PNL-4000 VOL. II
UC-62b

Assessment of Solar Options for Small Power Systems Applications

Volume II

Identification and Characterization of Concepts for Analysis

W. W. Laity
D. T. Aase
W. J. Apley
S. P. Bird
M. K. Drost
T. A. Williams

June 1980

Prepared for the U.S. Department of Energy
under Contract DE-AC06-76RLO 1830

Pacific Northwest Laboratory
Operated for the U.S. Department of Energy
by Battelle Memorial Institute

Battelle

PNL-4000 VOL. II

DISCLAIMER

PACIFIC NORTHWEST LABORATORY
operated by
BATTELLE
for the
UNITED STATES DEPARTMENT OF ENERGY
Under Contract DE-AC06-76RLO 1830

Printed in the United States of America
Available from
National Technical Information Service
United States Department of Commerce
5285 Port Royal Road
Springfield, Virginia 22151

Price: Printed Copy $_____*; Microfiche $3.00

*Pages	NTIS Selling Price
001-025	$4.00
026-050	$4.50
051-075	$5.25
076-100	$6.00
101-125	$6.50
126 150	$7.25
151-175	$8.00
176-200	$9.00
201-225	$9.25
226-250	$9.50
251-275	$10.75
276-300	$11.00

PNL-4000 VOL. II
UC-62b

ASSESSMENT OF SOLAR OPTIONS FOR SMALL POWER SYSTEMS APPLICATIONS

VOLUME II

IDENTIFICATION AND CHARACTERIZATION OF CONCEPTS FOR ANALYSIS

W. W. Laity
D. T. Aase
W. J. Apley
S. P. Bird
M. K. Drost
T. A. Williams

June 1980

Prepared for
the U.S. Department of Energy
under Contract DE-AC06-76RLO 1830

Pacific Northwest Laboratory
Richland, Washington 99352

DOE-Richland, WA

THIS PAGE

WAS INTENTIONALLY

LEFT BLANK

FOREWORD

Under the sponsorship of the U.S. Department of Energy's Division of Central Solar Technology, the Pacific Northwest Laboratory performed a comparative analysis of solar thermal conversion concepts that are potentially suitable for development as small electric power systems (1 to 10 MWe). Cogeneration and total energy systems were beyond the scope of this study.

Seven generic types of collectors, together with associated subsystems for electric power generation, were considered. The collectors can be classified into three categories: 1) two-axis tracking (with compound-curvature reflecting surfaces), 2) one-axis tracking (with single-curvature reflecting surfaces), and 3) nontracking (with low-concentration reflecting surfaces). All seven collectors were analyzed in conceptual system configurations with Rankine-cycle engines. In addition, two of the collectors (the Point Focus Central Receiver and the Point Focus Distributed Receiver) were analyzed with Brayton-cycle engines, and the latter of the two also was analyzed with Stirling-cycle engines. With these engine options, 10 systems were formulated for analysis.

This is the second volume of a five-volume report on the work performed to analyze the alternative concepts, and the results obtained. Included in this volume are detailed descriptions of the concepts analyzed, and the key ground rules, assumptions, and design constraints used in the analysis. The five volumes are:

Volume I	Executive Summary
Volume II	Identification and Characterization of Concepts for Analysis
Volume III	Analysis of Concepts
Volume IV	Comparative Ranking of Concepts
Volume V	SOLSTEP - A Computer Model for Solar Plant System Simulations.

THIS PAGE

WAS INTENTIONALLY

LEFT BLANK

CONTENTS

THIS PAGE

WAS INTENTIONALLY

LEFT BLANK

FIGURES

TABLES

ASSESSMENT OF SOLAR OPTIONS FOR SMALL POWER SYSTEMS APPLICATIONS

VOLUME II

IDENTIFICATION AND CHARACTERIZATION OF CONCEPTS FOR ANALYSIS

1.0 INTRODUCTION

Under the sponsorship of the U.S. Department of Energy's (DOE) Division of Central Solar Technology, the Pacific Northwest Laboratory (PNL) performed a comparative analysis of solar thermal conversion concepts for small electric power applications. This document is the second volume of the PNL report on the work performed.

1.1 STUDY PURPOSE

The primary purpose of this study is to provide DOE with an independent, objective assessment of the principal solar thermal conversion concepts that have the potential for achieving commercial success as small electric power systems in the 1- to 10-MWe range. This assessment was performed concurrently with a similar assessment by the Solar Energy Research Institute (SERI). The results of these assessments will serve as guidance for DOE to make decisions on which concepts warrant priority attention in further technology development.

1.2 STUDY SCOPE

Seven generic types of collectors, together with associated subsystems for electric power generation, were considered in this study. The collectors can be classified into three categories: 1) two-axis tracking (with compound curvature reflecting surfaces), 2) one-axis tracking (with single-curvature reflecting surfaces), and 3) nontracking (with low-concentration reflecting surfaces).

These collectors can be combined with energy transport, energy storage, and power conversion subsystems in a wide variety of ways to formulate conceptual systems for electric power generation. In this study, attention was restricted to configurations that are potentially suitable for development as small power systems (1 to 10 MWe) in the long term (1990 to 2000), with initial commercialization by the mid-1980s. Cogeneration and total energy systems were beyond the scope of this study.

All seven types of collectors were analyzed in conceptual system configurations with Rankine-cycle engines. Because they can operate at particularly high concentration ratios, two of the collectors (the Point Focus Central Receiver and the Point Focus Distributed Receiver) were also analyzed with Brayton-cycle engines. In addition, the latter of the two was analyzed with Stirling-cycle engines. With these engine options, 10 conceptual systems were formulated for analysis.

1.2.1 Principal Tasks

The four principal tasks included in this study are as follows:

- Task 1 - Determination and Characterization of Concepts for Analysis: The objectives of this task were to determine the solar thermal concepts that would be analyzed, and to acquire and evaluate the literature available on each.
- Task 2 - Systems Analysis: Each of the alternative concepts selected in Task 1 was analyzed to determine the levelized energy cost required for operation at a nominal power level of 5 MWe with an annual capacity factor of 0.4 and with costs amortized over 30 years.
- Task 3 - Sensitivity Analysis: The effect on each of the alternative concepts of varying rated power and annual capacity factor was determined.
- Task 4 - Concept Ranking: The alternative concepts were ranked on the basis of seven attributes considered in the analyses performed as part of Tasks 2 and 3, together with preference data for the attributes obtained from interviews of managers representing the utility industry and DOE. Multiattribute utility methodology was used to perform the ranking.

1.2.2 Limitations

Within the constraints imposed by the performance characteristics of the solar collector subsystems, the operating conditions (e.g., turbine inlet temperature) for alternative concepts that work on the same cycle (e.g., Rankine) were the same. This facilitated the identification of differences among concepts that could be attributed to the different collector subsystem designs. No attempt was made to perform a detailed optimization of each conceptual design. Rather, designs best suited for a comparative evaluation of the concepts were formulated.

1.3 SCOPE OF VOLUME II

The seven generic types of collectors considered in this study, and the conceptual system configurations in which they were analyzed, are described in detail in this volume. The manner in which the generic concepts were selected is described in Section 2.0. Presented in Section 3.0 are the key ground rules, assumptions, and design constraints used in the performance analyses. The alternative system configurations are described in Section 4.0, and the approach taken to estimate subsystem costs, replacement capital costs, and operating and maintenance costs is discussed in Section 5.0. Subsystems standardized for the concepts are described in Appendix A, and cost estimates for the concepts are summarized in Appendix B.

2.0 SELECTION OF CONCEPTS FOR ANALYSIS

The initial task of this study was to identify the generic types of solar thermal conversion concepts to be analyzed. In conjunction with this task an extensive literature search was performed, and specialists in solar thermal research and development who could later provide assistance were identified. The results of these initial efforts were documented in an earlier report (Apley 1978).

2.1 BASIS FOR SELECTION

Electric power may be produced from solar energy in a wide variety of ways. Attention was restricted in this study to solar energy systems that meet the following requisites: 1) power is generated via thermal energy conversion (rather than, say, by photovoltaic energy conversion), 2) the power range is 1 to 10 MWe, and 3) the concepts have the potential for commercialization in the 1990-2000 time frame.

The process followed in this study to categorize solar collectors and the power generation subsystems used with them is illustrated in Figure 2.1. Referring to Step 1 of that figure, solar collectors may be classified as either tracking or nontracking. Those in the former category use either one-axis or two-axis tracking systems (Figure 2.1, Step 2). Because any collector consists of a concentrator (with a highly reflective surface) and a receiver (with a heat absorption surface), tracking collectors may be further categorized according to whether the concentrator moves, the receiver moves, or both move (Figure 2.1, Step 3).

In a one-axis tracking collector it is necessary to move only the receiver or the concentrator to track the sun. Thus, the one-axis tracking concentrator/tracking receiver option is not carried beyond Step 3 in Figure 2.1. The other two options in this category, one with a tracking receiver and the other with a tracking concentrator, lead to several conceptual systems. In the former, the tracking system and flexible piping connections necessary for the relatively heavy receiver restrict the applicability of this option to distributed modules, as noted in Figure 2.1. The latter option leads to two

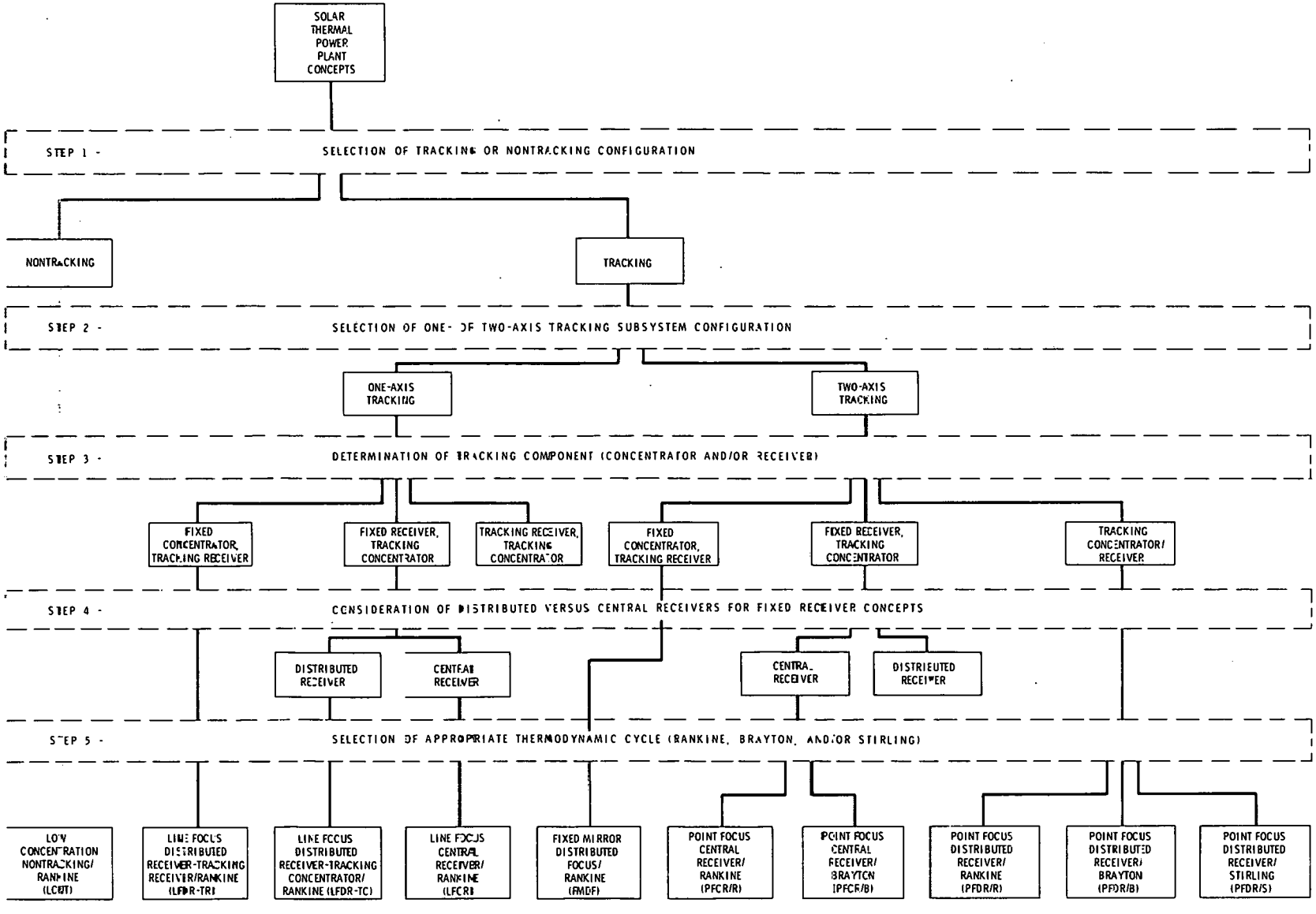

FIGURE 2.1. Determination of Generic Plant Concepts

alternatives. Fixed receivers with one-axis tracking concentrators can be used in distributed modules, or a single fixed receiver can be centrally located in a field of concentrators that direct incident solar energy to it.

Referring to Step 4 of Figure 2.1, one of the two-axis tracking options is the fixed, distributed receiver with a tracking concentrator. This option is not carried beyond Step 4 because its performance is substantially inferior to the alternative two-axis tracking, distributed receiver option with the receiver mounted at the focal point of, and tracking with, the concentrator.

The final step illustrated in Figure 2.1 involves the selection of appropriate thermodynamic cycles for power generation. Three cycles were considered: Brayton, Rankine, and Stirling.

Brayton engines and, to a lesser extent, Stirling engines operate economically only at high temperatures ($\sim 1500^{o}F$). Accordingly, these engines were considered for use only with two-axis tracking systems, which are capable of developing high temperatures because of their high concentration ratios. Brayton engines are available in unit sizes for a relatively large range of power levels; therefore, they were selected for analysis with both the Point Focus Central Receiver and the Point Focus Distributed Receiver concepts. Stirling engines show particular promise for modular applications and were, therefore, selected for analysis with the Point Focus Distributed Receiver concept.

Rankine-cycle engines have been developed for low-temperature as well as high-temperature applications. They were, therefore, selected for analysis with all types of collectors considered in this study. A centrally-located Rankine power plant, rather than distributed Rankine engines, is used in this study in conceptual systems with distributed collectors. Because of increasing demands for scarce water resources, particularly in the arid Southwest, this study is based on the use of dry cooling with all Rankine-cycle systems.

In summary, the process illustrated in Figure 2.1 led to the selection of seven generic types of collectors for analysis. All seven collectors were analyzed in conceptual system configurations with Rankine-cycle engines. In addition, two of the collectors (the Point Focus Central Receiver and the

Point Focus Distributed Receiver) were analyzed with Brayton-cycle engines; the latter of the two was also analyzed with Stirling-cycle engines. With these engine options, 10 conceptual systems were formulated for analysis. These are listed in Table 2.1, together with the nomenclature used to identify them in subsequent sections of this report.

2.2 SOURCES OF INFORMATION

Information needed for this study was acquired from two sources: available literature and individuals involved in the development of solar thermal power.

TABLE 2.1. Concepts Selected for Analysis

Concept	Thermodynamic Cycle	Symbol
TWO-AXIS TRACKING		
Point Focus Central Receiver	Rankine	PFCR/R
	Brayton	PFCR/B
Point Focus Distributed Receiver	Rankine	PFDR/R
	Brayton	PFDR/B
	Stirling	PFDR/S
Fixed Mirror Distributed Focus	Rankine	FMDF
ONE-AXIS TRACKING		
Line Focus Central Receiver	Rankine	LFCR
Line Focus Distributed Receiver		
• Tracking Concentrator	Rankine	LFDR-TC
• Tracking Receiver	Rankine	LFDR-TR
NONTRACKING		
Low-Concentration Nontracking	Rankine	LCNT

2.2.1 Literature Review

An extensive literature search was conducted during the initial phase of this study (January to June 1978). All solar energy updates, DOE/ERDA energy resource abstracts, government reports, announcements, and indices, solar directories, solar handbooks, engineering indices, and physics abstracts were reviewed, and a comprehensive computer search of all energy information data bases completed.

From the literature and from sources of information not yet published, an extensive data base for characterizing and evaluating the concepts was established. This included data from test facilities, information from organizations involved in the development of individual concepts, and cost and performance data from manufacturers.

The data base and reference materials were updated as new information became available during the course of the study. An index of this information was maintained on a magnetic card file for ease in updating it. All reference materials were readily available to members of the project team; these materials were used extensively throughout the study.

2.2.2 Contacts Made with Solar R&D Personnel

In conjunction with the literature review, a concerted effort was begun during the initial phase of this study to identify the major component manufacturers and system designers involved in solar thermal research and development. Over 50 sources were identified and contacted. These included individuals, institutions, and companies with experience in solar component design, power generation system layout, alternative thermal cycles, energy transport fluids, and advanced thermal and electrochemical storage methods.

As the study progressed, additional contacts were made as necessary to acquire needed information. Every effort was made to identify more than one source of information on any given topic, particularly when cost and/or performance data were needed.

Three consultants were placed under contract to assist in this study: 1) Dr. Lorin L. Vant-Hull of the University of Houston Solar Energy Laboratory, who assisted in the development of field layouts for the point focus, central receiver concepts; 2) Dr. William R. Martini of Richland, Washington, who provided information on Stirling engine performance, maintainability, and operating procedures; and 3) Bechtel National, Inc., which provided technical and cost information on components for energy conversion subsystems.

3.0 FORMULATION OF SYSTEM CONFIGURATIONS

This section briefly describes the methods PNL used to determine the cost and performance of each generic collector type.

3.1 OBJECTIVES

In developing performance and cost information for the seven generic concepts and alternative configurations considered in this study, the use of common performance and cost parameters was emphasized. The objective was to evaluate all the configurations on a common basis.

3.2 ENGINEERING GROUND RULES AND ASSUMPTIONS

Four key ground rules and assumptions were established at the outset of this study. They were selected to ensure that the small power systems ranked by PNL were comparable to those analyzed by SERI in its parallel study.

First, it was agreed that small power systems of 5 MWe would be compared. Sensitivity of the ranking to plant sizes of 1 MWe and 10 MWe would also be determined.

Second, all plants were to be designed to have a a capacity factor of 0.4. Capacity factor is defined as

$$CF = \frac{\text{Net energy generated annually (kWh)}}{\text{Rated capacity (kW) x number of hours in year}}$$

The net energy generated, used to calculate capacity factor, does not include forced outages. The sensitivity of the ranking at capacity factors of 0.7 and the optimum, i.e., lowest levelized energy cost, for each concept was also to be determined. As part of the sensitivity study, the concepts were also to be compared at capacity factors corresponding to zero storage for each system. By specifying capacity factor, the plants were compared at equivalent energy output, as well as at equivalent rating (power).

The third ground rule was that all the small power systems would be connected to a utility grid. This eliminated the need to match specific daily and seasonal load characteristics. The utility grid was assumed large enough to take the small power system's output and to supply power for specific peaks that would occur in any real load situation. Plant output was limited to nominal rating.

The fourth ground rule was that insolation data from Barstow, California would be used to determine plant output. The 1976 data collected by Aerospace Corporation were provided by the Jet Propulsion Laboratory.

3.3 DESIGN CONSTRAINTS

In addition to the four ground rules, PNL imposed several constraints in formulating the systems to be studied. The purposes of the additional constraints were to limit the scope of the engineering effort involved and to ensure that all concepts were evaluated on the same technological basis.

Descriptions of collector components (concentrator and receiver) were developed from designs representative of the generic concepts, to the extent that such design information was available. The descriptions were then modified to reflect proposed advances in structures, optical coatings, selective surfaces, and other features that would reflect the state of the art in the 1990s.

Common subsystems and components were used as much as possible in formulating the small power systems representing each generic concept. Subsystems such as thermal and electrical storage and power conversion were standardized and used as appropriate with the generic collector concepts.

The PNL studies minimized the subsystem optimization of design and operating parameters. Previous studies were relied on to establish appropriate operating temperatures and other parameters for this study. Exceptions were necessary for the small plant sizes. In these instances, some changes, such as field layout for central receiver concepts for small fields, are appropriate. Temperatures can be adjusted when cavity receivers are substituted for open receivers. No attempt was made, however, to perform extensive suboptimization, even when changes from previous designs were made.

4.0 CONCEPT DESCRIPTIONS

Each of the 10 generic concepts identified and analyzed in this study was organized into four subsystems:

- collector
- energy transport
- energy storage
- energy conversion.

Most of the concepts included a collector subsystem that collects incident solar radiation and converts it to thermal energy. The transport subsystem transports thermal energy from the collector subsystem to the energy storage and conversion subsystems. The energy storage subsystem stores excess thermal energy collected during periods of high insolation for use when little or no insolation is available. The energy conversion subsystem converts the thermal energy to electrical energy.

However, three concepts--the PFCR/B, PFDR/B, and PFDR/S--use a slightly different arrangement. The collector subsystem collects incident solar radiation and converts it to thermal energy, which is supplied directly to the energy conversion subsystem. The transport subsystem transports electric energy from the energy conversion subsystem to either the utility grid or the storage subsystem, where excess electric energy is stored for use during periods of little or no insolation.

For all 10 concepts, a base case arrangement was defined. The base case was to use near-term technology wherever possible. For most concepts, one or more alternative arrangements was considered. These alternative arrangements generally consisted of more advanced technology that could improve concept performance but would require additional research and development.

In this section, the general arrangement of each concept is outlined, followed by a detailed description of the collector subsystem. The other three subsystems are described in less detail. More complete discussions of the transport, storage, and energy conversion subsystems are presented in Appendix A. Finally, alternative arrangements, if any, are briefly described.

4.1 POINT FOCUS CENTRAL RECEIVER/RANKINE CYCLE

The concept consisting of a point focus central receiver and a Rankine-cycle heat engine will be discussed.

4.1.1 General Arrangement

The Point Focus Central Receiver is a two-axis tracking collector concept capable of generating very high operating temperatures. In the PFCR/R concept, the high temperatures available from the receiver are used to generate steam in a Rankine-cycle energy conversion subsystem, producing electric power. The concept has the advantage of high operating temperature and good energy conversion efficiency. However, the necessary components tend to be more expensive than those for lower temperature concepts.

The collector subsystem consists of a large array of heliostats (mirrors) that track the sun in two axes, redirecting the incident radiation onto a receiver located on the top of a fixed tower. Steam is generated at 510°C (950°F) and 10.0 MPa (1450 psi). The transport subsystem transports feedwater to the receiver and returns superheated steam to either the storage or energy conversion subsystem. The energy storage subsystem stores thermal energy in a mixed medium consisting of oil and rock. The thermal energy can be extracted to generate steam for the energy conversion subsystem. The energy conversion subsystem consists of a Rankine-cycle heat engine, which uses water as a working fluid, and a dry cooling tower for rejecting waste heat to the atmosphere. The PFCR/R concept is shown schematically in Figure 4.1.

4.1.2 Collector Subsystem

The same heliostat and support assembly were used for all PFCR cases. The selected design was very similar to both the Solaramics (Solaramics 1978) and McDonnell Douglas (MDAC) (Hallet and Gervais 1977a) prototype heliostat shown in Figure 4.2, sized to a 49-m^2 aperture area. Each heliostat had an individual tracking mechanism. The individual mirrors were focused but not canted.

Two different receivers were included in the analyses: an open and a cavity type. The open receiver was similar in design to the Martin Marietta

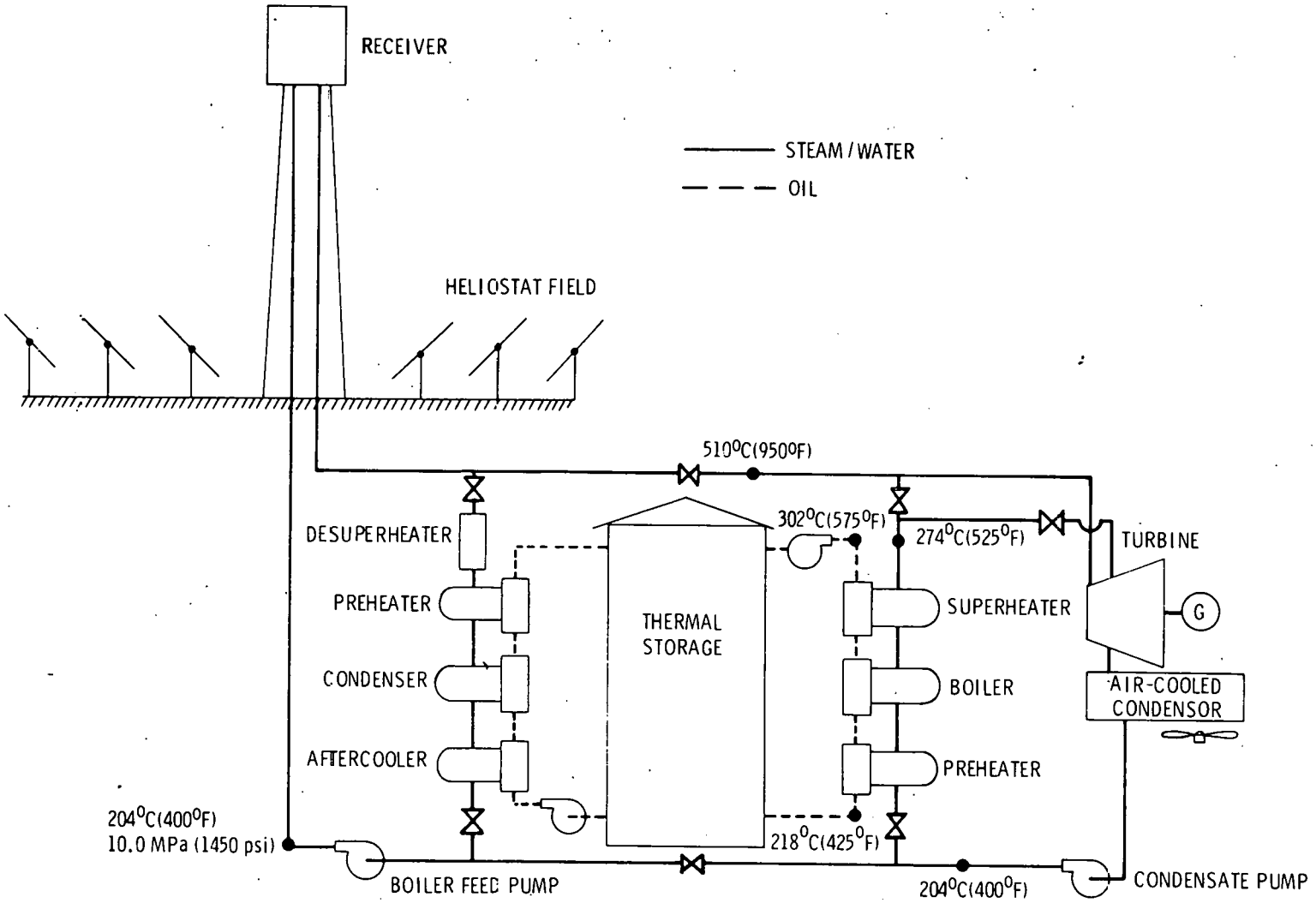

FIGURE 4.1. Point Focus Central Receiver/Rankine Cycle Concept Schematic

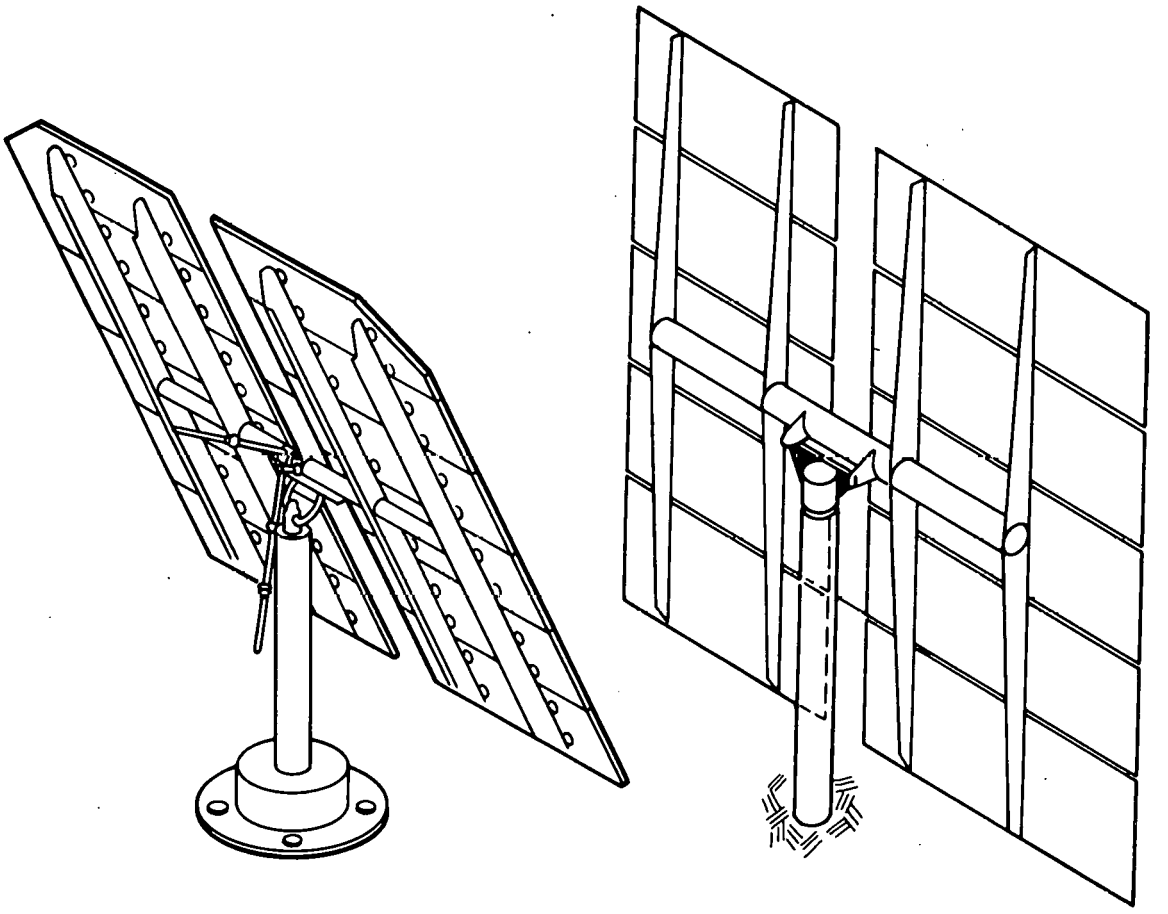

McDONNELL DOUGLAS ASTRONAUTICS CORP.
PROTOTYPE HELIOSTAT

SOLARAMICS PROTOTYPE HELIOSTAT

FIGURE 4.2. Point Focus Central Receiver Heliostat

molten salt receiver, while the cavity type was similar to the Boeing design (Sandia 1978); both designs are shown in Figure 4.3. Each receiver type was individually sized to match the power plant rating and hours-of-storage required. A maximum receiver loading of 0.3 MW/m^2 was used to determine heat transfer area. Additional receiver sizing was needed to ensure the optimal absorption/spillage/thermal loss combination.

The combined concentrator/receiver system is shown in Figure 4.4. It is important to note that the field shape can change dramatically when smaller plants or cavity receivers are considered. In both cases, the fraction of heliostats located in the southern portion of the field is reduced.

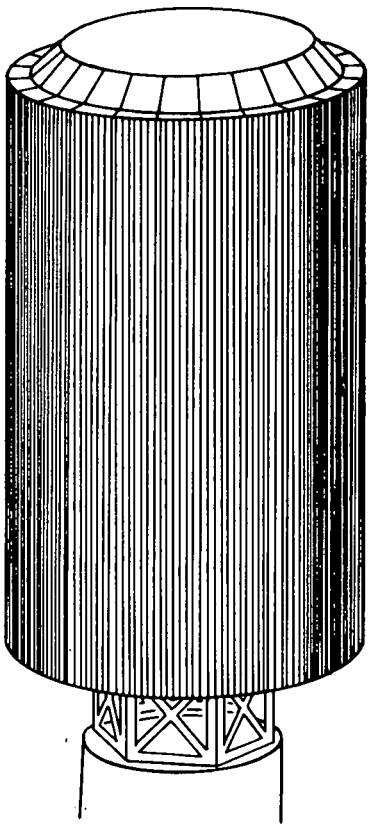

MARTIN MARIETTA
RECEIVER

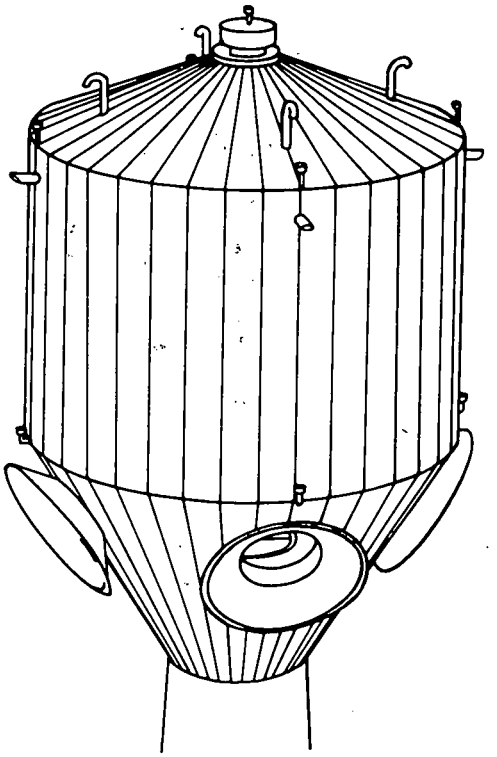

BOEING
RECEIVER

FIGURE 4.3. Receiver Types for Point Focus Central Receiver Concepts

4.1.3 Transport Subsystem

The PFCR/R transport subsystem transports feedwater from the energy conversion subsystem, located at ground level, to the receiver, located on top of the fixed tower. The transport subsystem returns superheated steam to either the energy conversion subsystem or the energy storage subsystem. When compared to other concepts, the PFCR/R transport subsystem is not extensive.

Several types of thermal energy transport subsystems were considered for application with the PFCR/R. The steam/water transport system was chosen for the base case arrangement because of component availability and extensive industrial experience with transporting steam and water. The steam/water transport subsystem will be discussed here; the alternative arrangements will be discussed in Section 4.1.6.

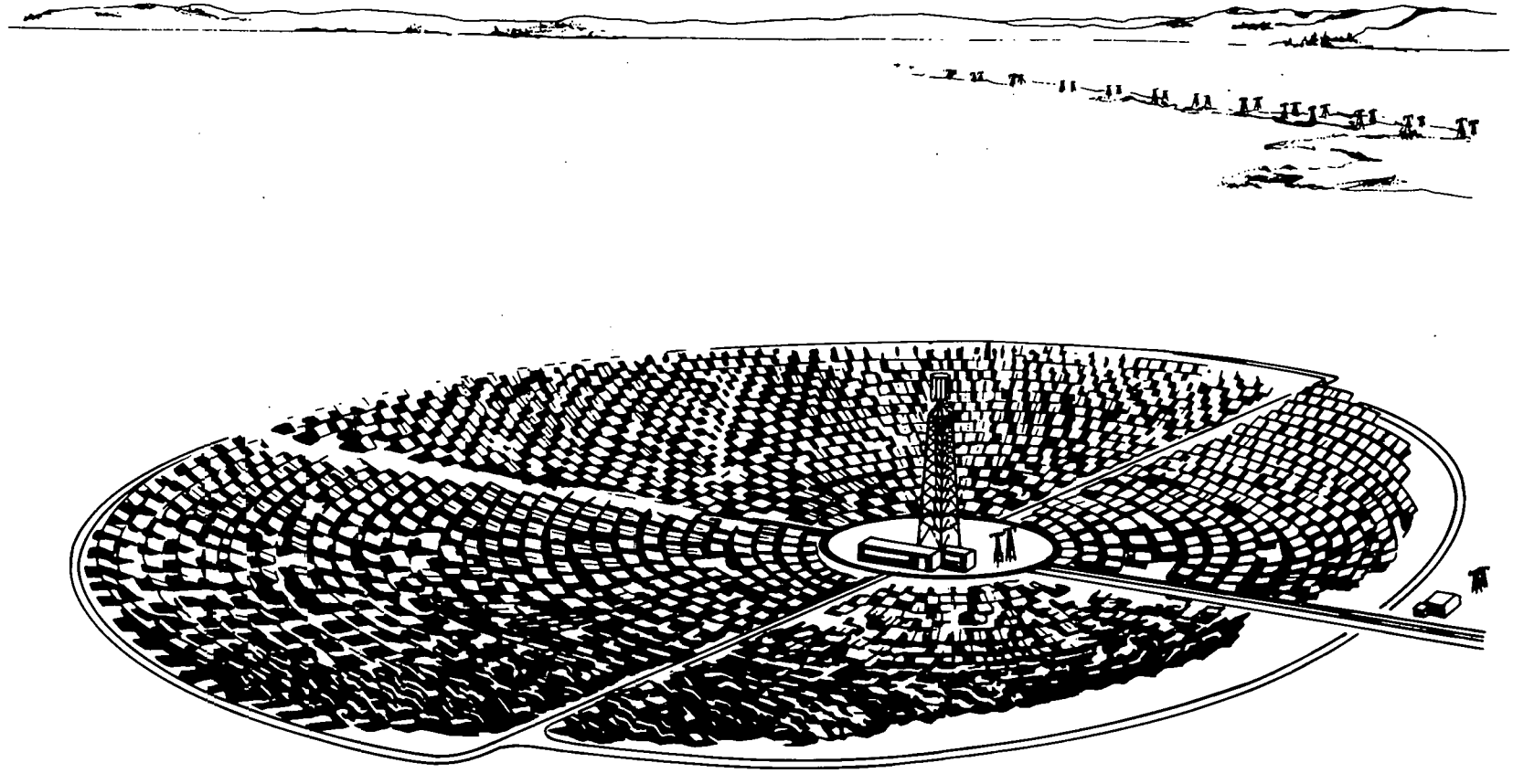

FIGURE 4.4. Point Focus Central Receiver

The transport subsystem supplies feedwater to the receiver distribution piping. The water is boiled and superheated in a once-through process. The superheated steam is either used in the energy conversion subsystem or desuperheated and used to charge the thermal energy storage subsystem. Steam returning from the tower is at 510°C (950°F) and 10.0 MPa (1450 psi).

The transport subsystem consists of the feedwater pump and the supply and return piping. Appropriate valves, expansion loops, and flexible coupling have been included to provide for thermal expansion during startup and operation. The supply piping is Schedule 160 carbon steel piping with calcium silicate insulation. The return piping is Schedule 160 low alloy steel piping with calcium silicate insulation. The feed pump is a carbon steel centrifugal pump with an electric motor for the driver. All valves are either carbon steel or low alloy steel, depending on temperature, with an appropriate pressure rating.

4.1.4 Storage Subsystem

Thermal energy collected in the collector field can be stored for use during the night or periods of low insolation. The thermal energy is stored as sensible heat in the energy storage subsystem. For the PFCR/R concept, several types of thermal energy storage subsystems were considered. The intermediate-temperature oil and rock subsystems was chosen for the base case because this approach is the closest to commercial availability. It will be described here; the alternative approaches will be discussed in Section 4.1.6.

The thermal energy storage subsystem consists of the storage medium, storage medium containment, charging heat exchanger, charging pump, discharge heat exchanger, discharge pump, and piping. The thermal energy storage subsystem is similar to that proposed by McDonnell Douglas for the Barstow Power Plant (Hallet and Gervais 1977b).

Thermal energy is stored as sensible heat in an oil and rock medium. The medium is contained in a tank arranged to maintain a thermocline between its hot and cool regions. River sand and pebbles were chosen as the rock component of the heat transfer medium. Caloria HT45® was selected as the heat transfer oil. Caloria HT45 cannot be used successfully above 304°C (580°F)

® Trademark of the Exxon Co., Houston, Texas.

because of thermal decomposition. Therefore, the selection of this oil requires that the maximum storage temperature be below 304°C (580°F).

During periods of high insolation, the thermal storage subsystem is charged by extracting steam returning from the collector subsystem. The steam is used to heat oil in the thermal storage charging loop, but is desuperheated to prevent excessive temperatures in the thermal storage unit. The charging loop consists of charging oil pumps, charging piping, charging heat exchangers, and appropriate controls.

During discharge the thermal storage unit provides heat to generate steam in the energy conversion subsystem. Steam is generated in the thermal storage discharge loop, containing a discharge oil pump, discharge piping, discharge heat exchangers, and appropriate controls.

The storage subsystem has two additional components that remove the residue of any thermal degradation of the heat transfer oil. The fluid maintenance system filters the oil to remove suspended solids, distills a side stream to remove high boiling polymeric compounds, and adds fresh makeup fluid to replace decomposed fluid. In addition to maintaining an oxygen-free gas above the heat transfer fluid, the ullage maintenance unit must also remove the volatile fractions of the degradation products that evaporate into the ullage space above the heat transfer fluid.

The oil and rock medium is contained in one or more carbon steel tanks, depending on the size of the thermal storage subsystem. The tanks are insulated to reduce heat loss from storage. Appropriate foundations and miscellaneous equipment are included. All piping is Schedule 40 carbon steel with calcium silicate insulation. All pumps are carbon steel centrifugal pumps with electric motor drives.

4.1.5 Energy Conversion Subsystem

The energy conversion subsystem takes thermal energy, supplied from either the field or storage, and converts it to electrical energy. This subsystem consists of the Rankine-cycle heat engine, generator, and air-cooled condenser.

The Rankine-cycle heat engine is a conventional steam power cycle. A detailed design of the Rankine cycle was beyond the scope of this study but performance and cost information were provided by a consultant for a representative Rankine-cycle engine steam power cycle. Accessories include three feedwater heaters, feedwater booster pump, feedwater pump, lubrication systems, steam seal systems, and controls.

The generator is a three-phase, four-pole synchronous unit. The generator is driven by the turbine through a double helical spur gear reduction unit. The air-cooled generator is equipped with a brushless exciter.

The waste heat from the Rankine cycle is rejected to the atmosphere in an air-cooled condenser. Exhaust steam from the turbine is ducted to the condenser where it is condensed in a steam/air heat exchanger. The steam/air heat exchangers are arranged in modules, each of which has a fan to force air past the heat transfer surfaces. Accessories include condensate pumps, piping, a mechanical vacuum pump, and auxiliary equipment.

4.1.6 Alternative Concept Arrangements

Once the base case concept arrangement was defined and analyzed, alternative components were considered because of their potential to either reduce cost or improve performance. In general, these alternatives represented advanced technology with more research and development risk. Five components were considered to estimate the 1990 performance of the PFCR/R concept using currently projected technology: a cavity receiver for the collector subsystem; a high-temperature HITEC® transport subsystem; a high-temperature HITEC storage subsystem; a high-temperature draw salt transport subsystem; and a high-temperature draw salt storage subsystem. These components were combined into three alternative arrangements.

4.1.6.1 PFCR/R Cavity Receiver Arrangement

In this arrangement, the base case open receiver is replaced by a cavity receiver, while maintaining the water/steam transport subsystem and

® HITEC is a trademark for heat transfer salt manufactured by E. I. DuPont de Nemours & Co., Wilmington, Delaware.

intermediate-temperature oil/rock storage subsystem. This arrangement has a higher optical efficiency for the small plant sizes considered in this study, particularly when a north field heliostat arrangement is used. In addition, thermal losses from the receiver are reduced.

4.1.6.2 PFCR/R Cavity Receiver, HITEC Arrangement

In this arrangement, the base case receiver is replaced by a cavity receiver, the water/steam transport subsystem is replaced with a HITEC transport subsystem, and the intermediate-temperature oil/rock storage is replaced by a high-temperature HITEC/rock storage subsystem. The HITEC is used to generate steam in heat exchangers for use in the energy conversion subsystem.

HITEC is heated in the receiver to 538^{o}C (1000^{o}F) and transported to the energy conversion or energy storage subsystem by the high-temperature HITEC transport subsystem. This system consists of supply piping, return piping, field circulation pump, and freeze protection equipment. Due to the high operating temperature of the HITEC, stainless steel piping must be used.

The storage subsystem stores thermal energy in a combination of molten salt and rock. The subsystem consists of the storage medium, medium containment, discharge loop, and medium treatment and makeup systems. A charging loop is not required because the same fluid is used for transport and storage. Thermal energy is discharged to the energy conversion subsystem in the discharge loop. The discharge loop consists of piping, HITEC pumps, heat exchangers, and miscellaneous equipment. Steam is generated at 510^{o}C (950^{o}F) and 10 MPa (1450 psi), regardless of whether energy is supplied from the field or from storage. Therefore, a single-admission turbine is used in the Rankine cycle.

4.1.6.3 PFCR/R Cavity Receiver, Draw Salt Arrangement

This arrangement is the same as the PFCR/R cavity receiver, HITEC arrangement except that the HITEC has been replaced by draw salt, a less expensive molten salt. Draw salt freezes at a higher temperature than HITEC and the materials compatibility has not been completely demonstrated. However, draw salt may have the potential for reducing storage and transport costs.

4.2 POINT FOCUS CENTRAL RECEIVER/BRAYTON CYCLE

The Point Focus Central Receiver/Brayton-cycle heat engine concept will be discussed in this section.

4.2.1 General Arrangement

The Point Focus Central Receiver is a two-axis tracking collector capable of generating very high operating temperatures. In the PFCR/B, the high temperatures available from the receiver are used in a closed-cycle Brayton energy conversion subsystem that produces electric power. The concept has the advantage of high operating temperature and very good energy conversion efficiency. However, the components tend to be more expensive than those for lower temperature concepts, and major research and development efforts will be required on certain high-temperature components.

The collector subsystem consists of a large array of heliostats (mirrors) that track the sun in two axes, redirecting the incident radiation onto a cavity receiver located on the top of a fixed tower. The receiver heats air to 816^{o}C (1500^{o}F), which is used in a closed-cycle Brayton engine energy conversion subsystem also located at the top of the tower. The transport subsystem transports electric energy from the energy conversion subsystem to either the storage subsystem or the utility power grid. The storage subsystem stores electric energy in one of several types of existing or proposed batteries. The PFCR/B concept is illustrated schematically in Figure 4.5.

4.2.2 Collector Subsystem

The concentrator subsystem was the same as that used for the PFCR/R concept, although a modified cavity receiver was used because of the higher temperatures (1500^{o}F) required for the Brayton cycle. The cavity aperture was optimized at a somewhat smaller size than for the Rankine cycle. This was due to balancing spillage and thermal losses. Because of the increased operating temperature, more expensive receiver materials and different selective surfaces with much lower performance capabilities were used.

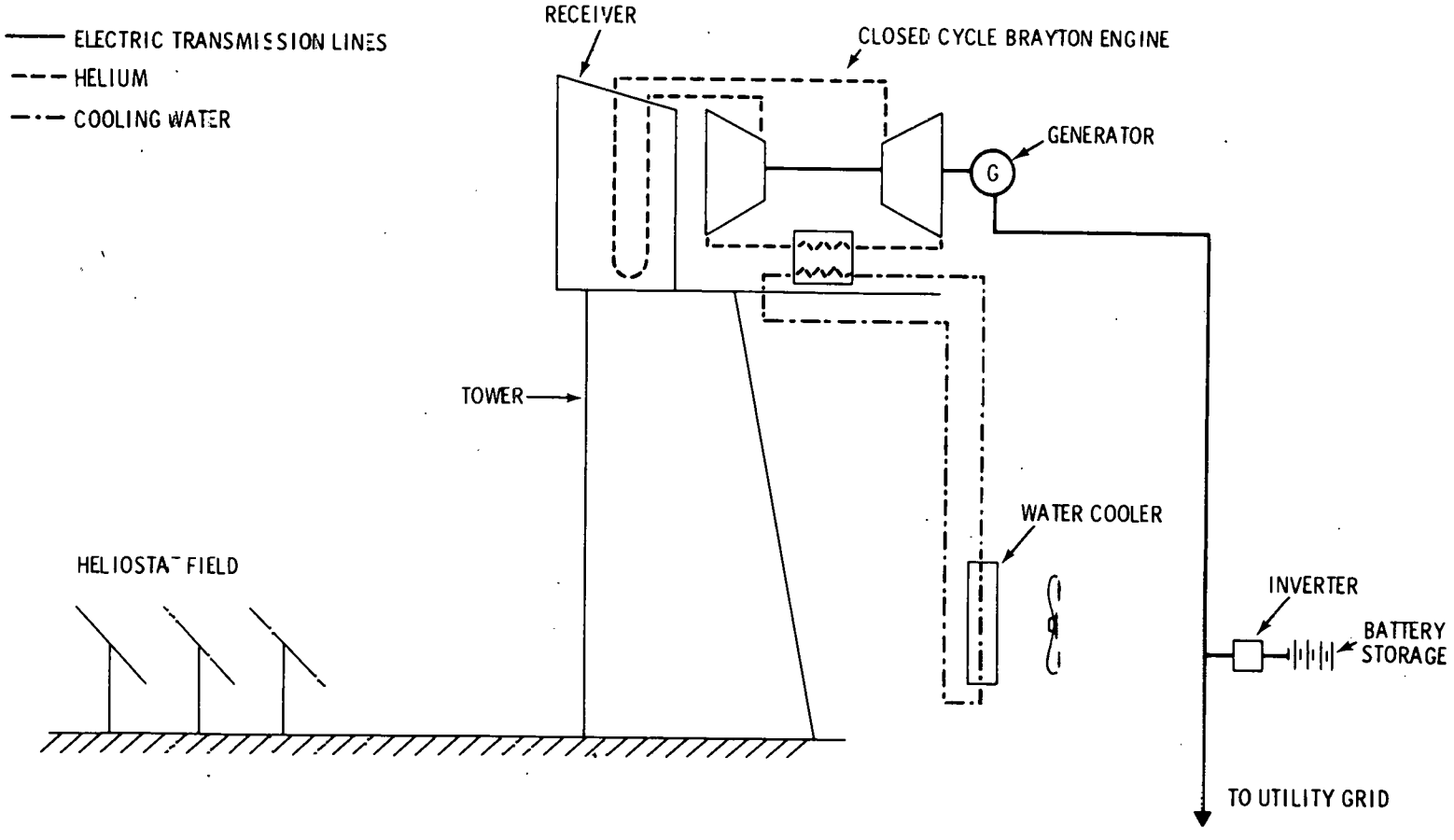

FIGURE 4.5. Point Focus Central Receiver/Brayton Cycle Concept Schematic

4.2.3 Transport Subsystem

The PFCR/B transport subsystem transports electric energy from the energy conversion subsystem located at the top of the tower to either the energy storage subsystem or the utility grid. When compared to other concepts using electric energy transport, the transport subsystem for the PFCR/B is not extensive; it is limited to the cable necessary to transfer power from the tower top to ground level.

4.2.4 Storage Subsystem

Electric energy generated in the energy conversion subsystem can be stored for use during the night or periods of low insolation. The electric energy is stored as electrochemical energy in batteries. Several types of electric energy storage subsystems were considered, each using a different type of battery. The lead acid battery was chosen for the base case because this approach is the closest to commercial availability. The lead acid battery energy storage subsystem will be discussed here; the alternative concepts will be discussed in Section 4.2.6.

The electric energy storage subsystem consists of the batteries, ac/dc converter, and miscellaneous equipment such as monitors, cooling water, makeup water, and wiring systems. The ac/dc converters convert the ac power from the energy conversion subsystem to dc power, which can be stored in the batteries.

The lead acid batteries are strings of sealed lead acid cells, physically arranged in a tri-stack configuration. Each string consists of series-connected cells. The number of cells depends on the power plant design rating. The individual cells are water-cooled by a closed-loop circulating system. The ac/dc converter equipment is sized for the maximum dc power input. The system includes the necessary SCR bridges, breakers, transformers, intermediate bus, and ancillary equipment.

4.2.5 Energy Conversion Subsystem

The energy conversion subsystem takes thermal energy supplied from the collector subsystem and converts it to electrical energy. The energy conversion subsystem consists of the Brayton engine, the generator, and a heat rejection unit.

The Brayton-cycle heat engine is a closed-cycle gas turbine with a recuperator. A detailed design of this component was beyond the scope of this study so vendor performance and cost information was used. The closed-cycle Brayton engine is water-cooled.

The generator is a three-phase, 60-Hz, four-pole synchronous unit. The generator is driven by the turbine through a speed reducer. The unit is air-cooled and equipped with a brushless exciter.

Waste heat from the Brayton engine is rejected to the atmosphere in an air cooler. Hot water from the Brayton cycle is piped to the cooler where it is cooled in a water/air heat exchanger. The water/air heat exchangers are arranged in modules, each with a fan to force air past the heat transfer surfaces. Accessories include pumps, piping, and auxiliary equipment.

4.2.6 Alternative Concept Arrangements

After the base case concept arrangement was defined and analyzed, alternative components were considered because of their potential for concept cost reduction or performance improvement. In general, the alternative components represent advanced technology with more research and development risk.

Two battery types were considered to give an estimate of the 1990 performance of the PFCR/B concept using currently projected technology: a generic advanced battery and a Redox advanced battery. These components were combined with the base case PFCR/B concept to provide two alternative arrangements.

4.2.6.1 PFCR/B Generic Advanced Battery

In this arrangement, the base case lead acid battery is replaced by an advanced battery having characteristics typical of a variety of solid anode/cathode battery systems currently under development.

4.2.6.2 PFCR/B Redox Battery

The base case lead acid battery is replaced by a Redox battery in this arrangement. The Redox battery uses fully soluble anode and cathode fluids separated by a selective ion exchange membrane. The reactants are normally

stored in tanks. During charge and discharge, the reactants are pumped through flow cells. The electrochemical reactions take place at separate inert porous carbon felt electrodes.

4.3 POINT FOCUS DISTRIBUTED RECEIVER/RANKINE CYCLE

The PFDR/R concept, which includes a point focus distributed receiver and a Rankine-cycle energy conversion subsystem, will be discussed in this section.

4.3.1 General Arrangement

The Point Focus Distributed Receiver is a distributed, dish-shaped, two-axis tracking collector capable of generating very high operating temperatures. In the PFDR/R concept, the high temperatures available from the receiver are used to generate steam for use in a Rankine-cycle energy conversion subsystem. The concept has the advantage of high operating temperature and good energy conversion efficiency. However, it requires an extensive transport subsystem, and the components tend to be more expensive than those for lower temperature concepts.

The collector subsystem consists of an array of parabolic dishes that track the sun in two axes, redirecting the incident radiation onto individual receivers located at the focal point of each separate parabolic concentrator. Steam is generated in the individual receivers, exiting at 510°C (950°F) and 10.0 MPa (1450 psi). The steam is transported to a central generation facility by the transport subsystem. The steam can be either used in the energy conversion subsystem or stored in the storage subsystem. The storage subsystem stores thermal energy in a mixed medium consisting of oil and rock. The thermal energy can be extracted to generate steam for the energy conversion subsystem. The energy conversion subsystem consists of a steam Rankine-cycle heat engine and a dry cooling tower for rejecting waste heat to the atmosphere. The PFDR/R concept is diagrammed schematically in Figure 4.6.

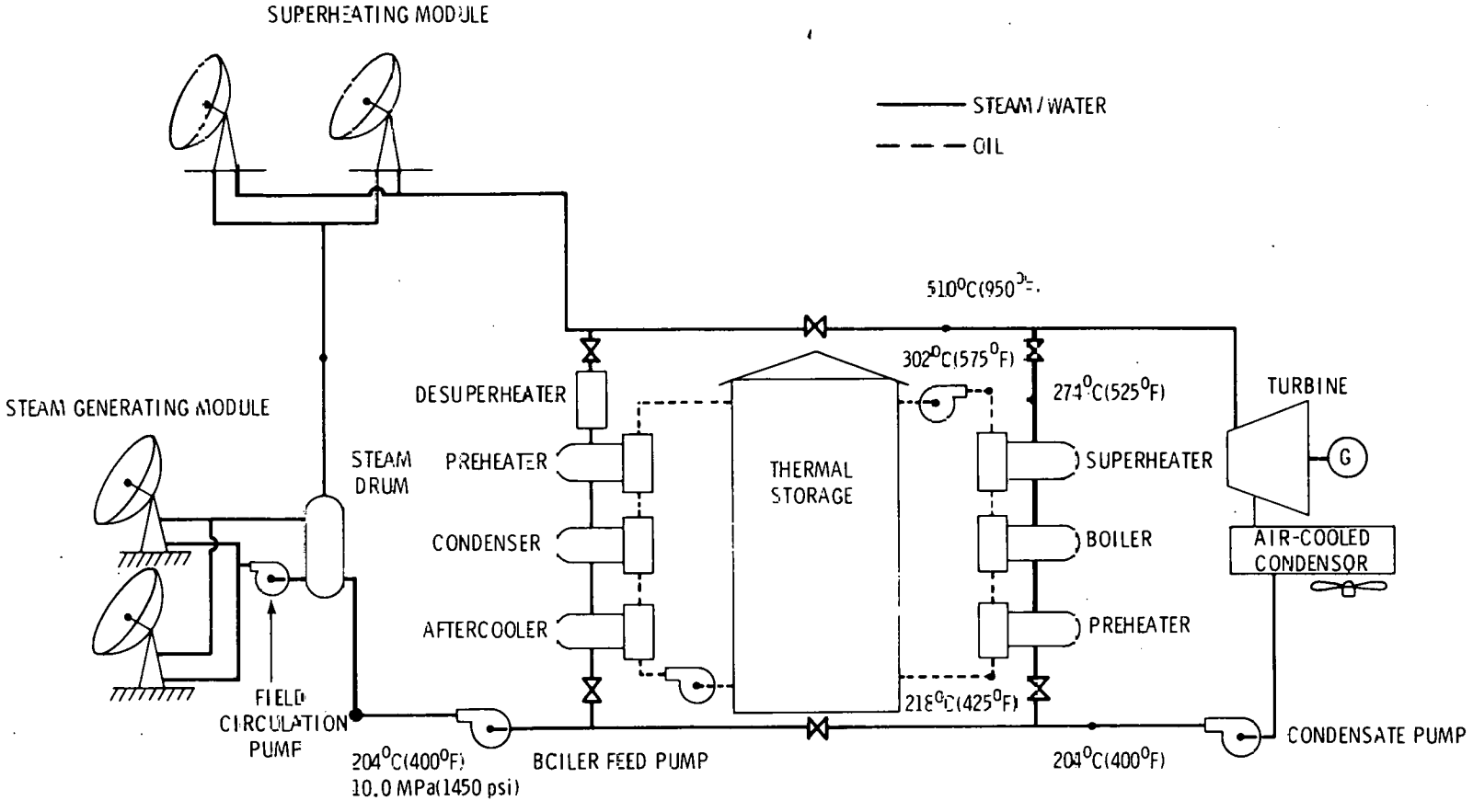

FIGURE 4.6. Point Focus Distributed Receiver/Rankine Cycle Concept Schematic

4.3.2 Collector Subsystem

The same concentrator was used for all PFDR concepts. It consisted of a parabolic dish with a 100-m^2 aperture, mounted on a tripod. The tripod could be rotated on a circular track and/or canted back by an individual tracking mechanism. The design is based on a configuration developed by the Jet Propulsion Laboratory (Truscello 1978), modified to be optimized using PNL economic and performance values.

Two high-temperature (1000^{o}F and 1500^{o}F) cavity-type receivers were included in the analysis. The 1500^{o}F subsystem included modifications to allow separate Brayton and Stirling engine operation. Features of both the General Electric (Zimmerman 1979) and Fairchild Stratos Division (Haglund and Tatge 1979) designs were combined with information from NASA-Lewis (Dochat and Cameron 1979) and the Jet Propulsion Laboratory (Caputo 1975; Wu and Wen 1978; Truscello 1978) to characterize the optimal receiver designs. Figure 4.7 shows a typical field configuration in which the receiver is mounted to the concentrator, and both are moved as part of the entire tracking assembly.

4.3.3 Transport Subsystem

The PFDR/R transport subsystem transports feedwater from the central generating facility to the distributed receivers and returns superheated steam to either the energy conversion or energy storage subsystem. The PFDR/R transport subsystem is quite extensive and involves a major capital cost.

Several types of thermal energy subsystems were considered for application with the PFDR/R. The steam/water transport system was chosen for the base case arrangement because of component availability and extensive industrial experience with transporting steam and water. The steam/water transport subsystem will be discussed here; the alternative arrangements will be discussed in Section 4.3.6.

The transport subsystem takes feedwater from the Rankine-cycle energy conversion subsystem and transports it through the supply piping to the collector array. The collector field is divided into steam generation and

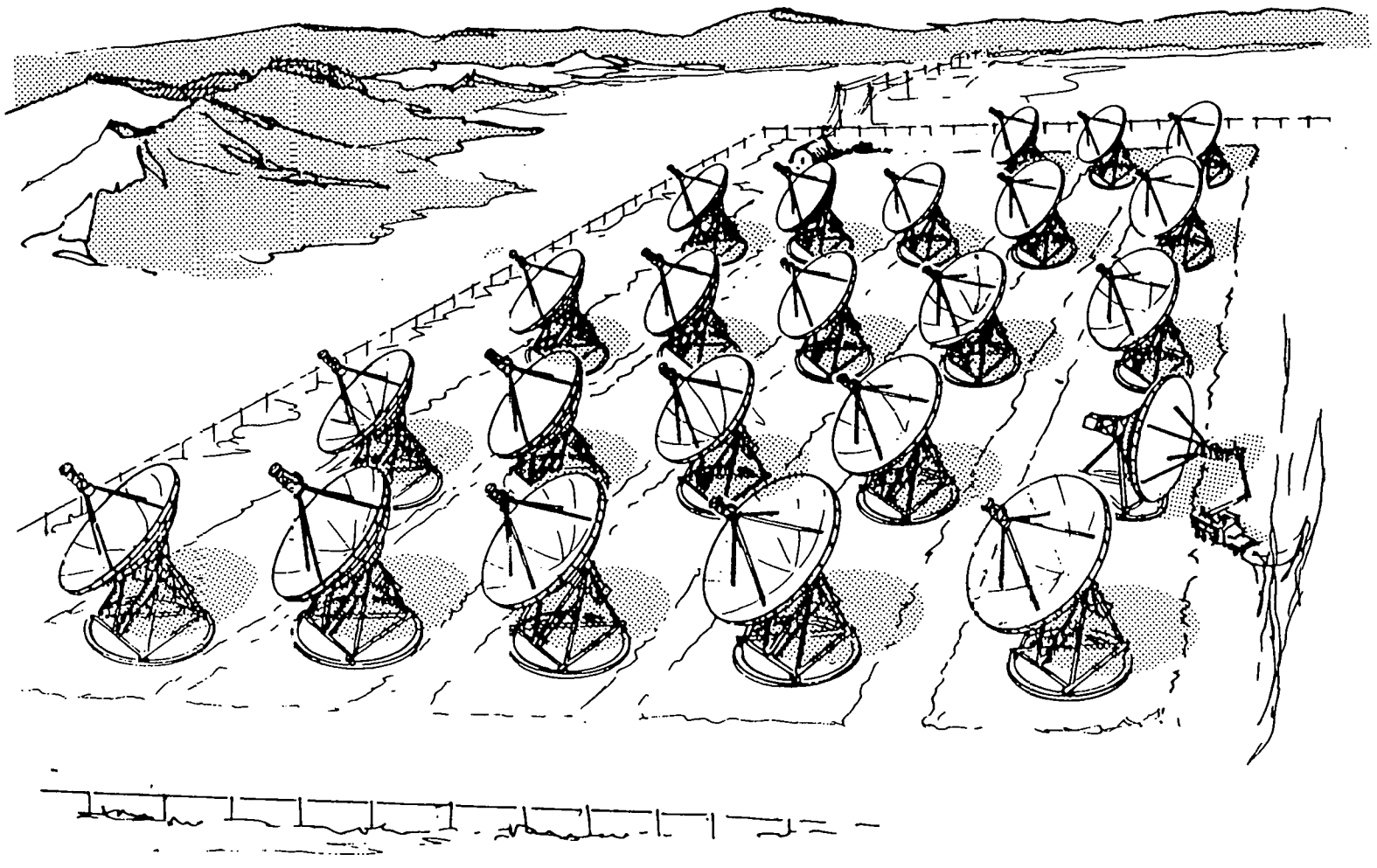

FIGURE 4.7. Point Focus Distributed Receiver

superheating modules. The feedwater is supplied to the steam generation module where the water is circulated through the collectors, producing a steam/water mixture. The steam is separated and transported to the superheating module; the water is recirculated through the steam generating module. Saturated steam from the steam generating module is superheated in the superheater module and returned to the central generating facility. Steam returning from the field is at 510°C (950°F) and 10.0 MPa (1450 psi).

The individual collectors are grouped into modules arranged to form the collector field. The transport subsystem can be divided into module supply piping, return piping, and internal piping. Supply piping for a steam generating module is shown in Figure 4.8. Isolation valves are included to allow for maintenance on individual collectors. Expansion loops and flexible coupling are included to accommodate thermal expansion.

A typical collector field for a 5-MWe plant is shown in Figure 4.9. In this arrangement, the superheating modules are the closest to the central generating facility. Module supply and return piping is included.

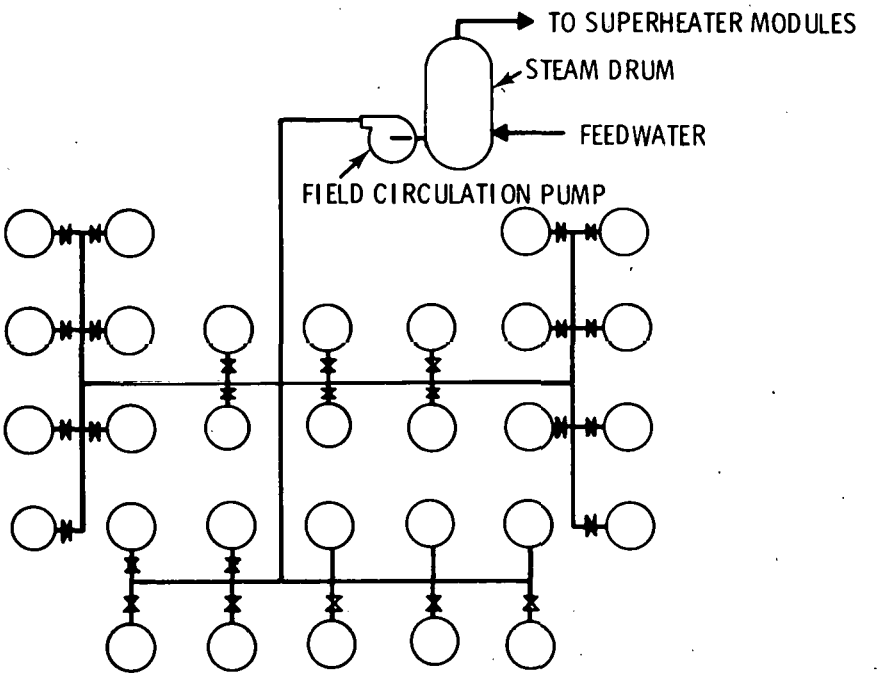

FIGURE 4.8. Steam Generator Module Supply Piping for the Point Focus Distributed Receiver/Rankine Cycle Concept

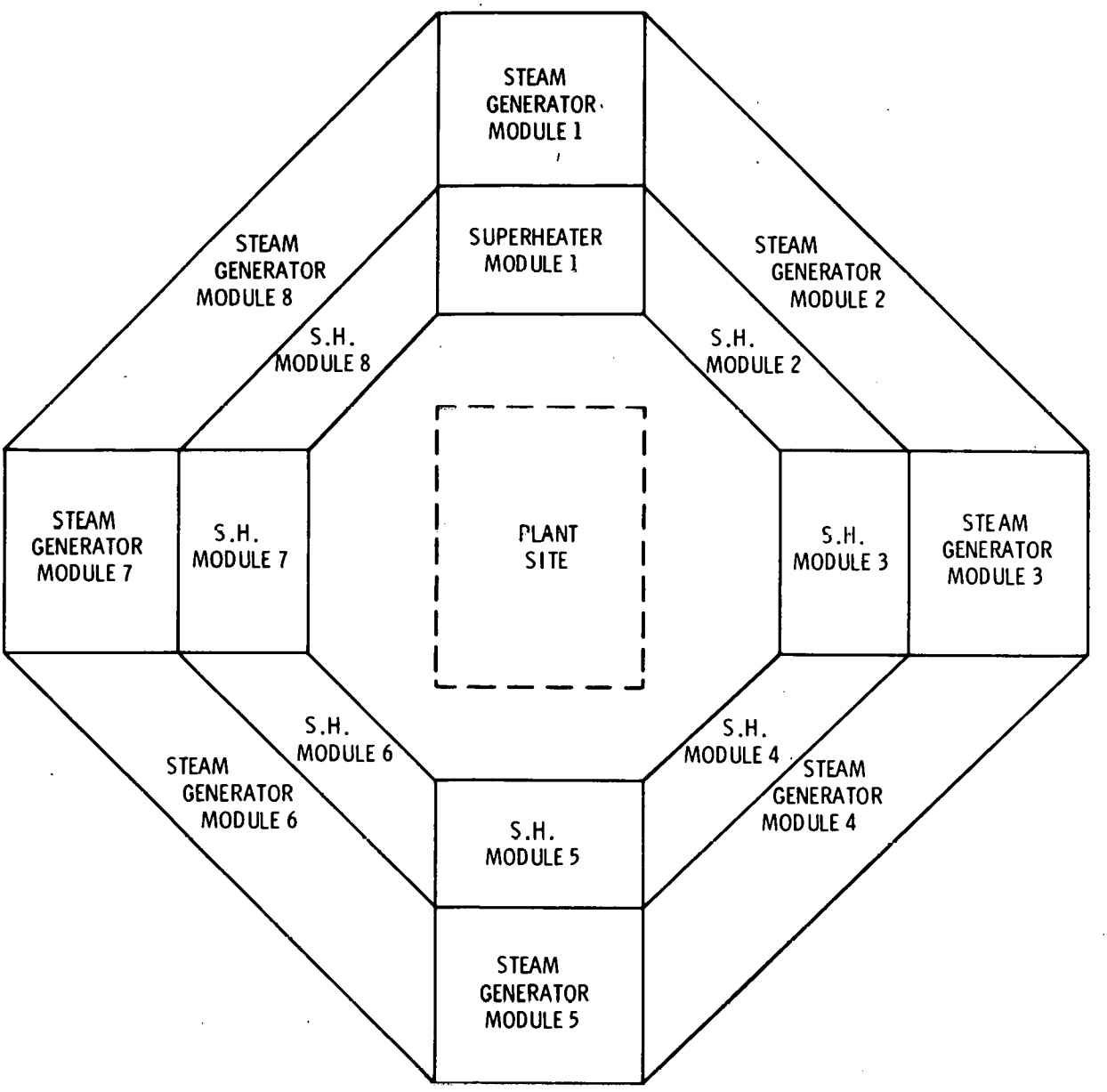

FIGURE 4.9. Typical Collector Field Layout, Point Focus Distributed Receiver/Rankine Cycle Concept

In all cases the piping is Schedule 160 carbon steel or low alloy steel with calcium silicate insulation. Module supply, return, and internal piping is welded and buried. The feed pump and field circulation pumps are carbon steel centrifugal pumps driven by electric motors. All valves are assumed to be carbon steel gate valves of the appropriate pressure rating.

4.3.4 Storage Subsystem

Thermal energy collected in the collector field can be stored for use during the night or periods of low insolation. The thermal energy is stored as sensible heat in the energy storage subsystem. For this concept, several types of thermal energy storage subsystems were considered. The intermediate temperature oil and rock type was chosen for the base case because it is the closest to commercial availability. The intermediate-temperature oil and rock subsystem will be described here. Alternative types will be discussed in Section 4.3.6.

The thermal energy storage subsystem consists of the storage medium, medium containment, charging heat exchangers, charging pump, discharge heat exchangers, discharge pump, and piping. The thermal energy storage subsystem is similar to that proposed by McDonnell Douglas for the Barstow Power Plant.

Thermal energy is stored as sensible heat in an oil and rock medium. The medium is contained in a tank arranged to maintain a thermocline between its hot and cool regions. Caloria HT45 was selected as the heat transfer oil; river sand and pebbles were chosen as the rock component of the heat transfer medium. Caloria HT45 cannot be used successfully at a temperature above 304°C (580°F), due to its thermal decomposition. Therefore, the maximum storage temperature must not exceed 304°C (580°F).

During periods of high insolation, the thermal storage subsystem is charged by extracting steam returning from the collector subsystem. The steam is used to heat oil in the thermal storage charging loop, but is desuperheated to prevent excessive temperatures in the thermal storage unit. The charging loop consists of charging oil pumps, charging piping, charging heat exchangers, and appropriate controls.

During discharge, the thermal storage unit provides heat to generate steam in the energy conversion subsystem. Steam is generated in the thermal storage discharge loop, which consists of a discharge oil pump, discharge piping, discharge heat exchangers, and appropriate controls.

The storage subsystem has two additional components that remove the residue of any thermal degradation of the heat transfer oil. The fluid maintenance system filters the oil to remove suspended solids, distills a side stream to remove high boiling polymeric compounds, and adds fresh makeup fluid to replace decomposed fluid. The ullage maintenance unit must remove the volatile fractions of the degradation products that evaporate into the ullage space above the heat transfer fluid, as well as maintain an oxygen-free gas above the heat transfer fluid

The oil and rock medium is contained in one or more carbon steel tanks, depending on the size of the thermal storage subsystem. The tanks are insulated to reduce heat loss from storage. Appropriate foundations and miscellaneous equipment are included. All piping is Schedule 40 carbon steel with calcium silicate insulation. All the pumps are carbon steel centrifugal pumps with electric motor drives.

4.3.5 Energy Conversion Subsystem

The energy conversion subsystem takes thermal energy, supplied from either the field or storage, and converts it to electrical energy. The energy conversion subsystem consists of the Rankine-cycle heat engine, generator, and air-cooled condenser.

The Rankine-cycle heat engine is a conventional steam power cycle. Although detailed design of the Rankine cycle was beyond the scope of this study, performance and cost information were provided by a consultant for a representative Rankine-cycle engine steam power cycle. Accessories include three feedwater heaters, feedwater booster pump, feedwater pump, lubrication system, steam seal system, and controls.

The generator is a three-phase, four-pole synchronous unit, driven by the turbine through a double helical spur gear reduction unit. The generator is air-cooled and equipped with a brushless exciter.

The waste heat from the Rankine cycle is rejected to the atmosphere in an air-cooled condenser. Exhaust steam from the turbine is ducted to the condenser where it is condensed in a steam/air heat exchanger. The steam/air heat

exchangers are arranged in modules, each with a fan to force air past the heat transfer surfaces. Accessories include condensate pumps, piping, mechanical vacuum pump, and auxiliary equipment.

4.3.6 Alternative Concept Arrangements

After the base case concept arrangement was defined and analyzed, alternative components were considered because of their potential to either reduce cost or improve performance. In general, these components represented advanced technology with more research and development risk.

Six alternative components were considered, to facilitate estimating the 1990 performance of the PFDR/R concept using currently projected technology:

- an intermediate-temperature HITEC transport subsystem
- a high-temperature HITEC subsystem
- an intermediate-temperature HITEC storage subsystem
- a high-temperature HITEC storage subsystem
- an intermediate-temperature draw salt transport subsystem
- an intermediate-temperature draw salt storage subsystem.

These components were combined with the base case PFDR/R concept to form three alternative arrangements.

4.3.6.1 PFDR/R Intermediate-Temperature HITEC Arrangement

In this arrangement, the base case steam/water transport subsystem is replaced with an intermediate-temperature HITEC transport subsystem; the base case oil/rock storage subsystem is replaced with an intermediate-temperature HITEC storage subsystem. The HITEC is used to generate steam in heat exchangers for use in the energy conversion subsystem.

HITEC is heated in the receiver to 454^{o}C (850^{o}F) and transported to the energy conversion or energy storage subsystem by the HITEC transport subsystem. This system consists of supply piping, return piping, field circulation pump, and freeze protection equipment. Because the maximum HITEC temperature is below 454^{o}C (850^{o}F), carbon steel piping can be used.

The storage subsystem stores thermal energy in a combination of molten salt and rock. The subsystem consists of the storage medium, medium containment, discharge loop, and medium treatment and makeup systems. A charging loop is not required because the same fluid is used for transport and storage. Thermal energy is discharged to the energy conversion subsystem in the discharge loop. The discharge loop consists of piping, HITEC pumps, heat exchangers, and miscellaneous equipment. Steam is generated at 427°C (800°F) and 10 MPa (1450 psi), regardless of whether energy is supplied from the field or from storage; therefore, a single-admission turbine is used in the Rankine cycle.

4.3.6.2 PFDR/R High-Temperature HITEC Arrangement

This arrangement is the same as the PFDR/R intermediate-temperature HITEC arrangement, except that the maximum temperature of the HITEC is raised to 538°C (1000°F). The higher maximum temperature requires the use of stainless steel in the high-temperature sections of the transport and storage subsystems.

4.3.6.3 PFDR/R Intermediate-Temperature Draw Salt Arrangement

This arrangement is the same as the PFDR/R intermediate-temperature HITEC arrangement except that the HITEC has been replaced by draw salt, a less expensive molten salt. Draw salt freezes at a higher temperature than HITEC and the materials compatibility has not been completely demonstrated. However, draw salt may have the potential for reducing storage and transport cost.

4.4 POINT FOCUS DISTRIBUTED RECEIVER/STIRLING CYCLE

The PFDR/S concept, which includes a point focus distributed receiver and a Stirling-cycle engine, is discussed in this section.

4.4.1 General Arrangement

The Point Focus Distributed Receiver is a distributed, dish-shaped, two-axis tracking collector capable of generating very high operating temperatures. In the PFDR/S concept, the high temperatures available from the receiver are used with a Stirling-cycle energy conversion subsystem. The concept has the

advantage of high operating temperature and a very good energy conversion efficiency. However, the components, particularly high-temperature components, tend to be more expensive than those for lower temperature concepts.

The collector subsystem consists of an array of parabolic dishes that track the sun in two axes, redirecting the incident radiation onto individual receivers located at the focal point of each separate parabolic concentrator. In the receiver, liquid metal is vaporized and then condensed on the heater tubes of a 17.5-kWe Stirling-cycle heat engine. The Stirling engine normally operates with a heater tube temperature of 816°C (1500°F) and drives a generator to produce electric power. The electric power is transported to storage or the utility power grid by the transport subsystem. The storage subsystem stores electric energy in one of several types of existing or proposed batteries. The PFDR/S concept is illustrated schematically in Figure 4.10.

4.4.2 Collector Subsystem

The concentrator used for the Stirling-cycle case was the same as that used for the Rankine and Brayton cycle cases. The receiver was a modified version of the Brayton-cycle design. The modification was necessary to take into account the lower volume area in which the heat source must be confined to enable efficient Stirling engine operation. Inclusion of a heat pipe subsystem was required to effectively concentrate the heat source.

4.4.3 Transport Subsystem

The PFDR/S transport subsystem transports electric energy from the Stirling-cycle energy conversion subsystem to either the energy storage subsystem or the utility grid. Because substantial technological improvements are not expected in electric power transmission, only one transport subsystem was considered in analyzing the PFDR/S concept. This subsystem is shown in Figure 4.11.

The transport subsystem is an ac power transmission network and consists of the cables, transformers, circuit breakers, and miscellaneous equipment necessary for transmitting power from the many small Stirling engines to the

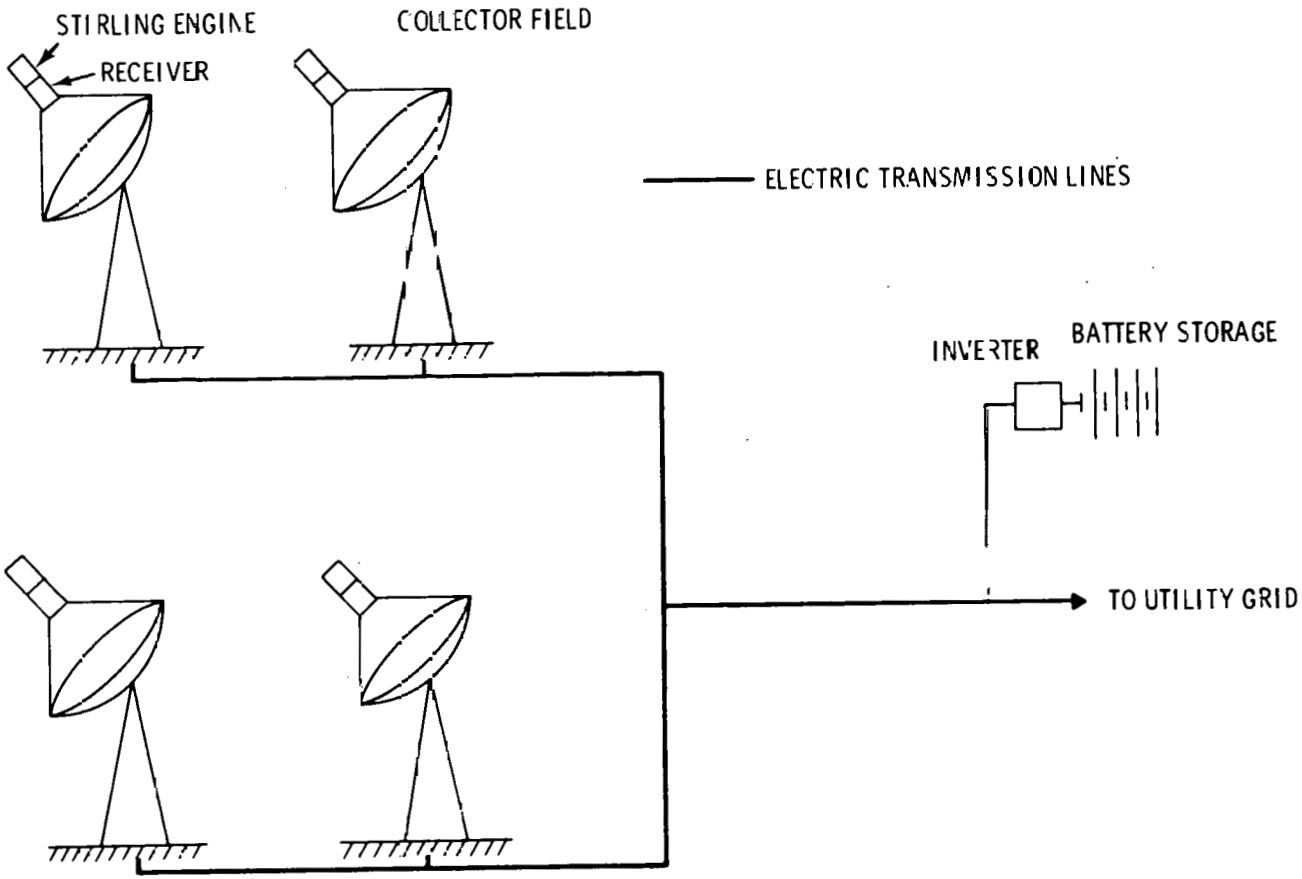

FIGURE 4.10. Point Focus Distributed Receiver/Stirling Cycle Concept Schematic

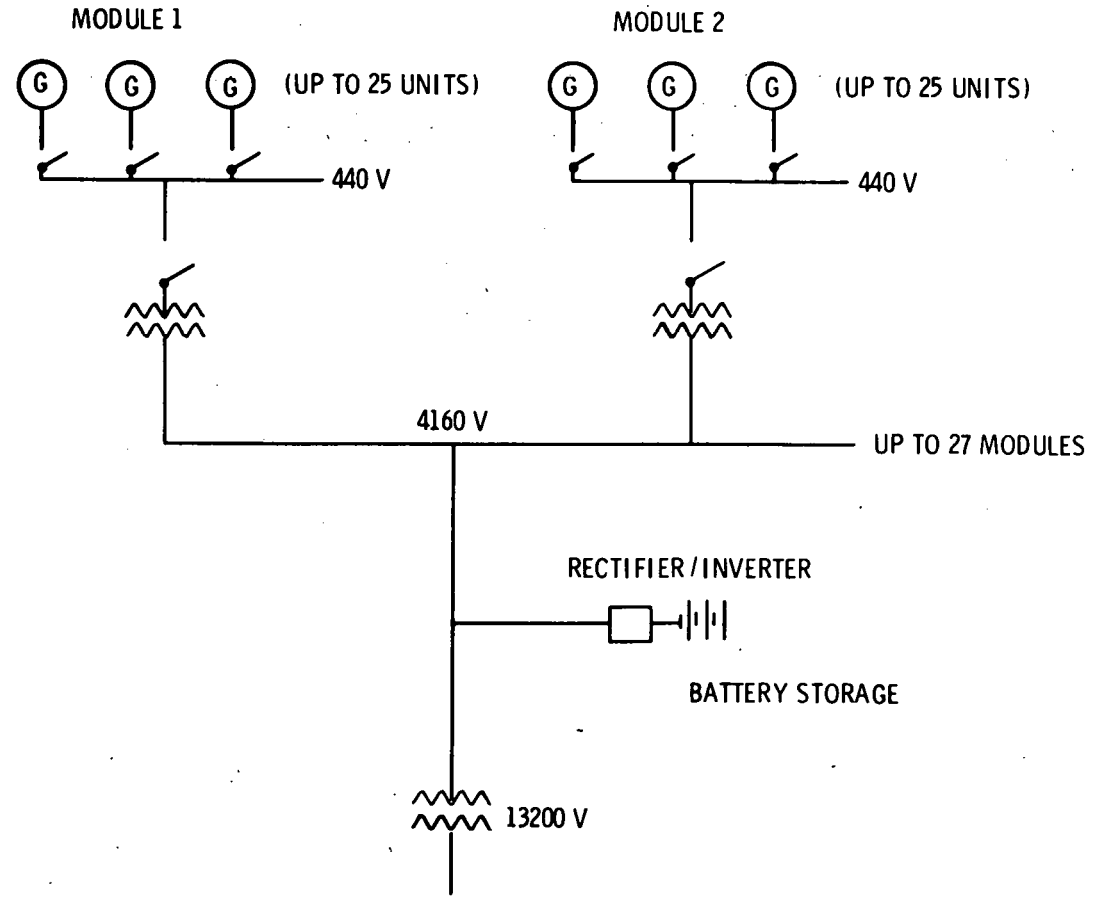

FIGURE 4.11. Transport Subsystem Schematic for the Point Focus Distributed Receiver/Stirling Cycle Concept

central storage facility. All transport subsystem components are commercially available and no problems are anticipated with either subsystem design or operation.

4.4.4 Storage Subsystem

Electric energy generated in the energy conversion subsystem can be stored for use during the night or periods of low insolation. The electric energy is stored as electrochemical energy in batteries. Several electric energy storage subsystem types were considered for the PFDR/S concept, each using a different type of battery. The lead acid battery was chosen for the base case because it is the closest to commercial availability. The lead acid battery energy storage subsystem will be discussed here. The alternative battery types will be discussed in Section 4.4.6.

The electric energy storage subsystem consists of the batteries, ac/dc converters, and miscellaneous equipment such as monitoring, cooling water, makeup water, and wiring systems. The ac/dc converters convert the ac power from the energy conversion subsystem to dc power, which can be stored in the batteries.

The lead acid batteries are strings of sealed lead acid cells, physically arranged in a tri-stack configuration. Each string consists of series-connected cells. The number of cells depends on the power plant design rating. The individual cells are water-cooled by a closed-loop circulating system. The ac/dc converter equipment is sized for the maximum dc power input. The system includes the necessary SCR bridges, breakers, transformers, intermediate bus, and ancillary equipment.

4.4.5 Energy Conversion Subsystem

The energy conversion subsystem takes thermal energy supplied from the collector subsystem and converts it to electrical energy. The energy conversion subsystem consists of the receiver, the Stirling engine, the generator, and the heat rejection unit.

The receiver consists of an annulus located inside a cavity receiver. The annulus acts as a vaporizor for liquid metal, which is condensed on the heater tubes of the Stirling engine. The receiver is intended to produce a heater tube temperature of 816^{o}C (1500^{o}F). The Stirling engine is a free-piston engine directly coupled to a linear alternator for power generation. The free-piston design was chosen over the kinematic designs because it has the potential for a longer operating life. The engine and generator are sized to produce 17.5 kWe. The Stirling engine is oil-cooled; the oil rejects heat to the atmosphere in an oil-to-air heat exchanger, which includes a fan to force air past the heat transfer surfaces.

4.4.6 Alternative Concept Arrangements

Other components were considered after the base case concept arrangement was defined and analyzed, because of their potential to either reduce cost or improve performance. These components generally represent advanced technology

with more research and development risk, and were considered to estimate future performance of the PFDR/S concept using currently projected technology.

Three components were considered: a thermal buffer, a generic advanced battery, and a Redox advanced battery. These were combined with the base case PFDR/S concept to yield three alternative concept arrangements.

4.4.6.1 PFDR/S Thermal Buffer

In this arrangement, a small thermal storage unit is installed between the liquid metal receiver and the Stirling engine. This allows the engine to operate during short periods of reduced insolation, "buffering out" the effects of short insolation transients. The thermal buffer consists of an insulated cylindrical vessel containing tubular capsules filled with a phase change salt. Thermal energy is stored as latent heat in the molten salt. The capsules are heated by condensing liquid metal from the receiver. The capsules give up heat to the Stirling engine heater tubes. The thermal buffer component proved to be quite expensive, indicating that other methods of handling short-term insolation transients should be explored.

4.4.6.2 PFDR/S Generic Advanced Battery

In this arrangement the base case lead acid battery is replaced by an advanced battery having characteristics typical of a variety of solid anode/cathode battery systems currently under development.

4.4.6.3 PFDR/S Redox Advanced Battery

The base case lead acid battery is replaced by a Redox battery in this arrangement. The Redox battery uses fully-soluble anode and cathode fluids separated by a selective ion exchange membrane. The reactants are normally stored in tanks. During charge and discharge, the reactants are pumped through flow cells. The electrochemical reactions take place at separate inert porous carbon felt electrodes.

4.5 POINT FOCUS DISTRIBUTED RECEIVER/BRAYTON CYCLE

The PFDR/B concept, which includes a point focus distributed receiver and a Brayton-cycle engine, is discussed in this section.

4.5.1 General Arrangement

The Point Focus Distributed Receiver is a distributed, dish-shaped, two-axis tracking collector capable of generating very high operating temperatures. The high temperatures available from the receiver are used in the PFDR/B concept with a Brayton-cycle energy conversion subsystem. The concept has the advantage of high operating temperature and a good energy conversion efficiency. However, the components, particularly high-temperature components, tend to be more expensive than those for lower temperature concepts.

The collector subsystem consists of an array of parabolic dishes that track the sun in two axes, redirecting the incident radiation onto individual receivers located at the focal point of each separate parabolic concentrator. In the receiver, liquid metal is vaporized and then condensed on the heater tubes of a 17.5-kWe Brayton-cycle heat engine. The Brayton engine normally operates with a heater tube temperature of 816^{o}C (1500^{o}F) and drives a generator to produce electric power. The electric power is transported to storage or the utility power grid by the transport subsystem. The storage subsystem stores electric energy in one of several types of near-term or advanced batteries. The PFDR/B concept is shown schematically in Figure 4.12.

4.5.2 Collector Subsystem

The concentrator used for the PFDR/B case was the same as that used for the Rankine cycle cases. The receiver was different due to the higher temperature requirements (1500^{o}F), and the design was reoptimized to trade off thermal losses against spillage losses.

4.5.3 Transport Subsystem

The PFDR/B transport subsystem transports electric energy from the Brayton-cycle energy conversion subsystem to either the energy storage subsystem or the utility power grid. Only one transport subsystem was considered for the PFDR/B concept because substantial technological improvements in electrical power transmission are not expected.

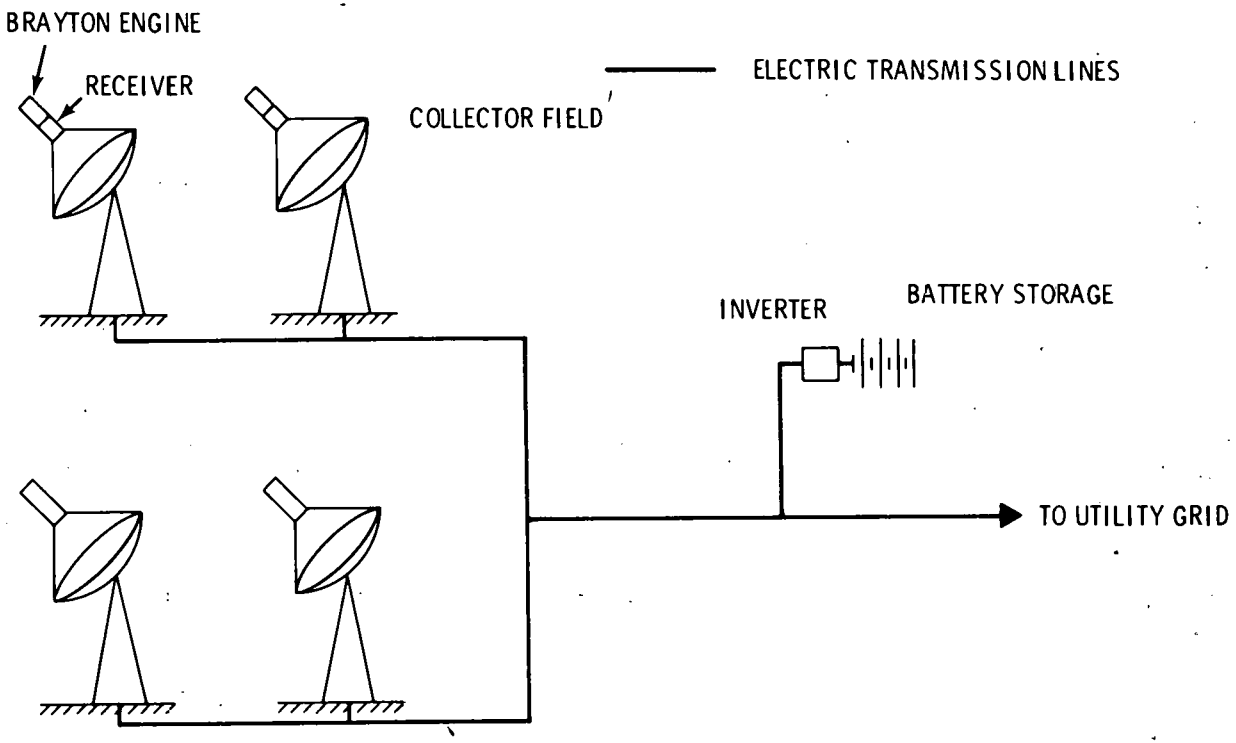

FIGURE 4.12. Point Focus Distributed Receiver/Brayton Cycle Concept Schematic

The transport subsystem shown in Figure 4.13 is an ac power transmission network and consists of the cables, transformers, circuit breakers, and miscellaneous equipment necessary for transmitting power from the many small Brayton engines to the central storage facility. All transport subsystem components are commercially available and no problems are anticipated with either subsystem design or operation.

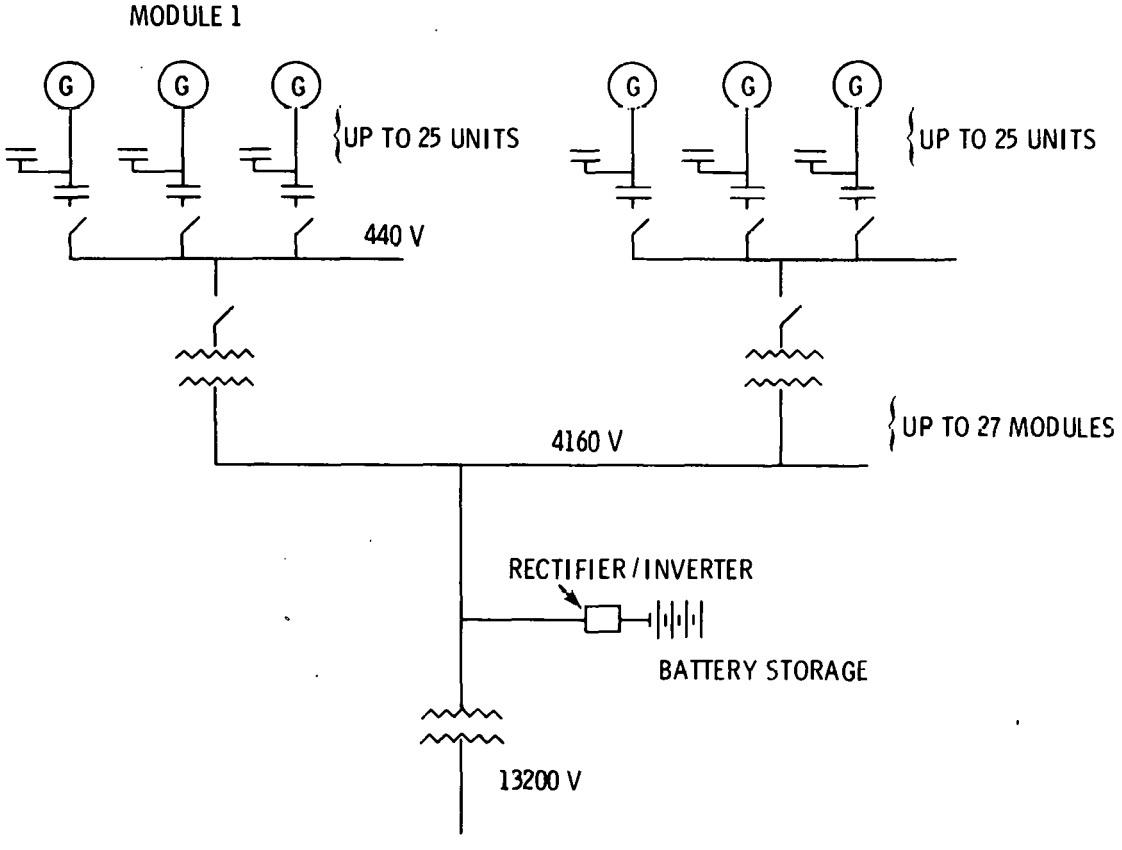

FIGURE 4.13. Transport Subsystem Schematic for the Point Focus Distributed Receiver/Brayton Cycle Concept

4.5.4 Storage Subsystem

Electric energy generated in the energy conversion subsystem can be stored for use during the night or periods of low insolation. The electric energy is stored as electrochemical energy in batteries. For the PFDR/B concept, several types of electric energy storage subsystems were considered, each using a different type of battery. The lead acid battery was chosen for the base case

because it is the closest to commercial availability. The lead acid battery energy storage subsystem will be discussed here; others will be discussed in Section 4.5.6.

The electric energy storage subsystem consists of the batteries, ac/dc converters, and miscellaneous equipment such as monitoring, cooling water, makeup water, and wiring systems. The ac/dc converters convert the ac power from the energy conversion subsystem to dc power, which can be stored in the batteries.

The lead acid batteries are strings of sealed lead acid cells, physically arranged in a tri-stack configuration. Each string consists of series-connected cells. The number of cells depends on the power plant design rating. The individual cells are water-cooled by a closed-loop circulating system. The ac/dc converter equipment is sized for the maximum dc power input. The system includes the necessary SCR bridges, breakers, transformers, intermediate bus, and ancillary equipment.

4.5.5 Energy Conversion Subsystem

The energy conversion subsystem takes thermal energy supplied from the collector subsystem and converts it to electrical energy. The energy conversion subsystem consists of the receiver, the Brayton engine, the generator, and the heat rejection unit.

The receiver consists of an annulus located inside the cavity receiver. The annulus acts as a vaporizor for liquid metal, which is condensed on the heater tubes of the Brayton engine. The receiver is intended to produce a heater tube temperature of 816^{o}C (1500^{o}F). The Brayton engine uses a closed cycle with air as the working fluid. The engine has a recuperator and rejects heat to a cooling oil. The engine has a rated output of 17.5 kWe. The Brayton engine drives a rotating induction generator. Waste heat is rejected to the atmosphere in an oil-to-air heat exchanger with a fan to force air past the heat transfer surfaces.

4.5.6 Alternative Concept Arrangements

After the base case concept arrangement was defined and analyzed, alternative components were considered because of their potential to either reduce

cost or improve performance. In general, these components represent advanced technology with more research and development risk. However, they were considered in order to give an estimate of the future performance of the PFDR/B concept using currently projected technology.

The three components considered were a thermal buffer, a generic advanced battery, and a Redox advanced battery. These alternatives were combined with the base case PFDR/B concept to create three other arrangements.

4.5.6.1 PFDR/B Thermal Buffer

In this arrangement, a small thermal storage unit is installed between the liquid metal receiver and the Brayton engine, allowing the engine to operate during short periods of reduced insolation. It "buffers out" the effects of short insolation transients. The thermal buffer consists of an insulated cylindrical vessel containing tubular capsules filled with a phase change salt. Thermal energy is stored as latent heat in the molten salt. The capsules are heated by condensing liquid metal from the receiver, and give up heat to the Brayton engine heater tubes. The thermal buffer component proved to be quite expensive. Exploration of other methods of handling short-term insolation transients is suggested.

4.5.6.2 PFDR/B Generic Advanced Battery

In this arrangement, the base case lead acid battery is replaced by an advanced battery with characteristics typical of a variety of solid anode/cathode battery systems currently under development.

4.5.6.3 PFDR/B Redox Advanced Battery

The base case lead acid battery is replaced by a Redox battery in this arrangement. The Redox battery uses fully-soluble anode and cathode fluids separated by a selective ion exchange membrane. The reactants are normally stored in tanks. During charge and discharge, the reactants are pumped through flow cells. The electrochemical reactions take place at separate inert porous carbon felt electrodes.

4.6 FIXED MIRROR DISTRIBUTED FOCUS/RANKINE CYCLE

The FMDF concept, which includes a fixed mirror distributed receiver and a Rankine-cycle engine, is discussed in this section.

4.6.1 General Arrangement

The fixed mirror distributed focus concept consists of a stationary concentrator and a two-axis tracking receiver capable of generating high operating temperatures. These high temperatures are used in the FMDF concept to generate steam in a Rankine-cycle energy conversion subsystem, which, in turn, produces electric power. High operating temperatures and good energy conversion efficiency are advantageous. However, the components tend to be more expensive than those for lower temperature concepts.

The collector subsystem is an array of large, bowl-like structures consisting of individual mirror panels attached to a criss-cross concrete frame. Steam is generated in the tracking receiver and exits at 510^{o}C (950^{o}F) and 10.0 MPa (1450 psi). The transport subsystem transports feedwater to the receiver and returns superheated steam to either the storage or the energy conversion subsystem. The energy storage subsystem stores the thermal energy in a mixed medium consisting of oil and rock. The thermal energy can be extracted to generate steam for the energy conversion subsystem. The energy conversion subsystem consists of a Rankine-cycle heat engine that uses water as a working fluid, and a dry cooling tower for rejecting waste heat to the atmosphere. The FMDF concept is illustrated schematically in Figure 4.14.

4.6.2 Collector Subsystem

The FMDF concentrator bowl is canted 15^{o} to the south, and is 200 ft in diameter. The generic plant, as developed by Texas Tech University and E-Systems, Inc., includes a number of these distributed bowls (Texas Tech and E-Systems 1977, 1978; Clements and Reichert 1979; Clausing 1976).

The receiver is a tube-wound cylinder moved by a boom/crane assembly that keeps the receiver in the moving focal region of the bowl during all daylight hours. The Inconel® 617 tubing with selective absorptive coating forms an open

® Brand name for nickel chromium alloys manufactured by Huntington Alloys, Inc., Huntington, West Virginia.

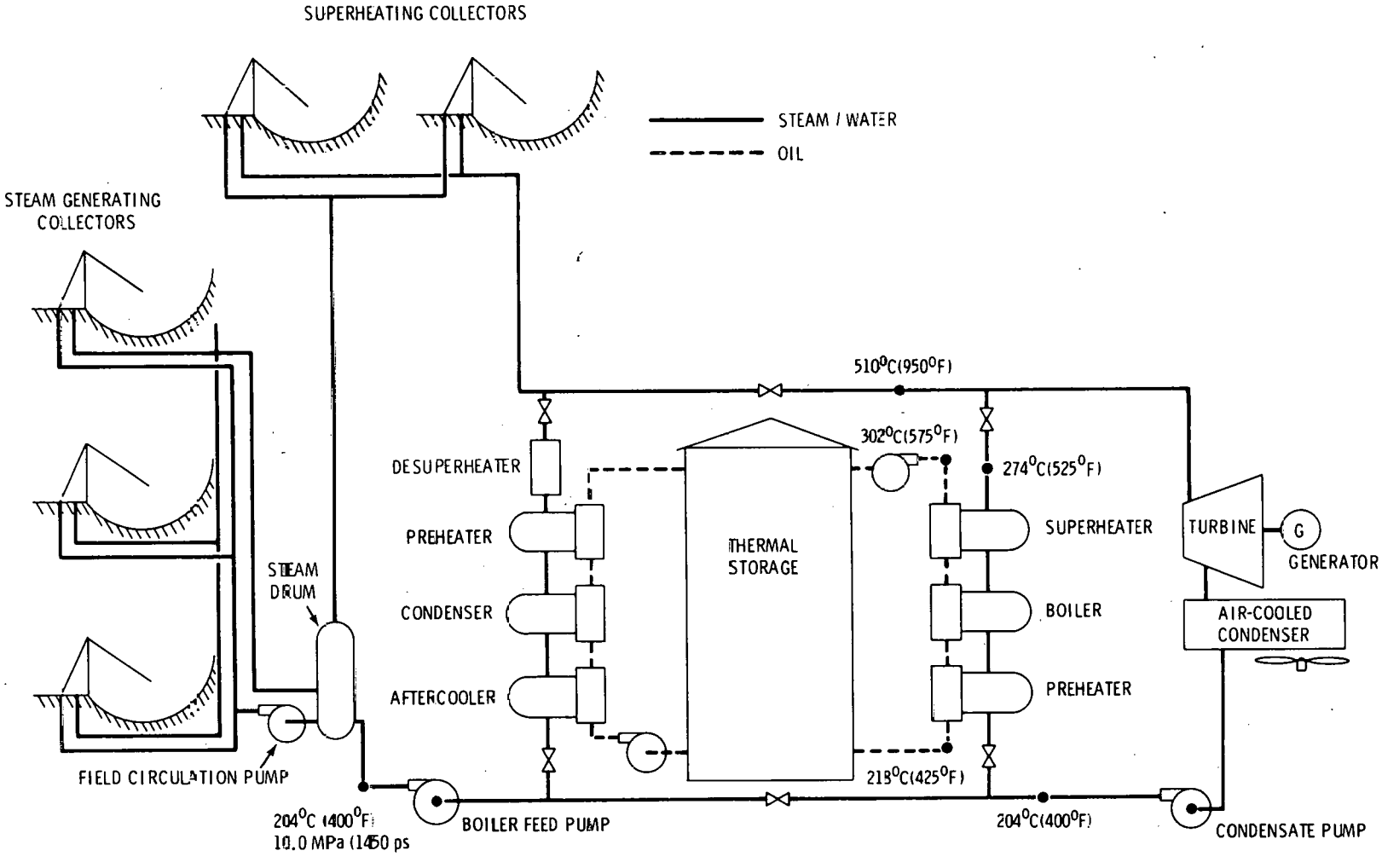

FIGURE 4.14. Fixed Mirror Distributed Focus Concept Schematic

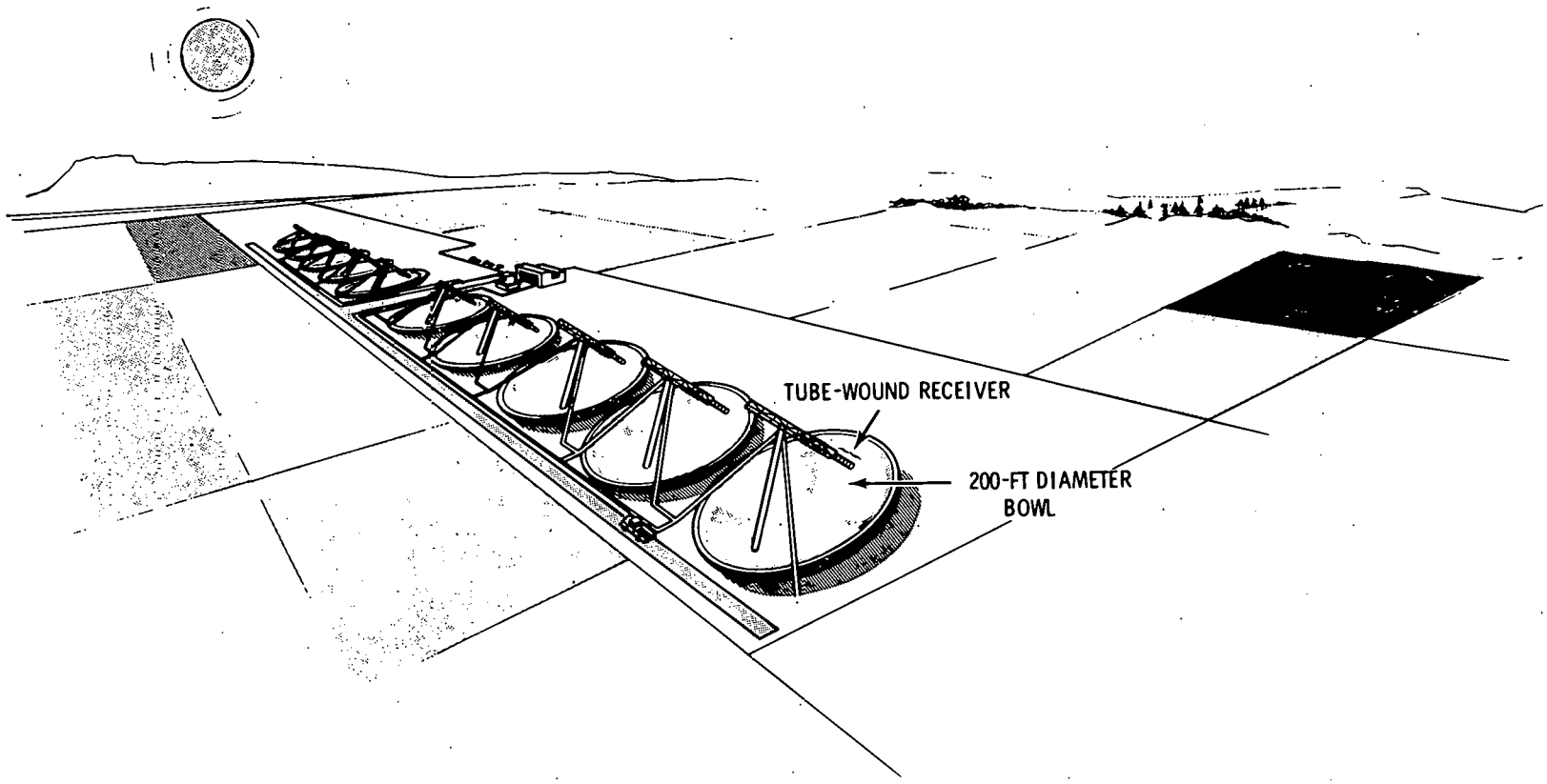

FIGURE 4.15. Fixed Mirror Distributed Focus Concept

receiver. An artist's conception of the combined concentrator/receiver system in operation is shown in Figure 4.15.

4.6.3 Transport Subsystem

The FMDF transport subsystem transports feedwater from the energy conversion subsystem to the collector array and returns superheated steam to either the energy conversion or energy storage subsystem. The FMDF transport subsystem appears to be a major component of the concept's capital cost.

Several types of thermal energy transport subsystems were considered for application with the FMDF. The steam/water transport system was chosen for the base case arrangement because of component availability and extensive industrial experience with transporting steam and water. The steam/water transport subsystem will be discussed here. Alternative transport subsystems will be discussed in Section 4.6.6.

The transport subsystem takes feedwater from the Rankine-cycle energy conversion subsystem and transports it through the supply piping to the collector array. The collector field is divided into steam generating and superheating collectors. The feedwater is supplied to the steam generation collectors through which the water is circulated, producing a steam/water mixture. The steam is separated and transported to the superheating collectors. The water is recirculated through the steam generating collector. Saturated steam from the steam generating collector is superheated in the superheating collectors and returned to the central generating facility. Steam returning from the field is at 510^{o}C (950^{o}F) and 10.0 MPa (1450 psi).

The individual collectors are arranged in modules to form the collector field. Each module consists of five steam generating collectors and two superheating collectors. The transport subsystem can be divided into module supply piping, return piping, and internal piping. Module internal piping is shown in Figure 4.16. Isolation valves are included to allow for individual collector maintenance. Expansion loops and flexible couplings are included to permit thermal expansion. A typical collector field for a 5-MWe plant is shown in Figure 4.17.

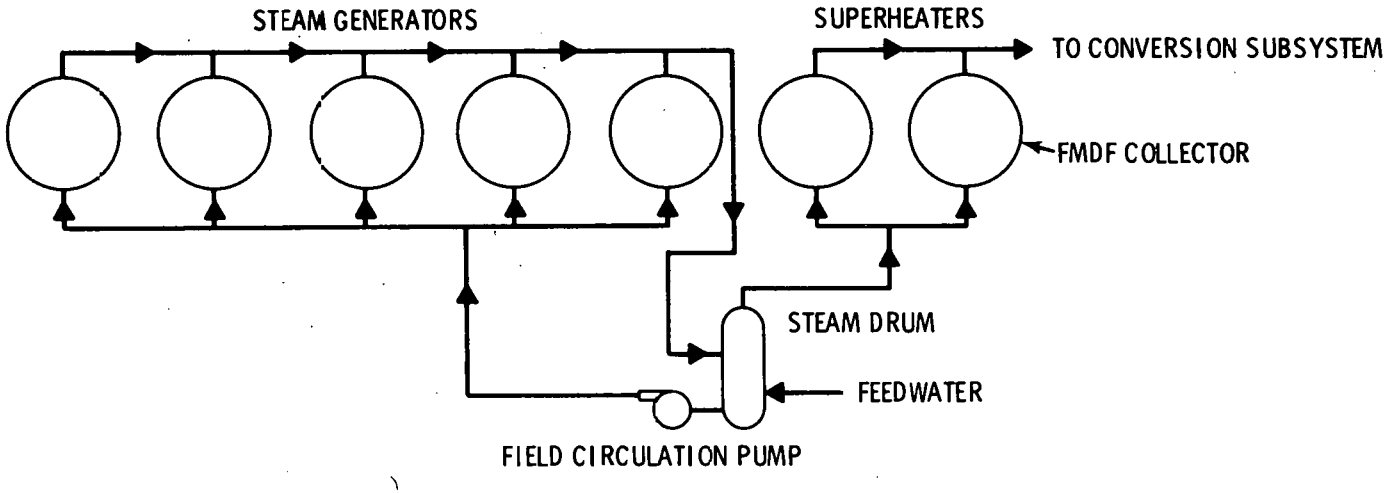

FIGURE 4.16. Transport Subsystem Piping for the Fixed Mirror Distributed Focus Concept

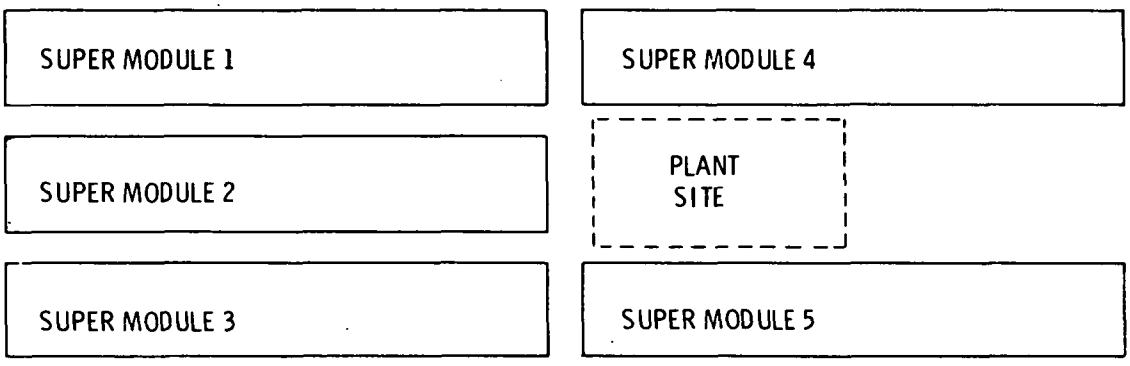

FIGURE 4.17. Typical Collector Field Layout, Fixed Mirror Distributed Focus Concept

In all cases, the piping is Schedule 160 carbon steel or low alloy steel with calcium silicate insulation. Module supply, return, and internal piping is welded and buried. The feed pumps and field circulation pumps are carbon steel centrifugal pumps driven by electric motors. All valves are assumed to be carbon steel gate valves of the appropriate pressure rating.

4.6.4 Storage Subsystem

Thermal energy collected in the collector field can be stored for use during the night or periods of low insolation. The thermal energy is stored as sensible heat in the energy storage subsystem. Several types of thermal energy storage subsystems were considered for the FMDF. The intermediate-temperature oil and rock subsystem was chosen for the base case because it is the closest to commercial availability. This subsystem will be described here. Storage subsystem alternatives will be discussed in Section 4.6.6.

The storage medium, storage medium containment, charging heat exchangers, charging pump, discharge heat exchangers, discharge pump, and piping compose the thermal energy storage subsystem. The arrangement is similar to that proposed by McDonnell Douglas for the Barstow Power Plant.

Thermal energy is stored as sensible heat in an oil and rock medium. The tank containing the medium is arranged so that a thermocline is maintained between the tank's hot and cool regions. Caloria HT45 was selected as the heat transfer oil; river sand and pebbles were chosen as the rock component of

the heat transfer medium. Because Caloria HT45 decomposes at temperatures above 304°C (580°F), maximum storage temperatures cannot exceed this level.

During periods of high insolation, the thermal storage subsystem is charged by extracting steam returning from the collector subsystem. The steam is used to heat oil in the thermal storage charging loop, but it is desuperheated to prevent excessive temperatures in the thermal storage unit. The charging loop consists of charging oil pumps, charging piping, charging heat exchangers, and appropriate controls.

During discharge, the thermal storage unit provides heat to generate steam in the energy conversion subsystem. Steam is generated in the thermal storage discharge loop, which consists of discharge oil pump, discharge piping, discharge heat exchangers, and appropriate controls.

Two additional components in this subsystem remove the residue of any heat transfer oil thermal degradation. The fluid maintenance system filters the oil to remove suspended solids, distills a side stream to remove high boiling polymeric compounds, and adds fresh makeup fluid to replace decomposed fluid. The ullage maintenance unit maintains an oxygen-free gas above the heat transfer fluid. It must also remove the volatile fractions of the degradation products that evaporate into the ullage space above the heat transfer fluid.

The oil and rock medium is contained in one or more carbon steel tanks, depending on the size of the thermal storage subsystem. The tanks are insulated to reduce heat loss from storage. Appropriate foundations and miscellaneous equipment are included. All piping is Schedule 40 carbon steel with calcium silicate insulation. All pumps are carbon steel centrifugal pumps with electric motor drives.

4.6.5 Energy Conversion Subsystem

The energy conversion subsystem takes thermal energy, supplied from either the field or storage, and converts it to electrical energy. This system includes the Rankine-cycle heat engine, generator, and an air-cooled condenser.

The Rankine-cycle heat engine is a conventional steam power cycle, based on performance and cost information provided by a consultant. Accessories

include three feedwater heaters, feedwater booster pump, feedwater pump, lubrication system, steam seal system, and controls.

The generator is a three-phase, four-pole synchronous unit. The generator is driven by the turbine through a double helical spur gear reduction unit. The air-cooled generator is equipped with a brushless exciter.

The waste heat from the Rankine cycle is rejected to the atmosphere in an air-cooled condenser. Exhaust steam from the turbine is ducted to the condenser where it is condensed in steam/air heat exchangers arranged in modules, each with a fan to force air past the heat transfer surfaces. Accessories include condensate pumps, piping, mechanical vacuum pump, and auxiliary equipment.

4.6.6 Alternative Concept Arrangements

After the base case FMDF concept arrangement was defined and analyzed, other components were considered for the same reasons as those alternatives assesed for the previously described concepts.

Four components were examined: an intermediate-temperature HITEC transport subsystem, an intermediate-temperature HITEC storage subsystem, an intermediate-temperature draw salt transport subsystem, and an intermediate-temperature draw salt storage subsystem. These components were combined with the base case FMDF concept to create two alternatives.

4.6.6.1 FMDF Intermediate-Temperature HITEC Arrangement

The base case water/steam transport subsystem is replaced in this arrangement with an intermediate-temperature HITEC transport subsystem. The base case oil/rock storage subsystem is replaced with an intermediate-temperature HITEC storage subsystem. The HITEC is used to generate steam in heat exchangers for use in the energy conversion subsystem.

HITEC is heated in the receiver to 454^{o}C (850^{o}F) and transported to the energy conversion or energy storage subsystem. The HITEC transport subsystem consists of supply piping, return piping, field circulation pump, and freeze protection equipment. Carbon steel piping can be used because the maximum HITEC temperature is below 454^{o}C (850^{o}F).

The storage subsystem stores thermal energy in a combination of molten salt and rock. The subsystem consists of the storage medium, medium containment, discharge loop, and medium treatment and makeup systems. A charging loop is not required because the same fluid is used for transport and storage. Thermal energy is discharged to the energy conversion subsystem in the discharge loop. The discharge loop consists of piping, HITEC pumps, heat exchangers, and miscellaneous equipment. Steam is generated at 427°C (800°F) and 10 MPa (1450 psi), regardless of whether energy is supplied from the field or from storage. Therefore, a single-admission turbine is used in the Rankine cycle.

4.6.6.2 FMDF Intermediate-Temperature Draw Salt Arrangement

This arrangement is the same as the HITEC arrangement just described except that the HITEC has been replaced by draw salt, a less expensive molten salt. Draw salt freezes at a higher temperature than HITEC and the materials compatability has not been completely demonstrated. However, draw salt may have the potential for reducing storage and transport cost.

4.7 LINE FOCUS CENTRAL RECEIVER/RANKINE CYCLE

The LFCR concept, which includes a line focus central receiver and a Rankine-cycle heat engine, is discussed in this section.

4.7.1 General Arrangement

The Line Focus Central Receiver is a one-axis tracking collector capable of generating high operating temperatures. These high temperatures are used to generate steam for use in a Rankine-cycle energy conversion subsystem. The LFCR concept has the advantage of high operating temperatures and good energy conversion efficiency. However, the receiver component tends to be more expensive than the same component for lower temperature concepts.

The collector subsystem consists of an array of rectangular single-axis heliostats that focus incident solar radiation onto an elevated line central receiver. The cavity-type line receiver is tower-mounted and generates steam with exit conditions of 510°C (950°F) and 10.0 MPa (1450 psi). The steam is transported to a central generation facility by the transport subsystem.

The steam can be either used in the energy conversion subsystem or stored in the storage subsystem. The storage subsystem stores thermal energy in a mixed medium consisting of oil and rock. The thermal energy can be extracted to generate steam for the energy conversion subsystem, consisting of a steam Rankine-cycle heat engine and a dry cooling tower for waste heat rejection to the atmosphere. Figure 4.18 presents a schematic of the LFCR concept.

4.7.2 Collector Subsystem

The LFCR concentrators are large (18.29 m long, 3.05 m wide), rectangular single-axis tracking heliostats. They are arranged on an E-W orientation to the north of the central line receiver. The heliostats, which have adjustable focal lengths, are arranged in rows that increase in length as distance from the receiver increases. There are 27 rows for 10-MWe plants, 26 rows for 5-MWe plants, and 20 rows for 1-MWe plants. The rows farthest from the plant are longer than the receiver; these outer heliostats form an area known as the "butterfly." Optimization of the butterfly area size is critical to the overall plant optimization, as is the calculation of heliostat row N-S distance separation. These size and separation optimizations were conducted for each plant being evaluated (e.g., each separate plant size and storage rating).

The LFCR concept receiver is a linear cavity type, canted at a 45^{o} downward angle to the north. Its design, like that of the concentrator, was developed by the FMC Corporation (FMC 1976, 1977, 1978; FMC and Stanford Research Institute 1976, 1977, 1978). The receiver and concentrator systems are combined as shown in Figure 4.19.

4.7.3 Transport Subsystem

The LFCR transport subsystem transports feedwater from the central generating facility to the line receivers and returns superheated steam to either the energy conversion or the energy storage subsystem.

Several types of thermal energy transport subsystems were considered for application with the LFCR. The steam/water transport system was chosen for the base case arrangement because of component availability and extensive

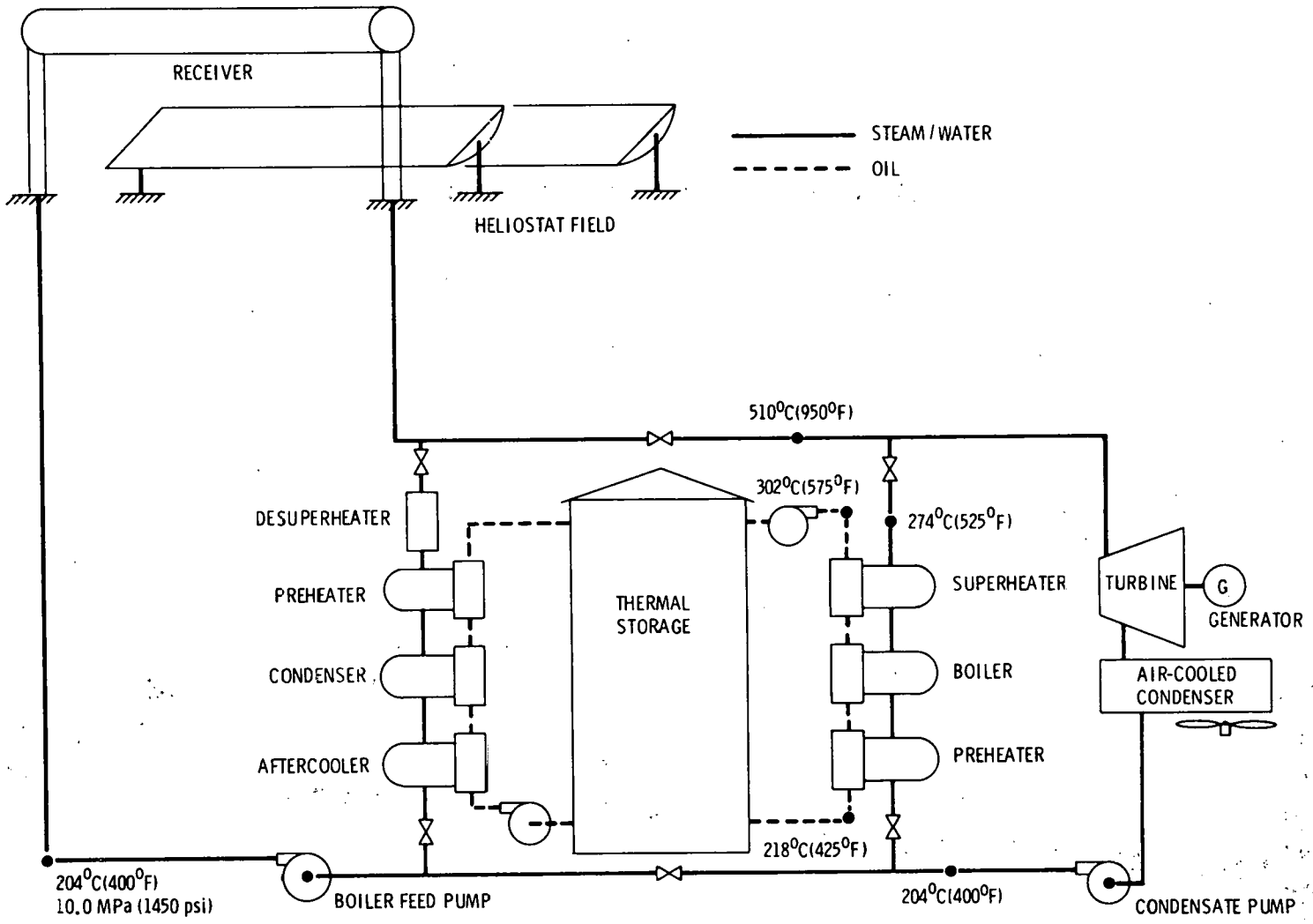

FIGURE 4.18. Line Focus Central Receiver Concept Schematic

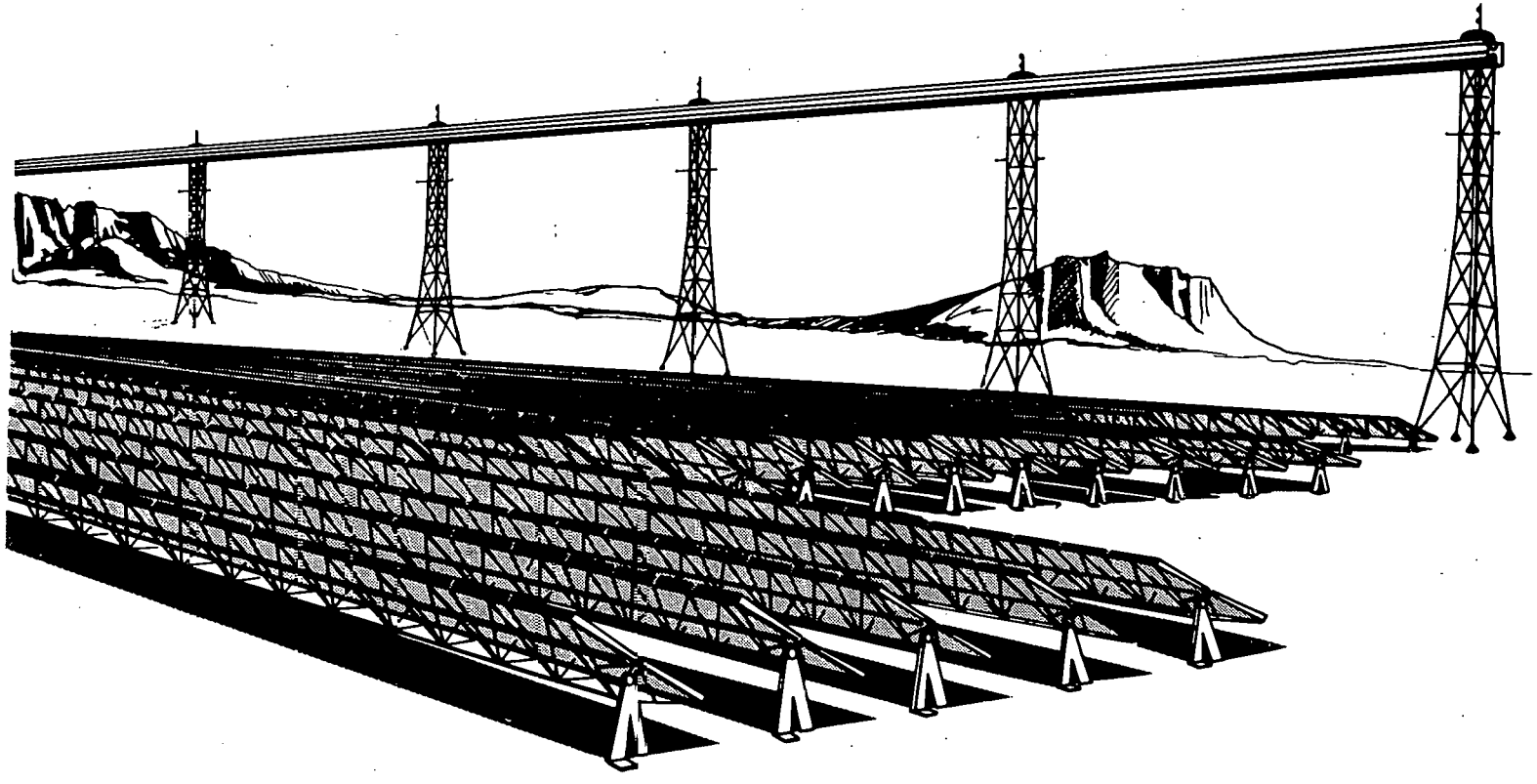

FIGURE 4.19. Line Focus Central Receiver

industrial experience with transporting steam and water. The steam/water transport subsystem will be discussed here. Other transport subsystems will be described in Section 4.7.6.

The transport subsystem transports feedwater from the Rankine-cycle energy conversion subsystem through the supply piping to the line receivers. Each receiver has steam generating and superheating sections internal to the receiver. Superheated steam leaves the receiver at 510°C (950°F) and 10.0 MPa (1450 psi).

The transport subsystem can be divided into supply and return piping. Isolation valves are included to allow for maintenance on individual receivers. Expansion loops and flexible couplings permit thermal expansion. A typical collector field for a 5-MWe plant is shown in Figure 4.20.

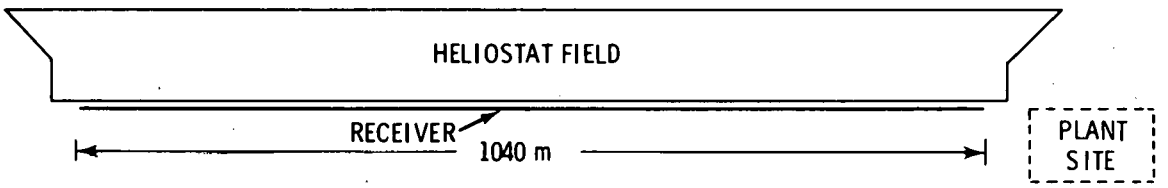

FIGURE 4.20. Typical Collector Field Layout, Line Focus Central Receiver Concept

In all cases, the piping is Schedule 160 carbon steel or low alloy steel with calcium silicate insulation. Module supply, return, and internal piping is welded and buried. The feed pump and field circulation pumps are carbon steel centrifugal pumps with electric motors for the driver. All valves are assumed to be carbon steel gate valves of appropriate pressure rating.

4.7.4 Storage Subsystem

Thermal energy collected in the collector field can be stored for use during the night or periods of low insolation. The thermal energy is stored as sensible heat in the energy storage subsystem. For the LFCR concept, several types of thermal energy storage subsystems were considered. The intermediate-temperature oil and rock subsystem was chosen for the base case because

it is the closest to commercial availability. The intermediate-temperature oil and rock subsystem will be described here. Alternative storage subsystems will be discussed in Section 4.7.6.

The thermal energy storage subsystem consists of the storage medium, storage medium containment, charging heat exchangers, charging pump, discharge heat exchangers, discharge pump, and piping. This subsystem is similar to that proposed by McDonnell Douglas for the Barstow Power Plant.

Thermal energy is stored as sensible heat in an oil and rock medium. The medium-containing tank is arranged so that a thermocline is maintained between the tank's hot and cool regions. Caloria HT45 was selected as the heat transfer oil; river sand and pebbles were chosen as the rock component. The maximum storage temperature cannot exceed 304°C (580°F) because Caloria HT45 will decompose above that level.

During periods of high insolation, the thermal storage subsystem is charged by extracting steam returning from the collector subsystem. The steam is used to heat oil in the thermal storage charging loop, but is desuperheated to prevent excessive temperatures in the thermal storage unit. The charging loop consists of charging oil pumps, charging piping, charging heat exchangers, and appropriate controls.

During discharge, the thermal storage unit provides heat to generate steam in the energy conversion subsystem. Steam is generated in the thermal storage discharge loop, which consists of a discharge oil pump, discharge piping, discharge heat exchangers, and appropriate controls.

Two additional components in the storage subsystem remove the residue of any heat transfer oil thermal degradation. The fluid maintenance system filters the oil to remove suspended solids, distills a side stream to remove high boiling polymeric compounds, and adds fresh makeup fluid to replace decomposed fluid. The ullage maintenance unit maintains an oxygen-free gas above the heat transfer fluid. This unit must also remove the volatile fractions of the degradation products that evaporate into the ullage space above the heat transfer fluid.

Depending on the size of the thermal storage subsystem, one or more carbon steel tanks contain the oil/rock medium. The tanks are insulated to reduce heat loss from storage. Appropriate foundations and miscellaneous equipment are included. All piping is Schedule 40 carbon steel with calcium silicate insulation. All pumps are carbon steel centrifugal pumps with electric motor drives.

4.7.5 Energy Conversion Subsystem

The energy conversion subsystem takes thermal energy, supplied from either the field or storage, and converts it to electrical energy. The energy conversion subsystem consists of the Rankine-cycle heat engine, generator and air-cooled condenser.

The Rankine-cycle heat engine is a conventional steam power cycle, based on performance and cost information provided by a consultant. Accessories include three feedwater heaters, feedwater booster pump, feedwater pump, lubrication system, steam seal system, and controls.

The generator is a three-phase, four-pole synchronous unit, driven by the turbine through a double helical spur gear reduction unit. The generator is air-cooled and equipped with a brushless exciter.

Waste heat from the Rankine cycle is rejected to the atmosphere in an air-cooled condenser. Exhaust steam from the turbine is ducted to the condenser where it is condensed in a steam/air heat exchanger. The steam/air heat exchangers are arranged in modules, each with a fan to force air past the heat transfer surfaces. Accessories include condensate pumps, piping, mechanical vacuum pump, and auxiliary equipment.

4.7.6 Alternative Concept Arrangements

After the base case concept arrangement was defined and analyzed, other components were considered to provide estimates of the future performance expected from the LFCR concept.

Four alternative components were considered: an intermediate-temperature HITEC transport subsystem, an intermediate-temperature HITEC storage subsystem, an intermediate-temperature draw salt transport subsystem, and an

intermediate-temperature draw salt storage subsystem. These were combined with the base case LFCR concept to yield two alternative arrangements.

4.7.6.1 LFCR Intermediate-Temperature HITEC Arrangement

In this arrangement, the base case steam/water transport subsystem is replaced with an intermediate-temperature HITEC transport subsystem. The base case oil/rock storage subsystem is replaced with an intermediate-temperature HITEC storage subsystem. The HITEC is used to generate steam in heat exchangers for use in the energy conversion subsystem.

HITEC is heated in the receiver to 454°C (850°F) and transported to the energy conversion or energy storage subsystem by the HITEC transport subsystem. This system consists of supply piping, return piping, field circulation pump, and freeze protection equipment. Carbon steel piping can be used because the maximum HITEC temperature is below 454°C (850°F).

The storage subsystem stores thermal energy in a combination of molten salt and rock. The subsystem consists of the storage medium, medium containment, discharge loop, and medium treatment and makeup systems. A charging loop is not required because the same fluid is used for transport and storage. Thermal energy is discharged to the energy conversion subsystem in the discharge loop. The discharge loop consists of piping, HITEC pumps, heat exchangers, and miscellaneous equipment. Steam is generated at 427°C (800°F) and 10 MPa (1450 psi) regardless of whether energy is supplied from the field or from storage; therefore, a single-admission turbine is used in the Rankine cycle.

4.7.6.2 LFCR Intermediate-Temperature Draw Salt Arrangement

This arrangement is the same as the HITEC arrangement just described, except that the HITEC is replaced by draw salt, a less expensive molten salt. Draw salt freezes at a higher temperature than HITEC and the materials compatibility has not been completely demonstrated. However, draw salt may have the potential for reducing storage and transport cost.

4.8 LINE FOCUS DISTRIBUTED RECEIVER - TRACKING RECEIVER/RANKINE CYCLE

The LFDR-TR concept, which includes a line focus distributed receiver with a tracking receiver and a Rankine-cycle heat engine, is discussed in this section.

4.8.1 General Arrangement

The Line Focus Distributed Receiver - Tracking Receiver is a one-axis tracking collector. This concept includes a receiver of advanced design, allowing the receiver to operate at a high temperature without excessive losses. In the LFDR-TR concept, the collector is used to generate steam for a Rankine-cycle energy conversion subsystem, which, in turn produces electric power. The concept has the advantage of high operating temperatures, but the collector is expensive and has poor optical efficiency.

The collector subsystem consists of an array of fixed mirror concentrators, each with a receiver that moves in a circular arc to track the focal line. Steam is generated in the receiver and exits at 510°C (950°F) and 10.0 MPa (1450 psi). The transport subsystem transports feedwater to the receiver and returns superheated steam to either the storage or energy conversion subsystem. The energy storage subsystem stores the thermal energy in a mixed oil/rock medium. The thermal energy can be extracted to generate steam for the energy conversion subsystem. The energy conversion subsystem consists of a Rankine-cycle heat engine, which uses water as a working fluid, and a dry cooling tower for rejecting waste heat to the atmosphere. The LFDR-TR concept is diagrammed schematically in Figure 4.21.

4.8.2 Collector Subsystem

The concentrator is a fixed mirror, slatted trough that produces a line focus regardless of the sun's position. This design consists of a concave array of long, narrow, flat mirror facets fixed to a concrete support. The mirror strips are bonded to the concrete moldings. This concentrator design, including the receiver, is very similar to the General Atomic configuration (Russell et al. 1977; Schuster et al. 1978; General Atomic 1979).

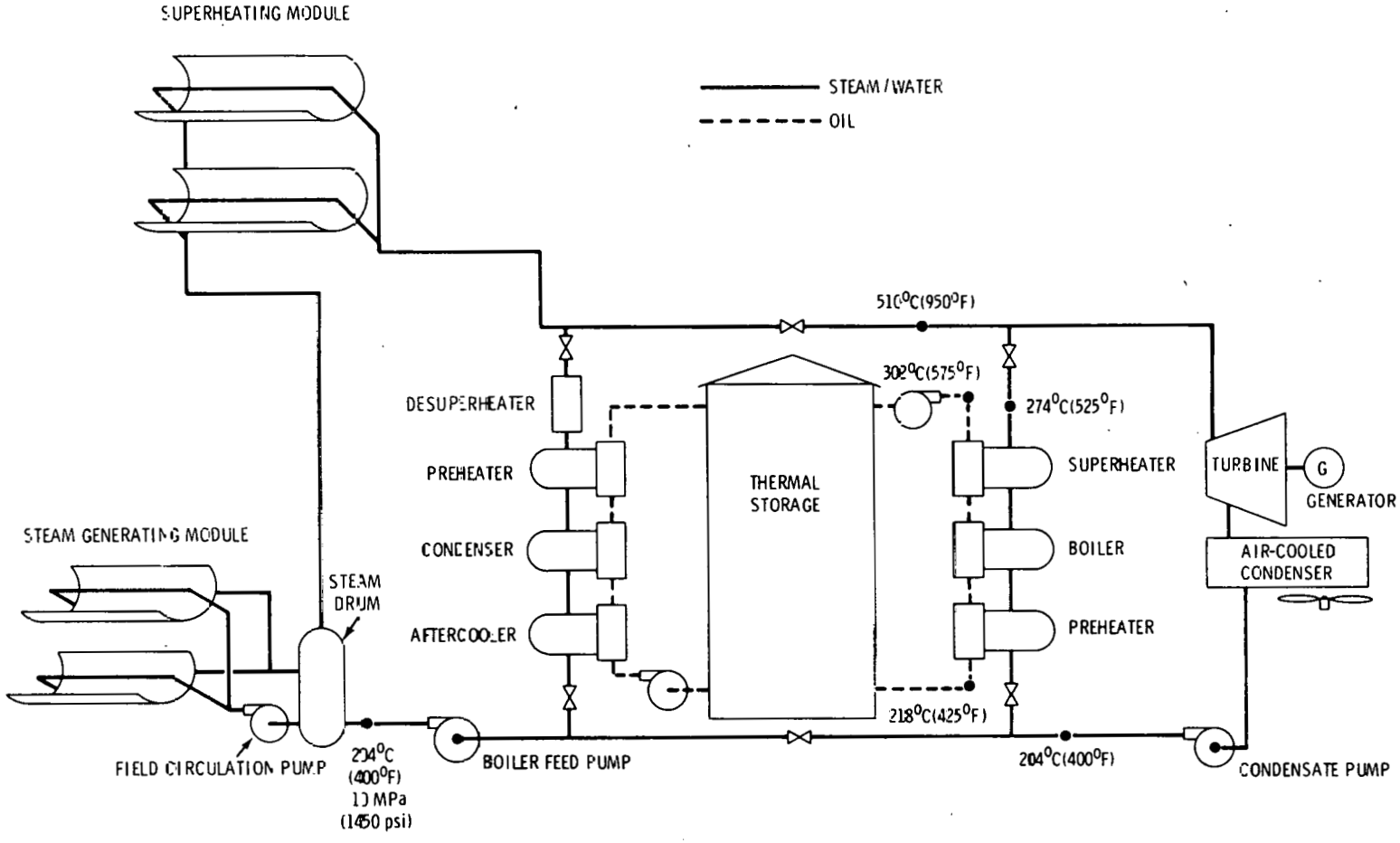

FIGURE 4.21. Line Focus Distributed Receiver - Tracking Receiver Concept Schematic

The receiver design, shown in Figure 4.22, is the moving mechanism of the LFDR-TR. It is moved in a circular arc to track the focal line. When this receiver and concentrator are combined, the resultant configuration is like that shown in Figure 4.23.

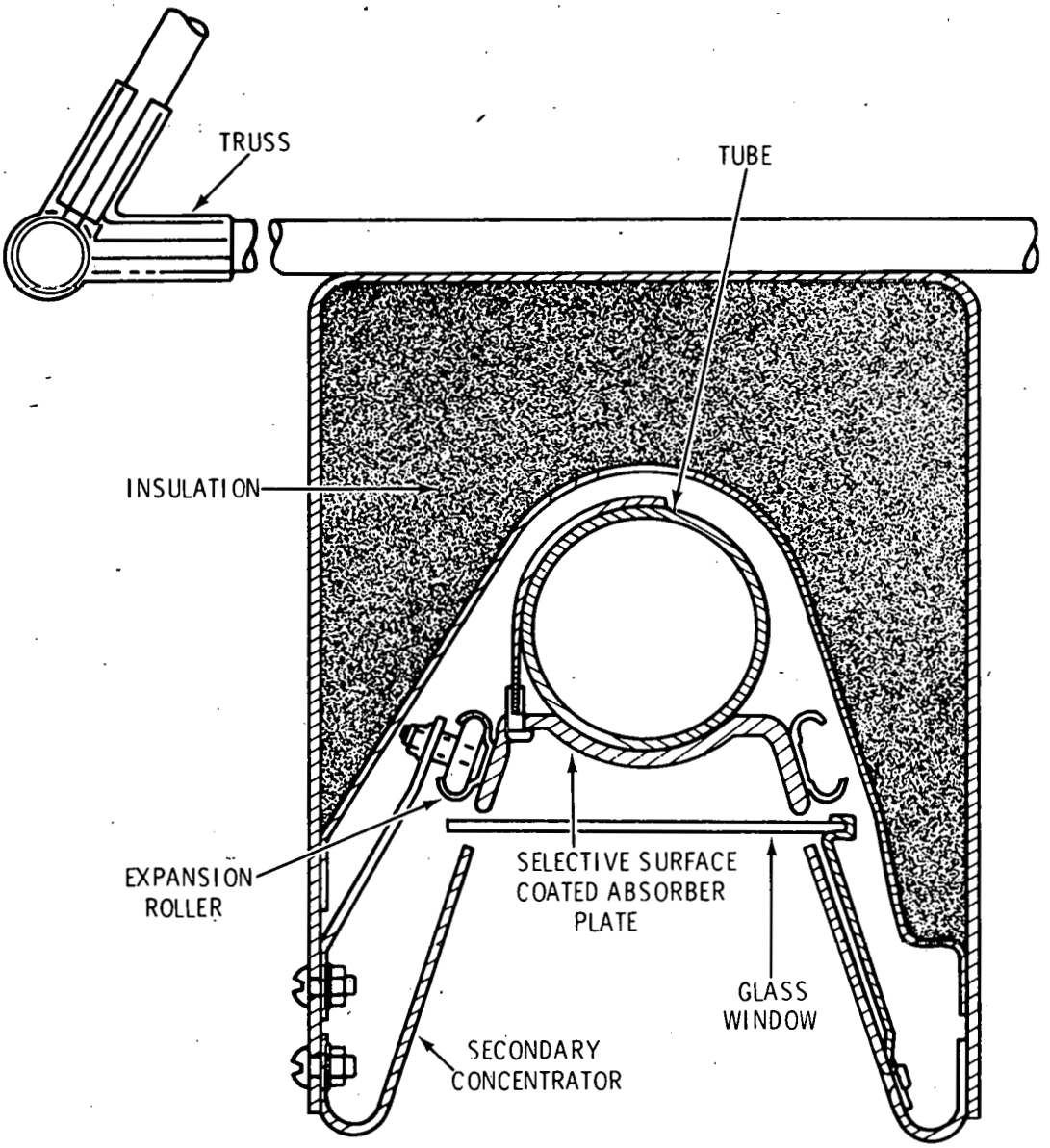

FIGURE 4.22 Receiver Design for the Line Focus Distributed Receiver - Tracking Receiver Concept

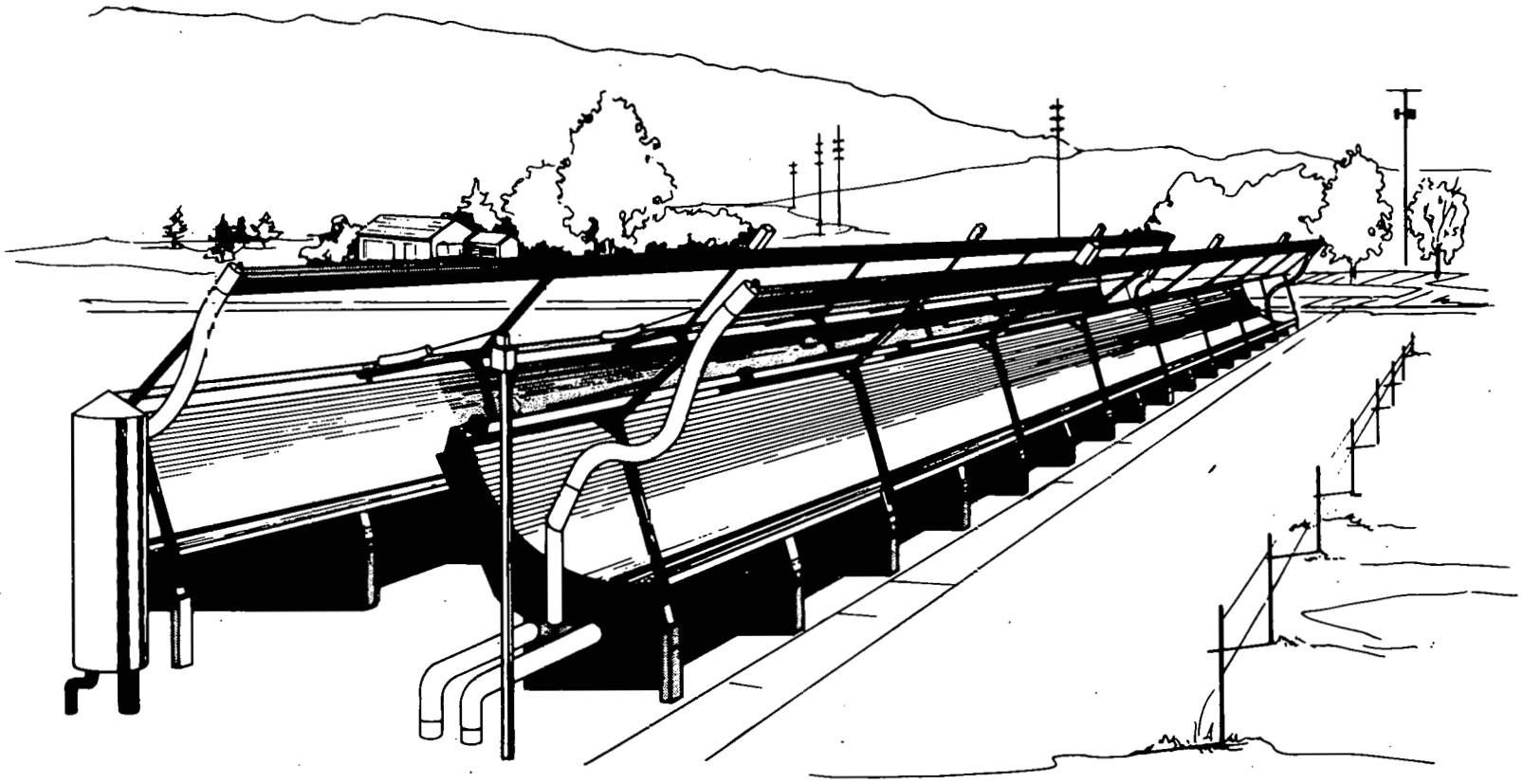

FIGURE 4.23. Line Focus Distributed Receiver - Tracking Receiver Concept

4.8.3 Transport Subsystem

The LFDR-TR transport subsystem transports feedwater from the energy conversion subsystem to the collector array and returns superheated steam to either the energy conversion or energy storage subsystem. The LFDR-TR transport subsystem is quite extensive and is a major component of the capital cost.

Several types of thermal energy transport subsystems were considered for application with the LFDR-TR. The steam/water transport subsystem was chosen for the base case arrangement because of component availability and extensive industrial experience with transporting steam and water. The steam/water transport subsystem will be discussed here. Alternative transport subsystems will be discussed in Section 4.8.6.

The transport subsystem transports feedwater from the Rankine-cycle energy conversion subsystem through the supply piping to the collector array. The collector field is divided into steam generation and superheating modules. The feedwater is supplied to the steam generation module where it is circulated through the collectors, producing a steam/water mixture. The steam is separated and transported to the superheating module; the water is recirculated through the steam generating module. Saturated steam from the steam generating module is superheated in the superheater module and returned to the central generating facility. Steam returning from the field is at 510^{o}C (950^{o}F) and 10.0 MPa (1450 psi).

The individual collectors are arranged in modules, which are, in turn, arranged to form the collector field. Each steam generating module has forty-five parallel 200-m flow paths. Each superheating module has twenty-four parallel flow paths, each 150 m long. The transport subsystem can be divided into module supply, return, and internal piping. Module internal piping for a steam generating module is shown in Figure 4.24. Isolation values are included to allow maintenance on individual flow paths. Expansion loops and flexible couplings provide for thermal expansion.

A typical collector field showing module supply and return piping is illustrated in Figure 4.25. This arrangement for a 5-MWe plant places the superheating modules closest to the central generating facility.

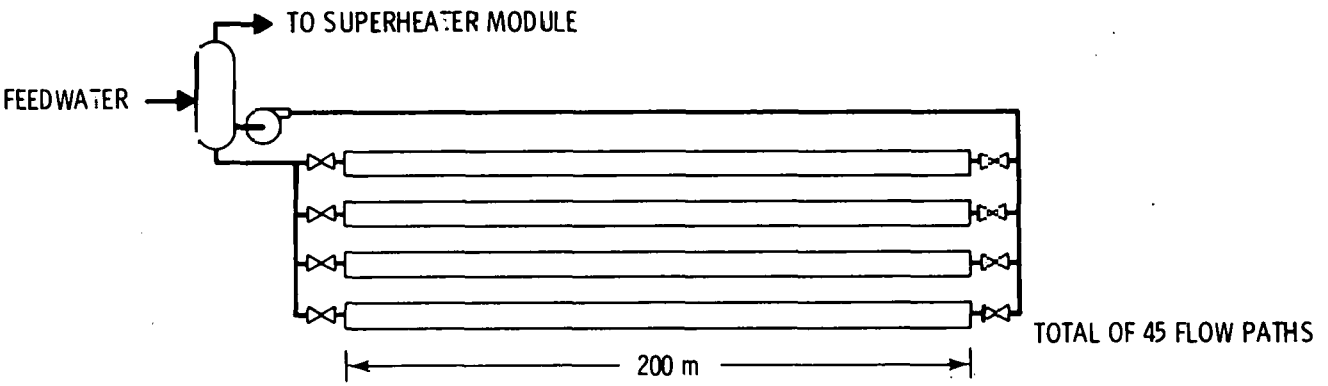

FIGURE 4.24. Steam Generator Module Piping for the Line Focus Distributed Receiver - Tracking Receiver Concept

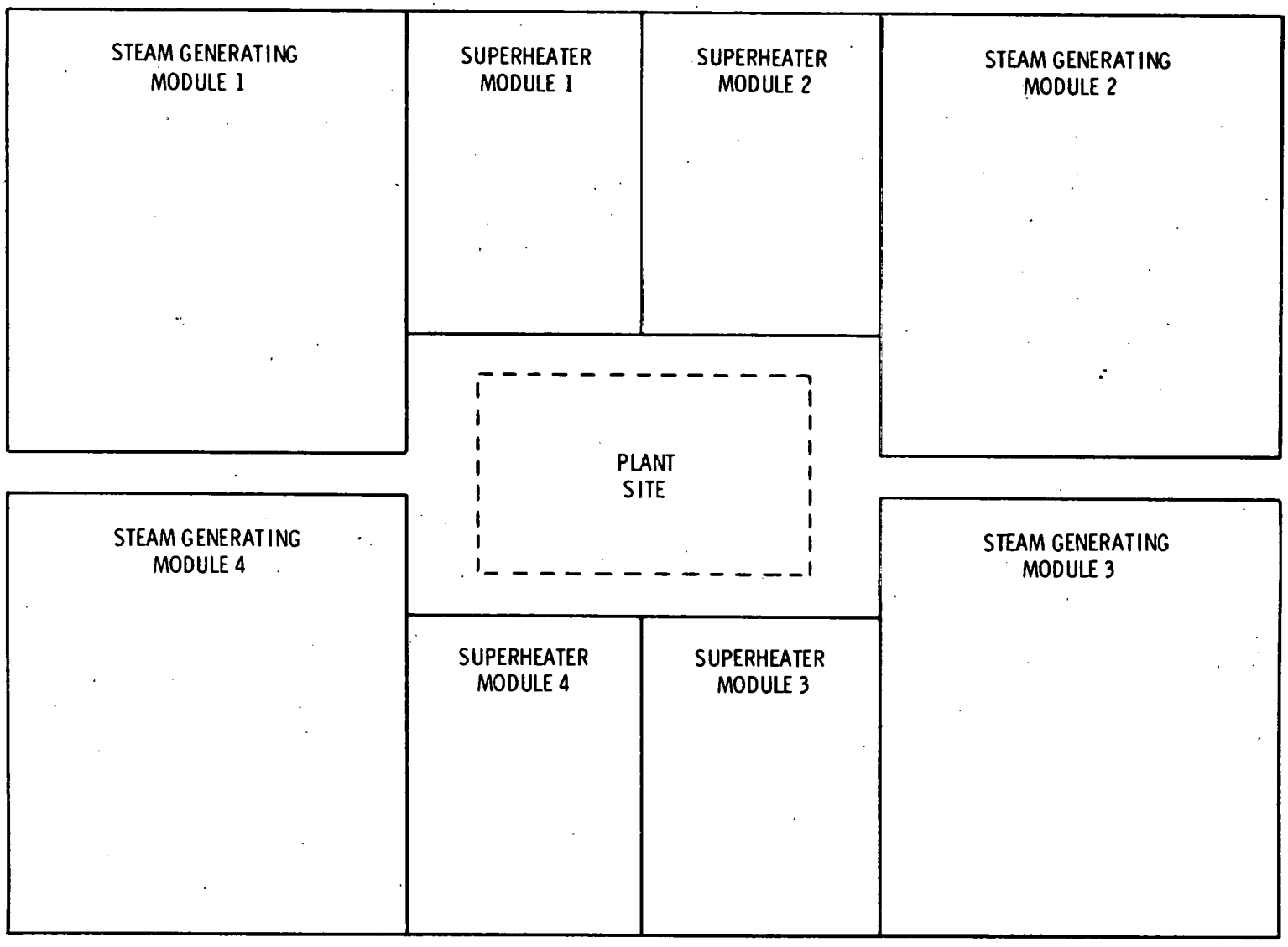

FIGURE 4.25. Typical Collector Field Layout, Line Focus Distributed Receiver - Tracking Receiver Concept

In all cases, the piping is Schedule 160 carbon steel or low alloy steel with calcium silicate insulation. Module supply, return and internal piping is welded and buried. The feed pump and field circulation pumps are carbon steel centrifugal pumps with electric motor drives. All valves are assumed to be carbon steel gate valves of the appropriate pressure rating.

4.8.4 Storage Subsystem

Thermal energy collected in the collector field can be stored for use during the night or periods of low insolation. The thermal energy is stored as sensible heat in the energy storage subsystem. Several types of thermal energy storage subsystems were considered for the LFDR-TR concept. The intermediate-temperature oil and rock subsystem was chosen for the base case because it is the closest to commercial availability. This storage subsystem will be described here. The two alternative subsystems will be discussed in Section 4.8.6.

The thermal energy storage subsystem consists of the storage medium, storage medium containment, charging heat exchangers, charging pump, discharge heat exchangers, discharge pump, and piping. The thermal energy storage subsystem is similar to that proposed by McDonnell Douglas for the Barstow Power Plant.

Thermal energy is stored as sensible heat in an oil and rock medium. The medium is contained in a tank arranged to maintain a thermocline between the hot and cool regions of the tank. Caloria HT45 was selected as the heat transfer oil; river sand and pebbles were chosen as the rock component of the heat transfer medium. Caloria HT45 cannot be used successfully above 304^{o}C (580^{o}F) due to thermal decomposition of the oil; therefore, the maximum storage temperature must be kept below 304^{o}C (580^{o}F).

During periods of high insolation, the thermal storage subsystem is charged by extracting steam returning from the collector subsystem. The steam is used to heat oil in the thermal storage charging loop, but is desuperheated to prevent excessive temperatures in the thermal storage unit. The charging loop consists of charging oil pumps, charging piping, charging heat exchangers, and appropriate controls.

During discharge, the thermal storage unit provides heat to generate steam in the energy conversion subsystem. Steam is generated in the thermal storage discharge loop, which consists of a discharge oil pump, discharge piping, discharge heat exchangers, and appropriate controls.

The storage subsystem has two additional components. These remove the residue of any thermal degradation of the heat transfer oil. The fluid maintenance system filters the oil to remove suspended solids, distills a side stream to remove high boiling polymeric compounds, and adds fresh makeup fluid to replace decomposed fluid. In addition to maintaining an oxygen-free gas above the heat transfer fluid, the ullage maintenance unit must also remove the volatile fractions of the degradation products that evaporate into the ullage space above the heat transfer fluid.

The oil/rock medium is contained in one or more carbon steel tanks, depending on the size of the thermal storage subsystem. The tanks are insulated to reduce heat loss from storage. Appropriate foundations and miscellaneous equipment are included. All piping is Schedule 40 carbon steel with calcium silicate insulation. All pumps are carbon steel centrifugal pumps with electric motor drives.

4.8.5 Energy Conversion Subsystem

The energy conversion subsystem takes thermal energy, supplied from either the field or storage, and converts it to electrical energy. The energy conversion subsystem consists of the Rankine-cycle heat engine, generator, and air-cooled condenser.

The Rankine-cycle heat engine is a conventional steam power cycle, based on performance and cost information provided by a consultant for a representative Rankine-cycle engine steam power cycle. Accessories include three feedwater heaters, feedwater booster pump, feedwater pump, lubrication system, steam seal system, and controls.

The generator is a three-phase, four-pole synchronous unit, driven by the turbine through a double helical spur gear reduction unit. The air-cooled generator is equipped with a brushless exciter.

The waste heat from the Rankine cycle is rejected to the atmosphere in an air-cooled condenser. Exhaust steam from the turbine is ducted to the condenser where it is condensed in a steam/air heat exchanger. The steam/air heat exchangers are arranged in modules, each with a fan to force air past the heat transfer surfaces. Accessories include condensate pumps, piping, mechanical pump, and auxiliary equipment.

4.8.6 Alternative Concept Arrangements

After the base case LFDR-TR concept arrangement was defined and analyzed, other components were considered. These alternatives had the potential to either reduce cost or improve performance, and were considered to estimate the future performance of the LFDR-TR concept using currently projected technology.

Four alternatives were considered: an intermediate-temperature HITEC transport subsystem, an intermediate-temperature HITEC storage subsystem, an intermediate-temperature draw salt transport subsystem, and an intermediate-temperature draw salt storage subsystem. These components were combined with the base case LFDR-TR to create two additional arrangements.

4.8.6.1 LFDR-TR Intermediate-Temperature HITEC Arrangement

In this arrangement, the base case steam/water transport subsystem is replaced with an intermediate-temperature HITEC transport subsystem. The base case oil/rock storage subsystem is replaced with an intermediate-temperature HITEC storage subsystem. The HITEC is used to generate steam in heat exchangers for use in the energy conversion subsystem.

HITEC is heated in the receiver to 454^{o}C (850^{o}F) and transported to the energy conversion or energy storage subsystem by the HITEC transport subsystem. This system consists of supply piping, return piping, field circulation pump, and freeze protection equipment. Because the maximum HITEC temperature is below 454^{o}C (850^{o}F), carbon steel piping can be used.

The storage subsystem stores thermal energy in a combination of molten salt and rock. The subsystem consists of the storage medium, medium containment, discharge loop, and medium treatment and makeup systems. A charging loop is not required because the same fluid is used for transport and storage.

Thermal energy is discharged to the energy conversion subsystem in the discharge loop. The discharge loop consists of piping, HITEC pumps, heat exchangers, and miscellaneous equipment. Steam is generated at 427°C (800°F) and 10 MPa (1450 psi) regardless of whether energy is supplied from the field or from storage; therefore, a single-admission turbine is used in the Rankine cycle.

4.8.6.2 LFDR-TR Intermediate-Temperature Draw Salt Arrangement

This arrangement is the same as the HITEC arrangement just discussed, except that draw salt (a less expensive molten salt) is used instead of HITEC. Draw salt freezes at a higher temperature than HITEC and the materials compatibility has not been completely demonstrated. However, draw salt may have the potential for reducing storage and transport cost.

4.9 LINE FOCUS DISTRIBUTED RECEIVER - TRACKING COLLECTOR/RANKINE CYCLE

The LFDR-TC concept, which includes a line focus distributed receiver with a tracking collector and a Rankine-cycle heat engine, is discussed in this section.

4.9.1 General Arrangement

The Line Focus Distributed Receiver - Tracking Collector is a one-axis tracking concept that can generate intermediate operating temperatures. In the LFDR-TC concept, the collector is used to generate steam for a Rankine-cycle energy conversion subsystem, which, in turn, produces electric power. The concept has the advantage of inexpensive components; however, the lower operating temperature causes a reduction in the energy conversion efficiency when compared to higher temperature concepts.

The collector subsystem consists of an array of single-curvature concentrators that focuses solar insolation on a fixed linear receiver. The concentrator is rotated around one axis to track the sun's diurnal motion. Steam is generated in the receiver and exits at 343°C (650°F) and 4.83 MPa (700 psi). The transport subsystem transports feedwater to the receiver and returns superheated steam to either storage or the energy conversion subsystem. The energy storage subsystem stores the thermal energy in a mixed oil and rock medium.

The thermal energy can be extracted to generate steam for the energy conversion subsystem. The energy conversion subsystem consists of a Rankine-cycle heat engine, which uses water as a working fluid, and a dry cooling tower for rejecting waste heat to the atmosphere. A schematic of the LFDR-TC concept appears in Figure 4.26.

4.9.2 Collector Subsystem

The LFDR-TC concentrator is a single-curvature design that focuses insolation onto a fixed linear receiver. The concentrator is rotated about one axis to track the sun's diurnal motion. The design selected for this evaluation closely models the Hexcel parabolic trough, chosen because that collector was the most efficient yet tested at the Sandia Collector Module Test Facility, effective March 1978 (Dudley and Workhoven 1978, p. 21). North-south, east-west, and polar orientations were evaluated.

The receiver used in this analysis was a modified version of the Hexcel design used with that concentrator subsystem. Figure 4.27 shows the receiver design. The concentrator and receiver subsystems are combined in forming the modular configuration shown in Figure 4.28.

4.9.3 Transport Subsystem

The LFDR-TC transport subsystem transports feedwater from the energy conversion subsystem to the collector array and returns superheated steam to either the energy conversion or energy storage subsystem. The LFDR-TC transport subsystem is quite extensive and is a major part of the concept's capital cost.

Several types of thermal energy transport subsystems were considered for application with the LFDR-TC. The steam/water transport subsystem was chosen for the base case arrangement because of component availability and extensive industrial experience with transporting steam and water. The steam/water transport subsystem will be discussed here. Alternative transport subsystems will be discussed in Section 4.9.6.

The transport subsystem takes feedwater from the Rankine-cycle energy conversion subsystem and transports it through the supply piping to the collector array. The collector field is divided into steam generation and

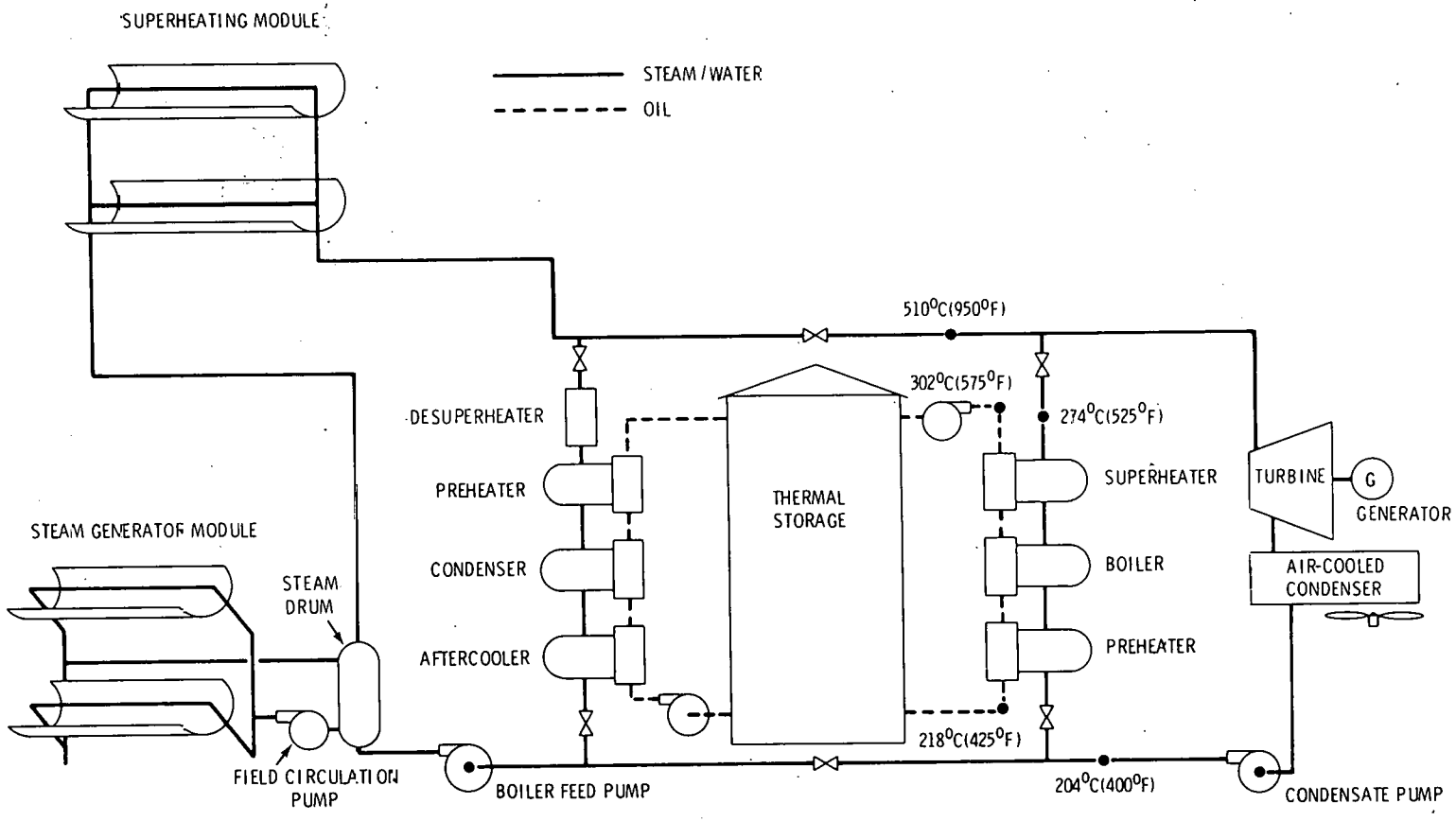

FIGURE 4.26. Line Focus Distributed Receiver - Tracking Collector Concept Schematic

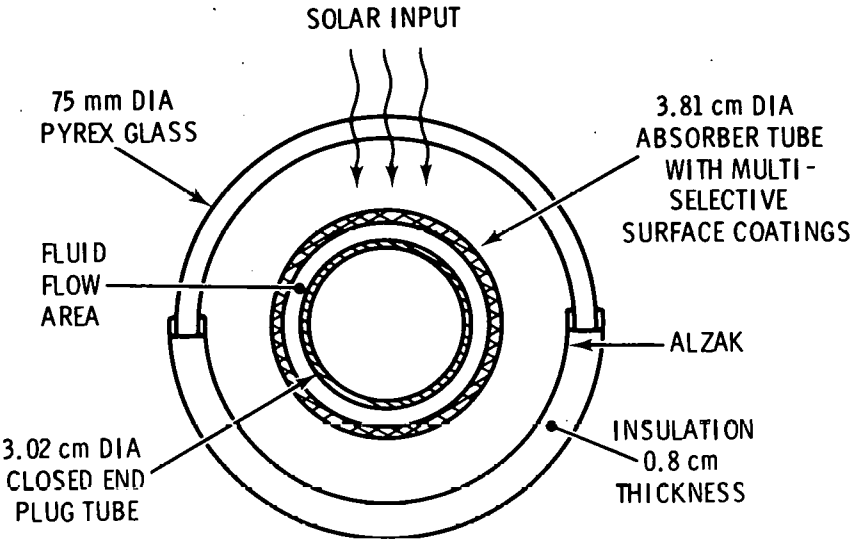

FIGURE 4.27. Receiver Assembly for the Line Focus Distributed Receiver - Tracking Collector Concept

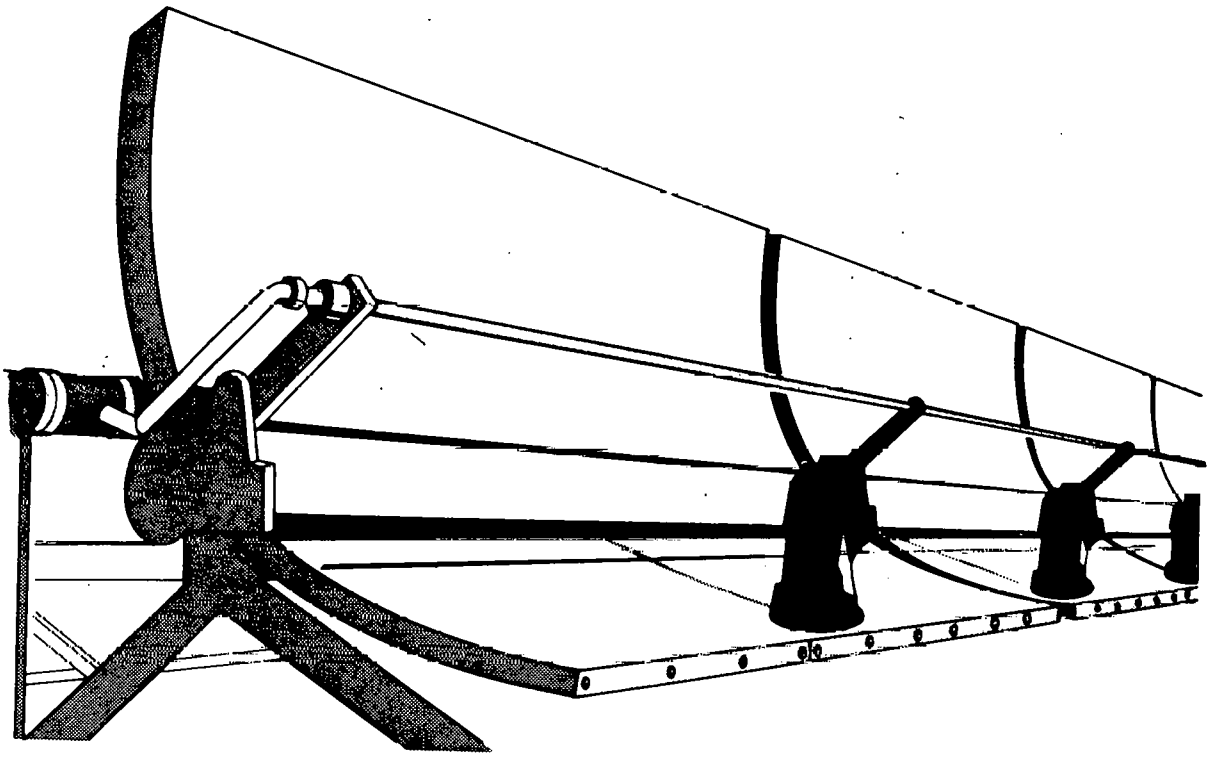

FIGURE 4.28. Line Focus Distributed Receiver - Tracking Collector Concept

superheating modules. The feedwater is supplied to the steam generation module where the water is circulated through the collectors, producing a steam/water mixture. The steam is separated and transported to the superheating module; the water is recirculated through the steam generating module. Saturated steam from the steam generating module is superheated in the superheater module and returned to the central generating facility. Steam returning from the field is at 343°C (650°F) and 4.83 MPa (700 psi).

The individual collectors are arranged in modules, which are, in turn arranged to form the collector field. Each steam generating module has forty parallel flow paths, each 190 m long. Each superheating module has fourteen parallel 90-m flow paths. The transport subsystem can be divided into module supply, return, and internal piping. Module piping and field layouts are similar to those discussed in Section 4.8.3 for the LFDR-TR concept. They are illustrated in Figures 4.29 and 4.30.

In all cases, the piping is Schedule 160 carbon steel or low alloy steel with calcium silicate insulation. Module supply, return, and internal piping is welded and buried. The feed pump and field circulation pumps are carbon steel centrifugal pumps with electric motor. All valves are assumed to be carbon steel gate valves of the appropriate pressure rating.

4.9.4 Storage Subsystem

Thermal energy collected in the collector field can be stored for use during the night or periods of low insolation. The thermal energy is stored as sensible heat in the energy storage subsystem. One type of thermal energy storage subsystem was considered for the LFDR-TC concept. The intermediate-temperature oil and rock subsystem was chosen for the base case because it is the closest to commercial availability; further, the high-temperature capabilities of other storage concepts were not required.

The thermal energy storage subsystem consists of the storage medium, storage medium containment, charging heat exchangers, charging pump, discharge heat exchangers, discharge pump, and piping. The thermal energy storage subsystem is similar to that proposed by McDonnell Douglas for the Barstow Power Plant.

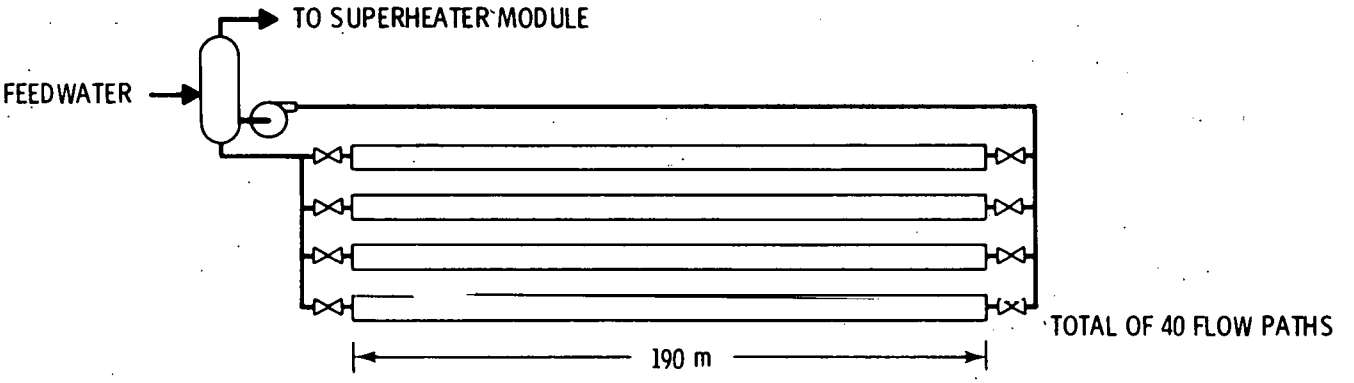

FIGURE 4.29. Steam Generator Module Piping for the Line Focus Distributed Receiver - Tracking Collector Concept

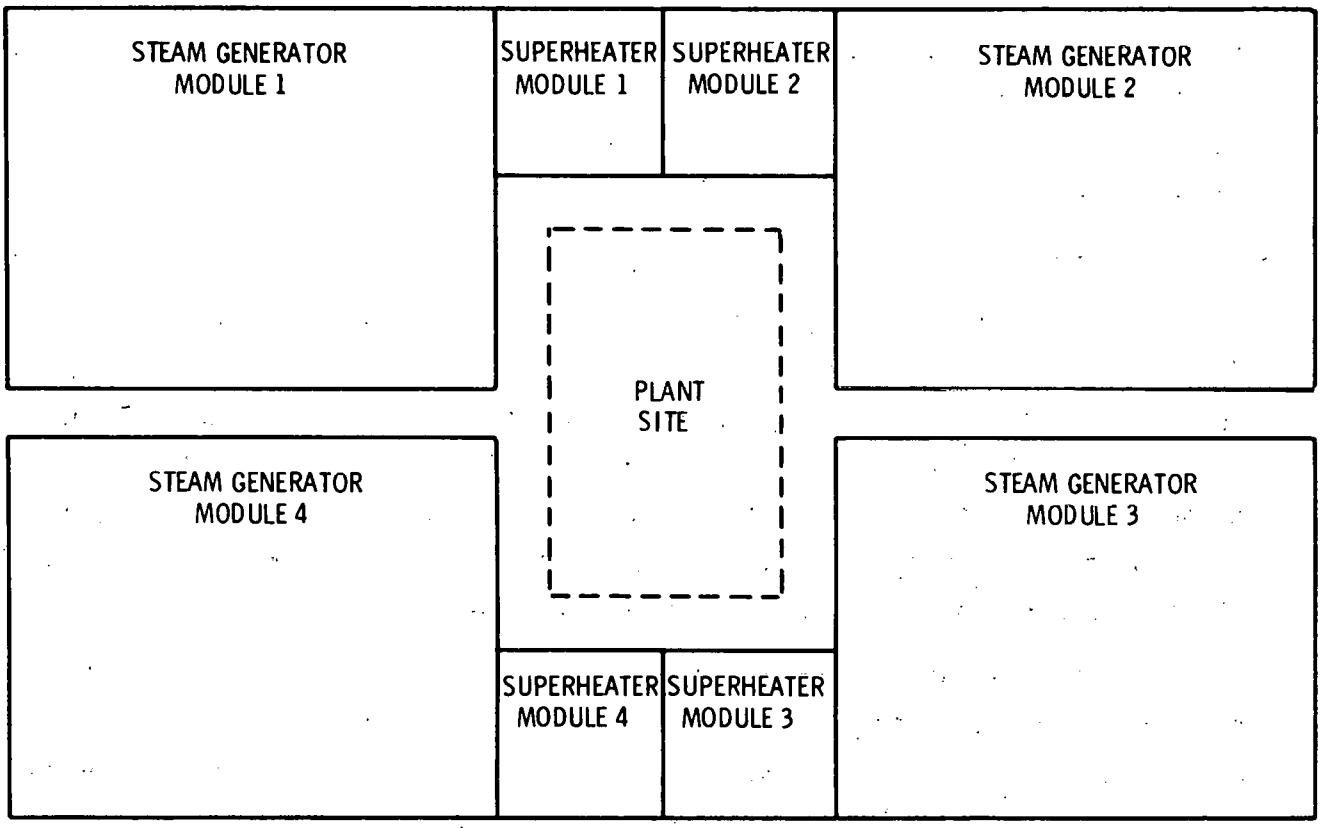

FIGURE 4.30. Typical Collector Field Layout, Line Focus Distributed Receiver - Tracking Collector Concept

Thermal energy is stored as sensible heat in an oil and rock medium, contained in a tank that is arranged to maintain a thermocline between the hot and cool regions of the tank. Caloria HT45 was selected as the heat transfer oil, and river sand and pebbles were chosen as the rock component of the heat transfer medium. Because Caloria HT45 thermally decomposes above 304°C (580°F), the maximum storage temperature must remain below that level.

During periods of high insolation the thermal storage subsystem is charged by extracting steam returning from the collector subsystem. The steam is used to heat oil in the thermal storage charging loop, but is desuperheated to prevent excessive temperatures in the thermal storage unit. The charging loop consists of charging oil pumps, charging piping, charging heat exchangers, and appropriate controls.

During discharge, the thermal storage unit provides heat to generate steam in the energy conversion subsystem. Steam is generated in the thermal storage discharge loop, which consists of a discharge oil pump, discharge piping, discharge heat exchangers, and appropriate controls.

Two additional components in the storage subsystem remove the residue of any heat transfer oil thermal degradation. The fluid maintenance system filters the oil to remove suspended solids, distills a side stream to remove high boiling polymeric compounds, and adds fresh makeup fluid to replace decomposed fluid. The ullage maintenance unit maintains an oxygen-free gas above the heat transfer fluid. It also removes the volatile fractions of the degradation products that evaporate into the ullage space above the heat transfer fluid.

The oil/rock medium is contained in one or more carbon steel tanks, depending on the size of the thermal storage subsystem. The tanks are insulated to reduce heat loss from storage. Appropriate foundations and miscellaneous equipment are included. All piping is Schedule 40 carbon steel with calcium silicate insulation. All pumps are carbon steel centrifugal pumps with electric motor drives.

4.9.5 Energy Conversion Subsystem

The energy conversion subsystem takes thermal energy, supplied from either the field or storage, and converts it to electrical energy. The energy conversion subsystem consists of the Rankine-cycle heat engine, generator, and air-cooled condenser.

The Rankine-cycle heat engine is a conventional steam power cycle, designed on the basis of performance and cost information provided by a consultant for a representative Rankine-cycle engine steam power cycle. Accessories include three feedwater heaters, feedwater booster pump, feedwater pump, lubrication system, steam seal system, and controls.

The generator is a three-phase, four-pole synchronous unit, driven by the turbine through a double helical spur gear reduction unit. It is air-cooled and equipped with a brushless exciter.

The waste heat from the Rankine cycle is rejected to the atmosphere in an air-cooled condenser. Exhaust steam from the turbine is ducted to the condenser where it is condensed in a steam/air heat exchanger. The steam/air heat exchangers are arranged in modules, each of which has a fan to force air past the heat transfer surfaces. Accessories include condensate pumps, piping, mechanical vacuum pump, and auxiliary equipment.

4.9.6 Alternative Concept Arrangements

After the base case LFDR-TC concept arrangement was defined and analyzed, one alternative was considered. In this arrangement, the steam/water transport subystem was replaced by an oil transport subsystem. The oil transport subsystem uses a heat transfer oil such as Caloria HT45 as the heat transfer fluid. Due to thermal decomposition, Caloria HT45 cannot be operated at a temperature above 304^{o}C (580^{o}F).

Caloria HT45 is heated in the collector field to 304^{o}C (580^{o}F) and returned to the storage subsystem. This system consists of supply and return piping and the field circulation pump. The same fluid is used in the transport subsystem as that used in the storage subsystem, so a charging loop is not required. In the Rankine cycle, steam is generated at 274^{o}C (525^{o}F) and

4.83 MPa (700 psi) regardless of whether energy is supplied from the field or from storage. Therefore, a single-admission turbine is used in the Rankine cycle.

The reduction in operating temperature when compared to the base case will reduce energy conversion efficiency. It was hoped that reduced high pressure piping cost, charging loop costs, and the elimination of the dual-admission turbine would offset the effects of the reduction in operating efficiency.

4.10 NONTRACKING CONCEPT

Any nontracking concept must have a low concentration ratio, which results in low operating temperatures. While the low operating temperature will reduce energy conversion subsystem efficiency, inexpensive nontracking collectors may substantially reduce the capital cost of the collector field. The trade-offs associated with operating temperature should indicate if low-cost, low-temperature concepts can successfully compete with the more expensive high-temperature concepts.

4.10.1 General Arrangement

The Low Concentration Nontracking concept analyzed in this study is designed to use the compound parabolic concentrator (CPC), which has a concentration ratio of 5.25. The CPC does not require daily tracking, but 12 adjustments must be made per year to take advantage of maximum solar energy acquisition time.

The LCNT concept is shown schematically in Figure 4.31. The CPC collector segments are arranged in a collector field consisting of standard modules. A heat transfer fluid circulated through the collector field is heated by the absorbed solar energy. The hot heat transfer fluid is either stored in the thermal storage subsystem or used to provide thermal energy to the energy conversion subsystem for conversion to electric power. The energy conversion subsystem is a Rankine-cycle heat engine with water as a working fluid. Waste heat from the Rankine cycle is rejected in an air-cooled condenser.

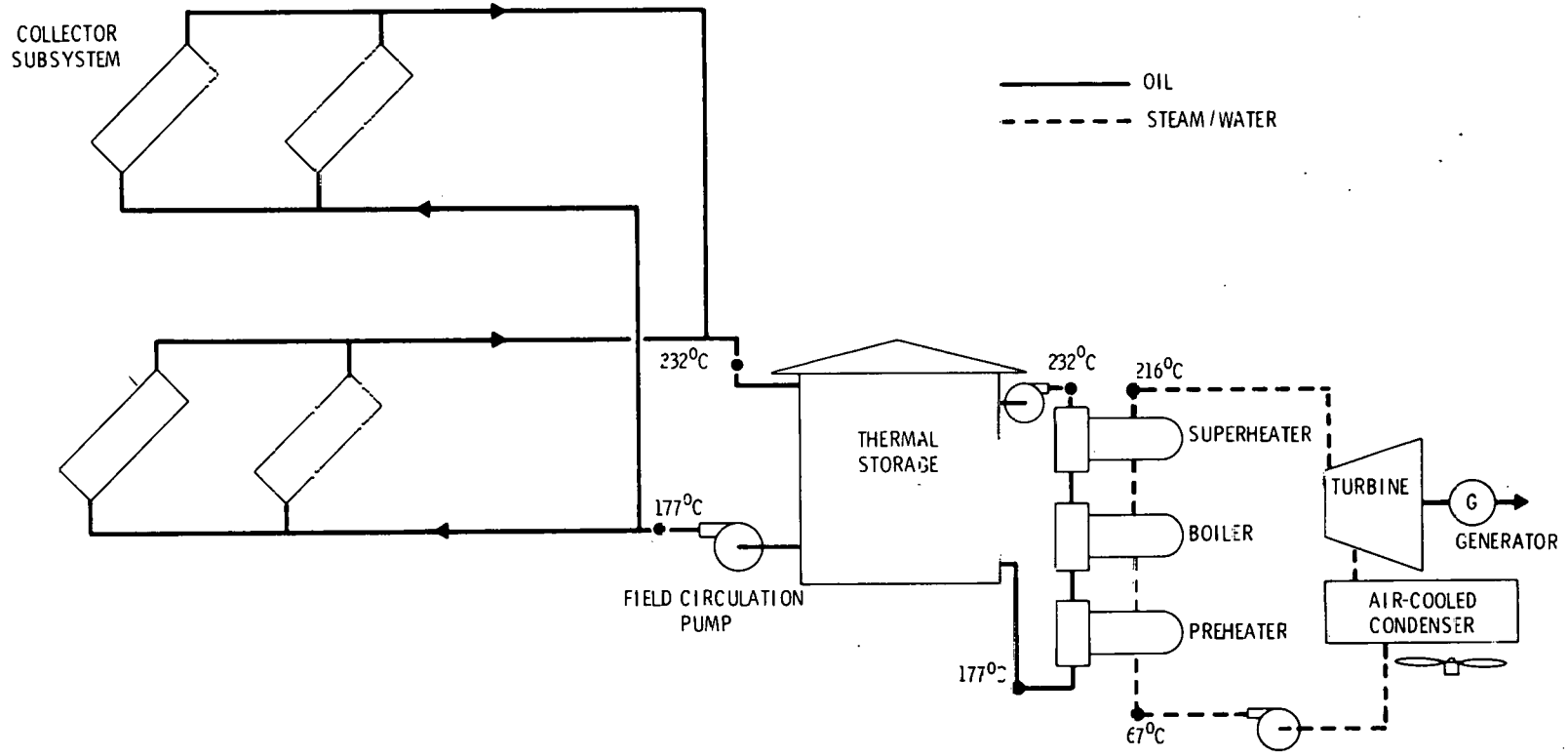

FIGURE 4.31. Low Concentration Nontracking Concept Schematic

4.10.2 Collector Subsystem

The LCNT concept uses a compound parabolic concentrator (CPC) collector. The CPC is a nonimaging concentrator, which, in theory, will concentrate any radiation within its acceptance angle. The solar radiation is redirected onto a selectively coated vacuum-enclosed receiver where it is absorbed and transferred to the heat transfer fluid. The concentration ratio can be increased by decreasing the acceptance angle. Because the CPC is a nontracking collector, a reduction in the acceptance angle will reduce the time that beam radiation from the sun is within the acceptance angle. To maintain a reasonable collector field efficiency, the compound parabolic collector must be adjusted to compensate for annual variations in the sun's elevation. For this study a truncated 7.2x compound parabolic collector with an effective concentration ratio of 5.25 was selected. The 5.25x collector requires 12 annual tilt adjustments.

The individual collector segment is based on the designs developed at the University of Chicago and Argonne National Laboratory, and has overall dimensions of 5.18 m (17 ft) by 2.74 m (9 ft) (Collares-Pereira et al. 1978; Cole et al. 1977; Little 1975; Allen et al. 1976). The concentrator is enclosed with a cover glass that reduces heat loss and surface degradation. The receiver is a selectively coated vacuum-enclosed tube. A bank of parallel collectors is arranged to form the collector segment, which includes a frame to support the collectors, manifolds, and an automatic shading system to prevent overheating in case of a loss of heat transfer fluid flow.

The collector segment structural support is designed to provide adequate support under conditions of sustained 90-mph winds. In addition, the collector segment must be able to have the tilt angle adjusted. The design shown in Figure 4.32 involves a manual tilt adjustment, but an automatic tilt adjustment is also feasible at an added cost of about $\$3/ft^2$.

The individual collector segments are arranged in a standard module. The collector field is a combination of standard modules with sufficient area to provide the required thermal energy. The standard module consists of 100 collector segments arranged in 10 rows and 10 columns. Each of 50 parallel

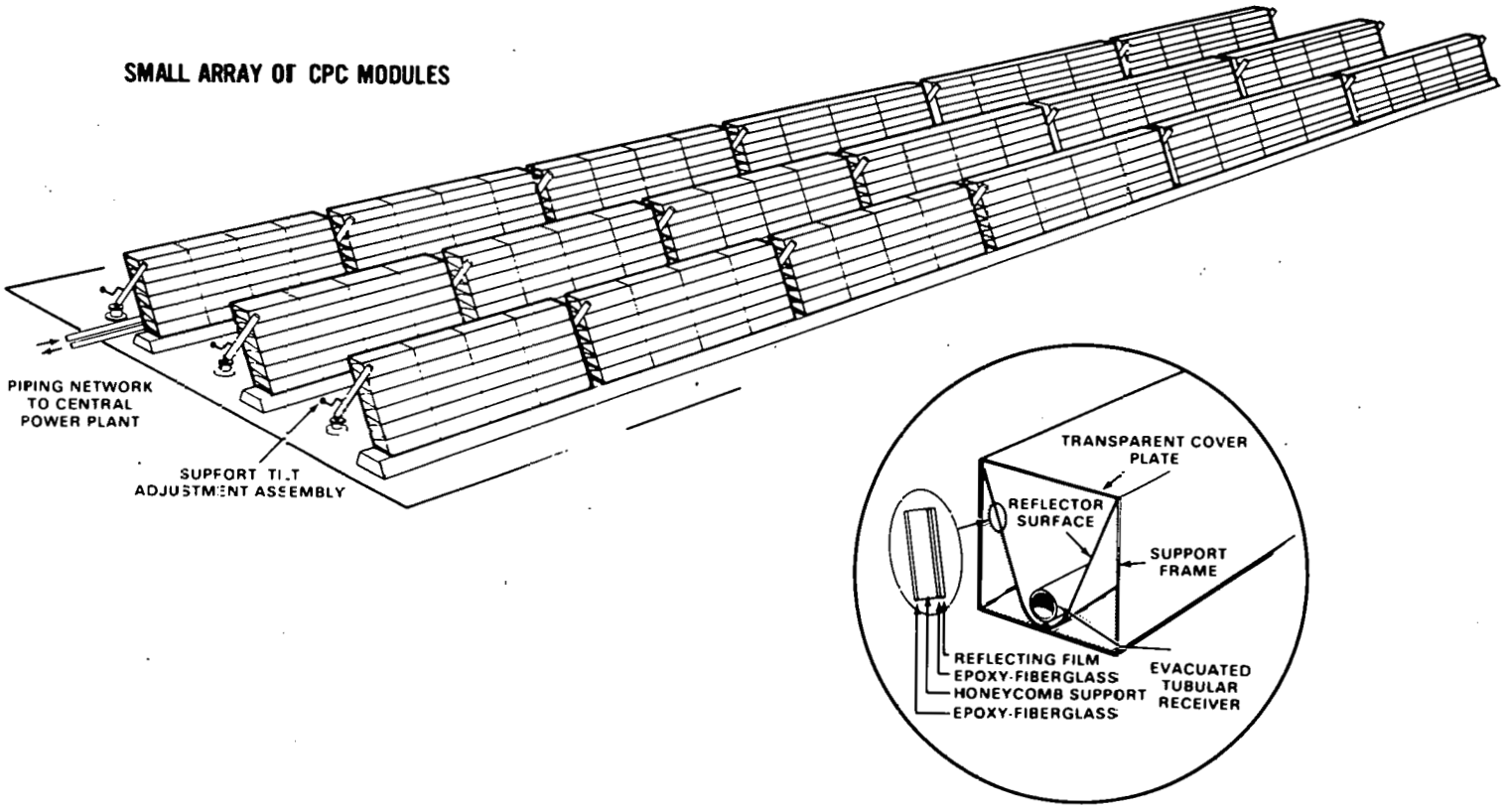

FIGURE 4.32. Low Concentration Nontracking Concept

flow paths consist of two collector segments arranged in series. Each standard module will provide around 550 kWh (1.9×10^6 Btu/hr) for an annual average insolation of 800 W/m^2. The standard module has a total effective aperture area of 1,254 m^2 (13,500 ft^2).

In determining the collector field optical performance, several variables were considered. These include ground cover ratio and collector tilt schedule. A ground cover ratio of 0.42, which relates to a 2.44-m (8.0-ft) spacing between rows, was used in this study. Other ground cover ratios were considered, but were found to have minimal effect upon CPC collector optical efficiency.

The compound parabolic collector with the selectively coated vacuum-enclosed receiver can operate at temperatures above 350°C (662°F). Above approximately 232°C (450°F), the increasing efficiency of the energy conversion subsystem does not compensate for the reduction in collector efficiency due to increased collector heat loss. For this study, a collector exit temperature of 232°C (450°F) was chosen.

4.10.3 Transport Subsystem

The transport subsystem consists of the pumps, piping, and heat transfer fluid necessary to transport the thermal energy collected in the collector field to the energy conversion and storage subsystems. The major components of the LCNT concept transport subsystem are the field circulating pump; module supply, internal, and return piping; and the heat transfer fluid.

The low operating temperature of the compound parabolic concentrator collector field allows a wide selection of heat transfer fluids. For the LCNT concept, a heat transfer oil such as Caloria HT45 was chosen. Caloria HT45 is also used as the storage medium in the energy storage subsystem. This dual application eliminates the need for the thermal energy storage charging heat exchangers, piping, and pumps.

Because Caloria HT45 does not experience a phase change while being heated in the collector field, once-through heating can be used with confidence, eliminating the need for recirculation pumps, steam drums, and accumulators in the transport subsystem. The field circulation pump pumps heat transfer oil

from the cool end of the thermal storage subsystem through the module supply piping to the standard module where the oil is distributed to the collector segments by means of the module internal piping. The oil is heated in the collector segments and returned via the module return piping to the thermal energy storage subsystem. The hot oil can go either into the thermal storage subsystem or directly to the steam generators for use in the energy conversion subsystem.

Module internal piping is shown in Figure 4.33. The collector segments are arranged in 50 parallel flow paths; each flow path consists of two collector segments. Valves are included to permit isolating a block of 20 collector segments for maintenance. Additional valves are included so that the complete standard module can be removed from service, if necessary. Expansion loops and flexible couplings provide for thermal expansion during startup and operation.

A typical collector field is shown in Figure 4.34. The standard modules are arranged in a rectangular grid with module supply and return piping arranged as shown. The field circulation pump located at the central power generation facility is sized to provide sufficient discharge pressure to pump the heat transfer oil through the transport piping network.

In all cases, the piping is Schedule 40 carbon steel with calcium silicate insulation. Module supply and return piping is welded and buried. The module internal piping is above ground but also welded. The field circulation pump is a carbon steel centrifugal pump with an electric motor for the driver. All valves are assumed to be carbon steel gate valves of the appropriate pressure rating.

4.10.4 Storage Subsystem

Thermal energy collected in the collector field can be stored for use during night or periods of low insolation. The thermal energy is stored as sensible heat in the energy storage subsystem. One type of thermal energy storage subsystems was considered for the LCNT concept. The low-temperature oil and rock subsystem was chosen for the base case because it is the closest to commercial availability. The high-temperature capabilities of the other storage types were not required.

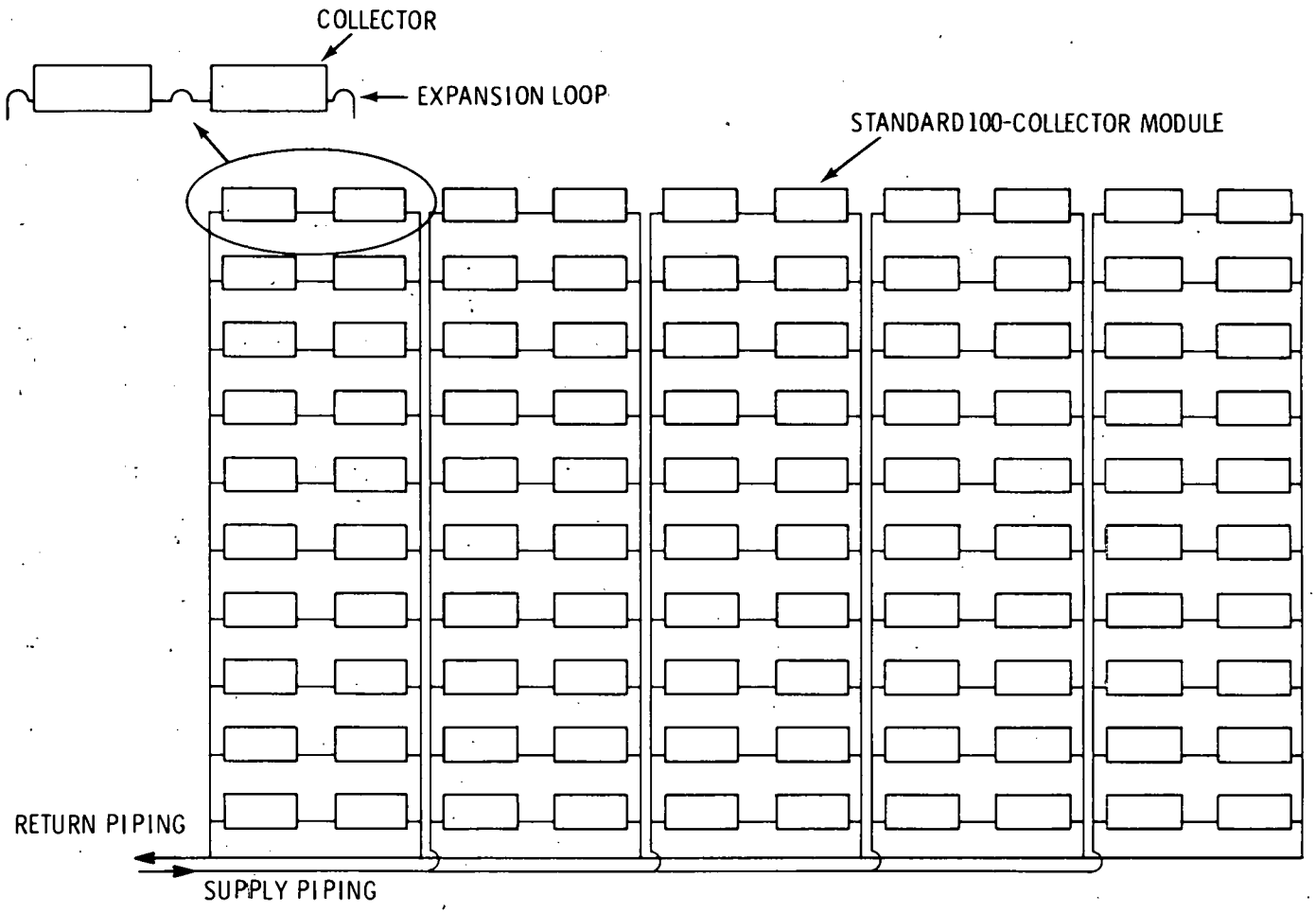

FIGURE 4.33. Module Internal Piping for the Low Concentration Nontracking Concept

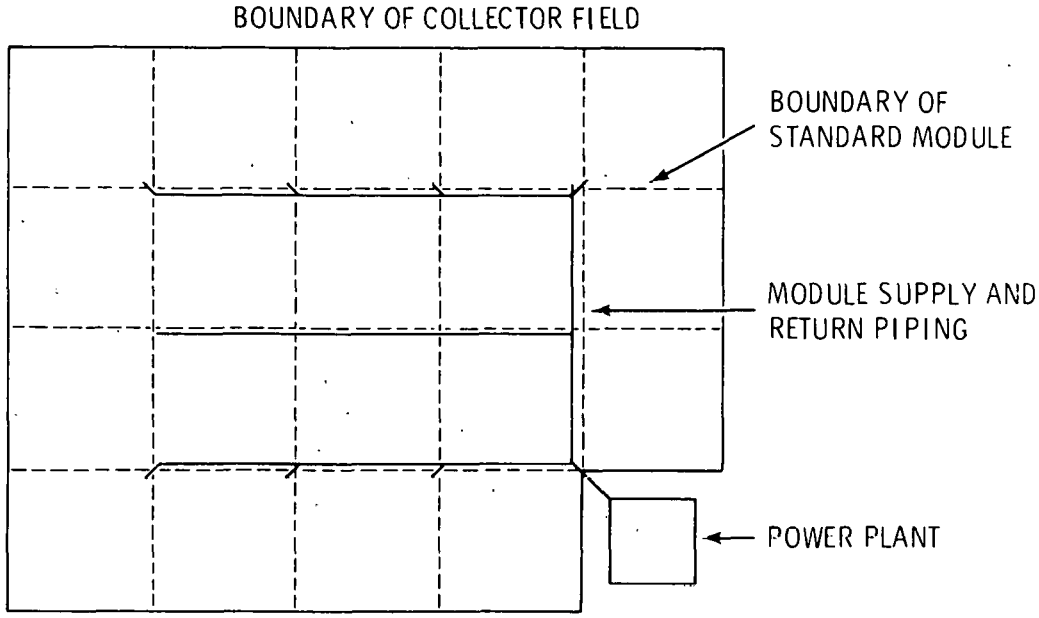

FIGURE 4.34. Typical Collector Field Layout, Low Concentration Nontracking Concept

The thermal energy storage subsystem consists of the storage medium, storage medium containment, charging heat exchangers, charging pump heat exchanger, discharge pump and piping. The thermal energy storage subsystem is similar to that proposed by McDonnell Douglas for the Barstow Power Plant.

Thermal energy is stored as sensible heat in an oil and rock medium. The medium is contained in a tank arranged to maintain a thermocline between the hot and cool regions of the tank. River sand and pebbles were chosen as the rock component of the heat transfer medium. Caloria HT45 was selected as the heat transfer oil. Caloria HT45 cannot be used successfully at a temperature above 304°C (580°F) due to thermal decomposition of the oil. This temperature limit was not a significant restraint because of the low collector operating temperature.

During periods of high insolation, the thermal storage subsystem is charged by extracting hot oil from the collector subsystem. Because Caloria HT45 is used in both the transport and storage subsystems, a charging loop is not required.

During discharge, the thermal storage unit provides heat to generate steam in the energy conversion subsystem. Steam is generated in the thermal storage discharge loop, which consists of discharge oil pump, discharge piping, discharge heat exchangers, and appropriate controls.

The storage subsystem has two additional components, which remove the residue of any heat transfer oil thermal degradation. The fluid maintenance system filters the oil to remove suspended solids, distills a side stream to remove high boiling polymeric compounds and adds fresh makeup fluid to replace decomposed fluid. The ullage maintenance unit maintains an oxygen-free gas above the heat transfer fluid. This unit also removes the volatile fractions of the degradation products that evaporate into the ullage space above the heat transfer fluid.

The oil/rock medium is contained in one or more carbon steel tanks, depending on the size of the thermal storage subsystem. The tanks are insulated to reduce heat loss from storage. Appropriate foundations and miscellaneous equipment are included. All piping is Schedule 40 carbon steel with calcium silicate insulation. All pumps are carbon steel centrifugal pumps with electric motor drives.

4.10.5 Energy Conversion Subsystem

The energy conversion subsystem consists of the Rankine-cycle heat engine, generator, and air-cooled condenser. Due to the low operating temperature of the compound parabolic concentrator, the energy conversion subsystem has a low conversion efficiency, particularly when waste heat is rejected through an air-cooled condenser.

Several Rankine-cycle engines were considered. At small sizes an organic Rankine cycle appeared to be slightly more efficient than the steam Rankine cycle. However, the added complexity and lack of industrial experience with large organic Rankine-cycle engines could offset any advantage gained by the increased efficiency. Therefore, a steam Rankine cycle was chosen for all plant sizes analyzed. A detailed design of the Rankine cycle was beyond the scope of this study. The Rankine cycle performance and cost information were provided by a consultant for a representative Rankine-cycle engine that

included a high-speed condensing steam turbine with three uncontrolled extraction connections. Accessories include three feedwater heaters, feedwater booster pump, feedwater pump, lubrication system, steam seal system, and controls.

The three-phase, 60-Hz, four-pole synchronous generator is driven by the turbine through a double helical spur gear reduction unit. The generator is air-cooled and equipped with a brushless exciter.

An air-cooled condenser rejects the waste heat from the Rankine cycle to the atmosphere. The condenser is located either adjacent to the turbine generator building or on the building roof. Exhaust steam from the turbine is ducted to the condenser where the steam is condensed by rejecting heat to ambient air in a steam/air heat exchanger. The steam/air heat exchangers are arranged in modules, each with a fan to force ambient air past the heat exchanger. Accessories include condensate pumps, piping, mechanical vacuum pump, and auxiliary equipment.

4.10.6 Alternative Concept Arrangements

No alternative arrangements were considered for the LCNT concept.

5.0 ESTIMATION OF COSTS

Estimation of costs for solar thermal power plants occurs in two distinct steps. Costs for equipment and services required for specific plant configurations are estimated, giving point estimates. These point estimates are then used to determine cost estimate scaling relationships relating component cost to variables such as nameplate plant rating, collector field size, capacity factor, and storage subsystem capacity. Cost estimate scaling relationships permit the analysis of a large number of plant configurations without requiring detailed estimation of costs for each.

The estimation of component costs at specific design points is by far the more time-consuming of these two steps. This step requires developing assumptions and ground rules, cost estimating methods, and unit costs for materials and labor. Finally, all these inputs are used to assemble cost estimates for each component of each system. This approach was used to establish costs in sufficient detail to detect differences among concepts that may not be apparent from a broader perspective.

Through standardizing inputs used in generating cost estimates for each concept, results obtained are on a comparable basis. This cost estimate normalization is important, because seemingly minor changes in assumptions, methodologies, or unit costs can have major impacts upon estimated costs and, hence, on concept ranking. Without normalization of cost estimates to a uniform basis, reasonable comparisons of concepts cannot be made.

5.1 ASSUMPTIONS AND GROUND RULES

Standardizing assumptions and ground rules used in estimating costs is critically important in generating comparable, or normalized, results. This is particularly true when conceptual designs are involved, as is the case for collectors. Changing assumptions and ground rules can radically affect collector cost estimates, which makes for uncertain comparisons between collectors when two concepts are evaluated using different bases. To ensure that consistent assumptions and ground rules were used, the PNL project team generated the cost estimates instead of relying on those available in the literature.

5.1.1 Industry Maturity and Production Rate Assumptions and Ground Rules

Assumptions and ground rules regarding industry maturity and production rates have large impacts upon component cost estimates. In general, costs for items produced by a mature, established industry are lower than those for identical items produced in a developing industry. Similarly, an item's cost tends to be inversely proportional to the item's production rate; as production rate increases, costs will decrease. These trends result from many factors; foremost are learning and economies of scale in materials, labor, and capital investments.

Collectors are a logical choice in standardizing production for different components. Collector cost estimates are very sensitive to assumed production rates, and collectors are the largest single cost element of solar plant costs. In the PNL study, the production rate for collectors is the yardstick used to determine production rate assumptions for other components. As an example, for concepts using distributed engine generators, with one engine per collector, engine production rates are assumed to correspond to collector production rates. In this way, cost estimates for specialized components not used by all concepts are equivalent with other estimates.

Several options exist for measuring collector production rates. Possibilities include measurement by the number of collectors produced per year, by the number of new installed capacity of solar plants each year, or by the collector aperture area produced per year. Basing production rate on the number of collectors produced tends to distort assumed markets for collectors, because a given number of large collectors receives more insolation than the same number of small collectors, implying a larger market for the large collector. Basing collector production rates on a number of installed solar MWe entails assuming that the only collector market is for electric applications, and ignores any nonelectric collector applications. Measuring production rate based on collector aperture area does not differentiate among collectors on the basis of size, and involves no assumptions concerning collector use. In addition, because aperture area is standardized, the insolation received by each concept will be exactly equivalent. Because of these advantages, aperture area was chosen as the variable from which to specify collector production rates.

A collector production level of 1,200,000 m^2 of aperture area per year was chosen as the reference at which to evaluate all concepts. This production level is large enough to allow collectors to experience significant cost reductions due to mass production, and was felt to be a conservative estimate for the time frame being considered in the overall project. This corresponds to roughly 100 to 200 MWe of new solar power each year, if all collectors were used for elecric power generation.

Assumed production rates for concentrator and receiver components for each concept are given in Table 5.1. Concentrator production rates are determined directly from the collector aperture area. Receiver production rates are dependent upon the number of receivers used per concentrator, which varies considerably from concept to concept. Central receiver concepts employ a large receiver surrounded by many smaller concentrators; the LCNT concept uses many small receiver tubes in each concentrator.

TABLE 5.1. Collector Component Production Levels[(a)]

Concept	Collector Aperture Area, m^2	Concentrator Production Rate, Units/Year	Receiver Production Rate, Units/Year
PFCR/R	49.0	25,000	30
PFCR/B	49.0	25,000	30
PFDR/R	100.0	12,000	12,000
PFDR/B	100.0	12,000	12,000
PFDR/S	100.0	12,000	12,000
FMDF	2920.0	411	411
LFCR	55.8	21,000	250
LFDR-TC	15.9	75,000	75,000
LFDR-TR	16.8	70,000	75,000
LCNT	14.2	85,000	2,550,000

(a) The reference production level is 1.2×10^6 m^2 aperture area yearly.

All cost estimates assume that a commercial solar industry has existed for several years. This avoids burdening concepts with one-time costs associated with new industry development, and reflects the level at which costs would stabilize under the assumed production rates.

5.1.2 Other Assumptions and Ground Rules

Economic assumptions and ground rules used in the PNL study can be categorized according to type:

- operation and maintenance of small power systems
- economic and financial parameters for the utility company operating the power system
- the solar industry in general
- collector manufacturing.

Table 5.2 summarizes the uniform economic assumptions and ground rules of each type used in the this study.

5.2 COST ESTIMATE REPORTING ACCOUNTS

Costs for solar thermal small power systems are summarized in 20 cost estimate reporting accounts. These accounts cover all costs from construction through plant operations, excluding plant decommissioning costs. Cost accounts are categorized as one of three types: initial capital costs, replacement costs, and operations and maintenance costs. Cost accounts for each type are listed in Table 5.3.

Initial capital costs consist of all costs incurred prior to plant startup. In addition to costs directly associated with the four primary plant subsystems (collectors, energy transport, energy storage, and energy conversion), a number of other plant costs exist. These include costs for structures, land, service facilities, power conditioning equipment, instrumentation and controls, and spare parts. Cost reporting accounts for these elements are grouped together as "other plant" costs. Indirect and contingency costs are compiled for plant construction as a whole rather than added to each reporting account, and are reported in individual reporting accounts.

TABLE 5.2 Economic Ground Rules and Assumptions

Category	Ground Rules and Assumptions
Solar Industry	• Concepts are analyzed assuming the power system operates as part of a commercial electricity production industry. • Capital investment costs for concepts are estimated assuming sophisticated fabrication, assembly, construction, and installation techniques. • Technological and economic risk as they may affect investment decisions for solar thermal small power systems are not considered. • R&D costs, development subsidies, and all other costs associated with solar thermal industry commercialization are not included. • Cost estimates do not include the effects of investment tax credits or other incentives. • Power plant decommissioning costs are not included in estimates.
Collector Manufacturing Process	• Concentrator costs are estimated assuming a reference production rate of 1.2×10^6 m^2/year concentrator reflective aperture area. • Collector manufacturing facilities are assumed to consist of highly automated processes, thereby minimizing production labor. Manufacturing process technology is assumed to be current state-of-the-art. • Collector cost estimates include manufacturing facility indirect costs, overhead, and allowances for a required return on investment. • Allowances for sales taxes, working capital, and manufacturing facility personnel training are included. • Manufacturing facility lifetime is 15 years. • Effective state and federal income tax rate burdened on manufacturing facility profits is 0.52. • Effective other taxes burdened on manufacturing facility profits are 0.02.
Small Power Systems Plant Operation and Maintenance	• Unscheduled maintenance requirements are assumed to be minimal. • Concentrator cleaning is performed weekly. • Plant control schemes are highly automated, requiring little interface with plant operators. • One operator is required for plant operations, and is present whenever the plant is operating. Operators perform scheduled maintenance when not actively involved in plant operations. • Owner home office expenses are not included in cost estimates. • All required maintenance is performed using subcontracted labor. Full-time maintenance crews are not used. • Small power systems are assumed to not require security personnel.
Economic Inputs	• Levelized energy costs are calculated using methodologies described in Doane et al. (1976). • Power licensing, construction, and start-up periods are assumed to be 4 years. • Capital recovery factor = 0.094 • Fixed charge rate = 0.157 • Nominal capital escalation rate = 0.06 • Nominal O&M expense escalation rate = 0.07 • Nominal general inflation rate = 0.06 • Cost of capital = 0.086 • Power system lifetime = 30 years • First year of power system commercial operation = 1985 • Base year of price levels = 1978

TABLE 5.3. Cost Reporting Accounts

Account Category	Account Included	Subsystem or Elements
Initial Capital Costs	Concentrator Costs	Collector
	Receiver Costs	
	Thermal Energy Transport Costs	Transport
	Electric Energy Transport Costs	
	Energy Conversion Costs	Energy Conversion
	Thermal/Electric Storage Costs	Energy Storage
	Structures Costs	Other Plant
	Land Costs	
	Service Facilities Costs	
	Power Conditioning Equipment Costs	
	Instrumentation and Control Costs	
	Spare Parts Costs	
	Indirect Construction Costs	Indirect and Contingency
	Contingency Costs	
Replacement Capital Costs	Collector Replacement	
	Engine Replacement	
	Storage Medium Replacement	
Operating and Maintenance Costs	Direct Production Cost	
	Maintenance Cost	
	Plant Overhead Cost	

Costs for the collector subsystem are reported in concentrator and receiver cost accounts. Included in both accounts are manufacturers' selling costs and costs of field installation and checkout. Field installation includes costs of construction tasks, such as foundation production, installation on foundations, and hookup to control and energy transport components. Costs for alignment, adjustment, and testing are included as checkout costs.

Elements of the thermal energy transport cost reporting account are pipe, pipe fittings, pipe trench, valves, insulation, pumps, and field storage tanks. Electric energy transport cost reporting account elements are electrical cable and ancillary field required transport equipment. Items in either account are used for the transport of energy from distributed locations in the collector field to a central location.

Components of the Rankine-cycle energy conversion cost reporting account are the steam turbogenerator, turbogenerator building, and air-cooled condensers for heat rejection. Components for Stirlingand Brayton-cycle energy conversion cost reporting accounts are the engine and generator, with costs of heat rejection equipment included in engine costs.

The energy storage cost reporting account includes all components required solely for the energy storage subsystem. The primary components for thermal energy storage subsystems are storage tanks, storage media, heat exchangers, pumps, and piping. For Redox battery electric energy storage subsystems, the primary components are the Redox battery, power inverter, and auxiliaries.

"Other plant" components are contained in six cost reporting accounts. The structures account reports costs for buildings used for control, maintenance, and storage. Costs for raw land, survey fees, site preparation, and site improvement are included in the land cost reporting account. Facilities for water treatment, water and electricity distribution, and plant communications, as well as fire protection and collector cleaning vehicles, are reported in the service facilities cost reporting account. Switchyard equipment for the plant is reported in the power conditioning cost reporting account. The instrumentation and control cost reporting account contains costs for overall plant control systems, excluding any individual control devices for collectors, which are included in concentrator costs. Costs of initial inventories of spare parts are included in the spare parts account.

The indirect construction cost reporting account covers engineering and field supervision expenses, general construction expenses, and contractors' fees for the construction of the entire power plant. Contingency allowances

for increases in cost due to equipment delivery problems, weather, labor conflicts, or other unforeseen difficulties are reported for the plant as a whole in the contingency cost reporting account.

Replacement capital cost reporting accounts correspond to capital costs occurring during the operating lifetime of the plant. These are incurred due to the replacement of equipment with life expectancies considerably less than the lifetime of the plant as a whole. Collector replacement costs include costs of replacing concentrator or receiver components. The engine replacement cost account corresponds to the cost of overhauling or replacing the engine portion of the energy conversion subsystem. Storage media replacement costs refer to the capital cost of replacing batteries or storage media in an energy storage system.

Operating and maintenance costs are reported in three accounts. Direct production costs are associated with plant operation, and consist of expenses for plant operating personnel. Maintenance costs consist of costs for scheduled and unscheduled system maintenance not performed during daily plant operations. These include costs for inspection, cleaning, equipment overhaul, and replacement of minor equipment, such as valves, due to unscheduled failure. Costs in addition to direct payments for direct production and maintenance costs are reported as plant overhead costs. Items in this account include administative costs and payroll burdens.

5.3 APPROACH FOR ESTIMATING SUBSYSTEM COSTS

Subsystem costs are aggregated from many component costs, with cost estimates for each component assessed in the same way for all concepts. This approach ensures that all concepts are uniformly evaluated, because the assumptions, ground rules, cost estimating methodologies, and unit cost inputs were carefully standardized by the PNL team.

Approaches used to estimate subsystem costs varied among subsystems. Costs for subsystems consisting of conventional, off-the-shelf items (such as thermal energy transport subsystems) were estimated using current component cost information. Subsystems containing nonconventional components, such as

the collector subsystem, require different estimating approaches, which can assess the impact of increased production over present-day levels on component costs. For most subsystems, cost estimates were developed independently from previous studies, using a detailed cost analysis. Because of the large number of components involved, this approach was not feasible for all components of all subsystems. For example, a detailed manufacturing cost analysis of small Stirling or Brayton engines was clearly beyond the scope of the project. When component costs were not independently estimated, cost information was assembled from previous studies in which detailed analysis had been made. Using cost estimates from previous studies requires careful interpretation of the studies' approach and results, because of the importance of evaluating all concepts on equivalent criteria.

Subsystem cost estimates were developed specifically to produce comparative estimates of concept costs, and should not replace or substitute for more detailed cost estimates necessary before actual pilot or commercial plant designs are designated for construction.

5.3.1 Collector

Collector subsystems consist of concentrator and receiver components, and are the single most distinguishing characteristic among concepts. Because of their importance in characterizing concepts and their major impact on installed system costs, a considerable amount of work was devoted to achieving realistic collector cost estimates. Rather than simply extract collector cost estimates directly from available literature, emphasis was placed on independently constructing collector manufacturing and field installation cost estimates for each concept.

The approach used was designed to obtain realistic collector cost estimates for each of the designs analyzed. In analyzing collector concepts, primary attention was given to major cost elements such as materials and labor cost. Less attention was given elements that contribute little to cost differences among collector concepts, such as manufacturing plant overheads, capital costs for constructing manufacturing facilities, and manufacturing facility return on investment requirements. A major benefit in using this

approach was the ability to analyze alternative collector concepts using a consistent data base of unit costs for materials and labor.

Unit costs for materials and labor common to all collector types were developed using a variety of sources. Unit costs for conventional items and tasks were developed from construction cost estimating guidebooks, vendor quotes, equipment cost guides, and other industry cost information. For cases in which component unit cost was highly dependent upon the specific applications of the component, unit costs were developed for each alternative application or location. An example of this is field-installed reinforced concrete, where the unit costs developed ranged from \$70 to \$450/yd^3, depending upon the complexity of the concrete placement. Some collector elements, such as tracking units, have not been produced in the quantities that would be required in an established solar thermal industry; therefore, unit costs at the increased production levels are somewhat uncertain. Several methods were used to establish unit costs for these items. In instances when manufacturers were able to estimate their selling cost at different production levels, these estimated unit cost measures were used. When these estimates were not available, they were made by comparing system components with other components of like size and configuration that do have cost information available.

An overview of the major steps in the collector cost estimating methodology is shown in Figure 5.1. In general, eight steps are involved in applying the methodology. To begin the process, a reference collector design is chosen and characterized, and an overall assembly/installation scenario devised. Costs for materials and assembly, as well as the manufacturing plant capital cost, are then estimated and combined. These combined costs are then used to calculate the selling price of the manufactured collector. Field installation/construction costs are estimated, then added to the manufactured collector selling price, determining the total installed collector cost. Each of these steps is described in greater detail in the following paragraphs. Collector costs are shown in Appendix B.

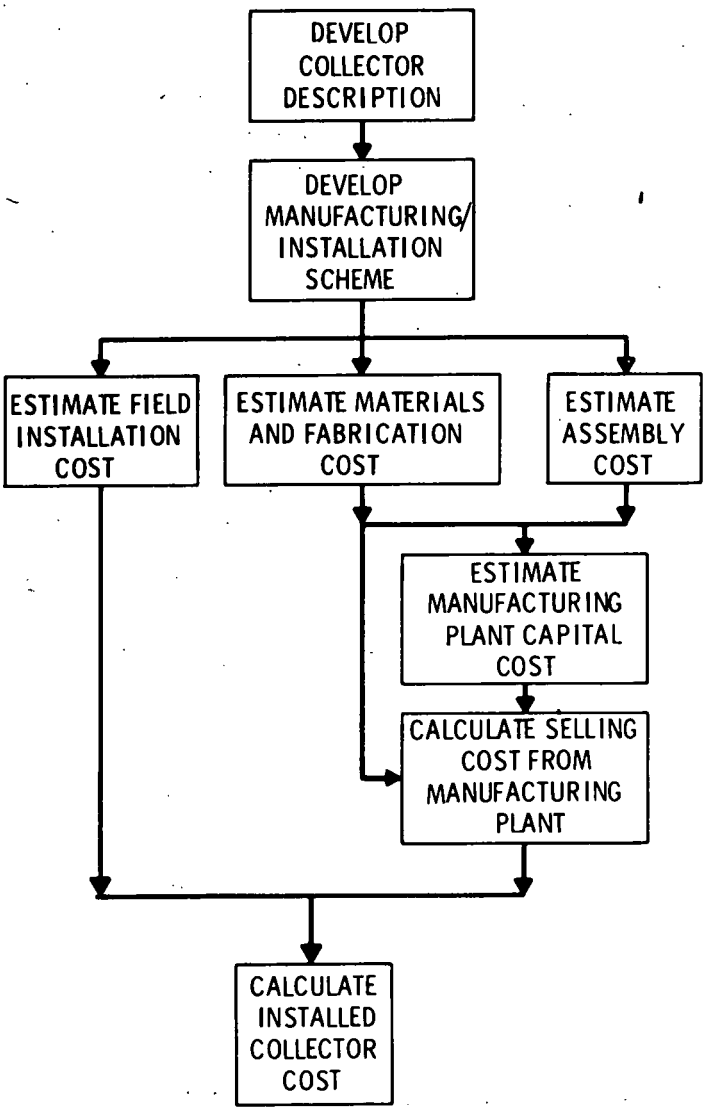

FIGURE 5.1. Collector Cost Estimating Methodology

5.3.1.1 Collector Description Development

Descriptions of each collector conceptual design must be developed in sufficient detail to allow estimation of materials, fabrication labor, and installation labor costs. Collector conceptual design documents and any existing prototype collectors are analyzed and used to construct a "straw man" collector design. This "straw man" collector design is then modified in two ways. Design optimization changes reflect the fact that designs appearing

optimal for near-term applications may not be optimal under mass production conditions. Design optimization is basically a subjective step involving changes such as small variations in concentrator size, different sizes of structural support members, or improved foundation designs. Input for design optimization changes came primarily from proponents of the different generic concepts, based on their opinions of what modifications would be done in mass production to lower overall collector cost. Changes in the "straw man" collector design due to component availability are similar to design optimization changes, and are a result of types of specialized collector components assumed to become available at the reference collector production rate. As an example, if low-cost tracking units are assumed to be available for one concept, the same tracking unit would be used for other concepts when applicable. Incorporating design optimization and component changes in the "straw man" collector conceptual design serves to standardize the basis on which the collector designs for alternative concepts are based.

5.3.1.2 Manufacturing/Installation Scheme Development

A manufacturing/installation scheme is outlined for each collector, dividing collector production tasks into those performed in the manufacturing facility and those performed in the field. Division of these tasks is a subjective judgment based on the overall collector size and complexity.

It is assumed that most tasks of collector production could be more economically performed in a manufacturing facility than in the field. One mitigating factor to this is collector size. Collector size relates to shipping considerations; namely, a maximum collector component size can be economically shipped. In addition, shipping costs for fully assembled collectors will be higher than for partly assembled collectors, due to packing efficiency. Size considerations can become critical as concentrator or receiver sizes approach the limits handled by conventional shipping. In most cases, concentrators were assumed to be shipped in several pieces, with simple assembly performed in the field.

Simple construction tasks, such as pouring foundations, pay little or no penalty for being performed in the field, and may, in fact, be more expensive

if performed in a manufacturing facility. Construction tasks that are traditionally performed in the field are assumed to be most economically performed in the field for collector cost estimating purposes.

Field installation tasks are dictated by collector construction methods and the extent of collector construction occurring at the plant site. Installation of assembled collectors typically consists of mounting on foundations, hookup to transport and control systems, alignment, and checkout.

5.3.1.3 Materials and Fabrication Cost Estimating

Materials and fabrication costs are incurred by the collector manufacturing facility during collector production. Direct materials costs are actual purchase costs of materials, while fabrication costs consist of labor costs required for cutting, shaping, or otherwise fabricating purchased materials into their final form.

Collector parts differ according to the form in which each may be purchased--raw materials to be completely fabricated in the manufacturing facility, a finished product ready for assembly, or something between the two. A complex component, such as an electric motor for a drive unit, is assumed to be bought, since the number required per year would not justify setting up an assembly line for motor production. Less complex items with larger requirements per collector, such as steel channels in structural supports, are assumed to be partially fabricated in the manufacturing facility. In no case was it assumed that collector parts would be produced at the manufacturing facility directly from raw materials, since complete fabrication of parts may not be economical except at higher production rates than assumed. At sufficiently high production rates, complete fabrication of collector parts could slightly lower materials and fabrication cost estimates formulated for this study.

General fabrication scenarios were developed for collector parts that are partially fabricated in the manufacturing facility. Fabrication is assumed to be carried out on highly automated production lines. Labor costs are generated using estimates of production line throughput and labor requirements.

5.3.1.4 Assembly Cost Estimation

Assembly costs are considered to consist solely of labor costs for assembling collectors at the manufacturing facility. Basic collector assembly scenarios were developed and used to designate assembly tasks. Simple assembly tasks were assumed to be performed on highly automated assembly lines requiring little direct operating labor. Tasks considered too complex for machine execution were assumed to be performed using a combination of machine and human labor. Having defined the assembly processes required, operator requirements were estimated for each process and summed to obtain total assembly man-hours. Total assembly cost was calculated using an average wage rate.

5.3.1.5 Manufacturing Plant Capital Cost Estimation

Capital costs for the collector manufacturing facility are required to calculate a collector selling cost. Estimates of manufacturing plant capital cost ranges for PFCR heliostats have been identified in previous studies; these provided the baseline used for estimating capital costs for other components. Manufacturing plant capital costs are subjectively scaled from the PFCR heliostat estimate based upon the complexity of fabricating and assembling the collector, and the required production rates for collector components. The relatively high uncertainty involved in this approach is compensated for by the minor contribution manufacturing plant capital costs make to collector selling cost. This result of the PNL analysis is upheld by other collector cost estimates (Drumheller 1978).

5.3.1.6 Collector Selling Cost Calculation

Collector manufacturing selling costs are defined as the cost at which collectors could be purchased by power plant constructors from an independent manufacturing facility. Collector selling costs include direct materials and labor costs, indirect materials and labor costs, capital investment depreciation, plant overhead costs, and manufacturers' profit.

Direct materials costs, described in Section 5.3.1.3, are what materials costs would be in an ideal process, with no materials wastage. Indirect materials costs stem from the fact that some materials wastage will occur

during collector production. This wastage is caused by rejection of parts not meeting specifications, breakage, and the inability to perfectly use all materials during fabrication steps. Indirect materials costs are calculated as a percentage of direct materials costs.

Direct labor costs consist of fabrication costs and assembly costs, as described in Sections 5.3.1.3 and 5.3.1.4, respectively. Indirect labor costs do not directly contribute to collector production, and are classified in three categories: supervisory labor, administrative expense, and plant maintenance costs. Supervisory labor costs account for inspection and quality control, shift supervisors, and other lower-level management personnel. Administrative expenses tally costs incurred for upper-level management and management support organizations. These include salaries and wages for administrators, clerical staff, and accountants. Both supervisory labor costs and administrative expenses are estimated as a percentage of direct production labor cost. Plant maintenance costs consist of expenses for scheduled maintenance and repair of the collector manufacturing facilities. These costs include materials, labor, and direct supervision. Plant maintenance costs are estimated as a percentage of plant capital costs.

Capital costs for the manufacturing facility are multiplied by the facilities' fixed charge rate to obtain an annualized cost contribution for capital costs. This approach is analogous to the use of the fixed charge rate in computing levelized busbar energy costs. Annualized contributions of capital cost obtained in this way account for both the depreciation of equipment and required rate of return on capital investment.

Plant overhead costs consist of expenses such as payroll burdens, employee benefits, safety inspections and equipment, and other general plant services unrelated to production. Plant overhead costs are computed as a percentage of direct and indirect labor costs.

Profit allowances are computed for both capital investment and manufacturing facility operating costs. Allowances for profit from capital investment are inherent in the treatment of capital investment cost. Profit allowances from operating costs are computed as a percentage of direct and indirect materials and labor cost, and plant overhead costs.

Collector manufacturing selling costs are calculated by adding direct and indirect materials and labor costs, capital investment depreciation, plant overhead costs, and manufacturing profit, and dividing this sum by the annual collector production rate. This yields the unit collector manufacturing cost, in $/collector.

5.3.1.7 Field Installation Cost Estimation

Field installation costs account for what happens to the collector after it leaves the manufacturing facility. All costs for field installation and construction tasks are considered field installation costs. These tasks typically consist of foundation construction, unpacking, and minor field assemblage of concentrators, installation of concentrator and receiver, and hookup to control and transport subsystems.

Based upon the manufacturing/installation scheme developed for each collector type, the major tasks to be performed in the field were identified. For conventional operations such as pouring foundations, costs are estimated using standard construction cost estimating information. For nonconventional operations such as collector installation and hookup, characterized by little or no available information, estimates are based on comparison to similar operations with known costs. Specialized vehicles are assumed to be available to facilitate field transportation and installation of the collectors.

Collector indirect construction costs are normally covered in the indirect cost reporting account. An exception is made when large field construction requirements indicate necessary additional indirect costs applicable only to collector construction. These indirect construction costs cover the additional supervision, engineering, and field mobilization costs incurred when a large percentage of collector construction occurs in the field. Collector indirect construction costs are estimated as a fraction of the field installation cost.

Collector manufacturing selling costs are added to the unit field installation cost to obtain the total installed collector cost.

5.3.2 Energy Conversion

The widely varying components used in alternative energy conversion subsystems are not conventional, off-the-shelf items. Rankine-cycle turbines as

a class have had extensive usage, but very few high-temperature and pressure turbines have been built in the 1 to 10 MWe capacity range. Similarly, Brayton-cycle engines have been used widely, but those designed specifically for solar applications have not been mass-produced. Only limited production experience exists for any Stirling-cycle engine.

Due to component nonconventionality, costs are strongly dependent on the component's assumed production rate. As production rate increases, component costs would decrease due to mass production benefits. The production dependence of energy conversion components requires that cost estimates be tied to a particular production rate, which for this study was the reference collector production rate. For distributed energy conversion systems using one engine per collector, assumed engine production rates correspond to collector production rates. For central energy conversion systems using one engine per power plant, engine production rates were chosen to correspond to the number of plants installed at the reference collector production rate. Assumed production rates and estimate costs for each energy conversion subsystem are found in Appendix B.

5.3.2.1 Rankine Cycle

Primary components of the Rankine-cycle energy conversion cost account are the heat engine, generator, and heat rejection units. High-temperature and pressure steam turbogenerators are used as engine/generator; heat is rejected by air-cooled condensers using no cooling water. Detailed component descriptions are given in Appendix A.3.3.

Steam turbogenerators are generally considered conventional technology, but production experience has been centered around much larger turbogenerators than are required for small power systems. Available cost information for small (1- to 10-MWe) turbogenerators is limited.

Cost estimates for turbogenerators in a wide range of sizes were compiled through literature reviews and contact with manufacturers. These cost estimates were used to judge the effects of economies of scale in steam turbogenerators, or how cost varies with unit size. Scaling exponents derived from these data were useful in interpreting cost estimates in the 1- to 10-MWe range, where data were scarce.

Turbogenerator cost information was also obtained from Bechtel National, Inc. In their report (Appendix C), they concluded that, although costs for turbogenerators in the 1- to 10-MWe range would be expected to decrease with increased production rates, no information is currently available to evaluate such an effect. This effect was taken into account in considering the cost data; turbogenerator cost estimates were developed assuming that some cost reduction would take place. The amount of cost reduction assumed was based upon cost estimates of the largest turbogenerators and estimated scaling parameters relating size to unit cost. It was assumed that decreases in cost due to increased production would not be enough to offset unit cost increases associated with decreasing turbogenerator size.

Current costs for state-of-the-art air-cooled condensers are quite high, in part because of limited production. It was assumed that, at the required production rates, costs for air-cooled condensers would fall in line with those of more conventional air-cooled heat rejection equipment. Air-cooled condenser costs were estimated using cost information for conventional air-cooled heat rejection equipment, with allowances for cost increases due to more sophisticated designs.

5.3.2.2 Brayton Cycle

Brayton-cycle engines are used for both distributed energy conversion, one per collector, and central energy conversion, one per plant. Design details of Brayton engines are found in Appendix A.3.2.

Brayton engines assumed for this study are not currently being produced, but are similar in design to units that have both limited and mass production experience. The principal information used in estimating the cost of Brayton engine/generators was obtained through AiResearch Manufacturing Company, and was the result of conceptual design studies for Brayton engines. A literature review was also used to establish costs for both current Brayton engines and proposed solar designs.

Installation costs were estimated separately from purchase price for Brayton engines, as opposed to Rankine engine estimates where costs in information sources were generally installed costs. Field installation tasks were

established for the engine/generator in the same manner as was described for the collector. Estimates of man-hours required per task were combined with average field wage rate to obtain installation costs.

5.3.2.3 Stirling Cycle

Stirling-cycle engines are used in distributed energy conversion subsystems, and are described in detail in Appendix A.3.1. As previously noted, little production experience exists with any Stirling engine, complicating the estimation of costs.

Stirling engine/generator costs were estimated using information from previous solar studies, manufacturing estimates of conceptual design Stirling engines, consultants, and cost information for Stirling engines that have been produced to date. These sources indicated that estimated costs were highly dependent upon assumed production rate. Care was taken in developing Stirling engine/generator cost estimates to ensure that the estimates were valid at the assumed engine production rate.

As with other cost estimates in this study, Stirling engine/generator estimated costs are actual selling costs, including indirect manufacturing costs, manufacturing overheads, and profit, in addition to direct manufacturing costs.

Installation costs for Stirling engine/generators were estimated separately from the purchase price. Installation costs were estimated similarly to those for Brayton engines, by identifying installation tasks, estimating man-hours to complete, and multiplying by an average wage rate to arrive at the installation cost.

5.3.3 Energy Storage

Energy storage subsystems are not conventional technology, and are not currently commercially produced. As such, cost estimates for energy storage subsystems depend considerably upon assumptions concerning industry maturity and component production rates. Energy storage subsystem cost estimates were developed assuming that energy storage technology had been demonstrated and was available for commercial application, under these assumptions. Costs associated with construction of "first of a kind" systems are not included.

Assumed production rates for energy storage subsystems were chosen to correspond to the number of solar plants installed under the reference collector production assumption. At these production rates it was assumed that indirect construction costs will be similar to those for other plant subsystems.

Although application of energy storage subsystems is considered nonconventional technology, the majority of storage system components are conventional, commercially available hardware, with cost levels unlikely to be affected by the commercial development of energy storage subsystems. Where possible, subsystem costs were developed by aggregation of component costs with costs for conventional components developed from vendors' quotes, cost estimating guides, and other current cost information.

5.3.3.1 Thermal Storage

Thermal storage subsystems considered differ primarily in the choice of storage medium: high-temperature storage subsystems use heat transfer salts; low-temperature storage subsystems use heat transfer oil. Detailed descriptions of both thermal storage subsystem types are found in Appendix A-2.1. Identical procedures were used in estimating costs of the high- and low-temperature subsystems.

Although thermal storage applications are not considered conventional technology, all subsystem components such as storage tanks, pumps, insulation and heat exchangers are conventional items. Cost estimates for thermal storage subsystems were developed by individually estimating costs for each subsystem component. Primary sources used were cost estimating manuals and contact with manufacturers and vendors. These sources, in many cases, were identical to sources used in developing component cost estimates for other subsystems, a factor contributing to consistency among estimates. In addition to the primary cost information sources, other studies discussing thermal storage subsystem costs were also reviewed, both as an aid in estimating component costs and a check on the overall subsystem cost estimate.

5.3.3.2 Electric Storage

Electric storage subsystems considered use lead acid, advanced generic, or Redox batteries. Lead acid batteries can be considered near-term technology

for storing electric energy, while advanced generic and Redox batteries use more advanced technologies. Descriptions of all battery types are contained in Appendix A.2.2.

Cost estimates for lead acid batteries were obtained from review of manufacturing cost estimates developed by major battery proponents. Cost estimates for other subsystem components were developed using information from other studies and independent estimates.

Redox battery electric storage subsystems offer promise of low-cost electric energy storage using advanced technology. Cost estimates for Redox battery and advanced generic subsystems were developed using information obtained through literature reviews.

5.3.4 Energy Transport

Energy transport subsystems use either electrical energy transport or thermal energy transport. Both types are described in detail in Appendix A. Conventional components and technologies are used in both thermal and electric transport subsystems, making cost estimates relatively insensitive to assumptions regarding the number of systems produced.

Cost estimates for energy transport subsystems were developed by aggregating individual cost estimates for major subsystem components. All estimates assume good labor productivity. Cost estimates do not contain contingency factors or indirect field construction costs, which are covered in separate cost accounts.

5.3.4.1 Thermal Energy Transport

Major components of thermal energy transport subsystems are piping runs, valves, pumps, and insulation. These components are conventional, and are described in detail in Appendix A.1. Cost estimates were developed using material requirements and specifications obtained from transport subsystem designs.

Cost estimates for pipe runs were based upon specifications of pipe diameter, schedule, construction material, and length. Pipe is assumed to run either along the ground or in pipe trenches. Pipe trench length was estimated

as a fraction of the length of the total piping run. A standardized unit cost base was developed for pipe and pipe trench, using cost estimating manuals, construction cost estimating guides, and information from vendors. This unit cost base was used in evaluating all concepts.

Cost estimates for pipe fittings were developed for several transport systems using specifications detailing types and numbers of fittings, as well as the same cost information sources used in estimating pipe costs. These detailed cost estimates were used to derive estimating relationships correlating fittings cost with pipe cost. The estimating relationships were then used to estimate fittings cost for the majority of transport subsystems.

Costs for valves, pumps, insulation, and other transport subsystem components were estimated using methods and cost information sources similar to those used in estimating pipe costs. Specifications and materials quantities were obtained for each of these components, and combined with other component costs to generate the overall thermal energy transport subsystem cost estimates.

5.3.4.2 Electric Energy Transport

Major elements of electric energy transport subsystems are electrical cable, capacitors, and switching equipment. Detailed subsystem descriptions are contained in Appendix A.

All components of electric energy transport subsystems are conventional hardware. Subsystem cost estimates were developed analogously to those for thermal energy transport subsystems, based upon materials requirements and specifications obtained from subsystem designs. A standardized set of materials and installation costs was developed, using construction cost estimating guides as sources, and used for all electric energy transport subsystem cost estimating.

5.3.5 Other Plant

Components making up "other plant" cost accounts tend to be common to broad groups of concepts. This commonality of "other plant" components makes them poor differentiators among concepts. Because of the small contribution

of "other plant" components to differences between concepts, primary attention in estimating system costs was focused upon the four primary subsystems: collectors, energy transport, energy conversion, and energy storage. The approach used to estimate "other plant" costs is described in the following six subsections.

5.3.5.1 Power Conditioning

Equipment required for the power conditioning cost account was assumed to be identical for all concepts. Therefore, costs for power conditioning equipment do not discriminate among concepts. Cost estimates for power conditioning equipment were obtained from a previous study assessing the costs for constructing geothermal power plants (Schulte 1977).

5.3.5.2 Structures

Building requirements contained in the structures cost account are assumed to be identical among concepts. Floor areas for each required structure were developed for 1-, 5-, and 10-MWe plants, and used as a basis to estimate structures costs. Average building costs on a $\$/ft^2$ basis were obtained from construction cost estimating manuals, and applied to floor area estimates to arrive at structures costs.

5.3.5.3 Land

Land requirements are determined by surface area required for the collector field, and surface area required for the remainder of the plant. Remainder of plant area requirements account for plant structures, access roads, and a plant perimeter, and were assumed to be identical for all concepts.

Unit costs for raw land were established as a study ground rule. Unit costs for site preparation were developed using information from construction cost estimating manuals. Site preparation requirements were assumed to be equivalent for all land, both collector field-related and remainder of plant-related.

5.3.5.4 Instrumentation and Control

Cost estimates for instrumentation and control components assume that major components are commercially available. Instrumentation and control

costs were assumed to be equal for concepts with similar collector tracking requirements and energy conversion systems.

Costs associated with central computer control for the plants were assumed to vary with nameplate plant rating, and to be relatively insensitive to changes in collector field size or storage subsystem size. Central computer control costs were estimated using information from cost estimates for the Barstow pilot plant (Honeywell, Inc. 1977). Cost reductions due to increased commercial production of control systems were factored in to these estimates. Costs for central computer control were assumed to be identical for concepts with similar tracking requirements, i.e., two-axis tracking, one-axis tracking, and nontracking.

Costs for instrumentation and control components other than central computer control were estimated as percentages of plant equipment costs. Estimating percentages used were based upon information obtained from cost estimating guides.

5.3.5.5 Spare Parts

Cost allowances required for spare parts were assumed to be similar for all concepts. Spare parts allowances were based upon subjective judgment and information from other studies. Estimated costs for spare parts were computed as a percentage of equipment costs.

5.3.5.6 Service Facilities

Differences in costs among concepts for service facilities were assumed to be related primarily to type of energy conversion subsystem employed and to the complexity of collector cleaning vehicles. Cost estimates for service facilities not related to collector cleaning were developed using information from cost estimating manuals. Cost estimates for collector cleaning systems were based upon comparison of conceptual design of cleaning systems to similar, currently available equipment. Service facilities costs were estimated as a percentage of plant equipment costs.

5.3.6 Indirect and Contingency

Indirect construction costs and contingency costs were estimated as percentages of direct capital costs. Estimating percentages were developed from a review of construction cost estimating guides, previous solar study cost estimates, and cost estimates for other advanced energy concepts.

Estimating percentages used for contingency costs were identical for all concepts. With exception of the portion of indirect costs allocated for engineering and field supervision, indirect construction cost estimating percentages were also identical for all concepts. Cost estimating percentages for engineering and field supervision costs varied between concepts, with variations based upon differences in the complexity of designing and constructing the concepts.

5.3.7 Cost Estimate Scaling Relationships

Cost estimate scaling relationships (CESRs) are mathematical relationships used to estimate how component costs will vary with changes in component physical parameters, such as size or power rating. The advantage of CESRs is that, once they are generated, they can be used to quickly estimate component costs over a wide range of component sizes and capacities. For each capital investment component, a CESR is developed and implemented in the plant simulation code SOLSTEP. This approach allows simulation of many plant configurations without developing detailed cost estimates for each. An additional benefit of using CESRs to estimate plant capital investment costs is that it allows a much more detailed analysis of how plant costs will vary with design changes. Plant design variations, such as changes in collector field size, will affect costs of each plant component differently. With proper use of CESRs for each component, the effects of plant design changes are readily known.

Development of CESRs involved defining any component-specific constraints, or assumptions, or both; determining which physical parameters can best be related to component costs; estimating costs for the component at several values of the physical scaling parameters; and using regression analysis to determine the form and coefficients of the CESR. Constraints and assumptions are necessary to reduce the complexity of developing CESRs because even simple,

off-the-shelf items rarely have costs which are a function of only several variables. Making qualifying constraints and assumptions allows one or two physical parameters to be chosen to which component cost can adequately be related. Ranges of interest were then established for the physical parameters and several component cost estimates were developed at points spanning the area of interest. Standard regression analysis was used to establish the CESR with the form of the relationship being chosen based upon statistical tests and graphical interpretation of the results.

Cost estimate scaling relationships used in this study generally have forms such as

$$\text{Cost} = A + B(X)^S + C(Y)^T$$

Here X and Y are physical scaling parameters, the component characteristics used to scale component costs. Fixed costs are any costs not related to the physical scaling parameters, and are represented by A. Variable costs coefficients are represented by B and C, and S and T represent scaling factors.

Functional forms of the CESR for each capital investment cost account are given in Table 5.4. Coefficient values for each concept are found in Appendix B. It should be noted that many restrictions apply toward the application of the CESRs to generate capital cost estimates and, as such, they should not be used as component cost predictors for other studies.

5.4 REPLACEMENT CAPITAL COST ESTIMATING

Assessing the economic significance of replacement capital costs requires estimates of both component replacement cost and component lifetime. This task is complicated by the fact that component lifetime and replacement costs are interrelated. From a broad perspective, component replacement would occur when the replacement resulted in the lowest lifetime cost of energy from the plant. For expensive components, the optimal economic solution may be to suffer degraded system performance for long periods rather than to pay for

TABLE 5.4. Cost Estimate Scaling Relationships for Capital Investment Cost Accounts

Subsystem	Relationship	Term Definition
Concentrator	$\text{Cost} = A + B(X)^S$	X = Collector field size, m^2
Receiver	$\text{Cost} = A + B(X)^S + C(X)^T$	X = Collector field size, m^2
Thermal Transport	$\text{Cost} = A + B(X)^S + \frac{C + D(X)^T}{Y^V}$	X = Number of collectors Y = Ground cover ratio
	$\text{Cost} = A + \left(\frac{X - B}{C}\right)^S$	X = Collector field size, m^2
Electric Transport	$\text{Cost} = A(X) + \left[\frac{B + C(X)}{Y^V}\right]$	X = Number of collectors Y = Ground cover ratio
Energy Conversion	$\text{Cost} = \left[A + B(X)^S\right]\left(Y^T\right)$	X = Nameplate plant rating, MWe Y = Number of collectors
Power Conditioning	$\text{Cost} = A + B(X)^S$	X = Nameplate plant rating, MWe
Thermal/Electric Storage	$\text{Cost} = A + B(X)^S$	X = Storage capacity, kWht
Structures	$\text{Cost} = A + B(X)^S$	X = Nameplate plant rating, MWe
Land	$\text{Cost} = A\left[B + C(X) + \frac{Y}{Z}\right]$	X = Nameplate plant rating, MWe Y = Collector field size, m^2 Z = Ground cover ratio
Instrumentation and Control	$\text{Cost} = A + B(X) + C(Y)$	X = Concentrator cost Y = Cost of receiver, structures, thermal transport, electric transport, power conditioning, energy conversion, land, thermal/electric storage
Spare Parts	$\text{Cost} = A(X)^S$	X = Cost of concentrator, receiver, thermal transport, electric transport, energy conversion, power conditioning, thermal/-electric storage, structures, and instrumentation and control
Service Facilities	$\text{Cost} = A(X)^S$	X = Cost of concentrator, receiver thermal transport, electric transport, energy conversion, power conditioning, thermal/electric storage, structures and instrumentation and control

component replacement. For relatively inexpensive components, optimal replacement may occur after only slight degradation of system performance.

A detailed analysis to determine optimal values of replacement capital costs was considered beyond the scope of this project. The approach used to estimate replacement capital costs was based upon expectations of maximum component lifetimes, degradation of component performance, and component replacement costs. If existing information on component lifetimes suggested a maximum lifetime less than the 30-year assumed plant lifetime, replacement was assumed to occur after the maximum component life. If component performance degradation was expected, and if replacement costs were low, component replacement was assumed to occur before complete failure at the end of its maximum lifetime. Unless otherwise specified, all components were assumed to have a 30-year lifetime.

5.4.1 Collector Replacement

Reflective surfaces not protected by glass covers were assumed to require replacement after 15 years due to surface degradation. Cost estimates for reflective surface replacement were based upon the original materials cost, plus an allowance for field installation of the surface. Installation costs assume that collectors are designed for easy reflective surface replacement, so only small costs for installation labor were involved.

The protective cover glass on the LCNT collector was assumed to be cost-effective to replace after 15 years. This assumption was based upon expectations of greater than normal surface scoring due to the inability of the LCNT collector to go to a stow position, and the low cost of replacing the cover glass.

All other collector components were assumed to have 30-year lifetimes.

5.4.2 Energy Conversion Replacement

Estimates of Stirling-cycle engine lifetimes from other studies (Fujita et al. 1978)[(a)] and contact with a consultant (Martini 1979) were used to

(a) Estimates were also obtained from Mechanical Technology, Inc.

develop Stirling engine lifetime assumptions. Free-piston Stirling engines were assumed to require major overhauls after 15 years of operation. This overhaul would be performed by detaching the engine in the field, shipping it to a repair facility, and installing a new one in its place. Overhaul costs were assumed to be 50% of the original engine cost.

Brayton-cycle engine lifetime assumptions were developed using information from other studies and contact with manufacturers. Small Brayton engines used in the PFDR/B concept were assumed to require a major overhaul every 15 years, which would be performed in a manner similar to the Stirling engine overhaul. Overhaul costs were assumed to be 50% of the original engine cost. The lifetime estimates for the Brayton engine used in the PFCR/B concept were based upon specific information obtained from AiResearch Manufacturing Company. The time between overhauls for this engine was assumed to be 23 years, with overhaul costs equaling 40% of the original engine cost.

5.5 OPERATING AND MAINTENANCE COSTS

Analysis by PNL has indicated that, under some conditions, O&M costs can become major determinants of levelized energy cost for solar thermal small power systems. Depending upon initial assumptions and operation scenarios used, O&M costs can constitute between 10% and 45% of total levelized energy costs for 1-MWe plants. Due to the potentially large impact of O&M costs, PNL spent considerable effort to identify key assumptions affecting O&M costs, and determine differences in O&M requirements for various concepts.

In general, two types of information are required for estimating O&M costs. System operating information relates to what the actual requirements for plant operations will be. Information regarding system integration into an existing utility grid dictates the administrative requirements for the plant, and determines the magnitude of operating, maintenance, and overhead costs that are assigned directly to the small power system, as opposed to being allocated against fixed overheads already present in the grid.

Systems operating information must determine both operating and maintenance requirements, and how these requirements will vary with plant size changes. The number of plant operators required, their duties, and the phases

of plant operation needing operators must all be determined. Scheduled maintenance must be identified, along with resources necessary for its completion. Items potentially needing unscheduled maintenance must be identified, and estimates of repair or replacement cost made.

Systems integration information relates primarily to the utility grid in which the small power system is installed, rather than to the power system itself. Large utility grids would have the capacity to absorb plant administrative costs and portions of plant operating and maintenance into an existing utility overhead. Smaller utility grids would be less capable of doing this, and consequently would have higher marginal costs associated with the solar plant addition.

Two primary assumptions concerning system integration were made by PNL in estimating small power systems O&M costs. First, it was assumed that the utility had the capacity to absorb the administrative costs associated with the small power system. This assumption should prove reasonable for all but very small utilities, and has the effect of deleting all administrative costs from O&M costs. Second, it was assumed that all required scheduled and unscheduled maintenance would be performed by a subcontractor. This would prove more economical than hiring a full-time maintenance crew. It also seemed more reasonable than assuming maintenance requirements would be absorbed by existing maintenance crews within the utility, because it was felt that utilities operating small solar power systems would not have this capability.

5.5.1 Direct Production Costs

Direct production costs consist of costs for plant operators. These are estimated based upon expectations of plant operating requirements. For each concept, plant operating tasks were described, assuming the use of highly automatic control subsystems. These plant operating tasks were used to develop estimates of plant operator requirements, or how long operators were required each day. Estimates of plant operator requirements are given in Appendix B.

Estimates of direct production costs were developed assuming that one operator would be present whenever each plant was operating, and that these operators would perform routine scheduled maintenance when not actively

involved in plant operations. The number of operators required for each plant configuration was determined by SOLSTEP, based upon the number of hours yearly the plant was operated and assuming a normal 40-hour work week for operators. Additional operators were added when plant operating hours would require operators working in excess of 8 overtime hours per week. Assumed salaries for plant operators were based upon average wage rates for similar positions.

5.5.2 Maintenance Costs

Scheduled maintenance includes collector cleaning, subsystem inspection, and regular required subsystem maintenance. Unscheduled maintenance consists of minor repair or replacement to items such as valves or controls.

Scheduled maintenance requirments are of two types: fixed and variable. Variable maintenance requirements change as collector field size changes. Fixed maintenance requirements remain constant as collector field size varies, and are assumed to remain constant as power plant rating changes as well.

Scheduled maintenance tasks are estimated for six major areas: collector subsystem, transport subsystem, energy conversion subsystem, storage subsystem, power conditioning subsystem, and plant grounds. Requirements for collector subsystem scheduled maintenance are inspection, lubrication, alignment and adjustment, and cleaning. Inspection is performed quarterly for all concepts, and consists of a check for defects such as mounting and foundation shifts, broken or degraded reflective surfaces, and malfunctioning tracking units. Lubrication includes greasing and cleaning contact surfaces in tracking mechanisms, and is performed quarterly for all tracking concepts. Alignment and adjustment are performed quarterly for tracking concepts, as is corrective action for errors in collector alignment. Monthly adjustments are made to the LCNT system to optimize energy collected. Cleaning is performed weekly for all concepts, and assumed to be done using specialized vehicles developed for collector cleaning. Estimated man-hour requirements to complete scheduled maintenance tasks are summarized in Appendix B.

Costs for scheduled maintenance were developed in SOLSTEP, based upon maintenance man-hour requirements and the number of hours operators were

available to perform maintenance. Hourly costs for maintenance personnel were assumed to be equivalent to average wage rates for construction labor.

Unscheduled maintenance costs were estimated as a percentage of equipment cost, with estimating percentages developed using information from cost estimating guides. These costs were developed assuming that systems have been designed to minimize unscheduled maintenance requirements.

5.5.3 Overhead Costs

Payroll overheads for operations and maintenance staff were estimated as a percentage of direct production cost and maintenance cost. Estimating percentages were based upon information from other industries.

REFERENCES

Allen, J. W., N. M. Levitz, A. Rabl, K. A. Reed, W. W. Schertz, G. Thodos, and R. Winston. 1976. Development and Demonstration of Compound Parabolic Concentrators for Solar Thermal Power Generation and Heating and Cooling Applications. ANL-76-71, Argonne National Laboratory, Argonne, Illinois.

Apley, W. J. 1978. Systems Analysis of Solar Thermal Power Systems, Report on Task 1 - Determination and Characterization of Solar Thermal Conversion Options. PNL-2693, Pacific Northwest Laboratory, Richland, Washington.

Arthur D. Little. 1975. Goals Study for Technical Development and Economic Evaluation of the Compound Parabolic Concentrator Concept for Solar Energy Collector Applications. Report No. 78372, Arthur D. Little, Inc., Cambridge, Massachusetts.

Caputo, R. S. 1975. An Initial Study of Solar Power Plants Using a Distributed Network of Point Focusing Collectors. Report No. EM342-308 (900-724), Jet Propulsion Laboratory, Pasadena, California.

Clausing, A. M. 1976. Potential of a Solar Collector with a Stationary Spherical Reflector and a Tracking Absorber for Electrical Power Production. SAND76-8039, Sandia Laboratories, Albuquerque, New Mexico.

Clements, L. D., and J. D. Reichert. 1979. "Optical-Thermal Performance Analysis for a Fixed Mirror Distributed Focal Solar-Thermal-Electric Power System." In Proceedings of 14th IECEC. Boston, Massachusetts.

Cole, R., W. Schertz, and W. P. Teagan. 1977. "Conceptual Design of a 5x CPC for Solar Total Energy Systems." In Proceedings of Concentrating Solar Collector Conference. CONF-770953-5, National Technical Information Service, Springfield, Virginia.

Collares-Pereira, M., J. J. O'Gallagher, A. Rabl, and R. Winston. 1978. "A Compound Parabolic Concentrator for a High Temperature Solar Collector Requiring Only Twelve Tilt Adjustments Per Year." In Proceedings of the January 1978 International Solar Energy Congress Meeting. New Delhi, India.

Dochat, G. R., and H. M. Cameron. 1979. "15 kW Free-Piston Solar Stirling Engine/Alternator." In Proceedings of 3rd Semi-Annual Advanced Technology Meeting, pp. 29-46. Long Beach, California.

Dudley, V. E., and R. M. Workhoven. 1978. Performance Testing of the Hexcel Parabolic-Trough Solar Collector. SAND78-0381, Sandia Laboratories, Albuquerque, New Mexico.

FMC Corporation. 1976. Central Receiver Research Study--Monthly Technical Progress Report #6. FMC Corporation, Santa Clara, California.

FMC Corporation. 1977. Central Receiver Research Study--Monthly Technical Progress Report #10. Report No. R-3630, FMC Corporation, Santa Clara, California.

FMC Corporation. 1978. Line Focus Solar Central Power System, Volume 1: Technical Report. FMC P-3750, FMC Corporation, Santa Clara, California.

FMC Corporation and Stanford Research Institute. 1976. Solar Thermal Electric Central Receiver Research Study, Semiannual Review. FMC Corporation, Santa Clara, California.

FMC Corporation and Stanford Research Institute. 1977. Solar Thermal Electric Central Receiver Research Study, Interim Report. FMC Corporation, Santa Clara, California.

General Atomic. 1978. Line Focus Solar Central Power Systems Phase 1 Midterm Topical Report for the Period September 30, 1978 through March 31, 1979. General Atomic, San Diego, California.

Haglund, R., and R. Tatge. 1979. "Dish Stirling Solar Receiver (DSSR)." In Proceeding of 3rd Semi-Annual Advanced Technology Meeting, pp. 20-28. Long Beach, California.

Hallet, R. W., and R. L. Gervais. 1977a. Central Receiver Solar Thermal Power System Phase 1, CDRL Item 2, Vol. 3. SAN/1108-8/2, McDonnell Douglas Astronautics Company, Huntington Beach, California.

Hallet, R. W., and R. L. Gervais. 1977b. Central Receiver Solar Thermal Power System Phase 1, CDRL Item 2, Vol. 5. SAN/1108-8/5, McDonnell Douglas Astronautics Company, Huntington Beach, California.

Russell, J. L., E. P. DePlomb, and R. K. Bansal. 1977. Principles of the Fixed Mirror Solar Concentrator. Report No. GA-A12902, General Atomic, San Diego, California.

Sandia Laboratories. 1978. Solar Central Receiver Systems. Livervmore, California.

Schuster, J. R., J. L. Russell, G. H. Eggers, and S. V. Shelton. 1978. Fixed Mirror Solar Concentrator for Power Generation. Report No. GA-A14883, General Atomic, San Diego, California.

Solaramics. 1978. Solar Central Receiver Prototype Heliostat. SAN-1745-1 (Vol. 1), El Segundo, California.

Texas Tech University and E-Systems, Inc. 1977. Crosbyton Solar Power Project - Phase 1, Vols. 1-3. CSP-TR-1, Texas Tech University, Lubbock, Texas.

Texas Tech University and E-Systems, Inc. 1978. Crosbyton Solar Power Project - Phase 1, Vols. 4-5. CSP-TR-2, Texas Tech University, Lubbock, Texas.

Truscello, V. C. 1978. "The Parabolic Concentrating Collector." In Proceedings of Solar Thermal Concentrating Collector Technology Symposium. Denver, Colorado.

Wu, Y., and L. Wen. 1978. Solar Receiver Performance in the Temperature Range of 300 to 1300°C. JPL-5102-82, Jet Propulsion Laboratory, Pasadena, California.

Zimmerman, W. F. 1979. "Heat Pipe Heat Receivers with TES." In Proceedings of 3rd Semi-Annual Advanced Technology Meeting, pp. 15-19. Long Beach, California.

APPENDIX A

STANDARDIZED SUBSYSTEMS

APPENDIX A

STANDARDIZED SUBSYSTEMS

A.1 TRANSPORT SUBSYSTEM

When considering the transport subsystem, the various concepts can be classified into one of two types: 1) those with energy storage between the collector subsystem and the energy conversion subsystem, and 2) those with energy storage after the energy conversion subsystem. Both arrangements are shown in Figure A.1. In concepts with energy storage between the collector and energy conversion subsystems, the collector subsystem absorbs thermal energy; the transport subsystem transfers this thermal energy to either the storage or energy conversion subsystem. The collector subsystem in concepts with energy storage after the energy conversion subsystem absorbs thermal energy. This energy is then converted to electrical energy in the energy conversion subsystem. The transport subsystem transfers the electrical energy to either the storage subsystem or the utility power grid.

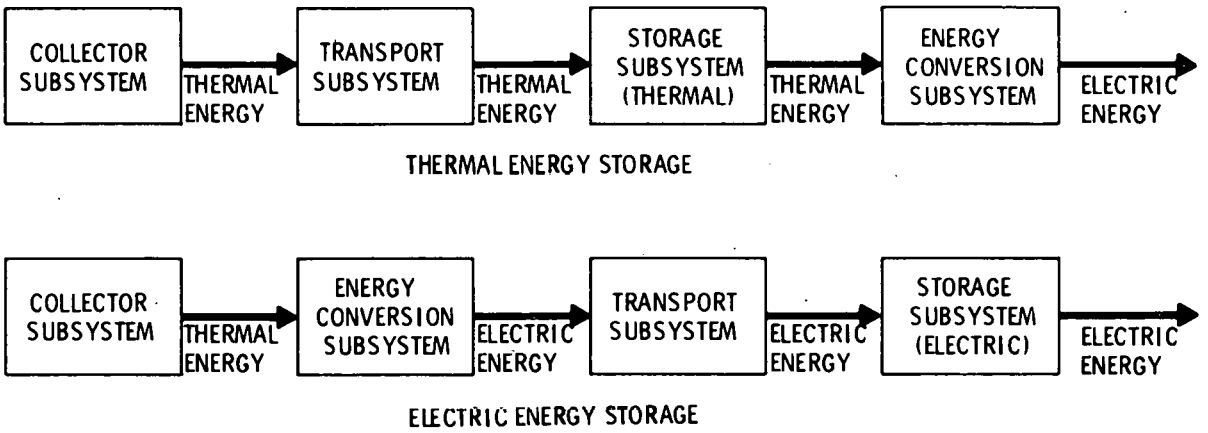

FIGURE A.1. Concept Arrangements for Thermal and Electric Storage

From the above discussion, it is obvious that two generic types of transport subsystems are required--a thermal energy transport subsystem and an electrical transport subsystem. Five alternative thermal transport subsystems, each using a different working fluid, were considered:

- Heat Transfer Oil Transport Subsystem - This subsystem uses a heat transfer oil such as Caloria HT45 for the heat transfer fluid. Because the decomposition rate of heat transfer oil is unacceptably high above an operating temperature of 304°C (580°F), this approach was considered for the low temperature concepts only, such as the LCNT and LFDR-TC.
- Water/Steam Transport Subsystem - This subsystem uses water/steam as the heat transfer fluid. This approach represents current technology, so it was considered the near-term heat transfer subsystem for the intermediate- and high-temperature thermal energy transport subsystems.
- Intermediate-Temperature Heat Transfer Salt Subsystem - This subsystem uses a heat transfer salt such as HITEC for the working fluid. The maximum operating temperature is limited to 454°C (850°F) to allow the use of carbon steel in the transport subsystem.
- High-Temperature Heat Transfer Salt Subsystem - This subsystem also uses a heat transfer salt such as HITEC for the working fluid. Operating temperatures are now limited to 538°C (1000°F), requiring the use of stainless steel in the high-temperature sections of the transport subsystem.
- Low-Cost Heat Transfer Salt Subsystem - This subsystem is similar to the intermediate-temperature heat transfer salt subsystem except that a low cost heat transfer salt such as less refined draw salt is assumed to be used in a transport subsystem.

These five transport subsystems will be discussed in Sections A.1.1 through A.1.5. Their arrangements and the methods used to analyze components and performance will be described.

Only one type of electrical transport subsystem was analyzed, because it was assumed that no substantial improvement would occur in its performance or cost. This subsystem is discussed in Section A.1.6.

A.1.1 Oil Transport Subsystem

The oil transport subsystem uses current technology with a relatively inexpensive heat transfer fluid, which exhibits good thermal properties. The primary disadvantage of using heat transfer oil as a working fluid is that it decomposes at high temperatures. Above 304°C (580°F) the decomposition rate is intolerably high. This limits the oil transport subsystem to lower temperature applications. The only concepts with sufficiently low maximum operating temperature are the LCNT (CPC), operating at 232°C (450°F) and the LFDR-TC, which operates at 304°C (580°F).

A.1.1.1 Subsystem Arrangement

In all distributed receiver concepts, the collectors are arranged in standard modules and the modules are arranged to form the collector field. The transport subsystem must supply low-temperature oil to the modules, distribute it through the module internal piping, and return it to the central generating facility. The subsystem consists of four components: heat transfer oil, module distribution piping, module internal piping, and feed pump. The components are arranged as shown in Figure A.2.

The oil transport subsystem arrangement is simpler than that of a similar water/steam system because oil does not experience a phase change; once-through heating can be used with confidence. In addition, the same fluid is used as

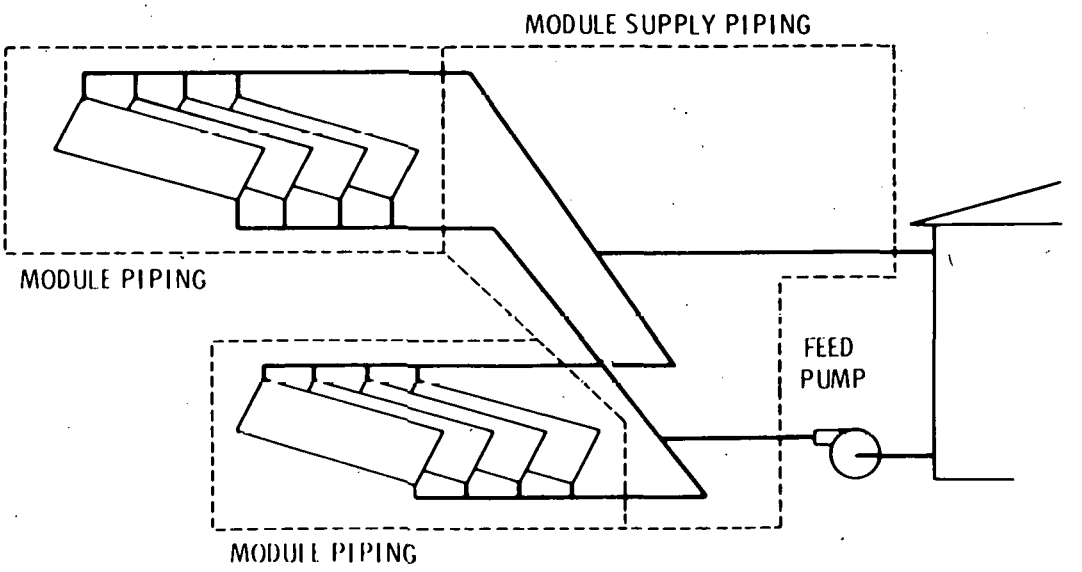

FIGURE A.2. Oil Transport Subsystem Component Arrangement

the working fluid in both the transport and storage subsystems; therefore, oil can be supplied directly from, and returned directly to, storage, eliminating the storage charging heat exchanger loop.

A.1.1.2 Component Analysis

Five components of the oil transport subsystem required either sizing or material selection:

- heat transfer fluid
- piping
- valves
- insulation
- feed pump.

Each is discussed in the following paragraphs.

Several heat transfer oils are available for high-temperature applications. Previous studies (Hallet and Gervais 1977, p. 4-23) have indicated that Caloria HT45 is the most attractive heat transfer oil from both volumetric storage and cost standpoints. In addition, Caloria has good stability and no fouling in the temperature range being considered. Because Caloria HT45 is also used in the thermal storage subsystem, it was decided to use Caloria as the heat transfer fluid. Properties of Caloria HT45 are given in Hallet and Gervais.

The transport subsystems have two types of piping: the module internal piping and the module distribution piping. Both were sized in a similar manner. First, an assumed piping layout was developed, which appeared to minimize the required length of piping, but the piping layout was not formally optimized. The mass flow rates of oil were determined from an energy balance on appropriate collectors, design temperature rise in the fluid, and the fluid specific heat. Based on the design mass flow rate of oil, the design velocity, and fluid density, the required pipe diameter was calculated for each component of the piping system. Using the pipe diameters, lengths, and design velocity, the pressure drop and pump work were calculated for the piping, system. If either the pipe diameters or the pump work seemed excessive, the design

velocity was modified and the process repeated until reasonable pipe diameters and pump work were obtained.

Thermal expansion of the piping required including expansion joints in the module internal piping design. In the longer module distribution piping, thermal expansion is handled by increasing the length of the piping by a factor of $\sqrt{2}$ to provide for either expansion loops or some other compensatory method.

In all cases, Schedule 40 carbon steel piping was assumed. Appropriate flanges and fittings were assumed and included in the cost estimate.

All valves were specified as #600 class carbon steel gate valves.

Insulation was specified as calcium silicate with appropriate lagging. Insulation thickness was based on optimal insulation thickness given in Perry, Chilton, and Kirkpatrick (1963).

The feed pump was sized using the transport system pumping power determined in the pipe sizing routine. A carbon steel, motor-driven centrifugal pump with a pump efficiency of 75% was assumed.

A.1.1.3 Performance Analysis

The transport subsystem impacts plant performance in two areas--heat loss from the subsystem itself and power used by the feed pumps.

Heat loss through the piping insulation was calculated assuming that the dominant resistance to heat transfer was the insulation so that the insulation inner wall temperature was that of the oil and the outer wall temperature was that of the ambient air. Ambient temperature was assumed to be 70^{o}F. Further thermal loss would occur when the transport subsystem cooled during periods of no insolation. This was not included in the transport subsystem heat loss because it was assumed that the subsystem would be warmed to operating temperature by the solar energy collected during the turbine startup procedure. If this energy were not used to warm the transport subsystem, it would be wasted because the turbine could operate only at some fraction of full load.

The base case pumping power was calculated in the pump sizing routine (see A.1.1.2) for full load using an assumed field size and ground cover ratio. Because the computer simulation considers a range of field sizes, the pumping power must be determined for varying field size, ground cover ratios, and part-load operation. The installed pumping power is assumed to vary linearly with field size and logarithmically with ground cover ratio.

$$\text{Installed pumping power} = (a + b\ln x)(cy)$$

where

x is ground cover ratio
y is field size
a, b, c are constants determined from the base case.

Actual pumping power includes the effect of part-load operation.

$$\text{Actual pumping power} = [0.25 + 0.75(dz)]\ (\text{installed pumping power})$$

where

z is the energy flow rate through the pump
d is a constant determined from the base case.

A.1.2 Water/Steam Transport

The water/steam transport subsystem has the advantage of using current technology with an extremely low-cost heat transfer fluid with excellent thermal properties. The primary disadvantage of the water/steam transport subsystem is that water experiences a phase change with a high vapor pressure. High pressure piping is required. In addition, heat exchangers are necessary to transfer energy into the storage subsystem, resulting in a loss of availability. The water/steam alternative is considered the near-term transport subsystem for all concepts using a thermal transport subsystem, except the LCNT and LFDR-TC concepts.

A.1.2.1 Subsystem Arrangement

In all distributed receiver concepts, the collectors are arranged in standard modules and the modules are arranged to form the collector field. For these concepts, the transport subsystem consists of the module distribution piping, module internal equipment, and the collector feed pump. The central receiver concepts have only one receiver, so modules are not required. For these concepts the transport subsystem consists of the receiver supply and return piping and the receiver feed pump.

There are two approaches to generating steam in the collector field or receiver. One method involves once-through steam generation in which the steam is preheated, boiled, and superheated in a single pass through the receiver. The second method involves separate steam generation and superheating receivers or modules. In such a system, feedwater from the plant is supplied to the steam drum of the steam generation module. A circulating pump takes water from the steam drum and circulates it through the steam generation module. The water is preheated; approximately one-sixth is evaporated. The water/steam mixture is returned to the steam drum, where the steam is separated from the water and sent to the superheater module. In the superheater module, the saturated steam is superheated and transported back to the central generation facility. Figure A.3 illustrates this transport subsystem. Due to the difficulties in once-through steam generation, particularly with many parallel flow paths, the approach using a steam generator followed by a superheater was used for all concepts except the PFCR.

The conditions of the steam exiting the superheater module are determined by a trade-off between receiver performance, which decreases with steam temperature, and heat engine efficiency, which increases with steam temperature. Standard steam conditions of 510°C (950°F) and 10,000 kPa (1450 psi) were used wherever possible. These steam conditions are the same as those used at the Barstow pilot plant. The one exception is the LFDR-TC, where steam conditions of 343°C (650°F) and 4830 kPa (700 psi) were used. In all cases the feedwater was assumed to be at 204°C (400°F).

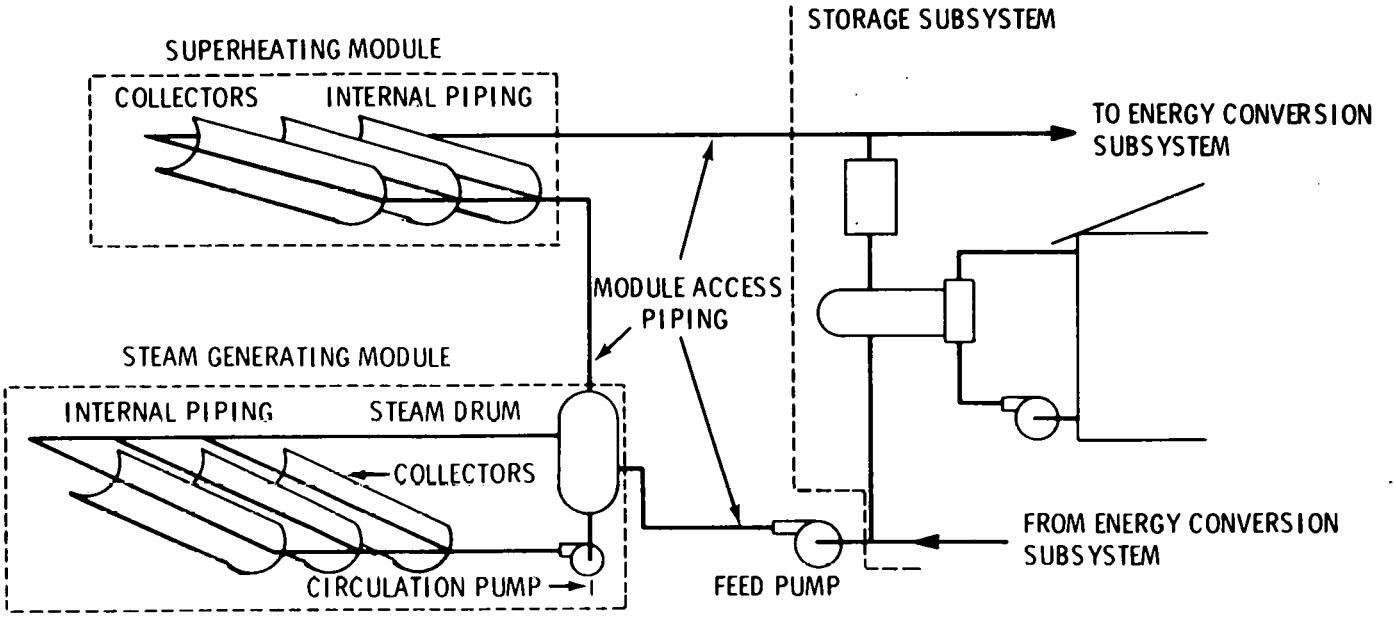

FIGURE A.3. Water/Steam Transport Subsystem Arrangement

This transport subsystem includes an accumulator and appropriate valves. Because oil is used as the energy storage fluid, the storage subsystem must include storage charging heat exchangers. In addition, the temperature of the oil cannot rise above 304°C (580°F), which may require desuperheating the steam before it enters the storage charging heat exchangers.

The distributed receiver concepts (PFDR/R, LFDR-TR, LFDR-TC, and FMDF) are arranged in standard modules. Each concept has a standard steam generator module and a standard superheater module. Each type of standard module is an arrangement of parallel and series flow paths. The standard steam generator module includes a steam drum and circulating pump.

A.1.2.2 Component Analysis

The water/steam transport subsystem has several components that require either sizing or material selection, including:

- heat transfer fluid
- piping
- valves
- insulation
- pumps.

The water used in the water/steam transport subsystem must be of sufficient purity to prevent scaling and corrosion in the receiver tubes.

Piping may be divided into five types: steam generator module feedwater supply piping, steam generator module internal piping, superheater module supply piping, superheater module internal piping, and superheated steam return piping. The steam generator module feedwater supply piping carries subcooled liquid at inlet conditions. The module internal piping carries either saturated liquid or low quality steam, depending on the location in the module. Superheater module supply piping carries saturated steam; the superheater internal and return piping carry superheated steam.

An assumed piping layout was developed for each piping type. The layout appeared to minimize the required length of piping, but was not optimized in a formal sense. The mass flow rate to the field was determined by the design energy input from the field and the design enthalpy rise in the water. The mass flow rate in the steam generator module was based on a recirculation ratio of 6:1.

Based on the design mass flow rate, the local specific volume, and the design velocity, the required pipe diameter was calculated for each piping system component. Different design velocities were used for the liquid, low quality steam, saturated steam, and superheated steam. The design velocities generally used were:

- 1.52 m/s (5 ft/sec) for liquid
- 6.1 m/s (20 ft/sec) for low quality steam
- 7.62 m/s (25 ft/sec) for superheated steam.

These velocities are lower than those usually used in power plant design, but the extensive distribution piping produced excessive pressure drops at higher velocities.

Using the pipe diameters, lengths, and design velocities, the pressure drops and pump work were calculated for the piping system. If either the pipe diameters or the pump work seemed excessive, the design velocity was modified and the process repeated until reasonable pipe diameters and pump work were obtained.

Thermal expansion of the piping requires including expansion joints in the design of the module internal piping. In the longer module distribution piping, thermal expansion is accommodated by increasing the piping length by a factor of $\sqrt{2}$ to provide for expansion loops or some other compensatory method.

In all cases, module supply piping, steam generator module internal piping, and superheater module supply piping were assumed to be of Schedule 160 carbon steel.

All valves were specified as #1500 class carbon steel or low alloy steel gate valves.

Insulation was specified as calcium silicate with appropriate lagging. Insulation thickness was based on those given in Perry, Chilton, and Kirkpatrick (1963).

The feed pump was sized using the transport system pumping power determined in the pipe sizing routine, minus the power used in the steam generator module. A carbon steel, motor-driven, centrifugal pump with a pump efficiency of 75% was assumed. The circulation pump was sized using the steam generator module pumping power determined in the pipe sizing routine. The circulation pump was of the same specifications and efficiency as the feed pump.

A.1.2.3 Performance Analysis

The water/steam transport subsystem performance was determined using the methods decribed in Section A.1.1.3 for the oil transport subsystem. Both the feed pump and the circulation pump use the same pump performance model as described in Section A.1.1.3.

A.1.3 Intermediate-Temperature Molten Salt Subsystem

Molten salts such as HITEC have been widely used, and their properties are well defined. While the use of molten salts in an extensive piping network exposed to low ambient temperatures cannot be considered current technology, it is reasonable to assume that such a system can be successfully designed. Molten salts have the advantage of being able to operate at high temperature without decomposition or high vapor pressure. In addition, a molten salt transport subsystem can be combined with a molten salt storage subsystem,

which eliminates the storage charging heat exchangers and resulting temperature drop. Molten salts have several disadvantages. They freeze at temperatures above ambient; they are expensive; and salts like HITEC are incompatible with carbon steel above 454°C (850°F). In this approach the molten salt operating temperature will be maintained below 454°C (850°F) to allow the use of carbon steel piping. The intermediate-temperature molten salt subsystem is considered an alternative for the high-temperature distributed receiver concepts and the LFCR concept because these concepts use extensive piping networks. The LFDR-TC and LCNT/R do not operate at a temperature high enough to gain any advantage from using molten salts. This approach was not considered for the PFCR/R because the extent of stainless steel piping required by a higher temperature system was not excessive.

A.1.3.1 Subsystem Arrangement

The subsystem arrangement is similar to that used with the water/steam transport subsystem, in which the collectors are arranged in standard modules for the distributed receiver concepts. The molten salt does not experience a phase change, so once-through heating can be used, eliminating the need for separate steam generation and superheating modules, circulation pumps, steam drums, and accumulators. In addition, the molten salt transport subsystem is used with a molten salt storage system. Because the same fluid is used as the working fluid in both the transport and storage subsystem, salt can be supplied directly from, and returned directly to, storage, eliminating the storage charging heat exchangers.

Molten salts have a melting point substantially above ambient temperature, so provisions for preventing freezing must be included in the transport subsystem design. A drain tank and a purge system are included in the design to allow drainage of the system during periods of no insolation or plant outage. A heated mixing tank with a solid HITEC storage facility is included to allow for adding makeup HITEC and for initially charging the system.

A.1.3.2 Component Analysis

Several components of this transport subsystem required either sizing or material selection. These components included:

- heat transfer fluid
- piping
- valves
- insulation
- feed pump.

This subsystem required a near-term molten salt, so HITEC or its equivalent was chosen from the array of available molten salts. The properties of HITEC used in this study are given in Table A.1.

TABLE A.1. Properties of HITEC

Maximum Temperature	565°C (1050°F)
Maximum Temperature for Compatibility with Carbon Steel	454°C (850°F)
Density	1909 kg/m^3 (119 lb/ft^3)
Specific Heat	1.558 kJ/kg °C (0.373 Btu/lb-°F)

The piping system was sized using the method described in Section A.1.1.2. All pipe was assumed to be of Schedule 40 carbon steel with appropriate flanges and fittings. The drain tank was also carbon steel.

All valves were specified as #600 class carbon steel gate valves.

Insulation was specified as calcium silicate with appropriate lagging. Insulation thickness was based on optimal insulation thickness given in Perry, Chilton, and Kirkpatrick (1963).

The feed pump was sized using the transport system pumping power determined in the pipe sizing routine. A carbon steel, motor-driven centrifugal pump with a pump efficiency of 75% was assumed.

A.1.3.3 Performance Analysis

The intermediate-temperature molten salt transport subsystem performance was determined using the methods described in Section A.1.1.3 for the oil transport subsystem.

A.1.4 High-Temperature Molten Salt Subsystem

Molten salts such as HITEC can operate at temperatures higher than those used in the intermediate-temperature molten salt system without decomposition, but stainless steel piping must be used. To examine the trade-off between better plant efficiency due to higher operating temperature and increased transport subsystem cost due to stainless steel piping, a high-temperature molten salt subsystem will be considered.

In the high-temperature molten salt system, the maximum molten salt temperature is limited to 538°C (1000°F). Above this temperature the decomposition of the molten salt becomes significant. All return piping from the receiver will see the maximum temperature and must be stainless steel. All receiver piping must also be stainless steel.

The high-temperature molten salt subsystem was considered as an alternative transport subsystem for the PFCR/R and PFDR/R. This approach was used with the PFCR/R because it has only a short run of return piping. The high-temperature molten salt system was used with the PFDR/R to provide data for comparison with the intermediate-temperature molten salt system.

A.1.4.1 Subsystem Arrangement

The subsystem arrangement is the same as that used with the intermediate-temperature molten salt system discussed in Section A.1.3.1.

A.1.4.2 Component Analysis

The subsystem components are the same as those used with the intermediate temperature molten salt system discussed in Section A.1.3.2, except that the high-temperature return piping is stainless steel, as are the valves on the return lines and the drain tank.

A.1.4.3 Performance Analysis

The high-temperature molten salt transport subsystem performance was determined using the methods described in Section A.1.1.3 for the oil transport subsystem.

A.1.5 Low-Cost Molten Salt Subsystem

It is possible that other, less expensive, molten salts would be suitable for use as the transport working fluid. The eutectic of sodium and potassium nitrate, known as draw salt, has also been considered (Hausz, Berkowitz, and Hare 1978). High-purity draw salt has been estimated to cost 30% less than HITEC. Draw salt of high purity appears to be compatible with carbon steel at intermediate temperatures. The suitability of less pure draw salt has not been determined. If it were proven suitable, working fluid cost could be substantially reduced, because commercial grade draw salt sells at around 4¢/lb (Hausz, Berkowitz, and Hare 1978). The real benefit of using draw salt is in reducing storage medium costs. However, to eliminate the storage charging heat exchangers, the transport working fluid and the storage working fluid must be the same.

For this transport subsystem, it was assumed that impure draw salt can be used as a heat transfer fluid, and that it was compatible with carbon steel at operating temperatures below 454°C (850°F) and stainless steel below 538°C (1000°F). The technology associated with low-cost molten salt subsystems has not been completely demonstrated, and there is a greater risk in specifying inexpensive draw salt as a suitable heat transfer/heat storage fluid. Although this subsystem is not so firmly based on existing technology, it does give indication of the best possible performance that could be expected in a thermal transport subsystem, extrapolating current procedures.

A.1.5.1 Subsystem Arrangement

The subsystem arrangement is the same as that used with the intermediate-temperature molten salt system discussed in Section A.1.3.1.

A.1.5.2 Component Analysis

The subsystem components are the same as those used with the intermediate-temperature molten salt system discussed in Section A.1.3.2, except that the high-temperature return piping is stainless steel, as are the valves on the return lines and drain tank.

A.1.5.3 Performance Analysis

The low-cost molten salt subsystem performance was determined using the methods described in Section A.1.1.3 for the oil transport subsystem.

A.1.6 Electric Transport Subsystem

The energy storage subsystem is located after the energy conversion subsystem in the PFDR/S, PFDR/B, and PFCR/B concepts. The PFDR/S and PFDR/B are distributed generation concepts that use a field of collectors, each with a small heat engine. These concepts require a transport subsystem that collects the electric energy from the field and transports it to either the energy storage subsystem or the utility grid. The PFCR/B consists of one tower-mounted Brayton-cycle engine. The transport subsystem for the PFCR/B is limited to the cable necessary to transfer the electric energy from the engine to the tower's base where the electric energy storage and the utility connections are located. Due to the simplicity of the PFCR/B transport subsystem this discussion will be limited to the distributed generation concepts. The electric transport subsystem is existing technology and all components are commercially available.

A.1.6.1 Subsystem Arrangement

In the distributed generation concepts, the collectors are arranged in standard modules; the modules are arranged to form the collector field. The transport subsystem collects the electric energy generated at the collectors, increases the voltage to levels suitable for the utility grid, and supplies the energy to the storage subsystem or the utility grid. The circuit is shown in Figure A.4. The heat engine generators are small ac induction generators, so the transport subsystem is ac; the energy storage subsystem has a rectifier/inverter for converting to dc for battery storage.

The standard module has twenty-one 17.5-kW generators in parallel, each at 440 V. A 440-V bus is located at each module. The bus receives the input from the generators and feeds it to a step-up transformer, which provides 4160 V power. The 4160-V cables combine at the 4160-V station bus. A circuit breaker is on the utility side of the bus for disconnecting the entire plant, with the exception of the storage subsystem. The rectifier/inverter of the

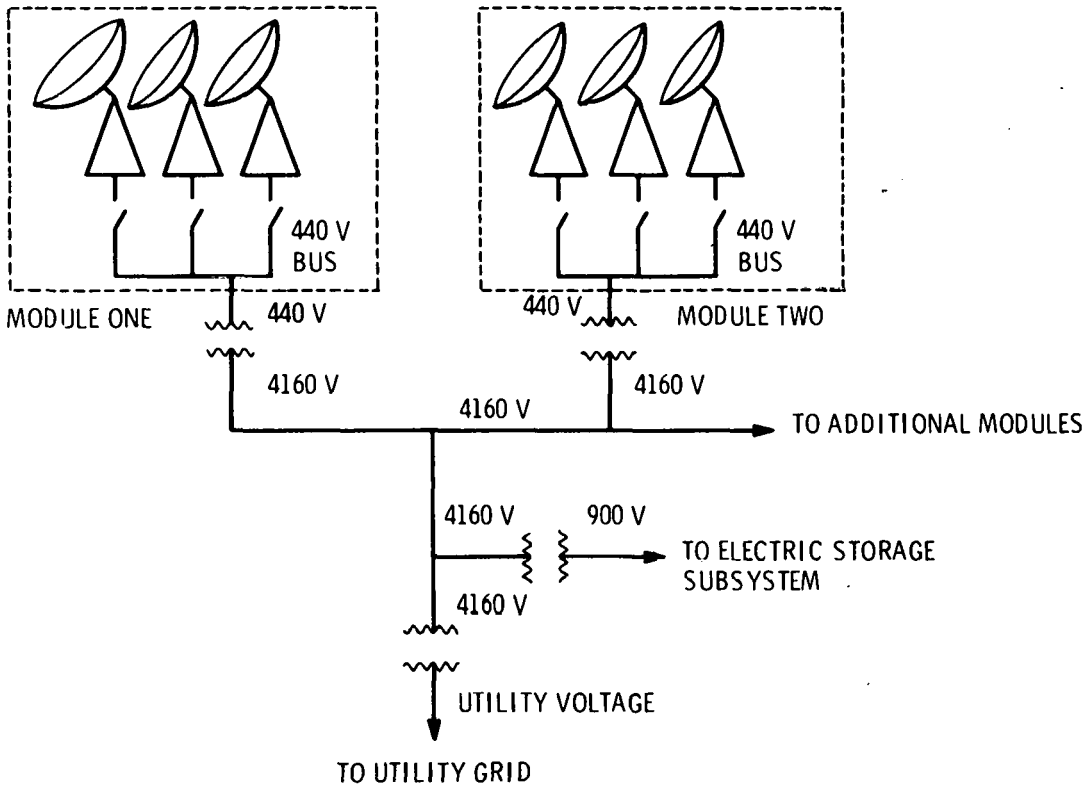

FIGURE A.4. Electric Transport Subsystem

energy storage subsystem requires 900 V power, so the transport subsystem includes 4160/900-V transformers for charging and discharging storage. When the transport subsystem is supplying power to the utility, the power is again stepped up to power grid voltage with another transformer.

A.1.6.2 Component Analysis

Several components of the electric transport subsystem required either sizing or material selection:

- 460-V cable - The 460-V cable is specified as 3 conductor, #4 Aluminum 600 V, Type UF cable with overall covering suitable for direct burial in earth. The cable is installed below ground.
- 4160-V cable - The 4160-V cable is specified as 3 conductor, #2 Aluminum 5000 V, Type UF cable with overall covering suitable for direct burial in earth. The cable is installed below ground.

- 4160/900-V transformer - The 4160/900-V transformer has three-phase six-pulse feeding into bridges with thyristors capable of operating at 1000 A or 2000 A for two in parallel.

A.1.6.3 Performance Analysis

The transport subsystem performance is based on component performance. The subsystem efficiency is the product of the efficiencies of the 460-V cable, 460/4160 tranformer, the 4160-V cable, and the 4160/grid voltage transformer. The efficiency of the 460-V cable for a standard module was calculated from resistance losses as 0.988. The efficiency of the 4160-V cable was also calculated from resistance losses, but the cable length varies depending on plant size. Because the variation was not large, an average value of 0.992 was used. The 460/4160-V transformer had an assumed efficiency of 0.985 and the 4160/grid voltage transformer had an assumed efficiency of 0.99. The electric transport subsystem efficiency is the product of the component efficiencies, or 0.955.

A.2 ENERGY STORAGE SUBSYSTEM

With respect to energy storage subsystem, the concepts analyzed in this study can be classified into one of two types: 1) those with energy storage between the collector subsystem and the energy conversion subsystem, and 2) those with energy storage after the energy conversion subsystem. The concepts with storage between the collector subsystem and the energy conversion subsystem collect and store thermal energy. Concepts with storage after the energy conversion subsystem must store electrical energy. Two generic types of energy storage subsystems are thus required--a thermal energy storage subsystem and an electrical energy storage subsystem.

A.2.1 Thermal Energy Storage

Five thermal energy storage subsystems were considered, each using either a different thermal energy storage medium or a different temperature range:

- Low-Temperature Oil and Rock Storage - This subsystem uses a heat transfer oil such as Caloria and rock as the thermal energy storage medium, and is used with the oil transport subsystem. The subsystem

operates at a maximum temperature of 232°C (450°F), which is well below the maximum operating temperature of Caloria.

- Intermediate-Temperature Oil and Rock Storage - This subsystem also uses heat transfer oil such as Caloria and rock as the thermal energy storage medium, but a maximum operating temperature of 304°C (580°F) is used. Above this temperature the decomposition rate of the heat transfer oil is unacceptably high. Because this storage subsystem is based on the McDonnell Douglas design for the Barstow plant, it is considered current technology and is used as the base case for all concepts except the LCNT using thermal storage. The low-temperature oil and rock alternative is the base case storage subsystem for the LCNT concept.
- Intermediate-Temperature Molten Salt and Rock Storage - This subsystem uses a molten salt such as HITEC and rock for the thermal storage medium. The subsystem operating temperature is limited to 454°C (850°F) to allow the use of carbon steel in the storage and transport subsystems.
- High-Temperature Molten Salt and Rock Storage - This subsystem also uses a molten salt such as HITEC and rock for the thermal storage medium, but the subsystem operating temperature is now limited to 538°C (1000°F), requiring that stainless steel be used in the storage subsystem and in the high-temperature sections of the transport subsystem.
- Low-Cost Molten Salt and Rock Storage - This subsystem is similar to the intermediate temperature molten salt subsystem except that a low-cost molten salt such as impure draw salt is assumed to be used.

Each type of storage will be discussed and the methods of subsystem arrangement, component analysis, and performance analysis will be described.

A.2.1.1 Low Temperature Oil and Rock Storage Subsystem

The low-temperature oil and rock storage subsystem is used with the oil transport subsystem, where oil is heated in the field and returned directly to the thermal energy storage subsystem. The low-temperature oil and rock storage subsystem is used only with the LCNT/R concept, operated at 232°C (450°F), which is well below the maximum operating temperature of heat transfer oil. The design is based on the McDonnell Douglas design for the Barstow power plant (Hallet and Gervais 1977).

A.2.1.1.1 Subsystem Arrangement. The low-temperature oil and rock storage subsystem uses an oil and rock thermocline storage medium. The oil and rock are contained in an insulated steel tank, where a substantial fraction of the volume is filled with inexpensive rock. The remaining tank volume is filled with more costly oil. Thermal energy is stored as sensible heat in the oil and rock. Hot oil is added or removed from the top of the tank; cool oil is added or removed from the bottom of the tank. This maintains the segregation (or thermocline) between the hot and cold oil in the tank.

The thermal storage subsystem does not include heat exchangers for charging storage because oil is pumped directly from the thermal storage tank to the field and returned directly to the top of the thermal storage tank. A storage discharge loop is required to transfer the thermal energy from the rock and oil storage to the water/steam used as the working fluid in the Rankine engine. The storage discharge loop includes piping, an oil discharge pump, a preheating heat exchanger, boiler, and superheating heat exchanger (see Figure A.5).

Heat transfer oils tend to degrade at elevated temperatures. Above 304°C (580°F), the degradation rate is very high and heat transfer oils cannot be successfully used. Below 304°C (580°F), degradation still occurs but at a substantially reduced rate. The low-temperature oil and rock storage subsystem operates at a temperature low enough to preclude major degradation problems. However, during operation, the products of degradation must be removed and replacement oil added (Hallet and Gervais 1977, p. 4-65).

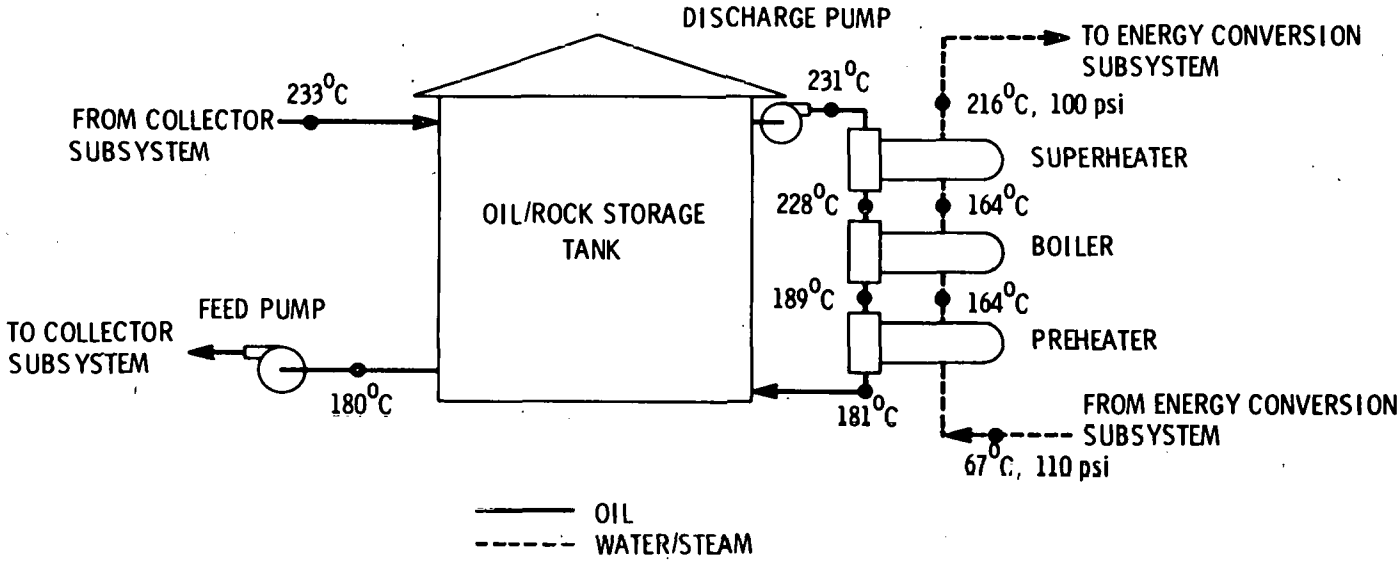

FIGURE A.5. Low-Temperature Oil and Rock Storage Subsystem

Two additional components are required to remove the oil degradation residue. The fluid maintenance system filters the oil to remove suspended solids, distills a side stream to remove high boiling polymeric compounds, and adds fresh makeup fluid to replace decomposed fluid (Hallet and Gervais 1977, p. 4-85). The ullage maintenance unit, in addition to maintaining an oxygen-free gas above the heat transfer fluid, also must remove the volatile fractions of the products of degradation which evaporate into the ullage space above the heat transfer fluid (p. 4-66).

The hot oil temperature in the thermal energy storage tank is at 231°C (447°F) and the cold oil is at 181°C (358°F), so cold oil is supplied to the field at approximately 178°C (350°F) and returns at 233°C (450°F). Similarly, hot oil is sent to the discharge heat exchangers at 231°C (447°F) and returns at 181°C (358°F). The oil and water/steam conditions exiting each discharge heat exchanger are given in Figure A.5.

A.2.1.1.2 Subsystem Sizing. In the concept characterization, three power plant sizes were considered--1-MWe, 5-MWe, and 10-MWe. Each size required a specific storage subsystem. In addition, a range of storage capacities was considered, which would allow the evaluation of plant performance over a range

of capacity factors. This necessitated characterizing storage subsystems capable of allowing plant operation for 3, 6, 9, or 18 hours after the collector subsystem was taken out of service.

The ideal storage medium volume was sized by determining the total quantity of thermal energy to be stored. This consists of thermal energy necessary for the next turbine startup, turbine seal steam, and thermal energy required to generate steam to run the turbine while the plant is generating power from storage. Thermal energy for startup has been estimated as 7.5 MWt-hr for a 10-MWe plant, assuming a hot start (Hallet and Gervais 1977, p. 4-6). This study assumed that thermal energy for startup varies linearly with plant size. Seal steam requires 0.33 MWt for each hour the turbine is down (p. 4-6). In this study, seal steam requirements were based on the hours of turbine downtime between starts, and were assumed to vary linearly with plant size.

The steam generator requirements are based on the energy conversion subsystem output when operating from storage, as well as the energy conversion subsystem overall efficiency,

$$\text{Storage (MWt)} = \text{ECS rated output (MWe)}/\text{ECS overall efficiency}$$

where the energy conversion subsystem output includes a 10% increase for parasitic loads. The overall conversion efficiency is discussed in Section 2.4.3.

The ideal medium volume can now be calculated using the volumetric specific heat of the oil/rock combination. For this study a value of 2.61 megajoule/m^3-^oC (32.9 Btu/ft^3-^oF) was used (Hallet and Gervais 1977, p. 4-25). This assumes a 25% void fraction so that 75% of the storage volume is rock and 25% is heat transfer oil. The ideal storage volume also depends on the temperature difference in storage between the hot and cold oil. For this subsystem the temperature difference is 56^oC (100^oF).

The ideal storage volume must be increased to account for nonideal factors, such as heat loss from storage and unavailable energy. Heat loss from storage represents energy loss by conduction and convection from the thermal energy storage tank. Unavailable energy represents a minimum amount of storage capacity that cannot be utilized, primarily because the thermocline breaks

down when the thermal energy storage tank is nearly drawn down. This would result in low-temperature oil being supplied to the discharge heat exchangers. Heat loss from storage for a 24-hour period is estimated to be between 2% and 6% of the stored energy, depending on tank size (Hallet and Gervais 1977, p. 4-42). Unavailable energy is estimated to be between 10% and 15% (p. 4-32). For this study an average value of 12.5% was used. The actual storage volume is given by

$$\text{Storage volume} = \frac{\text{Ideal storage volume}}{1 - (\text{heat loss} + \text{unavailable energy})}$$

where heat loss and unavailable energy are decimal fractions.

The maximum charge rate is influenced by both the plant's maximum output and the storage capacity. During periods of intermittent insolation, the output from the field must be buffered to prevent the energy conversion subsystem from experiencing large temperature swings. Buffering is accomplished by directing the field output through storage so that the charge rate must allow for the entire output of the field to be used to charge storage. Because the field is sized to operate the plant while charging storage, the maximum charge rate can be calculated as

$$\text{Maximum Charge Rate} = \frac{\text{Output}}{\eta_{ECS}} + \frac{\text{Ideal Maximum Storage}}{\eta_{Th} \times CT}$$

where

Output is plant gross output in MWe

η_{ECS} is energy conversion efficiency in MWe/MWt

Ideal maximum storage is the ideal maximum storage capacity in MWt

η_{Th} is thermal efficiency of storage

CT is charging time (assumed to be 8 hours).

The maximum charge rate would be used to size the charge loop and heat exchangers. However, the low-temperature oil and rock subsystem does not

require a charging heater because the transport and storage fluids are the same. The maximum extraction rate is used to size the discharge loop and heat exchangers.

Capacities of the ullage and fluid maintenance units are based on the rate of heat transfer oil degradation. The degradation rate for the selected heat transfer oil, Caloria HT45, is estimated from the rate equation obtained for the percentage weight loss of Caloria HT45 as a function of temperature (Hallet and Gervais 1977, p. 4-88):

$$R = 5.3 \times 10^{10} \exp [-17650/T]$$

where

R is weight percent per hour
T is temperature in ^{o}K.

The annual makeup requirement can now be determined using an assumed temperature cycle for the oil in the storage unit and the equation given above.

A.2.1.1.3 Component Analysis. Several storage subsystems components required either sizing or material selection. These included the storage medium, thermal storage tank, discharge heaters and loop, and ullage and fluid maintenance units.

Energy Storage Medium. A wide variety of media are available for sensible heat storage. Other studies (Hallet and Gervais 1977, p. 4-25) have indicated that, for storage temperatures below 304^{o}C (580^{o}F), the most attractive, sensible heat storage medium is a combination of Caloria HT45 and rock. Caloria HT45 is a heat transfer oil with good thermal performance. A void fraction of 0.25 was assumed for the oil and rock combination. Two rock sizes--large river gravel and No. 6 silica sand--were to be used.

Thermal Storage Tank. The details of the thermal storage tank are given in Hallet and Gervais (1977, p. 4-28). The thermal storage tank is assumed to have a maximum height of 44 ft, determined by the tank foundation design. The tank diameter is adjusted to give the required storage volume. In some cases, multiple tanks were used for concepts with large storage volumes. The tank is

constructed of A 547 high-strength steel with fiberglass insulation, 10 to 20 cm thick. The fiberglass insulation is covered with an aluminum weather cover.

Discharge Heaters. Three types of discharge heaters are used in the discharge loop: the preheater, the boiler, and the superheater. The 1- and 5-MWe plant storage subsystems have one of each. The 10-MWe plant storage subsystem has two of each. The discharge heaters are sized to take subcooled liquid at 100 psi and 67°C and generate steam at 100 psi and 216°C. The preheater raises the temperature of the subcooled liquid to saturation conditions. The boiler boils the saturated liquid and produces saturated vapor, which is superheated in the superheater. The heat transfer in each heater is determined by the required enthalpy change in the water and the mass flow rate of the water. Based on the required heat transfer in the heater, the temperature change in the oil can be calculated using the mass flow rate and specific heat of the oil. With the inlet conditions determined, the NTU method of heat exchanger analysis was used to determine the required area of the heaters. Heat transfer coefficients were assumed to be the same as those for the discharge heaters in the Barstow plant (Hallet and Gervais 1977, p. 4-138):

Discharge Heater	Overall Heat Transfer Coefficient (Btu/hr-°F-ft^2)
Superheater	44.6
Boiler	102.52
Preheater	86.8

The preheater was assumed to be a straight tube, floating head, counterflow heat exchanger. The boiler was assumed to be a horizontal U-tube kettle boiler. The superheater was assumed to be a horizontal U-tube crossflow heat exchanger.

Discharge Loop. The discharge loop consists of the discharge piping and discharge pump. The discharge piping was sized by assuming a design velocity for the oil and calculating a required diameter based on the oil volumetric

plant, using the 7/10 rule. The discharge pump was sized by calculating the headloss in the discharge piping and in the heaters. The pressure drop in the heaters was assumed to be the same as for the heaters in the Barstow plant. Based on the headloss, mass flow rate of oil, and an assumed pump efficiency of 0.75, the required pumping power was calculated. The pump and piping were assumed to be carbon steel. A centrifugal motor-driven pump was assumed.

Ullage Maintenance Unit, Fluid Maintenance Unit. The ullage and fluid maintenance units are described in Hallet and Gervais (1977, p. 4-23). Because they represent a small part of the storage system, no attempt was made to analyze these systems.

A.2.1.1.4 Performance Analysis. The storage subsystem impacts plant performance in several areas. The storage output efficiency, heat exchanger standby energy requirements, and storage energy loss reduce the amount of energy available in storage. In addition, parasitic loads such as discharge loop pumping power further reduce plant output when using storage.

Storage Output Efficiency. Because pumping power is considered below, the only loss associated with storage output is heat loss from the discharge piping and discharge heat exchangers. The heat loss was calculated assuming 4 in. of calcium silicate insulation on both the piping and the heat exchangers. Because the insulation provides the dominant resistance to heat transfer, the insulation inner-wall temperature was assumed to be that of the oil and the outer-wall temperature was assumed that of the ambient air, $70^{o}F$.

Storage Energy Loss. The storage thermal energy loss due to media cooling was taken from Hallet and Gervais (1977, p. 4-42) for a Barstow type rock and oil thermal storage unit.

Discharge Pump Performance. The SOLSTEP code calculated base case pumping power in the pump sizing routine for full-load operation. Because the computer simulation considers a range of operating conditions, the pumping power must be determined for part-load operation. Actual pumping power includes the effect of part-load operation and is given by

Actual pumping power = [0.25 + 0.75 (ab)] (Installed pumping power)

where

a is a constant determined from base case
b is the energy flow rate through the pump.

Storage Output Standby Energy. The energy required to keep the discharge heat exchangers at close to operating conditions is termed the storage output standby energy. The standby energy is assumed to equal the energy loss calculated in the storage output efficiency analysis.

A.2.1.2 Intermediate-Temperature Oil and Rock Storage Subsystem

Except for the LCNT/R and LFDR-TC, all concepts with thermal storage use water/steam as the base case heat transfer fluid. In addition, the steam returning from the field is at temperatures well above the maximum operating temperature of Caloria HT45. This requires considering a second oil and rock storage subsystem. This subsystem would require a storage charging loop with storage charging heat exchangers to transfer energy from the steam to the oil for storage. In addition, the storage subsystem can now be operated at its maximum temperature, around 304°C (580°F). Because the LFDR-TC concept uses an oil transport subsystem operating at 304°C (580°F), it does not require charging heat exchangers. The intermediate-temperature oil and rock storage subsystem is considered the base case storage subsystem for all concepts using intermediate-temperature thermal storage, and is based on the McDonnell Douglas design for the Barstow power plant.

A.2.1.2.1 Subsystem Arrangement. The subsystem arrangement for the intermediate-temperature oil and rock storage subsystem is similar to the low-temperature system described in Section A.2.1.1.1. However, it differs in two respects: the intermediate-temperature system operates at the maximum allowable temperature for Caloria HT45 and requires charging heaters.

The temperature of steam returning from the field is either 343°C (650°F) or 510°C (950°F), depending on the concept. In either case, the energy must be transferred from the steam to the storage system oil without exceeding the oil's maximum operating temperature. The charging loop, included to transfer

oil from the steam to the oil, consists of piping, an oil charging pump, and storage heaters. To prevent overheating the oil, the steam is desuperheated with a spray desuperheater before entering the storage heaters.

The hot oil in the thermal energy storage tank is at 304°C (580°F) and the cooler oil is at 218°C (425°F), so cold oil is supplied to the storage charging heaters at 218°C (425°F) and returns at 304°C (580°F). Similarly, hot oil is sent to the discharge heat exchangers at 304°C (580°F) and returns at 218°C (425°F). The oil and water steam conditions exiting each heat exchanger are given in Figure A.6.

A.2.1.2.2 Subsystem Sizing. The ideal and actual storage volumes for this subsystem were sized using the method described in Section A.2.1.1.2, with one exception. In the high-temperature system, the temperature change of the oil and rock between hot and cold conditions is 86°C (155°F), which means that more energy can be stored in a given volume of medium for the intermediate-temperature system than for the low-temperature system.

The maximum charge and discharge rates are determined using the method described in Section A.2.1.2 except that in this case, the charge rate is used to size the charging loop and heaters.

A.2.1.2.3 Component Analysis. The intermediate-temperature oil and rock storage subsystem has several components requiring either sizing or material selection. Because of similarity to the low-temperature system, analysis descriptions of the energy storage medium, thermal storage tank, discharge loop, and ullage and fluid maintenance units discussed in Section A.2.1.1.2 will apply here. The charging heaters and loop, as well as the discharge heaters and loop, are described in the next four subsections.

Charging Heaters. The charging heaters were sized using the maximum charge rate determined in A.2.1.2.2. Where possible, the charging heater designed for the Barstow plant was used. Multiple heaters were added for large storage sizes. For small storage sizes, the heater area was decreased linearly with required heat transfer. Because entrance and exit conditions are not influenced by unit size, this assumption resulted in an overall heat transfer coefficient constant with size. In all cases, the heat exchangers were horizontal steel U-tube heat exchangers.

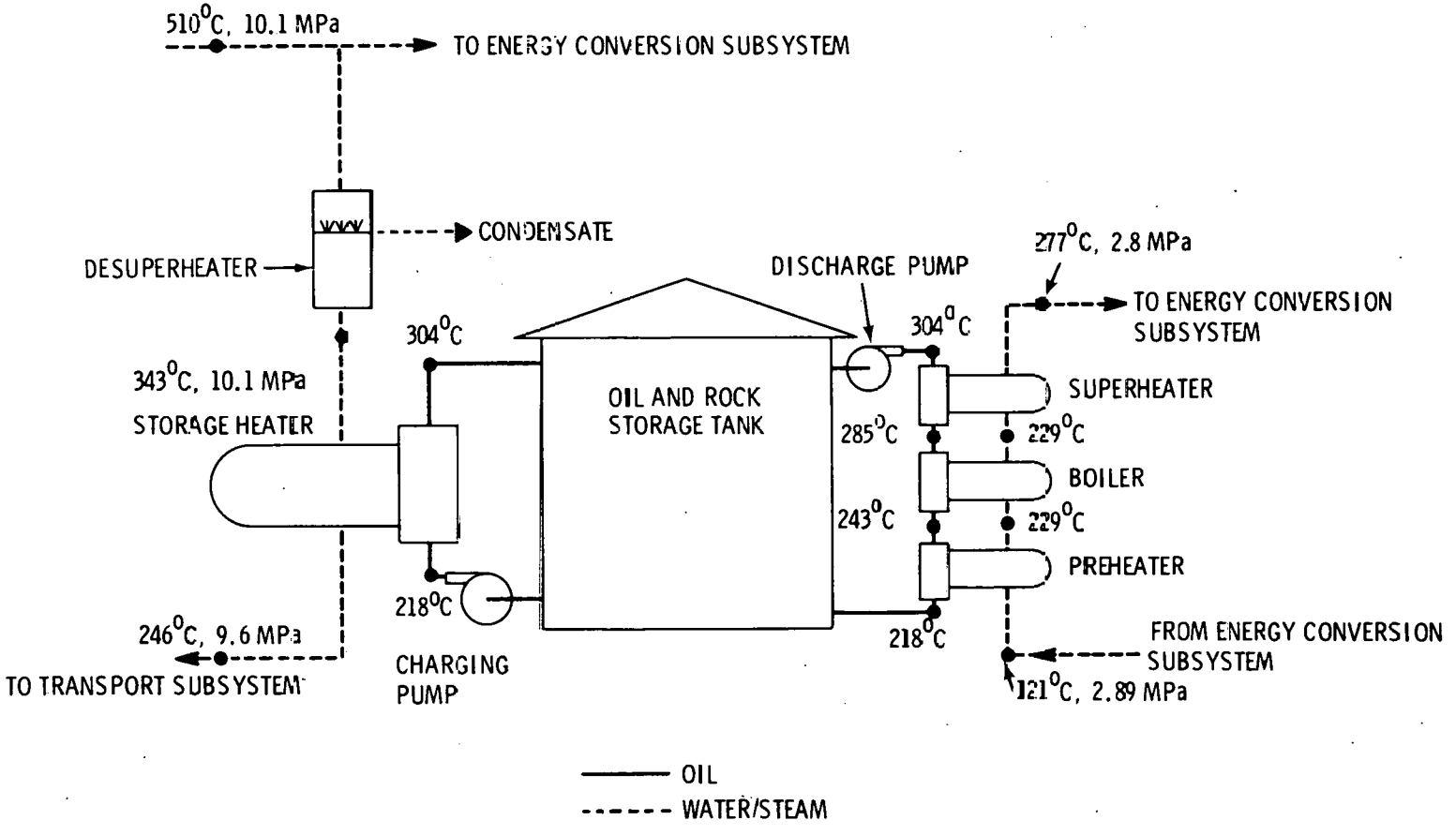

FIGURE A.6. Intermediate-Temperature Oil and Rock Storage Subsystem

Charging Loop. The charging loop piping and pump were sized using the method described in Section A.2.1.1.3.

Discharge Heaters. The discharge heaters in the intermediate temperature system are similar to those described in Section A.2.1.1.3, a superheater followed by a boiler and a preheater. Because the heaters operate at conditions identical to those used at the Barstow plant, the design information for the Barstow heaters (Hallet and Gervais 1977, p. 4-139) was used. The heaters used in the 5-MWe plant were identical to the Barstow heaters; the 10-MWe plant used two trains composed of the same heaters. The 1-MWe plant heaters were sized by assuming the required heat exchanger area was proportional to the required heat transfer.

Discharge Loop. The discharge loop piping and pump were sized using the method described in Section A.2.1.3.

A.2.1.2.4 Performance Analysis. The methods of determining storage output efficiency, storage energy loss, discharge pump performance, and storage output standby energy are described in Section A.2.1.1.4. Three other performance parameters were determined for the intermediate-temperature subsystem: storage input efficiency, charging pump performance, and storage output standby energy.

Storage Input Efficiency. The only loss associated with storage input is the heat loss from the charging piping and charging heat exchangers. The heat loss was calculated assuming 4 in. of calcium silicate insulation on both the piping and the heat exchangers. The insulation is the dominant resister of heat transfer, it was assumed that the insulation inner-wall temperature was that of the oil, and the outer-wall temperature was that of ambient air, $70^{o}F$.

Charging Pump Performance. The base case pumping power was calculated in SOLSTEP's pump sizing routine for full-load operation and an assumed field size. Because the computer simulation considers a range of field sizes, the pumping power had to be determined for varying field sizes and part-load operation. The installed pumping power was assumed to vary linearly with field size. Actual pumping power includes the effects of part-load operation:

Actual pumping power = [0.25 + 0.75(ax) (by)] (Installed pumping power)

where

x is energy flow rate through the pump
y is field size
a and b are constants determined from the base case.

Storage Input Standby Energy. Storage input standby energy is the energy required to keep the discharge heat exchangers at close to operating conditions. The standby energy is assumed to equal the energy loss calculated in the storage output efficiency analysis.

A.2.1.3 Intermediate-Temperature Molten Salt and Rock Storage Subsystem

Several attributes of molten salts such as HITEC make them attractive, sensible heat storage media. Molten salts can operate at high-temperatures without decomposition or high vapor pressure. In addition, a molten salt storage subsystem can be combined with a molten salt transport subsystem. This combination would eliminate the storage charging heaters and the resulting temperature drop.

Several disadvantages must be overcome before molten salt storage systems can be considered as a viable option. First, molten salts freeze at temperatures well above ambient. Second, molten salts operating above 454°C (850°F) are incompatible with carbon steel; more expensive stainless steel must be used. Third, high-purity molten salts such as HITEC are expensive. HITEC is approximately two and one-half times as expensive as oil and eight times more expensive than oil and rock on a cost per unit mass basis (Hallet and Gervais 1977, Table II, p. 6-27). After correcting for different specific heat and storage temperature, HITEC is still twice as expensive as oil and three times more expensive than oil and rock per unit of energy stored.

In the intermediate-temperature molten salt storage subsystem, the molten salt temperature is maintained below 454°C (850°F) to allow the use of carbon steel. To reduce the cost of the storage medium, use of a packed-bed/thermocline tank with HITEC and some compatible rock was assumed. This approach has been considered by Honeywell, Inc., and tests on degradation

rates of molten salt in the presence of various minerals have been conducted by DOE (Hallet and Gervais 1977, p. 6-35). It is not possible at this time to determine if a HITEC/rock packed-bed tank is feasible; therefore, this storage subsystem cannot be considered as near-term technology.

The intermediate temperature molten salt storage subsystem was considered as an alternative for the high-temperature distributed receiver concepts and the LFCR/R concept because it is compatible with the intermediate-temperature molten salt transport subsystem used on these concepts. The LFDR-TC and the LCNT/R do not operate at a temperature high enough to gain any advantage from using molten salts. This storage subsystem was not considered for use with the PFCR/R because this concept uses only the high-temperature molten salt transport subsystem.

A.2.1.3.1 Subsystem Arrangement. The intermediate-temperature molten salt and rock storage subsystem uses a molten salt and rock packed-bed/ thermocline storage. The molten salt and rock are contained in an insulated steel tank.

The thermal storage subsystem does not include heat exchangers for charging storage because molten salt is pumped directly from the thermal storage tank to the field and returned directly to the top of the thermal storage tank. A storage discharge loop is required to transfer the thermal energy from the molten salt and rock storage to the water/steam used as the working fluid in the Rankine engine. The storage discharge loop includes piping, molten salt discharge pump, a preheating heat exchanger, boiler and superheating heat exchanger. Figure A.7 illustrates this subsystem.

Because the degradation rate of molten salts such as HITEC is low at storage system operating temperatures, the fluid maintenance unit is not required. The ullage maintenance unit is still required to maintain an inert gas cover over the heat transfer molten salt in the storage tank. Provisions for preventing the freezing of the molten salt during long outages will be included. This would include heat tracing of pipes and storage tanks. Another method is to add water at an appropriate rate during the cooling period to assure that the molten salt mixture remains in liquid form (Hallet and Gervais 1977, p. 6-35).

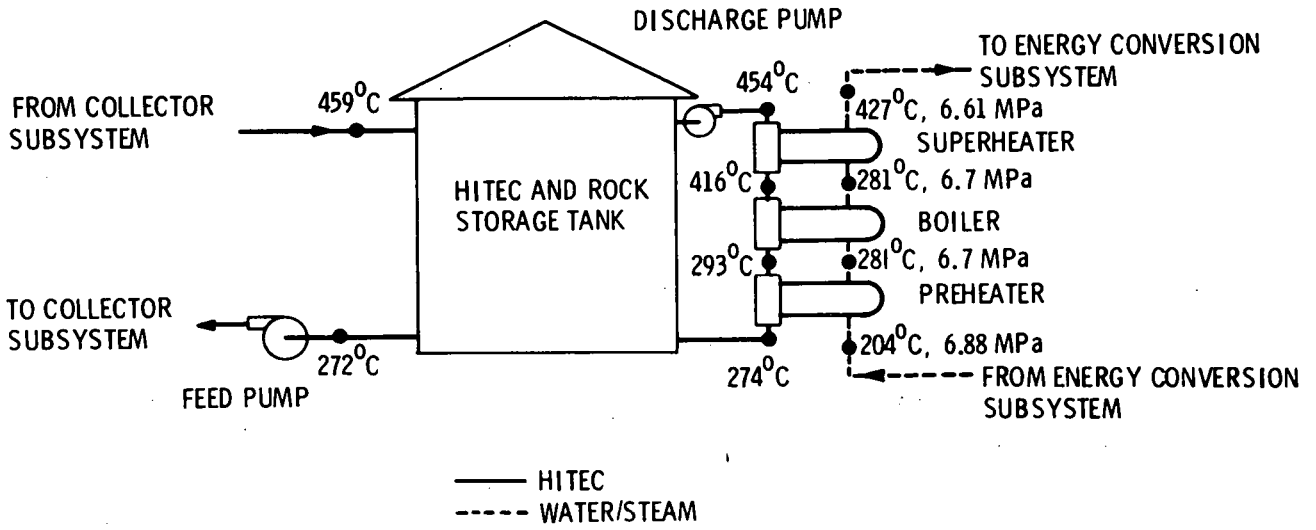

FIGURE A.7. Intermediate-Temperature Molten Salt and Rock Storage Subsystem

Hot molten salt in the thermal storage tank is maintained at 454°C (850°F), and the cold molten salt is maintained at 257°C (494°F), so cold molten salt is supplied to the field at 254°C (489°F) and returns at 454°C (850°F). Similarly, hot molten salt at 454°C (850°F) is supplied to the discharge loop heat exchangers and returns at 257°C (494°F). The molten salt and water steam conditons exiting each discharge heat exchanger are given in Figure A.7.

A.2.1.3.2 Subsystem Sizing. The required energy storage capacity was sized using the method described in Section A.2.1.1.2. The ideal storage volume was calculated using the volumetric specific heat of the molten salt/rock combination. For this study a value of 3.28 MJ/m^3-°C (41.4 Btu/ft^3-°F) was used (Hallet and Gervais 1977, p. 6-27). This assumes a 0.25 void fraction. The ideal storage volume also depends on the temperature difference in storage between the hot and cold molten salt. For this subsystem the temperature difference is 198°C (356°F).

The ideal storage volume must be increased to account for nonideal factors, such as heat loss from storage and unavailable energy. Heat loss from storage is determined in Section A.2.1.3.4. Unavailable energy was estimated

to be 12.5%, the same value as that used with the oil and rock subsystem. The actual storage volume, maximum extraction rate, and maximum charge rate were determined using the method described in Section A.2.1.1.2.

A.2.1.3.3 Component Analysis. Four components of the intermediate-temperature molten salt storage subsystem required either sizing or material selection. The analyses are described in the following paragraphs.

Energy Storage Media. Several heat transfer molten salts are available. HITEC is typical and will be used as the base case molten salt. The packed bed was assumed to be river rock and sand, but the actual packed bed medium has not been determined and must be compatible with HITEC.

Thermal Storage Tank. The thermal storage tank for HITEC and rock was assumed to be similar to that used for oil and rock, described in Section A.2.1.1.3.

Discharge Heaters. Three types of discharge heaters are used in the discharge loop: the preheater, the boiler, and the superheater. Storage subsystems for the 1- and 5-MWe plants have one heat exchanger train; the 10-MWe plant has two heat exchanger trains. The heat exchanger train takes subcooled water at 204°C (400°F) and 1000 psi and produces 427°C (800°F) steam at 900 psi. The heat transfer in each heat exchanger is determined by the enthalpy change in the water/steam and the mass flow rate of the water. Based on the heat transfer in each heat exchanger, the temperature change in the molten salt can be calculated using the mass flow rate and specific heat of the molten salt. With the inlet conditions determined, the log mean temperature difference method was used to determine the required area of the discharge heat exchangers. The heat transfer coefficients for the heat exchangers were taken from Martin Marietta (1977, p. D-12). All three were assumed to be counterflow heat exchangers.

Discharge Loop. The discharge loop consists of the discharge piping and discharge pump. The discharge piping was sized by assuming a design velocity for the molten salt and calculating a required diameter based on the molten salt volumetric flow rate. Because piping layouts were not developed, the

piping length was assumed to be the same as that for the oil and rock subsystem described in A.2.1.1.3. The pump was sized using the method described in Section A.2.1.1.3.

A.2.1.3.4 Performance Analysis. Subsystem performance was calculated using the method described in Section A.2.1.1.4.

A.2.1.4 High-Temperature Molten Salt and Rock Storage Subsystem

Molten salts such as HITEC can operate at temperatures higher than those used in the intermediate-temperature molten salt system without degradation, but stainless steel must be used in place of carbon steel. To examine the trade-off between better plant efficiency due to higher operating temperature and increased storage subsystem cost due to stainless steel piping, a high-temperature molten salt subsystem was considered.

In the high-temperature molten salt storage subsystem, the maximum molten salt temperature is limited to 538°C (1000°F). At higher temperatures the degradation of HITEC Increases to intolerable levels. The storage tank, sections of the discharge loop, discharge pump, and the superheating heat exchanger will be subjected to molten salt temperatures above 454°C (850°F) and must be constructed of stainless steel. With this exception, the subsystem arrangement and sizing, component analysis, and performance analysis were performed using the methods described in Sections A.2.1.3.1, A.2.1.3.2, A.2.1.3.3, and A.2.1.3.4.

A.2.1.5 Low-Cost Molten Salt Subsystem

One of the major drawbacks of using molten salt for sensible heat storage is the excessive cost of salts such as HITEC. Other, less expensive, molten salts may prove suitable for use as a thermal energy storage medium. Several other salts such as draw salt are being considered. High-purity draw salt has been estimated to cost 30% less than HITEC with suitable compatibility with carbon steel. Impure draw salt has been discussed as an alternative thermal energy storage medium. If impure draw salt is proven to be suitable, then a substantial cost reduction can be expected. Currently, the suitability of draw salt has not been completely demonstrated, and this concept must be considered as a higher-risk alternative.

For this storage concept it was assumed that impure draw salt can be used as a thermal energy storage medium and that it is compatible with carbon steel below 454°C (850°F) and stainless steel below 538°C (1000°F). This subsystem indicates the best performance in a thermal storage subsystem, extrapolating current procedures.

The low-cost molten salt subsystem is an alternative storage subsystem for all concepts using either the intermediateor high-temperature molten salt thermal storage subsystems. With the exception of the thermal storage medium, the subsystem arrangement, subsystem sizing, component analysis, and performance analysis are the same as those described in Sections A.2.1.3.1, A.2.1.3.2, A.2.1.3.3, and A.2.1.3.4.

A.2.2 Electrical Storage

The generic concepts using the Brayton and Stirling cycles required either very high-temperature thermal storage, involving an assumption of high-risk materials technology development, or electrical storage, which also has technical barriers to overcome, but does have more developed programs in place to overcome the barriers. Three distinct types of electrical storage were considered: lead acid, advanced conventional, and Redox. All three were evaluated and are later discussed in detail.

The three electrical storage subsystems have in common the interface converter equipment shown in Figure A.8. The converter equipment provides the rectification and inversion functions, thereby connecting the dc battery and the ac utility system. The output transformer, ac breaker, and lightning arrester, as well as all dc breakers, fuses, static interruptors, bridges, reactors, disconnects, filters, VAR compensation, controls, and cooling systems are included in the converter subsystem.

While it is possible to rate converter equipment power on several basis (dc power input, ac power input, product of maximum dc voltage and current, or product of average dc voltage and current), it was found that the dc power input was the most appropriate (Bechtel 1976, p. 4-6). An ac output voltage of 13.8 kV was chosen for connecting to the utility grid, while the maximum and minimum dc voltages are dictated by the battery type and size. Certain

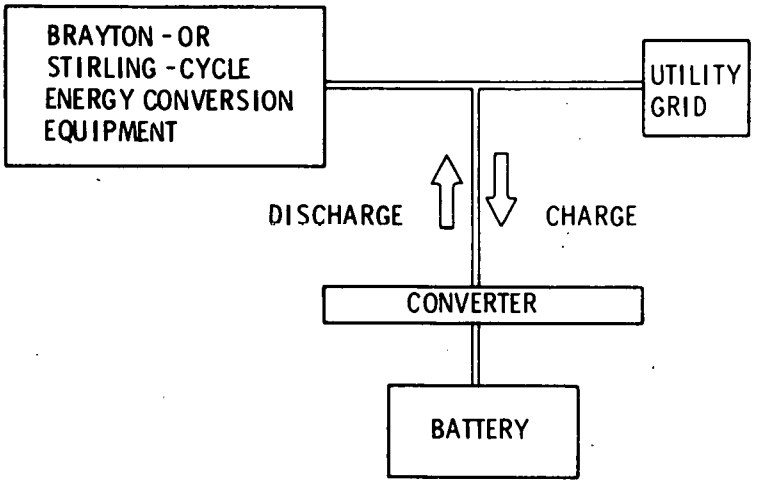

The output transformer, ac breaker and lightning arrester, as well as all dc breakers, fuses, static interruptors, bridges, reactors, disconnects, filters, VAR compensation, controls, and cooling systems, are included in the converter subsystem.

FIGURE A.8. Battery System Layout

design details are worth noting when the converter subsystem is compared to other configurations. These details have been collected by Bechtel in an assessment of similar sized electrical storage designs conducted in 1976, and presented here for information on assumptions used in the PNL study (Bechtel 1976, pp. 4-9 and 4-10):

- Converters form the entire link between the dc bus and ac grid. Hardware and logic are provided for complete self protection. This includes internal logic for SCR firing; breaker (or fuse), lightning arrester on the ac side; fuse (or breaker) backed solid state interruption on the dc side; and appropriate fault detection instrumentation and logic. All other ancillary systems (e.g., cooling, pulse generators) are also included.
- Converters are modular; several sets of SCR bridges are used and are housed in cabinets separate from other major equipment units such as the output transformer.

- Phasing of bridges and transformer design are used to aid in harmonic cancellation. All designs achieve a level of harmonic content adequate for connection to a utility system (e.g., less than 1% at any single frequency and less than 3% total).
- Both air and liquid cooling of internal components are used, but in all cases final rejection of waste heat is to the atmosphere without the need for any external cooling water.
- Both converter and battery manufacturers agree that the dc system should be floating so that battery ground faults require two coincident faults.
- All designs include adequate design for reactive power and for maintaining power factors above 0.9.
- Equipment space (exclusive of aisles, fence clearances, etc.) are 53 to 68 ft^2/MW, based on dc input power, with packing densities (including aisles and some clearance) ranging from 0.25 to 0.5.
- The bus systems are insulated to withstand 5 pu transients.

The estimates of the full-load, one-way efficiency for the converter range from 0.935 to 0.968, with an average of 0.951 based on the Bechtel manufacturer analysis. Advanced batteries (both conventional and Redox) can take advantage of full-load, one-way efficiencies approaching 0.98 due to a significantly narrower voltage range. For the PNL study the following converter efficiencies were used:

Battery Type	Converter Efficiency
Lead Acid	0.95
Advanced Conventional	0.98
Redox	0.98

These efficiencies were used in conjunction with the battery performance information given in the folowing subsections.

Another similarity of all three battery configurations is related to trickle discharge rate. Because of the potential for safety and performance degradation problems associated with alternately charging and discharging a battery, it is uncommon to run the battery with a zero float. A zero float implies that the battery is being neither charged nor discharged. However, because no instrumentation is 100% accurate, the battery is being alternately charged and discharged. This loss of control of the number of actual charge/discharge cycles actually conducted can void a manufacturer's warranty for the battery. To prevent this and maintain an accurate knowledge of how the battery has been operated, a trickle discharge of 15 amps is maintained for all three systems during periods when normal charge/discharge operations are not being conducted.

One other similarity among the three systems concerned "depth of discharge," which relates to what percentage of battery capacity can be used before discharge must be secured due to reaching minimum cell voltage. This factor affects initial cost in that a somewhat oversized storage device must be installed. It also affects performance in that the charging of that battery capacity below the "depth of discharge" limit cannot be recovered. Typical values for this limit are between 0.80 and 0.90.

A parameter that also impacts battery operation is the variation of capacity, from initial to end of life. This term is made up for again by oversizing the initial unit. The relationship between initial and end of life capacity for the lead acid battery is shown in Figure A.9 (Bechtel 1976, p. 4-149). This variation is also applicable to the advanced conventional battery, although the degradation is over a significantly longer lifetime (3x). The Redox battery system is able to purify, replace, and maintain (via a rebalance cell) the fluid reactants to all but eliminate capacity reduction.

A.2.2.1 Lead Acid Battery

In the 100-plus years the lead acid battery has been in use, significant improvements have been made to make it one of the least expensive, most reliable, and frequently used energy storage source today. The following excerpt is include to provide a brief description of the basics of a lead acid storage subsystem (Lee et al. 1978, p. IV-1,4,5):

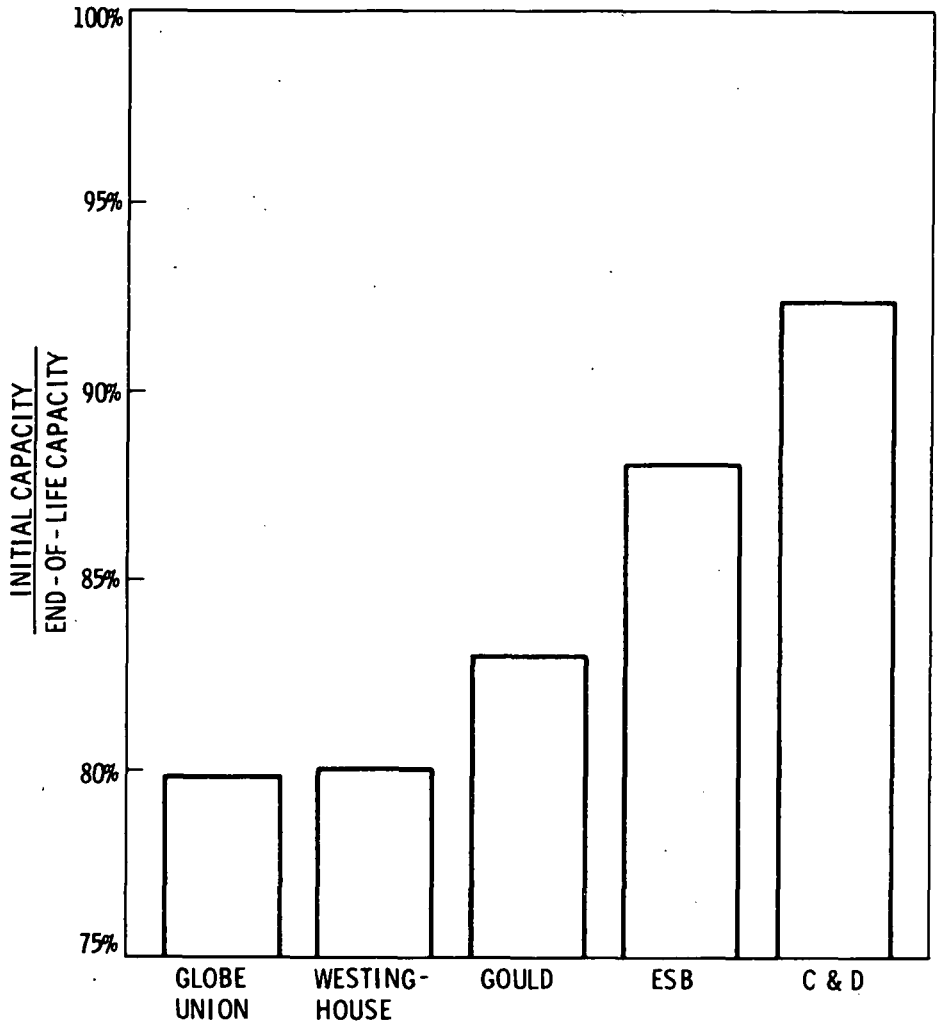

FIGURE A.9. Initial to End-of-Life Capacity Reduction for Lead Acid Battery System

The lead-acid battery contains plates made of sponge lead (Pb), which is a porous form of lead, and lead peroxide (PbO_2). These plates are immersed in a solution of sulfuric acid (H_2SO_4), which acts as the electrolyte for the battery. During discharge, the positive plate is changed from lead peroxide into lead sulfate ($PbSO_4$). At the negative plate, the sponge lead is oxidized into lead sulfate. While charging, the processes are reversed, and the lead sulfate at both plates is changed back into sponge lead and lead peroxide. The overall reaction for the charging-discharging process is:

$$PbO_2 + Pb + 2H_2SO_4 \underset{\text{discharge}}{\overset{\text{charge}}{\rightleftharpoons}} 2PbSO_4 + 2H_2O$$

The nominal voltage for this reaction is two volts per cell. Higher voltages are achieved by connecting individual cells in series.

A lead-acid battery is composed of a case, plates, separators, and sulfuric acid. The active materials in a battery are the positive plate, made from lead peroxide, the negative plate, made from lead, and sulfuric acid. The lead materials are formed from a paste composed of lead oxides and water.

Pastes are made from lead oxide and electrochemically converted into lead and lead peroxide after the pastes have been bonded to the grids. This process produces plates superior to those formed from lead peroxide and lead. The paste material is highly porous, giving the battery a large surface area. Since the reactions of the battery occur at the interface between the solid and liquid materials in the battery, a large surface area is essential for high capacity and power output.

The pastes used in battery manufacture are structurally very weak and also are poor conductors of electricity. In order to provide an even distribution of electricity to the paste and to support the paste structurally, a grid made from metallic lead is used. The grid consists of a lattice, cast from lead, which holds the paste in the spaces between the latticework. Antimonial lead has been the traditional material for lead grids, although recently other alloys, most notably calcium-lead alloys, have been used for grid material. These alloys have been developed primarily to reduce the decomposition of the water in the battery while charging. Electrolysis losses are a major reason why conventional batteries must have water added periodically.

In order to keep the positive and negative plates from contacting each other and short-circuiting the battery, thin insulators called separators are used. These separators, which may be made from glass, plastic, wood, asbestos, rubber, or fiberglass, are porous and allow the electrolyte to pass freely between the plates while preventing physical contact between the positive and negative plates. The separators also help to hold the active material onto the plates (loss of active material from positive plates is a common cause of battery failure).

Sulfuric acid forms the remaining portion of the active material. Sulfuric acid is usually diluted so that when the battery is fully charged, the specific gravity is 1.28 (37.5% sulfuric acid by weight). As the battery discharges, the sulfuric acid reacts with the lead materials to form lead sulfate, and the electrolyte becomes less acidic until, when the battery is fully discharged, the electrolyte is mostly water and the specific gravity approaches 1.12.

The plates and the sulfuric acid are contained in a plastic or rubber container. Polypropylene is the favored substance for cases because it is light, chemically inert, and strong, but any material that is nonporous and resistant to sulfuric acid may be used.

When a lead acid battery is being charged, losses above and beyond the ac/dc conversion efficiency occur. The ampere-hours and voltage required during recharge are higher than those of the discharge. This means that the energy efficiency is somewhat reduced from the simple converter throughput efficiency value. The subsystem design evaluated in the PNL study employed strings of sealed lead acid battery cells, stacked three high for compactness. Each string consists of series-connected ESB cells. The number of cells depends on the design power plant rating. The individual cells are water-cooled by a closed loop circulating system. Operating voltages are 1.65 volts per cell at maximum discharge condition, 2.35 volts per cell at final charging, and 2.65 volts per cell at the end of an equalizing charge. The nominal dc bus voltage range is from a minimum at (# series connected cells) (discharge cutoff = 1.65 V) to a maximum of (# series connected cells (equalizing charge voltage = 2.65 V). For a 900-cell string, the dc bus voltage would vary between ~1500 and 2400 volts. For the rated life of 2000 to 2500 cycles, the energy efficiency can be expected to be in range of 80 to 85% (Bechtel 1976, pp. 4-86,103). This configuration is described in greater detail in the Bechtel report, including all necessary buildings, cooling, ventilation, instrumentation and control circuitry, safety devices, and miscellaneous support equipment.

A.2.2.2 Advanced Conventional Battery

This subsystem uses an advanced battery of unspecified type with performance and cost representative of proposed advanced battery concepts. This approach was taken because of the numerous battery component development programs currently being conducted, including improvements in conventional lead acid designs. It is expected that the goals will be achieved or exceeded by a number of proposed advanced battery types; however, to couple the successful commercialization of a generic solar thermal power concept using electric storage to one particular battery development program is not appropriate.

Three major improvements will be required for the successful development of utility-oriented advanced batteries:

- increased battery efficiency
- longer battery lifetime
- reduced battery cost.

The utility applications may not require as high an energy density as certain transport applications, but high-current densities will still be needed to minimize the costly electrode and separator areas. This suggests that the most dramatic improvements may be in lifetime and cost, not in the efficiency, which is subject to a number of major technological constraints. Electrode (active) materials being studied as the basis for battery systems that may achieve the required goals include (Birk and Kalhammer 1976, p. A.11):

Negatives	Positives
sodium (liquid)	sulfur (liquid)
Lithium (liquid; alloy	chlorides (soluble)
zinc (soluble product)	sulfides (reversible solids)
iron (soluble product)	chlorine (soluble gas)
	bromine (soluble liquid).

The most promising combinations of these materials seem to be the

- sodium - sulfur
- sodium - antimony chloride
- lithium (alloy) - metal sulfide
- zinc - chlorine (bromine).

These systems and others appear to have the potential for achieving total battery effiencies of 83 to 85%, according to Argonne National Laboratory (1978, p. 22), Shimotake and Bartholme (1976 p. B-216), Bechtel Corporation (1976, P. 4-86), and General Electric Company (1978, p. C-6). These and other sources (Appleby and Gabano 1976, p. A.49; Cairns and Dunning 1976, p. A.91; Weiner 1976, p. B.225; Public Service Electric and Gas Company 1976, p. 1-19) suggest a theoretically predicted lifetime approaching 6000 cycles.

A.2.2.3 Redox Battery

The Redox system is an electrochemical storage device under development by NASA-Lewis Research Center, Oak Ridge National Laboratory, and others. It uses the reduction and oxidation of two full-soluble Redox couples (acidified chloride solution of chromium (Cr^{+2}/Cr^{+3}) and iron (Fe^{+2}/Fe^{+3}) for discharging and charging. The following description of the Redox battery system was provided by NASA-Lewis Research Center (Thaller 1979):

> Figure A.10 illustrates the system in its simplest form.
>
> This shows that the reactant solutions are stored in tanks outside the power conversion section in which the associated electrochemical reactions take place at inert electrodes. The Redox solutions that are pumped through the porous electrodes and kept separated by a highly selective ion exchange membrane. This membrane has been engineered to almost completely prohibit the passage of iron and chromium ions and yet allow easy passage of chloride and hydrogen ions. The reactant solutions are currently 1.0 molar in either iron or chromium chloride and 2.0 normal in hydrochloric acid. The inert electrodes are a highly porous carbon felt material. The electrode material used on the chromium side of the cell is catalyzed with small amounts of lead and gold.
>
> The electrochemical reactions are very simple and highly reversible. When the system is in the charged state, the chromium solution is mostly chromous ion and the iron solution, ferric ion. As the fluids are pumped through the system and they undergo discharge, the chromous ions are oxidized to chromic ions and the ferric ions are reduced to ferrous ions. To maintain overall charge neutrality in the system, these electrochemical reactions are accompanied by the gain of chloride ion (and/or loss of hydrogen ion) in the chromium solution and the commensurate loss of chloride ion (and/or gain of hydrogen ion) in the iron solution. The discharge processes may be summarized as follows:

At anode: $Cr^{+2} \rightleftharpoons Cr^{+3} + e^-$ (1)

At cathode: $Fe^{+3} + e^- \rightleftharpoons Fe^{+2}$ (2)

Across membrane: net positive charge from chromium solution to iron solution.

TWO - TANK ELECTRICALLY RECHARGEABLE
REDOX FLOW CELL

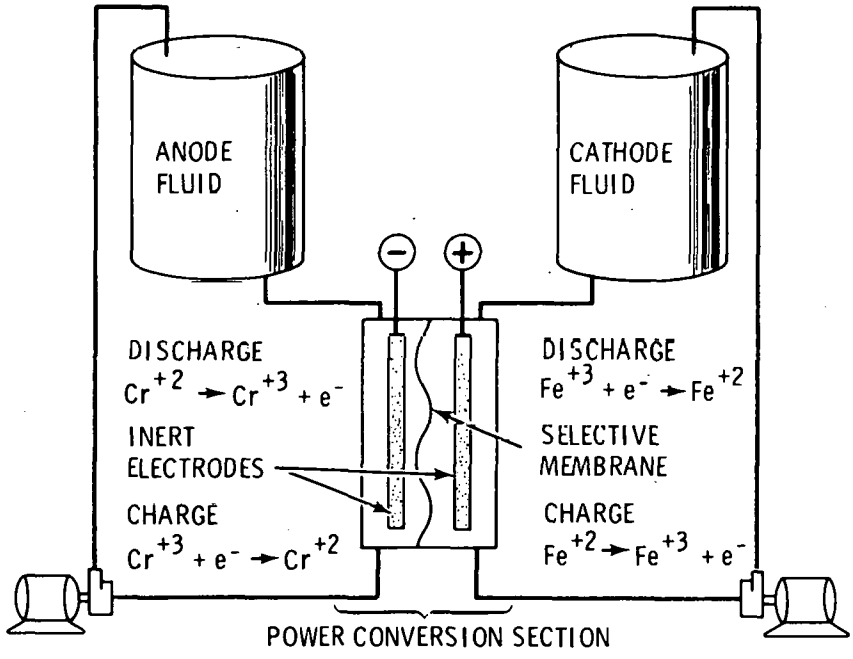

FIGURE A.10. Redox Battery System

As the discharge continues, there is a gradual change in ratio of the charged to discharged species in the two solutions and a point is reached where like any other secondary battery, it must be recharged. A power supply is connected to the terminals and the reverse electrochemical reactions take place. Although Figure A.10 shows only a single cell connected to the two Redox solutions, it is easy to see how a number of such cells could be connected together in parallel hydraulically and in series electrically. These stacks of cells closely resemble fuel cell batteries and water electrodialysis equipment.

The basic Redox system thus consists of a stack of cells, two pumps for circulating the Redox solutions, two tanks in which these fluids are stored, and some degree of control and switching equipment as with any other battery system. Several features of this system deserve further discussion.

1. The major feature of Redox systems that differentiate them from other battery systems is the complete independent sizing of the system storage capacity (kWh) by the selection of the tank

volumes and solution concentration and the system power (kW) by the grouping of cells in the Redox cell stack. This is particularly significant for long term storage applications where the relatively inexpensive part of the system (chemicals and tanks) account for a high proportion of the system cost.

2. Since the charge and discharge reactions involve simple Redox reactions, there are neither any plating/deplating reactions, nor any solid compound phase changes. There are thus no fundamental cycle life limitations from a electrochemical standpoint. Also, no capacity losses or failures caused by shape change, slumping, shedding or other phenomenon that are related to electrode morphology changes can occur.

3. The mild operating conditions associated with aqueous solutions permits the use of inexpensive carbon, graphite and plastic materials for the tanks, piping, pumps and stack components.

4. The absence of any highly reactive or toxic ingredients will minimize the safety and environmental hazards.

5. The existence of an applicable industrial technology base in both the fuel cell and water electrodialysis field is highly significant. These industries could well form the manufacturing base for the Redox hardware which is similar in many respects. This similarity has already been useful in making credible preliminary cost estimates for future Redox systems.

Only 1% of the system's energy is consumed in operating the circulating system, while a round-trip battery efficiency of 0.75 is obtainable. No solid compounds are formed in the Redox battery. Flow of the reactant fluids is uniform through all cells that make up the battery (Mechanical Engineering 1979, p. 55). The membrane material separating the two reactant fluids is the life-limiting component, but based on accelerated lifetime tests by NASA-Lewis (Thaller 1979), a 30-year period is estimated as feasible. While the efficiency gains are not impressive, the lower cost of the flow cells, ease of maintenance, and ability to simply increase tank size to increase storage capacity make the Redox battery system an attractive alternative. The documentation used in characterizing the cost and performance of the Redox system is sufficient to predict with some reliability the expected advantages of such an advanced storage device (Warshay and Wright 1975; Line 1975; Ciprios et al. 1977; Roy and Kaplan 1978; Thaller 1974; Mechanical Engineering 1979; Thaller 1979; NASA-Lewis Research Center 1977).

A.2.2.4 Comparison of Battery Input Parameters

Small changes needed to be made to account for different battery storage sizes, but, in general, the numbers presented in Table A.2 provide a basic comparison of the parameters used to characterize the alternate battery type. It can be noted that initial cost and system lifetime frequently provided for better economy than did minor improvements in efficiency.

TABLE A.2. Comparison of Battery Types

Performance Parameter	Battery Type		
	Lead Acid Battery	Advanced Conventional Battery	Redox Battery
One-way converter efficiency	0.95	0.98	0.98
Trickle discharge (amps)	15	15	15
Depth of discharge	0.80	0.90	0.90
Lifetime capacity reduction	0.93	0.93	1.00
Lifetime	2500 cycles	6000 cycles	30 yrs
Round-trip efficiency	0.83	0.85	0.75

A.3 ENERGY CONVERSION SUBSYSTEM

Two approaches to the energy conversion subsystem arrangement were considered:

- distributed generation
- central generation.

In the distributed generation concepts, the energy conversion subsystem is located at the collector and a large number of small heat engines is required. The central generation approach has only one heat engine and the energy collected in the collector field is transported to the heat engine the energy transport subsystem.

Two energy conversion subsystem types were considered for application with distributed generation concepts. They are:

- Stirling-cycle energy conversion subsystem - This subsystem uses a small (17.5-kW) Stirling-cycle engine attached to an ac linear alternator for the energy conversion subsystem. The engine is operated at 816°C (1500°F) and is located at the focal point of a two-axis tracking collector (PFDR).
- Small Brayton-cycle energy conversion subsystem - This subsystem uses a small (17.5-kW) closed-cycle Brayton engine attached to an ac induction generator for the energy conversion subsystem. The engine is operated at 816°C (1500°F) and is located at the focal point of a two-axis tracking collector (PFDR).

Two types of energy conversion subsystems were considered for the central generation concepts:

- Rankine-cycle energy conversion subsystem - This subsystem uses a Rankine-cycle engine attached to an ac synchronous generator for the energy conversion subsystem. Different Rankine cycles have been developed for concepts with different maximum operating temperatures. Rankine-cycle engines have been characterized for operating temperatures of 216°C (420°F), 274°C (525°F), 343°C (650°F), 427°C (800°F), 510°C (950°F). For each operating temperature, Rankine-cycle engines were characterized for facilities with a net output of 1 MWe, 5 MWe and 10 MWe. In all cases the energy conversion subsystem is located at a central facility with one engine installed.
- Large Brayton-cycle energy conversion subsystem - A closed-cycle Brayton engine is attached to an ac synchronous generator in this energy conversion subsystem. The single installed engine is operated at 816°C (1500°F) and is located at a central facility. Brayton-cycle engines were characterized for facilities with net outputs of 1 MWe, 5 MWe and 10 MWe.

All four energy conversion subsystems will be discussed. The methods of subsystem arrangement, component analysis, and performance analysis will be described.

A.3.1 Stirling-Cycle Energy Conversion Subsystem

The Stirling-cycle energy conversion subsystem is considered a distributed generation scheme for application with the Point Focus Distributed Receiver (PFDR) concept. The Stirling cycle has several advantages in this application. The PFDR collector is capable of producing temperatures above those used in Rankine cycles. The Stirling engine can operate with a heat source temperature of 816^{o}C (1500^{o}F) with a conversion efficiency well above those attainable from Rankine-cycle engines in the 1 MWe to 10 MWe range. The Stirling-cycle engine and the dish collector of the PFDR are matched so that a highly modular unit is available. The modularity of the PFDR/S concept is considered a major advantage in small power system applications.

The Stirling cycle has several disadvantages. The most significant is that Stirling engine technology cannot be considered as readily available in the near-term. The Stirling engine has not been extensively proven in field applications and a large, expensive research and development program would be required to commercialize Stirling technology. Previous studies have suggested that a Stirling engine for solar applications would require a thermal buffer between the collector and the engine to smooth out short-term variations in insolation (Jet Propulsion Laboratory 1978, pp. 2-9). Current proposals for the thermal buffer are unproven and estimated to be very expensive.

Stirling engines, in the size range of interest with characteristics specifically suitable for solar application, do not currently exist, even as prototypes. Because it was impossible to base Stirling engine characteristics on a machine suitable for solar application, it was decided to base the engine characteristics on a review of existing prototypes in the proper size range. The resulting description and performance was felt to be representative of existing Stirling engine technology.

A.3.1.1 Subsystem Arrangement

The Stirling-cycle energy conversion subsystem has four major components, illustrated in Figure A.11: the receiver/thermal buffer, the engine, the generator, and the heat rejection subsystem. The engine location has been discussed in other studies; an engine located at the focus of the concentrator has been determined as the optimal arrangement (Jet Propulsion Laboratory 1978, pp. 3-11). This arrangement requires that the receiver/thermal buffer, engine, and generator be located at the focus of the concentrator, with the heat rejection unit located on the ground adjacent to the collector.

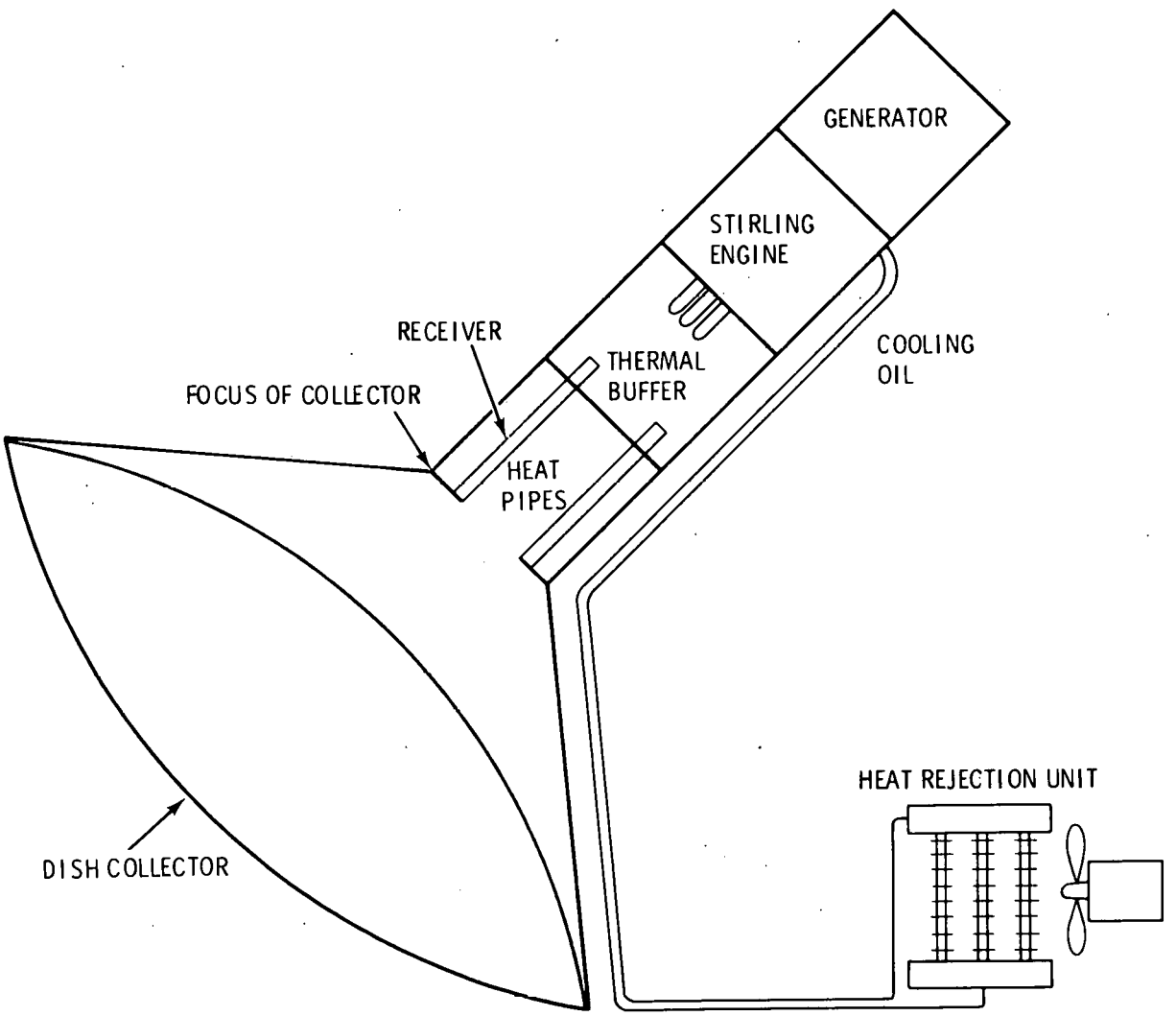

FIGURE A.11. Stirling-Cycle Energy Conversion Subsystem Arrangement

The receiver is an integral part of the thermal buffer and engine design. Therefore, the receiver's heat transfer components were considered as part of the energy conversion subsystem. The thermal buffer was considered an alternative to the base case. The thermal buffer has proven to be very expensive; thus, it was felt that accepting the performance penalty associated with large variations in insolation may prove to be cost-effective. The receiver uses liquid metal to transfer thermal energy from the receiver to the thermal buffer or directly to the Stirling engine heater tubes if the buffer is not included.

The Stirling engine receives heat from either the receiver or the thermal buffer in the Stirling engine heater tubes and rejects heat to oil which acts as a heat sink. The oil is cooled in the heat rejection unit. the Stirling engine converts heat to work in the form of a reciprocating shaft, which transmits work to the generator where the work is converted to electric energy. The Stirling engine receives thermal energy at 816^{o}C (1500^{o}F) and ultimately rejects heat to ambient conditions.

A.3.1.2 Component Analysis

Several components in the Stirling-cycle conversion subsystem are complicated and need further discussion. These include the receiver, thermal buffer, the Stirling-cycle engine, heat rejection unit, and generator.

A.3.1.2.1 Receiver. The receiver is assumed to be similar to the receiver proposed by Ford Aerospace. The receiver consists of an annulus filled with liquid sodium. The annulus forms the wall of the receiver cavity. The sodium is evaporated in the annulus and condensed on the heater tubes of the Stirling engine. The design includes a door to reduce heat loss (and freezing of sodium) during outages and a valve to control liquid sodium flow to the Stirling engine.

A.3.1.2.2 Thermal Buffer. The thermal buffer consists of an insulated cylindrical vessel containing 140 LiF-filled tubular capsules arranged in a hexagonal pattern. The condensing ends of the receiver heat pipes extend through the back end of the cylindrical vessel. The cylindrical vessel acts as a heat pipe. Sodium is evaporated at the front end of the cylinder and is condensed either on the LiF-filled tubular capsules or on the Stirling engine

heater tube depending on their respective temperatures. Energy is stored as latent heat in the LiF, which melts at 857°C (1575°F). Due to the high temperature, extensive use was made of expensive alloys such as Inconel 617, HA-188 and expensive insulation material. The resulting cost was very high. By derating the thermal buffer performance or incorporating some undetermined design change, a cost of $400/kWe is estimated for the buffer and receiver (Jet Propulsion Laboratory 1978, pp. 2-9).

A.3.1.2.3 Stirling Engine. The characteristics of the Stirling engine used in this study are based on a review of current Stirling engine technology and are representative of the MTI free-piston engine. The Stirling engine will have a free piston coupled directly to a linear alternator. Free-piston machines with linear alternators were chosen over kinematic Stirling engine designs because of the potential for increasing engine life.

The Stirling engine will have a heater tube external temperature of 816°C (1500°F) and will reject heat to cooling oil at a nominal temperature of 30°C (86°F). Other auxiliaries include the cooling oil pump and controls. In addition, the Stirling engine and generator must provide elecric power to operate the heat rejection unit.

A.3.1.2.4 Heat Rejection Unit. The heat rejection unit would consist of an oil-to-air heat exchanger, a fan and motor, and piping.

A.3.1.2.5 Generator. The type of generator for application with the free piston Stirling engine was reviewed by MTI. A linear alternator designed by MTI was chosen.

A.3.1.3 Performance Analysis

Energy conversion subsystem performance impacts plant performance in several ways. The major impact is the thermal energy to electric energy conversion efficiency. Other, less important impacts include the time required to reach full power during startup, standby load thermal energy requirements, and unrecoverable energy used during startup.

The thermal energy to electric energy conversion efficiency (η_{ECS}) is modeled as a nominal efficiency, corrected for part-load operation and ambient conditions. This conversion efficiency was determined for a nominal condition

[ambient air temperature of 21°C (70°F)] and full-load operation. Operating at less than full-load will change η_{ECS}; therefore, a correction curve was developed, relating the relative η_{ECS} to full-load fraction. In addition, as ambient air temperature changes, the temperature of the heat engine heat sink changes, which results in a variation in η_{ECS}.

The energy conversion subsystem performance is modeled as the product of four component efficiencies. The receiver efficiency is included in the collector performance model

$$\eta_{ECS} = \eta_{TB} \times \eta_{HE} \times \eta_g \times \eta_{AUX}$$

where

η_{TB} = thermal buffer efficiency
η_{HE} = heat engine efficiency
η_g = generator efficiency
$\eta_{AUX} = \frac{\text{gross ouput - auxiliary load}}{\text{gross output}}$

The thermal buffer is small and well-insulated so that η_{TB} can be assumed to be 1.00. The generator efficiency for the linear alternator is estimated as 0.9. η_{AUX}, which accounts for parasitic loads such as heat rejection unit fan power, is assumed to be 0.95.

The Stirling engine performance is assumed to be similar to the performance of the MTI free-piston design with a net efficiency of 41.8%. This gives a value of 0.36 for η_{ECS}.

Part-load operation was based on the part-load performance of the MTI free-piston engine. Figure A.12 presents the correction curve for part load operation.

Ambient air temperature correction was calculated by assuming that the actual η_{ECS} is a fixed fraction of the Carnot efficiency. By calculating the Carnot efficiency for varying ambient temperature, the relative variation in η_{ECS} can be determined. The correction curve for ambient air temperature appears in Figure A.13.

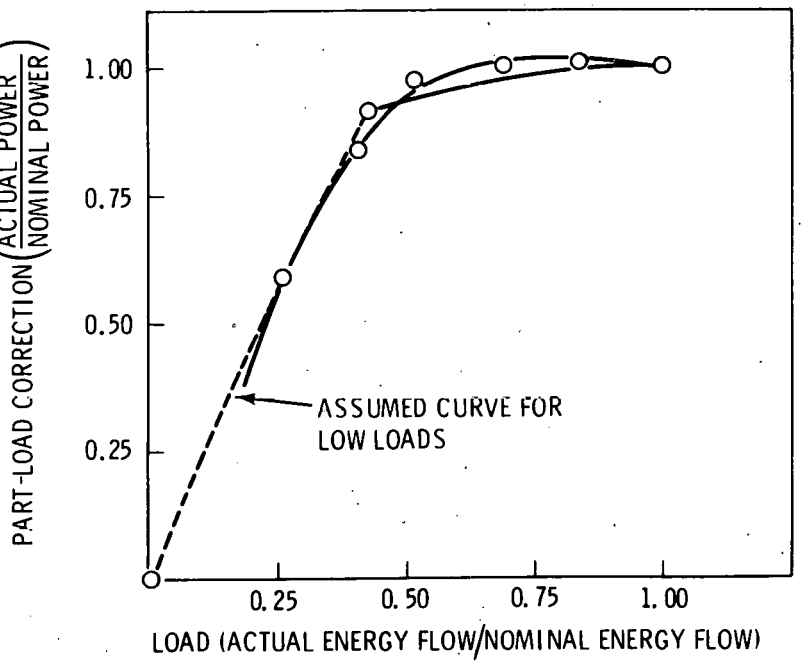

FIGURE A.12. Stirling-Cycle Part-Load Correction

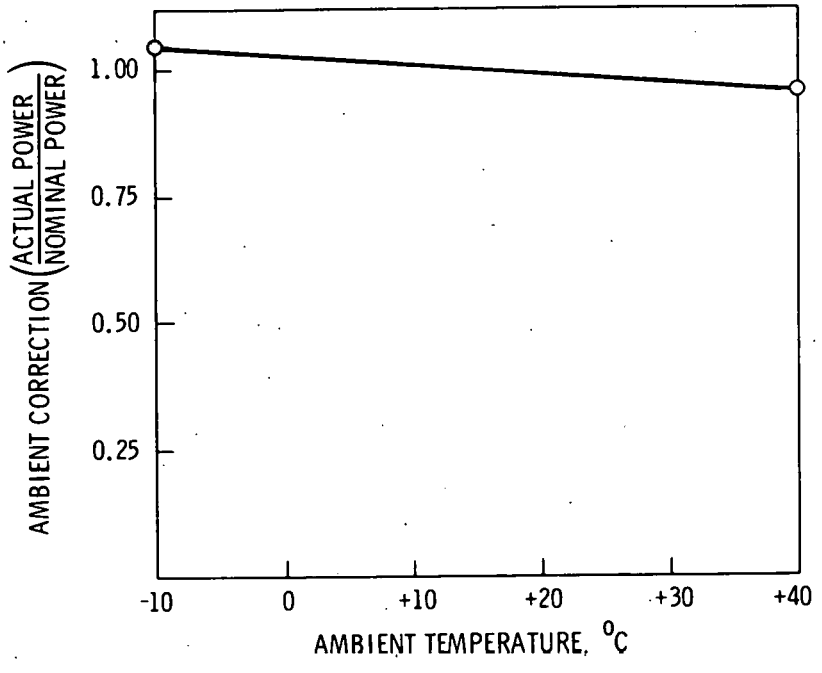

FIGURE A.13. Stirling-Cycle Ambient Temperature Correction

The Stirling engine should have good transient performance. The time required to reach full power is assumed to be 0.1 hour. Standby thermal load is negligible. The unrecoverable energy used during daily startup is estimated as 1 kWt-hr, which was calculated assuming that the engine would be ramped from no power to full power in 0.1 hour and that all energy used during startup was wasted.

A.3.2 Small Brayton-Cycle Engine Conversion Subsystem

The small Brayton-cycle energy conversion subsystem was considered as a distributed generation scheme for application with the Point Focus Distributed Receiver concept. The small Brayton engine has the same advantages as the Stirling engine just discussed except that the conversion efficiency of both an open- and closed-cycle Brayton engine are substantially below those estimated for the Stirling engine. The small Brayton-cycle engine has the advantage of being nearer-term technology than the Stirling engine.

The receiver for the small Brayton engine does not appear to have been studied in the same detail as for the Stirling. Although it is not clear whether a liquid metal heat pipe receiver and thermal buffer will be required for a Brayton-cycle engine, it does appear that they would be needed because of the difficulty in transferring large heat fluxes from the receiver absorption surfaces to a gas while maintaining a tolerable temperature drop across the receiver metal. For this study, the details of the closed-cycle Brayton engine were based on information provided by vendors.

A.3.2.1 Subsystem Arrangement

The Brayton cycle energy conversion subsystem consists of four major components: the receiver/thermal buffer, the engine, the generator, and the heat rejections subsystem. The receiver/thermal buffer, engine and generator are located at the focus of the concentrator. The heat rejection unit will be located on the ground adjacent to the collector.

The receiver is an integral part of the thermal buffer and Brayton cycle; therefore, the heat transfer components of the receiver were considered as part of the energy conversion subsystem. The thermal buffer was considered an alternative to the base case because the thermal buffer was proven very

expensive. It was felt that accepting the performance penalty associated with variations in insolation may prove to be more cost-effective. The receiver uses liquid metal heat pipes to transfer thermal energy from the receiver either to the thermal buffer or directly to the Brayton engine heater, depending on whether a thermal buffer is included.

The Brayton engine receives heat at 816°C (1500°F) in the heater and rejects heat to oil, which acts as the heat sink. The oil is cooled in the heat rejection unit. The Brayton engine converts heat to work in the form of a rotating shaft. Work is transmitted to the generator, where it is converted to electric energy. The Brayton engine receives thermal energy at 816°C (1500°F) and ultimately rejects heat to the atmosphere.

A.3.2.2 Component Analysis

The receiver, thermal buffer, and heat rejection unit used with the Brayton-cycle energy conversion subsystem are described in Section A.3.1.2 on Stirling cycle component analysis. The generators and Brayton-cycle engine are analyzed in the following paragraphs.

A.3.2.2.1 Generators. Several generator types were considered for application with the Brayton engine. Synchronous generators were rejected because each would require synchronizing and the 17.5-kWe size is too small to realize the advantages of a synchronous machine. Direct current generators were rejected because of difficulty in many controlling generators in parallel. Further, the plant's entire output would have to be converted to ac power for most applications.

An induction generator was chosen for this application because it is rugged, and requires no synchronizing and little attention. The induction generator does require a synchronous generator, a synchronous condenser, or capacitors in parallel with it to provide magnetizing current and any reactive power required by the load. Appropriate excitation must be included to render the generators operable at all loads and to ensure comparability of power output quality to that of other types of generators. A condenser can be used for this application.

A generator installed at the focus of the colector would consist of a completely enclosed induction machine with its leads to a terminal of the 460-V cable. The induction machine is an off the shelf item available for outdoor installation.

One condenser for each generator would be located on the ground. To prevent any unbalance between generating capacity and on-line capacitors the capacity rating will be about 15 kVA to ensure reliable generator operation and sufficient reactive kVA to meet the solar plant's appropriate share of reactive component in the average utility load.

A.3.2.2.2 Brayton Cycle Engine. The Brayton cycle engine will use a closed cycle with a recuperator. The engine is rated at 17.5 kWe output and will use air as the cycle working fluid.

A.3.2.3 Performance Analysis

The performance model used for the Brayton cycle energy conversion subsystem is the same as that of the Stirling engine described in Section A.3.1.3. As with the Stirling engine, the thermal buffer efficiency is assumed to be 1.0. Brayton-cycle performance is based on vendor-supplied performance curves, which include η_{HE}, η_g and η_{AUX}. A nominal efficiency of 0.32 was used. Part-load and ambient air temperature correction curves are shown in Figures A.14 and A.15.

The Brayton engine should have good transient performance. The time required to reach full power is assumed to be 0.1 hour. Standby thermal load is negligible. The unrecoverable energy used during daily startup is estimated as 1 kWt-hr, which was calculated assuming that the engine would be ramped from no power to full power in 0.1 hour and that all energy used during startup was wasted.

A.3.3 Rankine-Cycle Energy Conversion Subsystem

The Rankine cycle energy conversion subsystem was considered the base case energy conversion subsystem for all concepts using central generation. The Rankine-cycle central generation scheme requires a thermal transport subsystem to transfer heat from the receiver to a central facility containing the Rankine-cycle engine and auxiliary equipment.

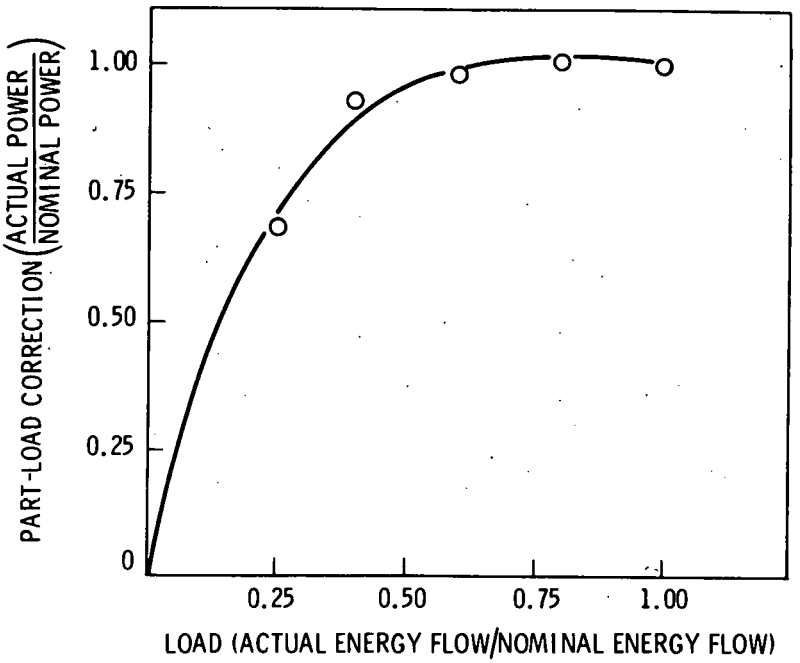

FIGURE A.14. Small Brayton-Cycle Part-Load Correction

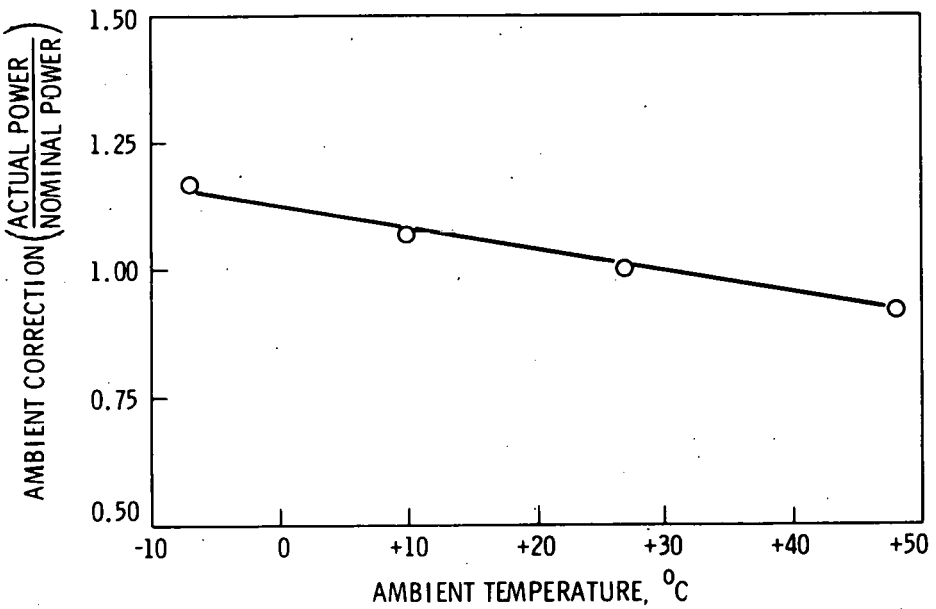

FIGURE A.15. Small Brayton-Cycle Ambient Temperature Correction

Rankine-cycle engines using steam as the working fluid are proven technology and can be expected to be highly reliable machines. The problems associated with operating a Rankine-cycle steam engine are well understood, and performance can be predicted with confidence. Rankine-cycle engines using organic working fluids do not have the operating experience of steam Rankine engines but can still be considered current technology.

Rankine-cycle engines have several disadvantages. Cycle efficiency is good for large engines but declines rapidly for smaller engines in the 1-MWe to 10-MWe range. In addition, cycle efficiency is sensitive to variations in the heat sink temperature. Because dry cooling towers are used for heat rejection, the cycle efficiency decreases rapidly with increasing ambient temperature, particularly for the low-temperature concepts.

Several Rankine cycles were considered because of differences in collector performance. Rankine-cycle performance improves with increasing heat source temperature. Conversely, collector subsystem performance worsens with increasing heat source temperature. In this study a heat source temperature (maximum temperature of Rankine-cycle working fluid) was chosen so that both the collector and the energy conversion subsystem exhibit reasonable performance. Because certain collector designs are better suited for high-temperature operation, it was decided to consider different maximum working fluid temperatures for different concepts. Six cycles were considered. Table A.3 includes the characteristics of each cycle.

Concepts using use oil and rock storage may have an additional temperature limitation when operating from storage. The maximum temperature limit of 304^{o}C (580^{o}F) for the oil dictates a maximum Rankine-cycle working fluid temperature of 274^{o}C (525^{o}F) when operating from storage. This limitation has no effect on the LCNT, which operates at 232^{o}C (420^{o}F). However, for concepts operating at 343^{o}C (650^{o}F) and 510^{o}C (950^{o}C), a reduction in working fluid temperature results. These concepts must to use a dual-admission turbine that can operate efficiently with either working fluid temperature.

TABLE A.3. Alternative Rankine Cycle Characteristics

Cycle	Steam Turbine Inlet Conditions	Applicable Concepts
1	510°C (950°F)	PFCR, PFDR/R, LFCR, LFDR-TR, FMDF
2	427°C (800°F)	PFDR/R, LFCR, LFDR-TR, FMDF
3	343°C (650°F)	LFDR-TC
4	216°C (420°F)	LCNT
5	274°C (525°F dual-admission)	PFCR, PFDR/R, LFCR, LFDR-TR, FMDF
6	274°C (525°F dual-admission)	LFDR-TC

The Rankine-cycle arrangements, component analysis, and performance analysis are based on a review of Rankine-cycle engines conducted by Bechtel National, Inc. under subcontract to PNL. The Bechtel report is reproduced in its entirety as Appendix C.

A.3.3.1 Subsystem Arrangement

The Rankine-cycle energy conversion subsystem consists of three components: the Rankine-cycle heat engine, the generator, and the heat rejection unit. The steam generator of the Rankine cycle is included in either the collector subsystem or the storage subsystem. The feed pump is included in the transport subsystem for all concepts except the PFCR. The feed pump was included in the PFCR energy conversion subsystem because its size was not a strong function of field size and layout. In the other central generation concepts, the feed pump size and parasitic load were strongly influenced by the collector field characteristics.

Rankine-cycle energy conversion subsystems were characterized for plants with net outputs of 1 MWe, 5 MWe and 10 MWe. In sizing the Rankine-cycle engine, a parasitic load of 10% was included so that the gross electric power output from the energy conversion subsystem was 1.1 MWe, 5.5 MWe, and 11 MWe.

A.3.3.2 Component Analysis

Because of their complexity, several components in the Rankine-cycle energy conversion subsystem need further discussion. These include the working fluid, turbine cycle equipment, and heat rejection unit.

A.3.3.2.1 Rankine Cycle Working Fluid. Several working fluids can be used in the Rankine-cycle energy conversion subsystem. The most common is water. At low and intermediate temperatures [less than 371°C (700°F)], other organic working fluids can be considered. The organic working fluids tend to have an advantage at lower temperatures and for small plants. A toluene working fluid was considered for the LCNT/R concept because of the low operating temperature. The toluene Rankine cycle showed a small increase in turbine efficiency for a 1-MW plant, but the increase was not sufficient to justify the added complication of using a working fluid other than water.

A.3.3.2.2 Turbine. The turbine for the 10-MWe 510°C (950°F) oil storage energy conversion subsystem is described in detail. Smaller systems and those with different operating conditions will be similar except that a dual-admission turbine will not be required for the 232°C (420°F), 274°C (525°F), 427°C (800°F) and 510°C (950°F) HITEC storage system.

The turbine is a single automatic extraction (admission) condensing steam turbine with three uncontrolled extraction connections. It consists of a two-stage, high pressure section supplied by main steam and a 19-stage low pressure section that operates on steam from the high pressure section and/or admission steam. The design speed of the turbine is 9500 rpm. A similar turbine rated at 1 MWe would operate at 13,000 rpm and have two uncontrolled extraction points. Because the steam is condensed in an air-cooled condenser, the turbine must be suitable for operating at higher than normal back pressure.

Bechtel National, Inc., has indicated that, for a 1-MWe turbine, efficiency is not improved by operating with an inlet steam pressure above 6.89 MPa (1000 psi). The high-temperature subsystems considered in this study are intended to operate at 10.0 MPa (1450 psi). It may be that the operating pressure of the 1-MWe systems can be reduced, but it has not been considered for this study.

Accessories for the turbine-generator include inlet steam stop and control valves, extraction stop valves, turning gear, lubrication system, steam seal system electrohydraulic control system, and foundation plate with bolts.

A.3.3.2.3 Generator. The turbine at 9500 rpm drives the generator at 1800 rpm through a double helical spur gear reduction unit. The generator is a three-phase, 60-Hz, four-pole synchronous unit rated at 13.8 kV with a power factor of 0.9. The generator is air-cooled and equipped with a brushless exciter.

A.3.3.2.4 Turbine Cycle Equipment. The turbine cycle equipment includes the feedwater heaters, the mechanical condensate pumps, booster pumps, miscellaneous piping and valves, condensate demineralizers, condensate makeup and storage, instruments and controls, and auxiliary equipment.

The lowest pressure of the three feedwater heaters would be of the open deaerating type, with the two intermediate pressure shell and tube heaters operating at approximately 0.344 MPa (50 psia) and 1.171 MPa (170 psia). The feedwater booster pumps draw from the deaerating heater drain tank and pump the condensate through the other two feedwater heaters to the feed pump suction. A 1-MWe cycle would have only one intermediate pressure heater, operating at approximately 0.55 MPa (80 psia).

A.3.3.2.5 Heat Rejection Unit. The heat rejection equipment consists of an air-cooled condenser, condensate pumps, piping, mechanical vacuum pump, and auxiliary equipment. The air-cooled condenser can be located either adjacent to the turbine generator building or on the building roof. Exhaust steam from the turbine is ducted to the condenser, which consists of a number of modules, each having one 75-kW fan and three air/steam heat exchangers. The condensed water is collected in the hot well and returned to the plant by the condensate pumps and piping. Approximately one module is required for each 1 MWe of plant size, assuming a design point of 24°C (75°F).

A.3.3.3 Performance Analysis

The thermal energy to electric energy conversion efficiency (η_{ECS}) was modeled using the method described in Section A.3.1.3. A nominal efficiency was determined for each size Rankine-cycle energy conversion subsystem. The

nominal efficiency was determined for full-load operating conditions and a design ambient air temperature of 23°C (75°F). Correction curves were developed to relate relative η_{ECS} of full-load fraction and ambient air temperature.

Bechtel National, Inc. has developed curves relating nominal engine efficiency to plant size and steam inlet conditions. Figure A.16 shows cycle efficiency for six inlet conditions over a size range of 1 MWe to 10 MWe. The data shown are for 3600-rpm addmission turbines. The net cycle efficiency is based on the net electrical output, which is equal to the gross electrical output less the auxiliary loads. The efficiency of the high speed turbine is assumed to be 8% higher than the 3600-rpm turbine. For some systems the feed pump has been included in the transport subsystem, so the nominal efficiency

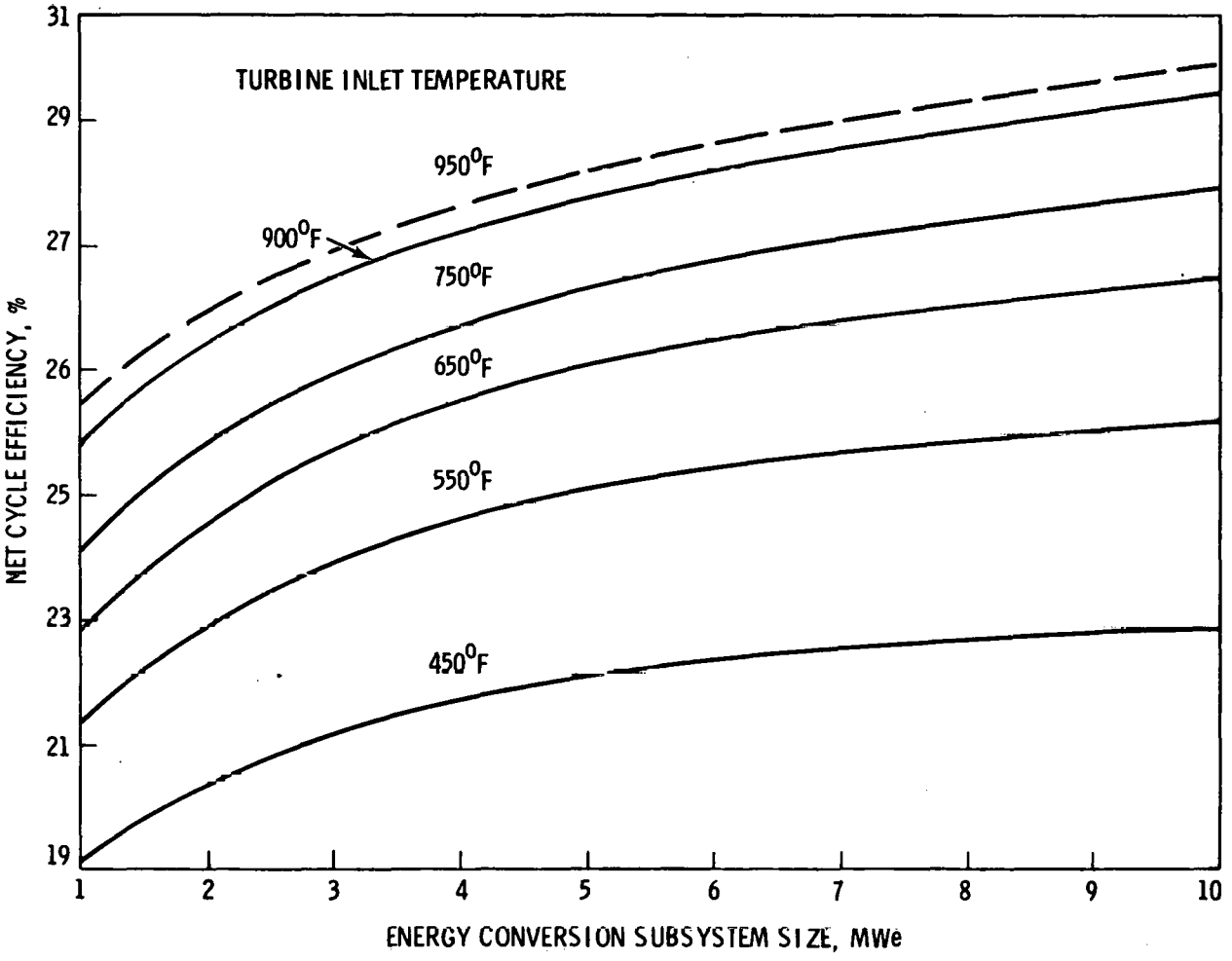

FIGURE A.16. Rankine Cycle Efficiency

must be increased to correct for the increased auxiliary load of the feed pump. The feed pump used in developing the performance curve requires 3.5% of the plant output. Nominal efficiency is given by

$$\eta_{ECS} = \frac{\eta_{ECS}\ 3600\ rpm}{(1 - 0.08)\ (1 - 0.035)}$$

For systems in which feedwater is not circulated through the field by the feed pump (LCNT, HITEC concepts) the feed pump is accounted for in the energy conversion subsystem efficiency. In these systems the energy conversion subsystem efficiency is not corrected for the 3.5% allotted to the feed pump. Table A.4 summarizes the nominal efficiency as a function of plant size and inlet conditions.

TABLE A.4. Nominal Efficiency(a)

Turbine Inlet Condition	Plant Size		
	1 MWe	5 MWe	10 MWe
950°F	0.293	0.323	0.337
800°F	0.277	0.305	0.324
650°F	0.256	0.283	0.305
420°F	0.219	0.239	0.252
525°F (dual-admission)	0.221	0.239	0.251
525°F (single-admission)	0.246	0.268	0.290

(a) Full load, 75°F ambient temperature, high speed turbine, no feed pump.

The variation of turbine cycle efficiency with operation at part load is shown in Figure A.17. The effect of auxiliary loads is included. This information is based on the preliminary design report for the 10-MWe Barstow pilot plant. The part-load correction curve for the 232°C (420°F) system is assumed to have the same shape as the admission steam only curve (274°C). The curves for the 343°C (650°F) and 427°C (800°F) systems were developed by assuming that

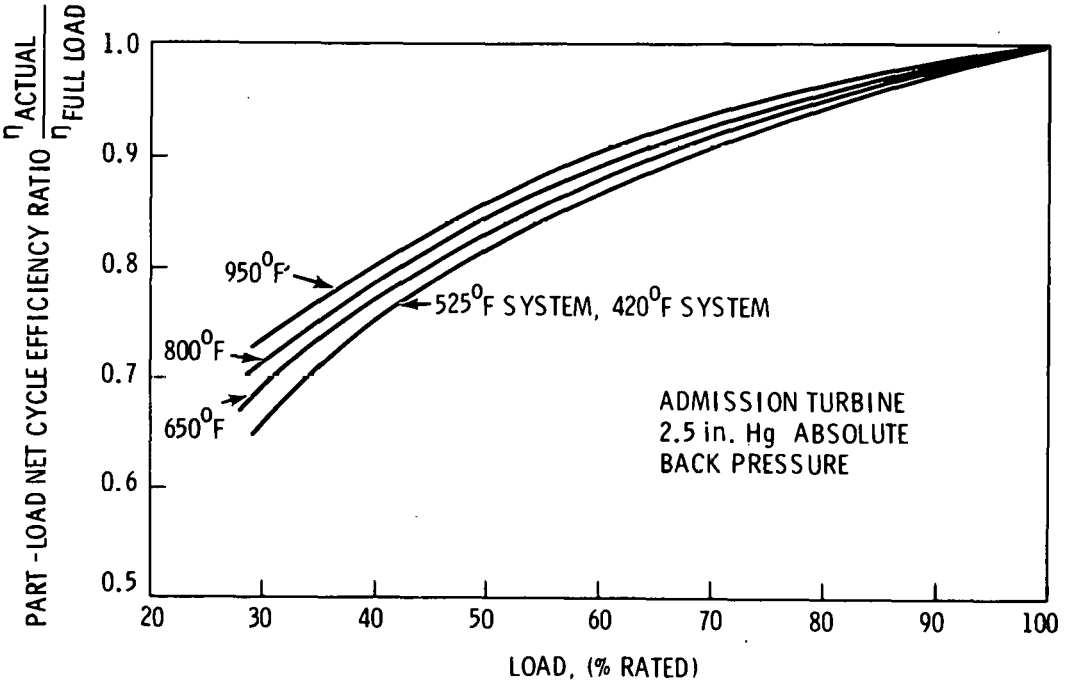

FIGURE A.17. Turbine Cycle Efficiency for Part-Load Operation

the correction factor was a linear function of inlet temperature between the main steam and admission steam lines for a given part load.

The variation of turbine cycle efficiency with ambient air temperature is shown in Figure A.18. The calculation of turbine efficiency variation with ambient air temperature is complicated because turbine and air-cooled condenser performance are coupled. In this analysis a turbine exit temperature was assumed, and the corresponding ambient temperature was calculated.

The Rankine-cycle engine has fair transient performance. Bechtel National has estimated the time required to reach full power as 45 minutes for a hot start. Standby thermal energy load is estimated to be 330 kWt for the 10-MWe turbine (Hallet and Gervais 1977, p. 4-14) and is assumed to decrease linearly with turbine size. The preliminary unrecoverable engine startup thermal load requirement is estimated to be 7500 kWt-hr for the 10-MWe turbine (p. 4-14) and is also assumed to decrease linearly with turbine size.

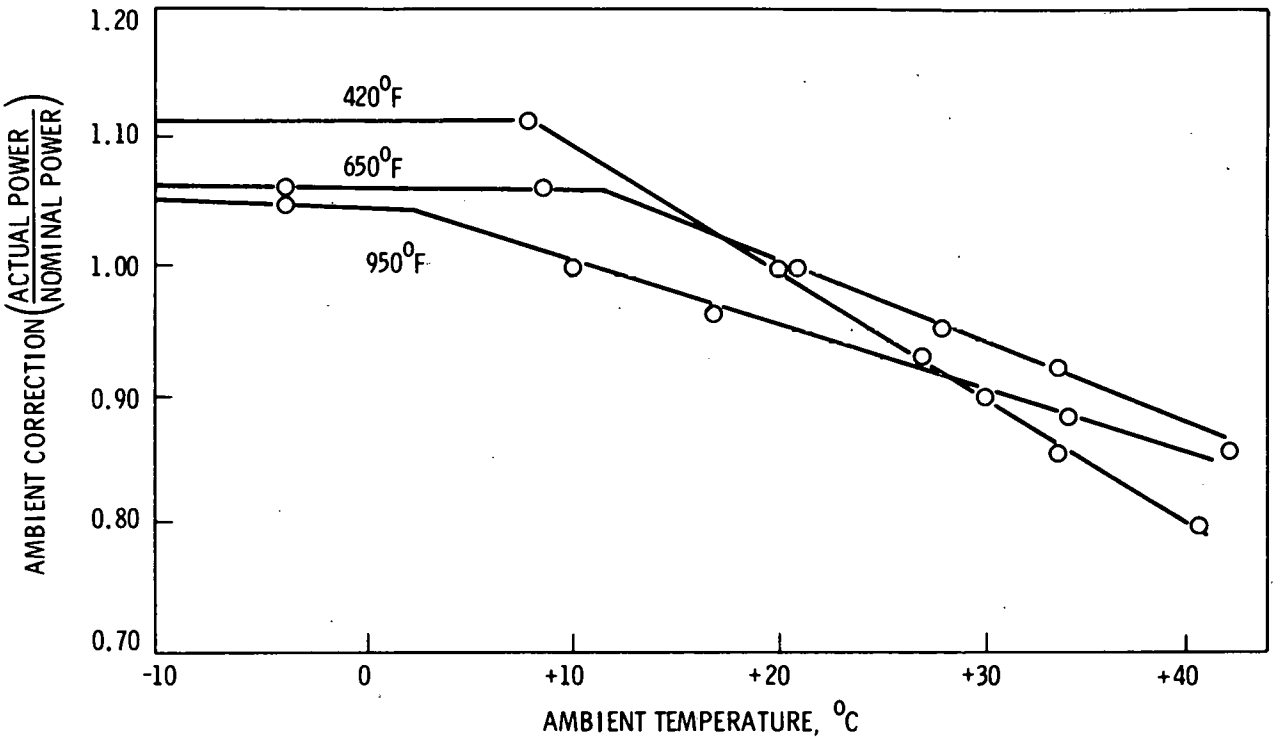

FIGURE A.18. Rankine-Cycle Energy Conversion Subsystem Ambient Temperature Correction Curves

A.3.4 Large Brayton-Cycle Energy Conversion Subsystem

The large Brayton-cycle energy conversion subsystem is considered an alternative energy conversion subsystem for the Point Focus Central Receiver concept. The large Brayton engine central generation scheme is located on the central receiver tower so that a thermal transport subsystem is not required. An electric transport subsystem transfers the electric power from the tower to either storage or the utility grid.

The closed-cycle large Brayton engine has been widely used, and the problems associated with operating the Brayton engine are well understood. Operating at the receiver temperature of approximately 816°C (1500°F) the Brayton-cycle operating conditions are well within current technology. At these operating conditions the large Brayton-cycle engine is more efficient than a similarly sized Rankine engine, assuming that the Brayton engine has an efficient recuperator.

The large Brayton-cycle engine arrangement, component analysis and performance analysis are based on vendor information. The Brayton engines are assumed to be similar to those supplied by AiResearch.

A.3.4.1 Subsystem Arrangement

The large Brayton-cycle energy conversion subsystem consists of two components, the Brayton engine and the generator. Because the Brayton engine uses a closed cycle, a heat rejection subsystem is required and would be located adjacent to the tower. The Brayton engine is a normal closed-cycle gas turbine except that the combustion chamber has been replaced with the solar thermal air heater in the central receiver. The air heater will be discussed as part of the collector subsystem. Both the Brayton engine and the generator are located on the tower close to the receiver and air heater.

Large Brayton-cycle energy conversion subsystems were characterized for plants with net output of 1 MWe, 5 MWe, and 10 MWe. In sizing the Brayton-cycle engine, a parasitic load of 2% was included so that the gross electric power output from each plant's energy conversion subsystem was 1.02 MWe, 5.1 MWe, and 10.2 MWe, respectively.

A.3.4.2 Component Analysis

Three components in the large Brayton-cycle energy conversion subsystem need further discussion: the Brayton engine, generator, and heat rejection unit.

A.3.4.2.1 Brayton Engine. The Brayton engine is a closed-cycle gas turbine with a recuperator. The cycle is shown schematically in Figure A.19. The gas turbines are similar to those supplied by AiResearch.

A.3.4.2.2 Generator. The gas turbine drives the generator through a speed reducer. The generator is a three-phase, 60-Hz, four-pole synchronous unit rated at 13.8 kV with a power factor of 0.9. The generator is air-cooled and equipped with a brushless exciter.

A.3.4.2.3 Heat Rejection Unit. The heat rejection unit would consist of a water/air heat exchanger, fans, motors, pumps, and piping.

POWER OUTPUT	30 kW
CYCLE EFFICIENCY	0.31
β = TURBINE PRESSURE RATIO / COMPRESSOR PRESSURE RATIO	0.933
SHAFT SPEED rpm	52,000
WORKING FLUID	ARGON
WORKING FLUID FLOW RATE	1.51 lb/sec (0.68 kg/sec)
COOLANT FLUID	WATER
COOLANT FLUID FLOW RATE	1.26 lb/sec (0.57 kg/sec)

T = °F (°C)
P = psia (ATMOS)
M = lb/sec (kg/sec)

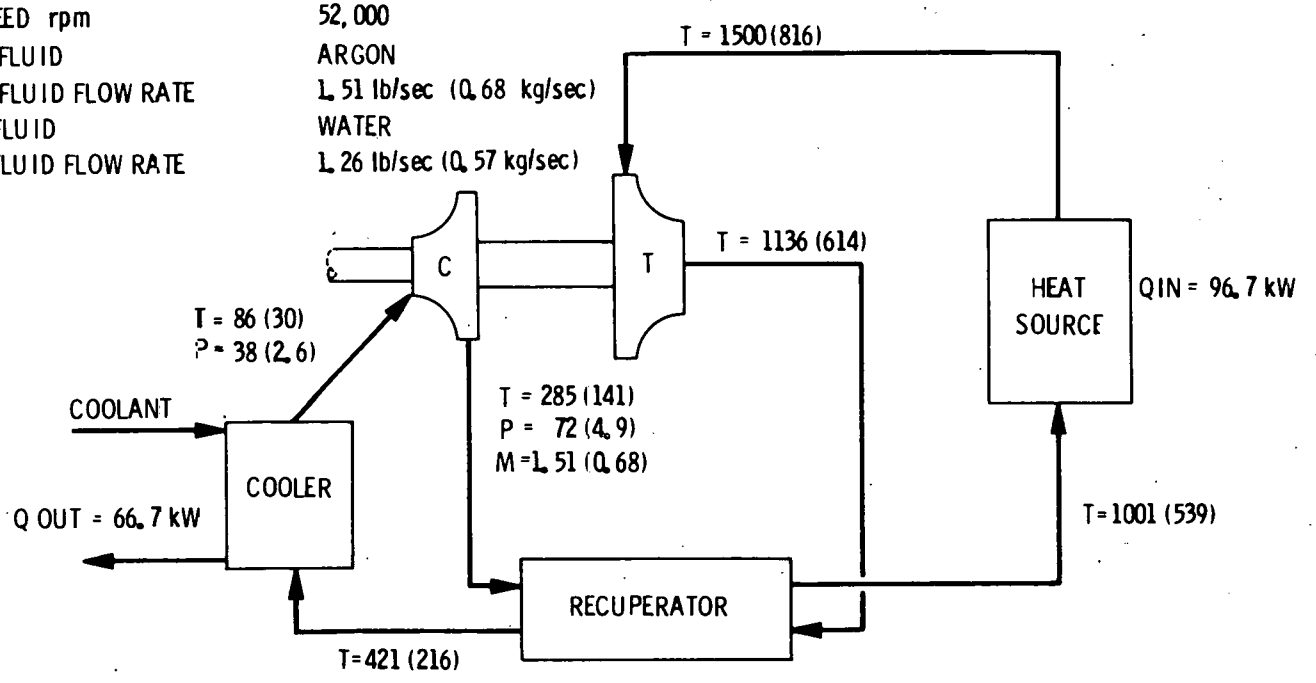

FIGURE A.19. Brayton Engine Cycle

A.3.4.3 Performance Analysis

The thermal energy to electric energy conversion efficiency (η_{ECS}) was modeled using the method described in Section A.3.1.3. A nominal efficiency was determined for each size of the large Brayton-cycle energy conversion subsystem. The nominal efficiency was determined for full-load operating conditions and a design ambient air temperature of 23°C (75°F). Correction curves were developed to relate relative η_{ECS} to full-load fraction and ambient air temperature.

APPENDIX A REFERENCES

Appleby, A. J., and J. P. Gabano. 1976. "Current Status and Prospects of the Zn-Air and Na-S Batteries in France." In Proceedings of the Symposium and Workshop on Advanced Battery Research and Design. ANL-76-8, Argonne National Laboratory, Argonne, Illinois.

Argonne National Laboratory. 1978. High Performance Batteries for Stationary Energy Storage and Electric-Vehicle Propulsion. ANL-77-75, Argonne, Illinois.

Bechtel National, Inc. 1976. An Engineering Study of a 20 MW Lead-Acid Battery Energy Storage Demonstration Plant. Report No. CONS/1205-1, San Francisco, California.

Birk, R., and F. R. Kalhammer. 1976. "Secondary Batteries for Load Leveling." In Proceedings of the Symposium and Workshop on Advanced Battery Research and Design. ANL-76-8, Argonne National Laboratory, Argonne, Illinois.

Ciprios, G., et al. 1977. Redox Bulk Energy Storage System Study, Vol. 1 and 2 Final Report, February 18, 1976-January 30, 1977. NASA-CR-135206 (Vol. 1&2), Exxon Corporation, Linden, New Jersey.

General Electric Company. 1978. Development of Sodium-Sulfur Batteries for Utility Application. EPRI EM-683, Electric Power Research Institute, Palo Alto, California.

Hallet, R. W., and R. L. Gervais. 1977. Central Receiver Solar Thermal Power System, Phase 1, CDRL Item 2, Vol. 5. SAN/1108-8/5, McDonnell Douglas Astronautics Company, Huntington Beach, California.

Hausz, W., B. J. Berkowitz, and R. C. Hare. 1978. Conceptual Design of Thermal Energy Storage Systems for Near-Term Electric Utility Applications, Vol1. GE 78 TMP-60 Vol. 1, General Electric Company, Schenectady, New York.

Jet Propulsion Laboratory. 1978. Thermal Power Systems Advanced Solar Thermal Technology Project, Advanced Subsystems Development, Second Semi-Annual Progress Report. DOE/JPL-1060-78/6, California Institute of Technology, Pasadena, California.

Lee, C., et al. 1978. Energy and Environmental Analysis of the Lead-Acid Battery Life Cycle. HIT-725, Hittman Associates, Columbia, Maryland.

Liu, C. C. 1975. The Research and Development of a Soluble Reactants and Products Secondary Battery System. NASA-CR-143510, Pittsburgh University, Pittsburgh, Pennsylvania.

Martin Marietta. 1977. Central Receiver Solar Thermal Power System, Phase 1, Preliminary Design Report, Vol. 5, Thermal Storage Subsystem. Denver, Colorado.

Mechanical Engineering. 1979. "System May Speed Growth of Solar Energy Storage." 101(6):55.

NASA-Lewis Research Center. 1977. Redox Flow Cell Development and Demonstration Project, Calendar Year 1976. NASA TM-73873, Cleveland, Ohio.

Perry, Chilton, and Kirkpatrick. 1963. Perry's Chemical Engineers' Handbook. McGraw-Hill Book Co., New York, New York.

Public Service Electric and Gas Company, New Jersey. 1976. An Assessment of Energy Storage Systems Suitable for Use by Electric Utilities. EPRI EM-264, Electric Power Research Institute, Palo Alto, California.

Roy, A. S., and S. I. Kaplan. 1978. "Analysis Performance Capabilities of Redox-Flow Storage Batteries." In Proceedings of Meeting of the American Section of the International Solar Energy Society. CONF-780808-20, National Technical Information Service, Springfield, Virginia.

Shimotake, H., and L. G. Bartholme. 1976. "Development of Uncharged Li-Al/FeS Cells." In Proceedings of the Synposium and Workshop on Advanced Battery Research and Design. ANL-76-8, Argonne National Laboratory, Argonne, Illinois.

Thaller, L. H. 1974. Electrically Rechargeable Redox Flow Cells. NASA TM X-71540, NASA-Lewis Research Center, Cleveland, Ohio.

Thaller, H. 1979. "Redox Flow Cell Energy Storage Systems." In Proceedings of AIAA Terrestrial Energy Systems Conference. CONF-79-0989, National Technical Information Service, Springfield, Virginia.

Warshay, M., and L. O. Wright. 1975. "Cost and Size Estimates for an Electrochemical Bulk Energy Storage Concept." In Proceedings of Energy Storage Symposium, Fall Meeting of the Electrochemical Society, pp. 130-140. CONF-751032, National Technical Information Service, Springfield, Virginia.

Weiner, S. A. 1976. "The Sodium/Sulfur Battery: A Progress Report." In Proceedings of the Symposium and Workshop on Advanced Battery Research and Design. ANL-76-8, Argonne National Laboratory, Argonne, Illinois.

APPENDIX B

COST ESTIMATES

APPENDIX B
COST ESTIMATES

Determination of the levelized energy cost (LEC) attribute and the fixed cost as a percentage of levelized energy cost (FIX) attribute requires estimating costs of capital investment, operating and maintenance, and replacement capital. Of these, the capital investment costs are the most important; they are the primary determinants of levelized energy cost and vary widely among concepts. Unit cost estimates and cost estimate scaling relationships used in determining capital investment costs are discussed in this appendix.

B.1 COLLECTOR COST ESTIMATES

Costs for concentrators and receivers, which jointly comprise the collector subsystem, were estimated using approaches described in Section 5.3.1. The level of detail in the estimates varied among components due to differences in their documentation and design detail.

For some collector components, design information was very limited, resulting in rough estimates of component cost.

B.1.1 Material and Labor Estimate Bases

Collector cost estimates were developed using information from a variety of sources. Design information was obtained primarily through concept proponents and, for some collectors, was acquired from several sources. Sources for cost estimates varied considerably among concepts and were determined principally by the level of detail available in collector designs. Cost estimates for well-defined components were developed using information from vendors, average unit costs for materials, and information from other collector cost studies. Cost estimates for components that were not well-defined were based principally upon estimates from concept proponents and other collector cost studies.

The general basis for estimates of materials and labor costs is described below for each concept.

B.1.1.1 PFCR/R Estimate Basis

The baseline design for the PFCR/R heliostat (concentrator) is very similar to both the McDonnell Douglas (MDAC) and Solaramics prototype heliostats. Primary materials requirements were obtained from MDAC design descriptions and manufacturing analysis of heliostats (McDonnell Douglas 1977; Drumheller 1978). Specifications assumed for heliostat costing purposes are given in Table B.1.

TABLE B.1. Materials Specifications Assumed for PFCR/R Heliostat

Item	Specification	Quantity
Reflective Surface	Second surface mirror laminated to glass back panel	49 m^2
Mirror Structural Support	Galvanized steel	1012 lb
Support Structure	Galvanized steel	351 lb
Drive/Tracking Unit	Two-axis drive/tracking mechanism	1 per heliostat
Pedestal	Galvanized steel	306 lb
Foundation	Concrete, average reinforcing	2.8 yd^3
Foundation	Galvanized steel form	75 lb

Heliostat cost estimates were developed assuming that most materials would be purchased fully fabricated, with some materials partly fabricated in the heliostat manufacturing facility. Minimal field assembly of the heliostat would be required, because any parts requiring complex assembly could be shipped fully assembled from the manufacturing facility. Field installation costs assure the use of specialized installation equipment such as is discussed by McDonnell Douglas (1977).

Material costs for galvanized and carbon steel components were developed from information in cost estimating guides, industry cost trends, and previous solar costing reports (Robert Snow Means Co. 1976, 1977; Dodge 1977; Mitre

Corp. 1977; Guthrie 1974). Unit costs for reflective surfaces were developed using estimates from previous solar costing reports as guidelines, and are based upon optimistic assumptions regarding potential cost reductions due to increased solar production (Mitre Corp. 1977; Drumheller 1978). The drive/tracking unit was considered to consist of motors, gearbox, and tracking unit, with each of these components treated essentially as a "black box." Cost estimates for drive/tracking components were developed from information in other cost studies, contact with solar manufacturers, contact with concept proponents, and comparison with current motor and gearing costs for nonsolar applications (McDonnell Douglas 1977; Drumheller 1978; Robert Snow Means Co. 1976, 1977). An overall materials and installation cost was developed for the foundation concrete work, and was obtained from the Robert Snow Means Co. construction cost estimating guides (1976, 1977).

Receiver cost estimation for the PFCR/R concept was complicated by the fact that receiver size varied as concentrator field size varied. Hence, a standard receiver could not be used for all plants. Receiver cost estimates were based primarily on information for small central receivers reported by Sandia Laboratories (Holl 1978). The effects of receiver size on cost were accounted for by using cost estimate scaling relationships for various portions of the receiver costs. Cost estimate scaling relationships were of the form

$$\text{Cost}_A = \text{Cost}_B \left(\frac{\text{Size}_A}{\text{Size}_B}\right)^S$$

where

Cost_A = cost of component A
Cost_B = cost of component B
Size_A = capacity of component A
Size_B = capacity of component B
S = scaling parameter.

Estimates for receivers of various sizes were developed using receiver steam flow rates as capacity parameters for all portions of receiver cost. Assumed scaling parameters were based upon known scaling parameters for similar equipment and operations.

Receiver costs from other solar cost studies were compared to the PNL cost estimates obtained by scaling the Sandia cost information (Mitre Corp. 1977; Fujita et al. 1978; Selcuk 1975; Martin Marietta 1975; McDonnell Douglas 1976). Although strict comparisons of the estimates are not feasible because of differences in receiver size, costing assumptions, and design assumptions, it was felt that the PNL estimates fell within an appropriate range.

Towers for supporting central receivers were costed separately from receivers and were included in the receiver cost account. Tower costs for towers of various heights and land-bearing capabilities were obtained from a number of sources, and used to determine average tower cost as a function of tower height (Mitre Corp. 1977; Selcuk 1975; Martin Marietta 1975; McDonnell Douglas 1976; Honeywell, Inc. 1977). Tower cost estimates assume a production rate of 20 to 40 similar towers yearly.

B.1.1.2 PFCR/B Estimate Basis

The concentrator portion of the PFCR/B collector subsystem is identical to that of the PFCR/R concept described in Section B.1.1.1.

The conceptual design receiver for the PFCR/B concept was assumed to be similar in configuration to the PFCR/R receiver but would use liquid metal heat pipes to enhance heat transfer. Incremental costs of using heat pipes in the receiver design were assessed by comparison to the additional costs for small distributed receivers. Receivers for the PFDR/S concept were estimated as 60% more expensive than lower temperature receivers not using heat pipes. Because central receivers would be produced at much lower rates than distributed receivers, it was estimated that heat pipe technology would experience fewer mass production benefits and cost reductions for central receivers than for distributed receivers. For these reasons, it was estimated that the receiver for the PFCR/B concept would be 80% more expensive overall than the counterpart PFCR/R receiver. An inherent liability in this estimate is that, even if there

were no uncertainty on the additional costs for a specific design, the percentage additional costs could vary substantially over the receiver size range considered. Until more detailed designs become available, assessing potential variations in cost for the PFCR/B receiver will remain somewhat speculative.

The tower used to support the receiver and engine was assumed to cost the same as towers for the PFCR/R concept, as discussed in Section B.1.1.1. Although the tower for the PFCR/B concept would be required to support more weight than the tower for the PFCR/R concept, information on tower costs suggests that cost increases for the PFCR/B towers are minimal. A much more detailed analysis would be required to assess exact differences in cost between PFCR/B and PFCR/R towers, as a number of tower heights and receiver weights must be considered for each concept.

B.1.1.3 PFDR/R Estimate Basis

The baseline design for the PFDR/R concentrator uses a parabolic concentrator with a 100-m^2 aperture area that tracks the sun in two axes. At the time of this report, conceptual designs for PFDR/R concentrators were generally less defined than for other concepts; as such, their material requirements and cost estimates are based upon more subjective judgments than those used for other concepts.

Conceptual designs for a PFDR concentrator are discussed in general in several previous solar reports (Selcuk 1976; Fujita et al. 1977; Mitre Corp. 1977). Estimated materials quantities were developed based upon preliminary design calculations for these conceptual designs and are shown in Table B.2. Basic specifications for the reflective surface were assumed to be identical to those for the PFDR/R heliostat. The drive/tracking unit was assumed to be similar to the unit used for the PFDR/R heliostat, with allowance for increased drive capacity required because of the larger surface area and greater concentrator weight. Reflective surface supports are used to structurally strengthen reflective surfaces and to provide for easy mounting to the mirror structural supports.

Concentrator cost estimates were developed assuming that the majority of materials would be purchased fully fabricated, with partial fabrication of some

TABLE B.2. Materials Specifications Assumed for PFDR/R Concentrator

Item	Specification	Quantity
Reflective Surface	Second surface mirror laminated to glass back panel	106 m^2
Reflective Surface Support	Galvanized steel	180 lb
Mirror Structural Support	Galvanized steel	2050 lb
Support Structure	Galvanized steel	1110 lb
Drive/Tracking Unit	Two-axis drive/tracking mechanism	1 per concentrator
Pedestal	Galvanized steel	850
Foundation	Concrete, average reinforcing	3.5 yd^3
Foundation	Galvanized steel form	380 lb

components performed in the concentrator manufacturing facility. Concentrator assembly is assumed to be performed on an assembly line in the manufacturing facility with concentrators shipped in several pieces for field installation. Final concentrator assembly would be performed at the power plant site and is included under field costs. Field installation costs assume the use of specialized installation equipment similar to that used for the PFCR/R heliostat.

Unit costs for reflective surfaces were the same as those used for the PFCR/R heliostat. Material costs for galvanized steel components were developed using the same data base as was used for the PFCR/R heliostat (Robert Snow Means Co. 1976, 1977; Dodge 1977; Miska 1978; Mitre Corp. 1977; Guthrie 1974). Costs for the drive/tracking unit were based upon drive/tracking unit costs for the PFDR/R heliostat, with additional cost allowances to reflect increased drive capacity. An overall materials and installation cost was developed for the foundation concrete work based upon information from construction cost estimating guides (Robert Snow Means Co. 1976, 1977).

The PFDR/R receiver is a cavity receiver mounted at the focal point of the concentrator. Receiver costs were estimated based upon conceptual design information and checked by comparison to other receiver cost estimates.

Receiver conceptual design information was obtained from the same sources used in establishing concentrator design (Selcuk 1976; Fujita 1977; Mitre Corp. 1977). This information was then used in establishing baseline estimates of material quantities for heat exchanger tubing, insulation, and the receiver structural support. Estimates of the purchase price of these materials were developed from cost estimating guides and combined with assembly labor cost estimates and manufacturing overheads to obtain an estimate of receiver manufacturing cost (Robert Snow Means Co. 1976, 1977; Dodge 1977; Miska 1978; Mitre Corp. 1977; Guthrie 1974; Peters and Timmerhaus 1968). Field installation costs were estimated assuming a simple bolt-on attachment of receiver to concentrator and quick connection of the receiver to the transport subsystem.

Although collector cost estimates for all concepts were compared to estimates of other sources as a check, special effort was put into comparison of the PFDR/R receiver cost estimate. In addition to estimates found in previous solar designs studies (Fujita 1977; Fujita et al. 1978), organizations involved in receiver R&D (Fairchild, GE, Ford Aerospace) provided information. In general, the PNL receiver cost estimates were higher than those from other sources. This discrepancy resulted from differences in assumed receiver production rates and differences in cost accounting procedures. Estimates from other sources often used production rates an order of magnitude greater than the reference production rate assumed for this study. The larger production rates lowered manufacturing cost estimates due to learning and production economies of scale. In addition, many of the other receiver cost estimates differed in the way costs were reported, with some giving only direct materials and labor cost for a given production scenario. The PNL receiver cost estimates include direct costs, indirect costs, factory overheads, and profits and field installation costs. After accounting for discrepancies in estimates due to accounting differences and differences in production rate assumptions, it was concluded that PNL estimates were comparable to other estimates checked.

B.1.1.4 PFDR/B Estimate Basis

The concentrator portion of the PFDR/B collector subsystem is assumed to be identical to that of the PFDR/R concept, and is described in Section B.1.1.3.

The conceptual design developed for the receiver was similar enough to the receiver of the PFDR/R concept that, for costing purposes, it was estimated in the same manner. This resulted in an overall collector cost identical to that for the PFDR/R concept.

B.1.1.5 PFDR/S Estimate Basis

The concentrator portion of the PFDR/S collector subsystem is assumed to be identical to that of the PFDR/R concept described in Section B.1.1.3.

The PFDR/S receiver, described in more detail in Section A.3.1.2.1, utilizes a liquid sodium-filled annulus to enhance heat transfer. Cost estimates were based upon information received from Ford Aerospace and cost analysis of another receiver proposed for small Stirling-cycle engines (Jet Propulsion Laboratory 1978). Receiver manufacturing costs include materials and labor, indirect costs, overheads, and profit. Field installation costs were assumed to be the same as for the PFDR/R receiver.

B.1.1.6 FMDF Estimate Basis

Several approaches to conceptual designs for the FMDF concentrator have been described, differing in the type of structural supports used, the amount of excavation required, and in general, the type and quantity of materials required (E-Systems, Inc. 1978a, 1978b; Texas Tech University 1977). The conceptual concentrator design analyzed in this study consists of a large bowl-like structure made up of individual mirror panels attached to a criss-cross concrete frame. Partial excavation is used in the bowl construction.

Materials specifications and quantities were for the FMDF concentrator obtained from E-Systems, Inc., and are shown in Table B.3. These materials quantities are for a specific FMDF design, and are not universally characteristic of all conceptual designs for FMDF concentrators discussed in the literature (E-Systems, Inc. 1978a, 1978b; Texas Tech University 1977).

TABLE B.3. Materials Specifications Assumed for FMDF Concentrator

Item	Quantity (Units)
Reflective Panel (Average Size)	
Backsheet - 28 ga. galv. sheet metal - 23.7 lb	1307
Edgesheet - 28 ga. galv. sheet metal 2.74 lb	1307
Honeycomb - 2 in. x 48 in. x 96 in.	1307
Back-Silvered Glass - 48 in. x 96 in.	1307
Attachment Brackets	3921
Adhesive - 0.2 lb/ft^2	8365 lb
Panel Attachments	
Threaded Rod - 1/2 in. x 1 3/8 in.	3921
Nuts - 1/2 in.	15,684
Washer	15,684
Channel Bolts	3921
Channel - 1 in. x 2 in. x 12 in.	3921
6 KWIK-SET Bolts	7842
Mirror Wash	
Pump & Motor	1
Brushes	120 ft
Support Structure	120 ft
Drive Mechanism & Drive Motor	1
Pipe	150 ft
Concrete Support Framework	
Panel Support Structure	25.9 yd^3
Main Beams	67.7 yd^3
Substructure	37.8 yd^3
Foundation	
Pier - 16 in. diameter, 10 ft deep	107
Excavation	
Excavation	18,617 yd^3
Receiver Drive/Tracking Unit	1 per concentrator

Concentrator cost estimates were developed assuming that panel fabrication would be carried out in a manufacturing facility, and construction of the concrete support framework performed in the field. Components of the reflective panel were assumed to be purchased by the manufacturing facility either fully or partially fabricated, with minimal fabrication for some components performed in the manufacturing facility. Reflective panels would be shipped to the plant site where they would be attached to the completed concrete support framework and aligned for proper position. Installation costs for reflector panels assume the use of a laser alignment system to expedite proper positioning of panels, but would require no unique equipment for initial panel attachment to the support structure.

Materials costs for galvanized and carbon steel components were obtained from the same cost data base used to evaluate the PFCR/R heliostat (Robert Snow Means Co. 1976, 1977; Dodge 1977; Miska 1978; Mitre Corp. 1977; Guthrie 1974). Unit costs for back-silvered glass were assumed to be the same as for the PFCR/R heliostat. Cost estimates for mirror wash systems and the receiver drive/tracking unit were based upon analysis of E-Systems cost estimates for these items.

Field construction of the concentrator foundation would involve standard construction techniques, similar to those used for other concentrator applications. Cost estimates for foundation concrete work were obtained from the Robert Snow Means Co. construction cost estimating guides (1976, 1977). Estimated costs for the concrete support framework assumed that, at the reference concentrator production rate, installed concrete costs will be similar to installed concrete costs for high-rise building construction. Cost estimates for concrete support framework were developed using information from the Robert Snow Means Co. construction cost estimating guides (1976, 1977).

Receiver cost was based upon analysis of receiver cost estimates provided by E-Systems (1978a). Although these estimates were based upon somewhat different assumptions and unit costs than PNL estimates for other receivers, it was concluded that differences tended to offset each other. For this reason, the overall estimate of receiver cost obtained from E-Systems was used in the analysis.

B.1.1.7 LFCR Estimate Basis

The conceptual design for the LFCR concentrator includes one-axis tracking heliostats with an adjustable focal length. Estimated heliostat materials requirements were developed using information obtained from LFCR design documents (FMC Corporation 1978) and contacts with concept proponents. Heliostat materials specifications used for costing purposes are given in Table B.4.

TABLE B.4. Materials Specifications Assumed for LFCR Heliostat

Item	Specification	Quantity
Reflective Surface	Second surface mirror laminated to glass back panel	55.8 m^2
Mirror Structural Support	Galvanized steel	384 lb
Support Structure	Galvanized steel	2580 lb
Drive/Tracking/Focus Unit	Axis/drive/tracking mechanism, focal length adjustment	1/2 per collector
Pedestal	Galvanized steel	100 lb
Foundation	Concrete, average reinforcing	1.6 yd^3

Heliostat cost estimates were developed assuming that most materials would be purchased fully fabricated, with partial fabrication for some materials done in the heliostat manufacturing facility. Minimal field assembly of the heliostat would be required because all parts requiring complex assembly could be shipped fully assembled from the manufacturing facility. Except for heliostat checkout, all field installation tasks were assumed to be performed using conventional construction equipment.

Materials costs for galvanized steel components were developed from the same cost data base established for the PFCR/R concept, as described in Section B.1.1.1. Reflective panel materials and construction were identical to the PFCR/R heliostat, and were costed using the same unit costs as for the PFCR/R heliostat. As with other concepts, the drive/tracking unit was treated as a "black box" with cost estimates based upon allowances for motors, gearbox, and tracking unit. Estimates for the drive/tracking unit were developed

from information in other cost studies, contact with solar manufacturers, contact with concept proponents, and comparison with current motor and gearing costs for nonsolar applications (McDonnell Douglas 1977; Drumheller 1978; Robert Snow Means Co. 1976, 1977). Focal length adjustment would be provided by a small, centrally-controlled motor. Motor costs were estimated using information from cost estimating guides, with allowances for gearing and control costs based upon information developed for drive/tracking units (Robert Snow Means Co. 1976, 1977). An overall cost estimate for foundation materials and labor was obtained based upon information in the Robert Snow Means Co. construction cost estimating guides (1976, 1977).

Receiver cost estimates were based upon cost estimates published in the literature. These receiver costs were judged to be reasonable for the conditions modeled by this study, and were used without modification (FMC Corp. 1978).

Towers used for receiver support were costed separately from receivers, and included in the receiver cost account. The estimates of LFCR towers examined (FMC Corp. 1978) were considered to be too low. Cost estimates for PFCR/R towers were used as a baseline to establish reasonable ranges for LFCR tower costs (Mitre Corp. 1977; Selcuk 1976; Martin Marietta 1975; McDonnell Douglas 1976; Honeywell, Inc. 1977). Based upon information from these sources, and estimated weights for LFCR receiver sections, it was judged that any differences in structural requirements between LFCR towers and PFCR towers of equivalent height would not have a significant impact upon the cost of LFCR towers. Reductions in cost for LFCR towers would be expected due to mass production benefits and the effects of learning. At the reference production rate assumption of 1.2×10^6 m^2 concentrator aperture area produced per year, approximately 250 LFCR towers would be required compared to 10 to 20 towers for the PFCR/R. Mass production benefits were assessed assuming that no reduction in tower materials cost would take place, while tower labor and indirect costs would be lowered. Taking production benefits and learning effects into account resulted in a tower cost for the LFCR 29% lower than an equivalent tower for the PFCR/R.

B.1.1.8 LFDR-TC Estimate Basis

Primary materials requirements for the LFDR-TC concentrator were estimated based on examination of designs currently produced by Accurex Corporation and Hexcel Corporation, and conversations with manufacturers concerning potential design improvements feasible at larger production rates. Materials requirements and specifications developed for costing purposes are given in Table B.5.

TABLE B.5. Materials Specifications Assumed for LFDR-TC Concentrator

Item	Specification	Quantity
Reflective Surface	Polished aluminum	16.8 m^2
Mirror Structural Support	Galvanized steel	150 lb
Support Structure	Galvanized steel	250 lb
Drive/Tracking Unit	One-axis drive/tracking unit	1/8 per concentrator
Pedestal	Galvanized steel	20 lb
Foundation	Concrete, average reinforcing	1.6 yd^3

Concentrator cost estimates were developed assuming that the majority of materials would be purchased fully fabricated, with partial fabrication for some components performed in the concentrator manufacturing facility. Installation costs assume that the concentrator was shipped from the manufacturing facility fully assembled except for drive unit and pedestal. This would minimize field assembly labor at the expense of increased shipping and handling costs. Field installation costs assume the use of conventional construction equipment.

Materials costs for galvanized steel components were estimated using the same cost data base developed for the PFCR/R heliostat, as discussed in Section B.1.1.1. Information regarding current prices of aluminum reflective surfaces was obtained through conversations with current manufacturers. Unit costs for aluminum reflective surfaces were developed using current cost information as guidelines, and are based upon optimistic assumptions concerning potential cost reductions due to increased production of solar hardware.

Cost allowances for the drive/tracking unit were determined using the same information sources as described for the PFCR/R heliostat in Section B.1.1.1. An overall materials and installation cost was developed for the foundation, based upon information from the Robert Snow Means Co. construction cost estimating guides (1976, 1977).

Sources for receiver cost estimates included previous solar studies (Fujita et al. 1977; Mitre Corp. 1977) and contact with solar manufacturers. An overall estimate of receiver materials cost was developed, based primarily on information received from Hexcel Corporation. It was assumed in developing the materials cost estimate that receiver components would be purchased fully fabricated, and require only assembly in the manufacturing facility.

B.1.1.9 LFDR-TR Estimate Basis

Materials requirements for the LFDR-TR concentrator were estimated based upon examination of prototype concentrators already constructed, concentrator conceptual designs, and contact with concept proponents. Materials requirements and specifications developed for costing purposes are given in Table B.6.

TABLE B.6. Materials Specifications Assumed for LFDR-TR Concentrator

Item	Specification	Quantity
Reflective Surface	Second surface mirror	18.1 m^2
Support Structure	Concrete with wire fiber reinforcing	4.5 yd^3
Drive/Tracking Unit	One-axis drive/tracking unit	1 per concentrator
Foundation	Concrete with wire fiber reinforcing	0.9 yd^3

Concentrator cost estimates assume that drive/tracking unit components would be purchased fully fabricated, and reflective surface materials purchased partially fabricated. Concentrator support structure and foundation would be field fabricated, with the reflective surface installed as part of

support structure fabrication. Field installation and construction costs assume the use of reusable forms for concrete work, and conventional construction equipment.

Unit costs for reflective surfaces and drive/tracking units were developed using the same cost bases established for the PFCR/R heliostat, as described in Section B.1.1.1. Materials costs for concrete with wire fiber reinforcing were developed using information from the Robert Snow Means Co. construction cost estimating manuals (1976, 1977) and information obtained from General Atomic Company.

Receiver conceptual design information was obtained from design documents, examination of prototype receivers, and discussion with concept proponents. Materials costs for the receiver were estimated using the same cost data as developed for concentrator materials, and assume that receiver materials are purchased partially or fully fabricated.

B.1.1.10 LCNT Estimate Basis

The LCNT concentrator conceptual design is similar to nonimaging concentrators being developed at Argonne National Laboratory and the University of Chicago. Materials specifications and quantities were based principally on design information published by Arthur D. Little, Inc. (1977), and are shown in Table B.7.

TABLE B.7. Materials Specifications Assumed for LCNT Concentrator

Item	Specification	Quantity
Reflective Surface	Polished aluminum	51.2 m^2
Cover Glass	Glass	14.2 m^2
Support Structure	Galvanized steel	240 lb
Support Structure	Carbon steel	230 lb
Tilt Assembly	Manual tilt adjustment	1 per concentrator
Foundation	Concrete, average reinforcing	1.6 yd^3

Concentrator cost estimates were developed assuming that most materials would be purchased fully fabricated, with partial fabrication of some components done in the concentrator manufacturing facility. Concentrators would be shipped from the manufacturing facility essentially fully assembled, requiring only mounting on foundations and installation of the tilt assembly in the field. Field installation costs assume the use of conventional construction equipment.

Materials costs for galvanized and carbon steel components were developed using the same cost data base established for the PFCR/R heliostat, as described in Section B.1.1.1. Materials costs for aluminum reflective surfaces were obtained using unit cost estimates developed for the LFDR-TC concentrator, as discussed in Section B.1.1.8. The tilt assembly was assumed to consist of cable, drums, and pipe. Costs for pipe were obtained from construction cost estimating manuals (Robert Snow Means Co. 1976, 1977; Guthrie 1974). Cost allowances for cable and cable drums were based upon consideration of current costs for similar applications. An overall materials and installation cost was developed for the concentrator foundation, and was obtained from construction cost estimating guides (Robert Snow Means Co. 1976, 1977).

Estimates of receiver cost were based upon current costs of vacuum tube receivers, and expectations for cost reductions at increased production volumes (Arthur D. Little 1977). Receiver costs assume that receiver tubes would be purchased fully fabricated from a specialty manufacturer, and installed in the concentrator at the collector manufacturing facility.

B.1.2 Concentrator Cost Estimates

Concentrator cost estimates are shown in Table B.8. Cost estimates are also reported on a unit cost basis, in $\$/m^2$, in Table B.9. Concentrator costs are broken out into major accounts, namely materials, labor, fixed charges, manufacturing markup, and field costs. Materials, labor, fixed charges, and manufacturing markup are costs incurred at the concentrator manufacturing facility. It should be noted that the estimates in Table B.8 do not include standard field indirect costs or contingencies, which are contained in separate accounts.

TABLE B.8. Concentrator Cost Estimates ($/Concentrator, 1978 $)

	PFCR/R	PFCR/B	PFDR/R	PFDR/B	PFDR/S	FMDF	LFCR	LFDR-TC	LFDR-TR	LCNT
MATERIALS										
Reflective Surface	400	400	1,230	1,230	1,230	16,950	460	150	100	390
Reflective Surface Support	--	--	90	90	90	46,140	--	--	--	--
Main Structural Support	500	500	1,400	1,400	1,400	--	1,130	140	--	73
Pedestal	110	110	480	480	480	--	90	10	--	20
Drive/Tracking	1,400	1,400	1,535	1,535	1,535	18,350	820	196	380	--
Miscellaneous	145	145	560	560	560	7,900	178	34	30	12
LABOR										
Direct Production	47	47	840	840	840	2,530	108	30	6	19
Direct Supervisory and Clerical	7	7	126	126	126	380	16	4	1	3
Administrative	19	19	336	336	336	1,013	43	12	3	7
Manufacturing Plant Maintenance	11	11	33	33	33	422	16	3	1	1
Overheads	16	16	250	250	250	834	35	9	2	6
FIXED CHARGES	266	266	857	857	857	10,554	401	87	25	35
MANUFACTURING MARKUP	317	317	1,116	1,116	1,116	9,110	346	72	61	68
FIELD COSTS										
Foundation	310	310	1,100	1,100	1,100	7,317	200	200	59	220
Field Construction	--	--	--	--	--	49,500	--	--	381	--
Installation and Checkout	350	350	1,700	1,700	1,700	19,000	180	123	130	35
TOTAL COST	3,898	3,898	11,653	11,653	11,653	190,000	4,023	1,070	1,179	889

TABLE B.9. Concentrator Unit Cost Estimates ($/m^2, 1978 $)

	PFCR/R	PFCR/B	PFDR/R	PFDR/B	PFDR/S	FMDF	LFCR	LFDR-TC	LFDR-TR	LCNT
MATERIALS										
Reflective Surface	8.2	8.2	12.3	12.3	12.3	5.8	8.2	9.4	6.0	27.5
Reflective Surface Support	--	--	0.9	0.9	0.9	15.8	--	--	--	--
Main Structural Support	10.2	10.2	14.0	14.0	14.0	--	20.3	8.8	--	5.1
Pedestal	2.2	2.2	4.8	4.8	4.8	--	1.6	0.6	--	1.4
Drive/Tracking	28.6	28.6	15.4	15.4	15.4	6.3	14.7	12.3	22.7	--
Miscellaneous	3.0	3.0	5.6	5.6	5.6	2.7	3.2	2.1	1.8	0.8
LABOR										
Direct Production	1.0	1.0	8.4	8.4	8.4	0.9	1.9	1.9	0.4	1.3
Direct Supervisory and Clerical	0.1	0.1	1.3	1.3	1.3	0.1	0.3	0.3	0.1	0.2
Administrative	0.4	0.4	3.4	3.4	3.4	0.3	0.8	0.8	0.2	0.5
Manufacturing Plant Maintenance	0.2	0.2	0.3	0.3	0.3	0.1	0.3	0.2	0.1	0.1
Overheads	0.3	0.3	2.5	2.5	2.5	0.3	0.6	0.6	0.1	0.4
FIXED CHARGES	5.4	5.4	8.6	8.6	8.6	3.6	7.2	5.5	1.5	2.5
MANUFACTURING MARKUP	6.5	6.5	11.2	11.2	11.2	3.1	6.2	4.5	3.6	4.8
FIELD COSTS										
Foundation	6.3	6.3	11.0	11.0	11.0	2.5	3.6	12.6	3.5	15.5
Field Construction	--	--	--	--	--	17.0	--	--	22.8	--
Installation and Checkout	7.1	7.1	17.0	17.0	17.0	6.5	3.2	7.7	7.8	2.5
TOTAL UNIT COST, $/m^2	80	80	116	116	116	65	72	67	70	62

General trends in the concentrator cost estimates can be observed most easily from Table B.9, where unit costs are shown. Differences among estimated concentrator unit costs are discussed and rationalized below.

B.1.2.1 Materials

All materials purchased by the concentrator manufacturing facility are included in the materials account. Materials are broken out further into major subaccounts. The reflective surface subaccount covers all materials used in the concentrator reflective surface, but excludes anything relating to the structural rigidity of the reflective panel. Panel stiffening members are included in the reflective surface support subaccount. Primary concentrator structural members are contained in the main structural support subaccount. The distinction between the reflective surface support and the concentrator structural support subaccounts is subjective, and is intended to highlight differences between reflective panels using integral structural support and panels bolted directly to the main concentrator support structure. Components in the pedestal subaccount are used to raise the concentrator above ground level. The drive/tracking subaccount contains all motors, gearing, and tracking units required for the collector, regardless of whether the concept has a tracking concentrator or tracking receiver. Attachment brackets, allowances for wastage, and similar materials not fitting into other subaccounts are included in the miscellaneous subaccount.

Reflective surface costs differ among concepts principally because of the type of material used (i.e., glass versus aluminized) and the ratio of aperture area to total reflective surface area. Among the concepts using a glass mirror, the lowest reflective surface cost is achieved by the FMDF and LFDR-TR concepts, which do not use a glass back panel. This can be somewhat deceptive, however. In the case of the FMDF, deletion of the glass back panel necessitates a more complicated, and expensive, reflective surface support to protect the mirror silvering. The PFDR concepts have somewhat higher reflective surface costs than other concepts using glass mirrors due to more complex formation of the mirror to achieve a parabolic structure. The highest reflective surface cost for any concept was achieved by the LCNT concept, which resulted from a large surface area-to-aperture area ratio, and inclusion of the cover glass in the reflective surface cost accounting.

Reflective surface support was used in the construction of mirror panels for the PFDR concepts and the FMDF concept. In the case of the PFDR concepts, reflective surface support was achieved with an economy of materials, resulting in a low cost. Reflective surface support for the FMDF used a much more complicated mirror panel construction, involving both advantages and disadvantages. The advantages of this construction are that the need for a glass back panel to the reflective panel is eliminated, and requirements for concentrator structural support are simplified. The primary disadvantage to this approach is the substantial added cost to mirror panel construction.

Materials costs for the concentrator main structural support vary considerably for two concepts, the LFCR and LCNT. Structural support costs for the LCNT are the lowest of any concept. This results from low requirements for concentrator rigidity, and a very light concentrator construction. At the high end of the scale, structural support costs for the LFCR concentrator are roughly twice those of the other heliostat concepts, the PFCR/R and PFCR/B. The large cost increase results from the requirement for a variable focal length on the LFCR concentrator. Achieving the focal length adjustment necessitates a much more complicated concentrator support structure than would otherwise be required.

Main structural support costs tend to be grouped fairly close for the PFCR, PFDR, and LFDR-TC concepts. Differences among these concepts are attributed to both the concentrator weight that must be supported and the complexity of the support structure. Materials costs for main structural supports are not listed for the FMDF and LFDR-TR concentrators, as these concepts employ field-constructed concrete support structures, which are included under field costs.

Pedestal materials costs are lowest for line focus concentrators, which are supported relatively close to ground level. Of the point focusing concepts using pedestals, the PFCR concepts have somewhat lower costs than the PFDR concepts, because pedestal heights are lower and pedestals are required to support less weight for the PFCR concepts. Pedestal materials costs are

not listed for the FMDF and LFDR-TR concepts; because pedestal costs are inherent in their concrete support structures, they are included under field-incurred costs.

Drive/tracking units vary over a range of $\$28/m^2$ among the concepts, and hence have a significant impact upon concentrator cost estimates. Among the two-axis tracking concepts, economies of scale play a major role in the relative costs of drive units. Many drive/tracking components remain fixed, or increase only moderately in price, as concentrator aperture area increases. This effect is responsible for the lower unit cost for the drive/tracking portion of the PFDR concepts in comparison to the PFCR concepts, and partially explains why the two-axis tracking FMDF concentrator has lower drive/tracking costs than either the PFCR or PFDR concentrators.

In addition to economies of scale, design differences among the two-axis tracking systems must also be considered in examining relative drive/tracking unit costs. Differences between the drive/tracking costs of the FMDF and the other two-axis tracking concepts are partly due to the use of a tracking receiver rather than a tracking concentrator. Unfortunately, there is not sufficient information to ferret out what portion of the FMDF concept's advantage in drive unit cost is due to economies of scale, and what portion is related to the cost advantages or disadvantages of using a tracking receiver. It is noted, however, that using a tracking receiver concept seems to be the only feasible approach for concentrators as large as the FMDF, suggesting that, to obtain maximum economies of scale benefits in drive/tracking unit costs, tracking receivers must be used.

Relative drive/tracking unit costs for one-axis tracking concentrators tend to be affected by economies of scale, as are the two-axis tracking concentrators. Minimizing drive/tracking unit costs can be done to a great extent by operating a number of concentrators ganged to a common drive/tracking unit. The LFDR-TC concept achieved the lowest overall drive/tracking cost using eight concentrators, a total of 128 m^2, ganged to a common unit. The LFCR concept employed a common drive/tracking unit ganged to a total of 112 m^2 and achieved a cost slightly greater than the LFDR-TC concept. A significant portion of the LFCR drive/tracking unit cost is incurred for the focus unit,

used to adjust concentrator focal length. The LFDR-TR concept uses a tracking jack for each concentrator section, and so cannot gang a number of concentrators to a common drive. This results in a much higher cost for the LFDR-TR drive/tracking unit than for other one-axis tracking concepts.

Because of its nontracking configuration, the LCNT concept incurs no cost for a drive/tracking unit. Mechanisms providing manual tilt adjustments to the LCNT concentrator are included under concentrator main structural support.

Miscellaneous materials cost allowances reflect the complexity of concentrator designs. Concentrators with complicated support structures and more complicated reflective panel attachment incurred higher costs for miscellaneous materials than did concentrators with simpler designs.

B.1.2.2 Labor

This account includes all direct and indirect labor-oriented costs incurred in the concentrator manufacturing facility. The direct production subaccount includes all estimated costs for direct manufacturing labor and assembly labor. Labor costs that are not directly related to concentrator production are contained in the direct supervisory and clerical, administrative, and manufacturing plant maintenance subaccounts. Labor overheads are contained in the overheads subaccount.

Direct production labor costs are directly proportional to the number and complexity of concentrator components that must be fabricated and assembled in the concentrator manufacturing facility. Direct production labor costs are lowest for the LFDR-TR and FMDF concepts, both of which employ extensive field construction. The use of field construction reduces direct production costs at the expense of an increase in field construction costs. Concentrator complexity and number of parts is sufficiently similar for the PFCR/R, PFCR/B, LFCR, LFDR-TC, and LCNT concepts that only relatively minor variations in direct production costs occur. Because of their large size and complex structure, direct production costs are higher for the PFDR/R, PFDR/B, and PFDR/S concentrators than for those of other concepts. The complexity of assembling PFDR concentrators requires assembly scenarios with a higher percentage of human labor than other concepts, where more automation is feasible.

Direct supervisory and clerical, administrative, and manufacturing plant maintenance are all indirect labor costs. These were calculated in the same way for all concepts, based upon other manufacturing inputs. Calculation methods for each subaccount are given in Table B.10. These estimating rules are essentially assumptions regarding the amount of indirect labor required in the concentrator manufacturing industry. This somewhat simplified approach was possible because of the relative nature of the concentrator comparison. Use of a standard estimating method tends to affect all concepts equally, without disrupting relative cost ranking.

TABLE B.10. Calculation Methods for Indirect Labor Costs

Subaccount	Calculation Method
Direct supervisory and clerical labor cost	15% of direct production labor cost
Administrative costs	40% of direct production labor cost
Manufacturing plant maintenance	1% of manufacturing plant capital cost

Overheads on labor cost were estimated as 25% of the costs for direct production labor, direct supervisory and clerical labor, and manufacturing plant maintenance. As with indirect labor costs, this was essentially an assumption that was applied equally to all concepts.

B.1.2.3 Fixed Charges

Fixed charges associated with the concentrator manufacturing facility include return on investment, depreciation, annual taxes, and other payments. Fixed charges were calculated as a percentage of the capital investment for the concentrator manufacturing facility.

Estimates of the overall collector manufacturing facility capital cost for the PFCR concepts were developed based upon information in heliostat manufacturing studies (Drumheller 1978). Manufacturing facility capital cost estimates for other types of collectors were subjectively scaled from the PFCR estimate, based on the complexity of collector fabrication and assembly.

The judgments of collector fabrication and assembly complexity are shown in Table B.11. Fabrication complexity was judged by the number of collector components fabricated in the manufacturing facility and the degree of fabrication involved. Assembly complexity was judged by the number of collector components assembled in the manufacturing facility, and the type of assemblage required. Both fabrication and assemblage complexity are affected by collector production rates, with higher production rates increasing complexity.

TABLE B.11. Collector Fabrication and Assemblage Complexity

Fabrication Complexity

Low	Moderately Low	Baseline	Moderately High	High
LCNT	FMDF	PFCR/R	LFCR	PFDR/R
LFDR-TR		PFCR/B	LFDR-TC	PFDR/B
				PFDR/S

Assemblage Complexity

Low	Moderately Low	Baseline	Moderately High	High
FMDF	LFDR-TC	PFCR/R	LCNT	PFDR/R
LFDR-TR		PFCR/B	LFCR	PFDR/B
				PFDR/S

Capital cost estimates were developed based on estimates of PFCR heliostat manufacturing facility capital costs and the judgments of Table B.11, and are shown in Table B.12. The estimates are for all collector manufacturing facility capital costs, and not specifically for items relating to concentrators only.

Estimates of fixed charges were developed using an annual fixed charge rate of 25%. Fixed charges were allocated between concentrator and receiver components based upon considerations of the overall production scenario.

TABLE B.12. Collector Manufacturing Facility Capital Cost Estimates (1978 $)

Concept	Facility Capital Cost
LFDR-TR	$12,000,000
FMDF	$17,000,000
LCNT	$18,000,000
PFCR/R	$26,000,000
PFCR/B	$26,000,000
LFDR-TC	$29,000,000
LFCR	$33,000,000
PFDR/R	$40,000,000
PFDR/B	$40,000,000
PFDR/S	$40,000,000

Uncertainties involved in estimates of fixed charges are relatively large. However, the effects of these uncertainties in the overall concentrator cost estimate are small, because of the small percentage of collector costs constituted by fixed charges.

B.1.2.4 Manufacturing Markups

The manufacturing markup account consists of a standard profit markup applied to concentrator materials and labor costs. This markup was calculated as 12% of materials and labor costs for all concepts.

B.1.2.5 Field Costs

Field costs summarize all concentrator costs incurred outside the concentrator manufacturing facility. The foundation subaccount consists of costs for materials and labor for the concentrator foundation. The field construction subaccount contains costs for major concentrator fabrication and construction performed in the field, and consists of materials and labor costs, and remote construction burdens. The installation and checkout subaccount consists of costs for field installation of concentrator components, hookup to control systems, and concentrator checkout.

Foundation costs show effects of economies of scale for most concepts, with foundation costs decreasing as concentrator aperture area increases. This is evident from examining the range of foundation costs. Lowest foundation costs were achieved by the FMDF concentrator, which is by far the largest concentrator. The highest foundation costs were incurred for the LCNT concentrator, the smallest concentrator of the group.

Two of the concepts analyzed show exception to the economies-of-scale trend in foundation costs. The LFDR-TR concentrator has significantly lower foundation costs than other concentrators in the same size range. Low foundation costs for the LFDR-TR concentrator are due to the incorporation of an integral foundation pad during field construction of the concrete main structural support. The PFDR concentrators stand out as not having cost reductions due to economies of scale. Relatively high foundation costs for the PFDR concentrators could be the result of a nonoptimal foundation design, or some diseconomies of scale that may exist for large concentrators using a single foundation.

Field construction costs are incurred by the FMDF and LFDR-TR concepts during construction of their concrete structural supports. Costs are lower for the FMDF concept, although it uses a much more complex construction, because of its use of criss-cross concrete support beams. The LFDR-TR concentrator requires a solid concrete support structure, which uses much more concrete per square meter aperture area than does the FMDF concentrator.

Installation and checkout costs are directly related to the complexity of concentrator field assembly. The LCNT concentrator, which is shipped fully assembled, requires only quick mounting on its foundation, and no precise alignment. Complex field assembly and more precise alignment is required for the PFDR concentrators, which result in costs almost $\$15/m^2$ higher than for the LCNT. Installation and checkout costs for other concepts fall between the LCNT concept at the low end of the scale and the PFDR concepts at the high end of the scale.

B.1.3 Receiver Cost Estimates

Reeiver cost estimates can best be discussed as two groups: distributed receivers and central receivers. Distributed receiver concepts use a receiver of constant design, and use receivers in a constant proportion to concentrators (generally one receiver per concentrator). Central receiver concepts use one receiver for any number of concentrators, and vary receiver design as the size of the concentrator field changes. These approaches to collector design lead to fundamentally different receiver cost behavior. Receiver unit costs for distributed receiver concepts are constant for any collector field size, while unit costs for central receivers vary with changing collector field size.

B.1.3.1 Distributed Receiver Costs

Receiver cost estimates for the seven distributed receiver concepts analyzed are shown in Table B.13, on a $\$/m^2$ unit cost basis. Table B.13 presents an aggregated cost estimate for the FMDF receiver, because it was not possible to generate more detailed cost breakdowns within the scope of this study. Estimated costs for field installation, fixed charges, and manufacturing markups were, in most cases, generated for an overall collector cost estimate, and split out later for allocation between concentrator and receiver components. Division of these costs among concentrator and receiver components was determined somewhat subjectively, depending upon collector design and assembly scenarios.

TABLE B.13. Distributed Receiver Unit Costs ($\$/m^2$, 1978 $)

	PFDR/R	PFDR/B	PFDR/S	FMDF	LFDR-TC	LFDR-TR	LCNT
Materials	20	20	32	--	4.6	21	21
Labor (Direct and Indirect)	0.8	0.8	1.5	--	0.5	0.6	2.5
Fixed Charges and Manufacturing Markup	3.5	3.5	6.3	--	1.4	3.3	3.5
Field Installation	0.7	0.7	0.7	--	1.1	3.6	2.5
Total Unit Cost	25	25	40	24.8	7.8	28	29

Materials costs account for approximately 60 to 80% of the total installed receiver cost. The LFDR-TC receiver attains the lowest unit cost by a considerable margin. A large portion of the advantage in materials cost of the LFDR-TC receiver is due to its considerably lower operating temperature compared to all concepts other than the LCNT. The lower temperature characteristics of the LFDR-TC receiver allow the use of a relatively simple design using standard, inexpensive components. The LCNT concept, using a relatively low-temperature receiver design, does not experience materials cost advantages over other concepts due to the overall collector design. By using a low concentration concentrator, the LCNT reduces concentrator costs at the expense of receiver costs. The low concentration ratio requires a large number of receiver tubes per collector, greatly increasing receiver unit cost. In addition, the vacuum tube receivers required for the LCNT are significantly more expensive than the nonvacuum receiver used on the LFDR-TC.

Material costs are highest for the PFDR/S receiver, because it uses sodium heat pipes. The heat pipe design adds 60% to the materials cost of the nonheat pipe PFDR/B receiver.

Labor costs are affected by the degree of fabrication required for receiver components and the complexity of receiver assembly. Lowest labor costs were required for the LFDR-TC and LFDR-TR receivers, because of the small amount of fabrication assumed and the relatively simple assembly of receiver components. Labor costs for the PFDR/R and PFDR/B receivers were slightly higher than the lowest group due to somewhat more complex assembly. Assembly was significantly more difficult for the PFDR/S receiver with its heat pipe design, and was reflected in higher labor costs. Highest labor costs were incurred for the LCNT receiver, and account purely for factory installation of the receiver in the concentrator, because LCNT receivers were assumed to be purchased fully fabricated. Installation of the LCNT receiver was complicated by the large number of receiver tubes to be installed and connected within each concentrator.

Fixed charges and manufacturing markup follow exactly the same order as labor costs, with the exception of the LCNT concept. The trend is established

largely by the fixed charge component, which is related to the capital investment required to fabricate and assemble receiver components. Costs for the LCNT receiver are no longer at the top of the group as they were for labor costs, because a relatively large portion of LCNT labor is performed by hand, minimizing capital investment. For all other concepts, the relative order of fixed charges and manufacturing markup is the same as for labor costs. The manufacturing markup component is proportional to materials costs, and results in a larger spread among concepts for fixed charges and manufacturing markup than was present for labor costs.

Field installation costs were assumed to be the same for the PFDR/R, PFDR/B, and PFDR/S receivers, and were the lowest of any concept. Although field installation of the PFDR receivers was relatively complex, this cost was spread out over a large concentrator area, resulting in a low unit cost. Differences among installation costs for the LFDR-TC, LFDR-TR, and LCNT concepts are due to differences in the type of installation tasks required and in the allocation of costs for installation tasks among concentrator and receiver components.

Receiver unit costs for the FMDF concept are based upon E-Systems estimates and presented as an aggregated cost. The PFDR/R receiver is most similar in function to the FMDF receiver, and so provides a baseline for a subjective comparison of designs and cost estimates. The FMDF receiver is more complicated in structural support than the PFDR/R receiver, because of the FMDF's tracking receiver design. Neglecting structural supports, the FMDF receiver is inherently simpler than the PFDR/R receiver on the basis of its open, rather than cavity, design. From a cost standpoint, two factors are potentially of great importance: mass production cost benefits favor the PFDR/R receiver, since it was assumed to be produced at larger production rates than the FMDF. Economies of scale favor the FMDF, since its receiver is much larger than the PFDR/R receiver. It was judged that economies of scale and an overall simpler receiver design would outweigh factors favoring the PFDR/R receiver, so that the unit cost for the FMDF would be the lower of the two. For these reasons, the E-Systems overall estimate of receiver cost was considered to be sufficiently conservative for use in this study.

B.1.3.2 Central Receiver Costs

Unlike distributed receiver concepts, central receiver concepts were analyzed using receiver configurations that were varied for different collector field sizes. For the PFCR/R and PFCR/B concepts, adding heliostats to the collector field required increasing tower height and receiver size. For the LFCR concept, increasing the number of heliostats necessitated adding a linear receiver segment and support tower. Because no single receiver configuration was used, receiver costs vary with heliostat field size.

Central receiver costs can be broken down into costs for the receiver itself, and costs for towers. In this definition, all structural support components from the receiver base down are considered as part of the tower; all other components are part of the receiver.

Tower costs as a function of tower height are shown in Figure B.1. A range of tower heights is used for the PFCR/R and PFCR/B, while a single size tower, 61 m high, is used for the LFCR concept. The LFCR tower costs approximately 28% less than towers of similar height for the PFCR concepts because of mass production benefits. By using a large number of identical towers, tower engineering and construction costs can be greatly reduced. PFCR/R and PFCR/B concepts do not experience these effects to the same degree as the LFCR because they use a number of different-sized towers.

Tower costs for PFCR/R and PFCR/B concepts vary with heliostat field size because taller towers are required as more heliostats are added to the field. Additional towers are required for the LFCR concept as heliostats are added to the field. Estimated tower costs for a matrix of heliostat field sizes are shown in Table B.14. Tower costs for the PFCR/R and PFCR/B concepts exhibit economies of scale, with tower unit cost decreasing as heliostat field size increases. Tower costs for the LFCR show diseconomies of scale, with tower unit cost becoming progressively higher for larger heliostat field areas. The diseconomies of scale stem from larger ratios of heliostat field area to the number of receiver sections at smaller field sizes. Unlike the PFCR/R and PFCR/B concepts, the LFCR uses different heliostat arrangements for alternative power plant ratings. Therefore, LFCR receiver costs vary with both heliostat field area and power plant rating.

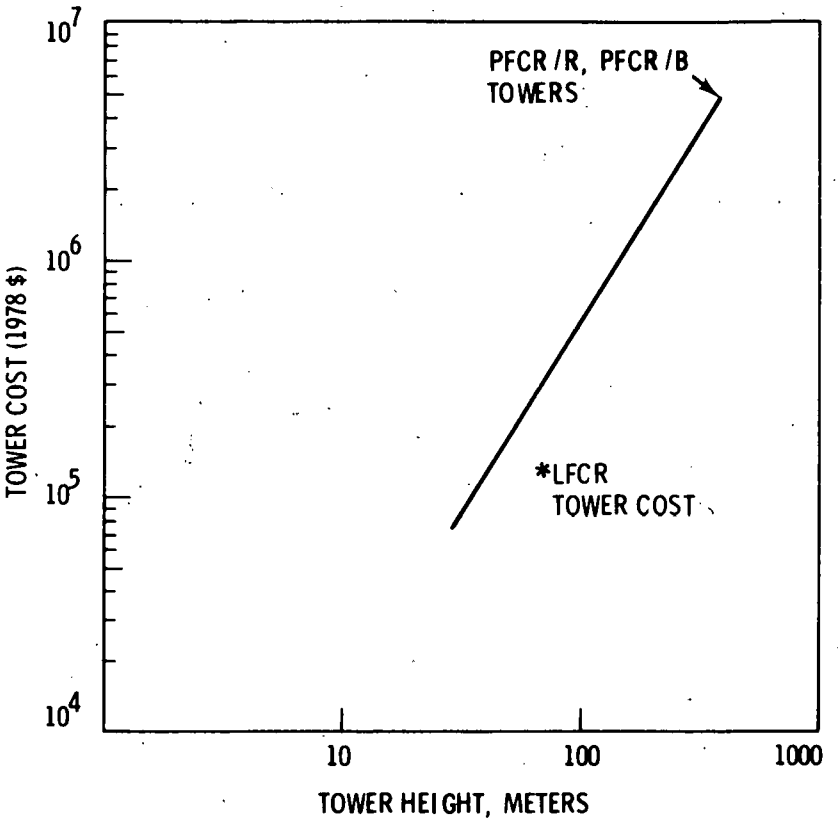

FIGURE B.1. Central Receiver Tower Cost Estimates

TABLE B.14. Central Receiver Tower Costs ($/m^2, 1978 $)

Concept	Concentrator Area 10,000 m^2	40,000 m^2	100,000 m^2	400,000 m^2
PFCR/R	7.8	7.6	7.5	7.3
PFCR/B	7.8	7.6	7.5	7.3
LFCR, 1 MW	41	46	47	--
LFCR, 5 MW	--	33	36	37
LFCR, 10 MW	--	32	34	35

Total receiver costs, including towers, are shown in Table B.15. Receiver costs follow the same general trends as do tower costs, with economies of scale present for the PFCR/R and PFCR/B concepts, and diseconomies of scale present

for the LFCR concept. In general, costs for LFCR receivers are significantly higher than for PFCR receivers. The major portion of this cost differential is due to tower costs. Both PFCR concepts experience significant savings at all field sizes by using one support tower, rather than many.

TABLE B.15. Central Receiver Costs, Tower and Receiver ($/m^2, 1978 $)

	Concentrator Area			
Concept	10,000 m^2	40,000 m^2	100,000 m^2	400,000 m^2
PFCR/R	36	26	21	16
PFCR/B	52	37	30	22
LFCR, 1 MW	56	72	75	--
LFCR, 5 MW	--	51	56	59
LFCR, 10 MW	--	49	54	57

Of the two PFCR concepts, the PFCR/B receiver is significantly more expensive at all field sizes because of its sodium heat pipes. Cost differences between the two receivers decrease slightly at large field sizes, as components common to both receivers become larger percentages of overall receiver costs.

B.2 ENERGY CONVERSION SUBSYSTEM COST ESTIMATES

Costs for energy conversion subsystems were estimated using information from a variety of sources, including previous studies, contact with manufacturers, and information from subcontractors. Estimated costs are sensitive to assumptions regarding maturity of the industry producing the energy conversion subsystems and assumed production rates. All cost estimates assume the energy conversion subsystem is produced by a commercial industry at production rates to match the production of solar thermal power plants. Cost estimates do not include R&D costs and other one-time costs associated with initial industry commercialization.

B.2.1 Rankine Cycle

The Rankine-cycle energy conversion subsystems are described in detail in Appendix A.3.1. Basically, two Rankine-cycle subsystems were considered: a low-temperature subsystem for the LFDR-TC and LCNT concepts, and a high-temperature subsystem for other concepts. Both the low- and high-temperature subsystems are central generating types, using one turbogenerator per plant, and so require the use of different capacity components as overall plant nameplate rating changes.

Cost estimates for Rankine-cycle energy conversion were based upon information obtained from previous studies, published cost information, and information obtained through subcontractors (Honeywell, Inc. 1977; Sterlich 1975; Guthrie 1974; Meador 1977). Estimated costs are shown in Table B.16.

Significant economies of scale are present for both the low- and high-temperature systems. These economies of scale cause costs for the conversion subsystems to be higher than for larger, more conventional power plants. The high-temperature Rankine subsystems experience greater benefits from economies of scale, and are less expensive than the low-temperature subsystems in all but the 1-MWe case.

TABLE B.16. Rankine-Cycle Energy Conversion Subsystem Costs (1978 $)

Subsystem Type	Rated Capacity MWe	Total Cost $/kW
High-Temperature Rankine	1	860
	5	427
	10	325
Low-Temperature Rankine	1	860
	5	559
	10	490

B.2.2 Brayton Cycle

Brayton-cycle energy conversion subsystems are decribed in detail in Appendix A.3.2. A central Brayton-cycle engine was used for the PFCR/B concept, and small, distributed engines were used for the PFDR/B concept.

Sources used in determining Brayton-cycle energy conversion subsystem costs included previous studies and contact with manufacturers (Selcuk 1976; Fujita et al. 1978; AiResearch 1975).

Data supplied by AiResearch Manufacturing Company were heavily weighted in developing cost estimates used in the analysis. These cost estimates are shown in Table B.17.

TABLE B.17. Brayton-Cycle Energy Conversion Subsystem Costs (1978 $)

Subsystem Type	Rated Capacity MWe	Cost $/kW
Central Brayton	1	162
	5	155
	10	154
Distributed Brayton	0.0175	246

Although the distributed Brayton conversion subsystem reaps greater benefit from mass production than do the central conversion subsystems, economies of scale make the central subsystems considerably less expensive.

B.2.3 Stirling Cycle

Stirling-cycle energy conversion subsystems are described in detail in Appendix A.3.3. The subsystem consists of a small Stirling engine/generator mounted on each collector.

Sources used in estimating Stirling engine costs included previous cost studies and subcontractor information concerning present-day Stirling costs and expected costs in mass production (Fujita et al. 1978; Martini 1979; Selcuk 1976). Information from these sources indicated that Stirling engine costs were very dependent upon assumed production rates. Sorting out actual differences in cost estimates from alternative sources is complicated by varying standards for cost reporting; some sources reported only direct manufacturing costs, while others estimated total manufacturing selling cost.

Costs estimated for the Stirling energy conversion subsystem are summarized in Table B.18 for an engine with a 17.5-kW rated capacity. Costs are broken out to show contributions of the various cost elements, and to facilitate comparison with estimates from other sources. Overall estimated costs are higher than those reported in several other sources because of the assumed engine production rate, which is more than an order of magnitude less than production rates of 400,000 engines/year assumed in some studies.

TABLE B.18. Stirling-Cycle Energy Conversion Subsystem Costs (1978 $)

Component	Cost, $/kW
Direct Manufacturing Materials, Labor	113
Overheads, Indirects	68
Manufacturers Profit	18
Field Installation	6
Total	$205/kW

B.3 ENERGY STORAGE COST ESTIMATES

Cost estimates for energy storage subsystems assume that these subsystems are constructed as part of the commercial solar industry, using proven technology. Cost estimates do not reflect R&D costs or other one-time costs associated with developing a commercial energy storage industry.

It should be noted that estimates for energy storage subsystems are reported in either 1977 or 1978 price levels. Those reported in 1977 price levels were escalated to 1978 levels by SOLSTEP during computer simulation.

B.3.1 Thermal Storage

Thermal storage cost estimates were based upon analysis of the costs of major subsystem components. Information sources consisted primarily of published cost information for conventional, off-the-shelf hardware. Previous studies were consulted for comparison, and for obtaining cost information for some components (Electric Power Research Institute 1976; Mitre Corp. 1977; Fujita et al. 1978; Fujita 1977; Department of Energy 1978).

Estimated costs for draw salt thermal storage subsystems for various subsystem configurations are shown in Tables B.19 and B.20. Costs are higher for the high-temperature subsystem because stainless steel is substituted for carbon steel in many of the components. Cost estimates for oil and rock thermal storage subsystems are given in Tables B.21 and B.22.

B.3.2 Electric Energy Storage

Cost estimates for Redox battery electric energy storage subsystems were based upon information reported in other studies and discussions with energy storage R&D personnel (Warshey and Wright 1975; Thaller 1974, 1979). Storage cost estimates for Redox batteries consist of a cost related to the maximum storage power, in $/kW, and a cost related to the total energy stored, in $/kWh. Redox battery cost estimates used for the analysis were $160/kW for power related costs, and $14/kWh for capacity related costs, both in 1978 price levels.

B.4 ENERGY TRANSPORT SUBSYSTEM COST ESTIMATES

A number of information sources were used in developing cost estimates for energy transport subsystems, including cost estimating guides, published cost information, and contact with vendors. A standard set of unit costs and estimating procedures was developed and used in estimating component costs for all concepts, so that cost differences among concepts reflect design differences only.

Energy transport subsystem cost estimates are found in Tables B.23 through B.29. Estimates do not appear for the PFCR/R and PFCR/B concepts because transport costs are included with receiver costs for those concepts.

B.5 OTHER PLANT

Costs for power conditioning equipment, structures, land, instrumentation and control, spare parts, and service facilities are grouped under "other plant" costs. Unit costs for these accounts tend to vary little among concepts, because the components are more or less common to all concepts.

TABLE B.19. Draw Salt Thermal Energy Storage Subsystem Costs, 950°F Heat Storage (1977 $)

Nameplate Plant Rating, MWe	Storage Capacity, kWt-h	Tank	Insulation	Piping	Pumps	Draw Salt	Heat Exchangers	Charging/Freeze Protection System	Total
1	12,500	$43,000	$10,000	$ 2,000	$12,000	$ 7,000	$166,000	$19,000	$ 259,000
1	23,800	59,000	14,000	2,000	12,000	14,000	166,000	19,000	286,000
1	35,000	80,000	17,000	2,000	12,000	20,000	166,000	19,000	316,000
1	68,800	123,000	25,000	2,000	12,000	41,000	166,000	19,000	388,000
5	57,000	107,000	25,000	11,000	22,000	34,000	470,000	22,000	691,000
5	108,000	166,000	34,000	11,000	22,000	63,000	470,000	22,000	788,000
5	159,000	215,000	42,000	11,000	22,000	94,000	470,000	22,000	876,000
5	312,000	327,000	60,000	11,000	22,000	184,000	470,000	22,000	1,096,000
10	111,000	172,000	39,000	33,000	55,000	67,000	940,000	26,000	1,332,000
10	209,000	252,000	52,000	33,000	55,000	123,000	940,000	26,000	1,481,000
10	307,000	322,000	64,000	33,000	55,000	181,000	940,000	26,000	1,621,000
10	600,000	494,000	91,000	33,000	55,000	347,000	940,000	26,000	1,986,000

TABLE B.20. Draw Salt Thermal Energy Storage Subsystem Costs, 800°F Heat Storage (1977 $)

Nameplate Plant Rating, MWe	Storage Capacity, kWt-h	Tank	Insulation	Piping	Pumps	Draw Salt	Heat Exchangers	Charging/Freeze Protection System	Total
1	13,200	$ 23,000	$13,000	$1,000	$12,000	$ 11,000	$ 79,000	$19,000	$ 158,000
1	25,100	36,000	18,000	1,000	12,000	21,000	79,000	19,000	186,000
1	37,000	45,000	21,000	1,000	12,000	31,000	79,000	19,000	208,000
1	72,800	70,000	31,000	1,000	12,000	61,000	79,000	19,000	273,000
5	60,000	62,000	30,000	2,000	26,000	50,000	236,000	22,000	428,000
5	114,000	93,000	42,000	2,000	26,000	95,000	236,000	22,000	516,000
5	168,000	119,000	52,000	2,000	26,000	140,000	236,000	22,000	597,000
5	330,000	183,000	76,000	2,000	26,000	276,000	236,000	22,000	821,000
10	114,000	93,000	48,000	9,000	38,000	96,000	449,000	26,000	759,000
10	217,000	140,000	66,000	9,000	38,000	181,000	449,000	26,000	909,000
10	318,000	179,000	80,000	9,000	38,000	266,000	449,000	26,000	1,047,000
10	624,000	275,000	117,000	9,000	38,000	522,000	449,000	26,000	1,436,000

TABLE B.21. Oil and Rock Thermal Energy Storage Subsystem Costs, 450°F Heat Storage (1977 $)

Nameplate Plant Rating, MWe	Storage Capacity, kWt-h	Tank	Insulation	Piping	Pumps	Heat Transfer Oil	Heat Exchangers	Ullage and Fluid Maintenance	Total
1	19,250	$ 65,000	$ 25,000	$2,000	$ 15,000	$ 35,000	$ 64,000	$14,000	$ 220,000
1	37,040	86,000	37,000	2,000	15,000	68,000	64,000	14,000	286,000
1	54,800	123,000	46,000	2,000	15,000	100,000	64,000	14,000	364,000
1	108,000	175,000	70,000	2,000	15,000	198,000	64,000	18,000	542,000
5	94,100	168,000	64,000	4,000	78,000	173,000	239,000	18,000	744,000
5	180,900	251,000	97,000	4,000	78,000	331,000	239,000	18,000	1,020,000
5	260,400	272,000	123,000	4,000	78,000	477,000	239,000	18,000	1,210,000
5	528,120	456,000	200,000	4,000	78,000	968,000	239,000	22,000	1,970,000
10	188,000	168,000	99,000	9,000	116,000	214,000	433,000	22,000	1,060,000
10	361,800	353,000	154,000	9,000	116,000	411,000	433,000	22,000	1,500,000
10	535,300	456,000	202,000	9,000	116,000	608,000	433,000	22,000	1,850,000
10	1,055,000	659,0004	331,000	9,000	116,000	1,200,000	433,000	26,000	2,770,000

TABLE B.22. Oil and Rock Thermal Energy Storage Subsystem Costs, 580°F Heat Storage (1977 $)

Nameplate Plant Rating, MWe	Storage Capacity, kWt-h	Tank	Insulation	Piping	Pumps	Heat Transfer Oil	Heat Exchangers	Ullage and Fluid Maintenance	Total
1	13,400	$ 38,000	$ 15,000	$1,000	$ 5,000	$ 17,000	$ 80,000	$ 7,000	$ 163,000
1	25,000	65,000	22,000	1,000	5,000	31,000	80,000	7,000	211,000
1	36,700	69,000	27,000	1,000	5,000	450,000	80,000	7,000	234,000
1	69,000	107,000	45,000	1,000	5,000	85,000	80,000	9,000	332,000
5	65,000	107,000	45,000	3,000	23,000	79,000	240,000	9,000	506,000
5	121,000	154,000	64,000	3,000	23,000	150,000	240,000	9,000	643,00
5	176,000	189,000	81,000	3,000	23,000	210,000	240,000	9,000	755,000
5	346,000	271,000	122,000	3,000	23,000	422,000	240,000	11,000	1,090,000
10	128,000	154,000	66,000	6,000	46,000	160,000	480,000	11,000	923,000
10	240,000	230,000	98,000	6,000	46,000	290,000	480,000	11,000	1,160,000
10	353,000	271,000	126,000	6,000	46,000	430,000	480,000	11,000	1,370,000
10	693,000	424,000	202,000	6,000	46,000	844,000	480,000	13,000	2,020,000

TABLE B.23. Point Focus Distributed Receiver 850°F Draw Salt Transport System Costs (1977 $; GCR = 0.44)

Field Size m^2	Pipe and Fittings	Pipe Trench	Insulation	Valves	Pumps	Draw Salt	Storage Tank	Total
10,000	$ 45,600	$ 43,600	$ 75,700	$ 78,000	$ 24,500	$ 1,100	$ 4,800	$ 273,000
50,000	228,000	222,000	372,000	390,000	81,400	5,400	12,600	1,310,000
100,000	474,000	446,000	757,000	780,000	158,000	12,000	16,100	2,640,000

TABLE B.24. Electric Energy Transport Costs for the PFDR/B, S Concepts (1977 $; GCR = 0.11)

Protective m^2	Cable	Capacitors	Equipment	Total
6,700	$ 63,000	$ 17,000	$ 4,000	$ 84,000
40,000	402,000	104,000	16,000	352,000
66,700	691,000	174,000	27,000	892,000

TABLE B.25. Fixed Mirror Distributed Focus 850°F HITEC Transport System Costs (1977 $; GCR = 0.55)

Field Size m^2	Pipe and Fittings	Pipe Trench	Insulation	Valves	Pumps	Draw Salt	Salt Storage Tank	Total
19,500	$ 15,600	$ 8,200	$ 21,100	$ 3,000	$ 20,400	$ 1,100	$ 4,600	$ 74,000
97,500	117,000	52,400	154,000	14,900	87,300	8,100	13,500	447,000
184,000	196,000	91,800	273,000	26,500	151,000	14,400	17,000	770,000

TABLE B.26. Line Focus Central Receiver 850°F Draw Salt Transport System Costs (1977 $; GCR = 0.47)

Field Size m^2	Pipe and Fittings	Pipe Trench	Insulation	Valves	Pumps	Draw Salt	Salt Storage Tank	Total
35,000	$ 12,100	$ 6,700	$ 16,200	$ 3,000	$ 23,300	$ 1,100	$ 4,700	$ 67,000
100,000	106,000	24,100	150,000	14,100	87,300	28,000	20,700	430,000
175,000	277,000	46,600	355,000	26,600	262,000	56,000	26,100	1,049,000

TABLE B.27. Line Focus Distributed Receiver - Tracking Collector Thermal Energy Transport Costs (1977 $; GCR = 0.50)

Field Size m^2	Pipe and Fittings	Pipe Trench	Insulation	Valves	Pumps	Total
20,000	$ 30,000	$10,000	$ 36,000	$ 15,000	$ 25,000	$ 116,000
80,000	191,000	48,000	208,000	67,000	70,000	584,000
161,000	331,000	97,000	334,000	133,000	163,000	1,060,000

TABLE B.28. Line Focus Distributed Receiver - Tracking Receiver 850°F Draw Salt Transport Costs (1977 $; GCR = 0.25)

Field Size m^2	Pipe and Fittings	Pipe Trench	Insulation	Valves	Pumps	Draw Salt	Salt Storage Tank	Total
19,800	$ 9,600	$ 5,600	$ 14,500	$ 14,600	$12,300	$ 1,300	$ 5,000	$ 63,400
79,200	54,000	25,700	71,300	58,600	30,900	5,600	13,500	260,000
158,000	122,000	54,900	159,000	119,000	69,900	20,000	17,400	562,000

TABLE B.29. Low Concentration Nontracking Thermal Energy Transport Costs (1977 $; GCR = 0.53)

Field Size m^2	Pipe and Fittings	Pipe Trench	Insulation	Valves	Pumps	Heat Transfer Oil	Total
27,000	$ 142,000	$ 159,000	$ 296,000	$ 9,000	$ 26,000	$ 9,000	$ 641,000
136,000	876,000	815,000	1,860,000	46,000	154,000	87,000	3,740,000
270,000	1,820,000	1,610,000	3,960,000	91,000	317,000	211,000	8,010,000

Power conditioning equipment varies only with rated plant capacity, and was assumed to be common to all concepts. Cost estimates for power conditioning equipment were based upon information from previous studies, and are shown in Table B.30 (Schulte 1977).

TABLE B.30. Power Conditioning Account Cost Estimates (1977 $)

Plant Capacity, MWe	Power Conditioning Costs
1	$128,000
5	285,000
10	405,000

Included in the structures account were the main control building, a general maintenance building, and a storage building for equipment and spares. These buildings were assumed to be common to all concepts, and to vary only with rated plant capacity. Structures cost estimates were based upon information from construction cost estimating guides (Robert Snow Means Co. 1976, 1977; Guthrie 1974). Structures cost estimates are given in Table B.31.

Unit costs for land were assumed to be the same for all concepts, and consist of costs for raw land and site preparation. Raw land costs were established as a study ground rule, with site preparation costs developed from information in cost estimating guides (Robert Snow Means Co. 1976, 1977; Dodge 1977). Land costs are shown in Table B.32. Costs for grading and site surveys are based upon optimistic assumptions regarding the plant site, and could be considerably higher in some locations.

TABLE B.31. Structures Account Cost Estimates (1977 $)

Plant Capacity, MWe	Control Building	Maintenance Building	Storage Building	Total
1	$ 80,000	$ 66,000	$25,000	$171,000
5	88,000	116,000	42,000	246,000
10	100,000	132,000	53,000	285,000

TABLE B.32. Land Account Cost Estimates (1978 $)

Component	Cost, $/Acre
Raw Land	$5,000
Survey Fee	200
Grading	387
Dust Suppression (crushed stone)	984
Total	$6,600

Cost estimates for instrumentation and control, spare parts, and service facilities were developed as functions of costs for other accounts, rather than as explicitly estimated costs. Cost estimating relationships for these accounts are given in Section B.7.

B.6 OPERATION AND MAINTENANCE COSTS

Estimates of labor required for scheduled operation and maintenance are shown in Table B.33. Plant operation quantifies the amount of time plant operators would be actively involved in plant control, and unavailable for other tasks. Scheduled maintenance tasks for the collector subsystem include inspection for potential defects, lubrication of moving parts, optical alignment and adjustments, and reflective surface cleaning. Transport system scheduled maintenance consists of inspection, system testing, and preventive maintenance. Heat engine and energy storage maintenance requirements cover preventive maintenance and inspection for the energy conversion and energy storage subsystems. General scheduled maintenance for plant grounds and miscellaneous plant equipment is reported as plant grounds maintenance.

Scheduled operation and maintenance was assumed to be performed by plant operators and maintenance personnel. Wage rates used in estimating O&M costs are shown in Table B.34.

TABLE B.33. Scheduled Operation and Maintenance Man-Hour Requirements

Concept	Plant Operation, hr/yr	Collector Maintenance, hr/m^2-yr[a]	Transport Maintenance, hr/m^2-yr	Heat Engine Maintenance, hr/m^2-yr	Plant Grounds Maintenance, hr/m^2-yr	Energy Storage Maintenence, hr/yr
PFCR/R	730	0.035	52[b]	417[b]	0.013	52
PFCR/B	730	0.035	52[b]	417[b]	0.013	52
PFDR/R	1460	0.052	0.008	417[b]	0.013	52
PFDR/B	365	0.052	0	0.052	0.013	0
PFDR/S	365	0.052	0	0.052	0.013	0
FMDF	1460	0.026	0.008	417[b]	0.013	52
LFCR	730	0.016	104[b]	417[b]	0.013	52
LFDR-TC	1460	0.050	0.008	417[b]	0.013	52
LFDR-TR	1460	0.061	0.008	417[b]	0.013	52
LCNT	1460	0.019	0.008	417[b]	0.013	52

(a) Concentrator aperture area, m^2
(b) hr/yr

TABLE B.34. Assumed Wage Rate for Operation and Maintenance Personnel (1978 $/hr)

	Base Rate	Payroll Burden	Subcontractor Fee	Total Direct Cost
Plant Operators	10.00	2.20	--	12.20
Maintenance Personnel	7.00	1.54	0.91	9.45

Unscheduled maintenance costs were estimated as a percentage of installed equipment costs, and assure that systems have been designed to minimize unscheduled maintenance. Allowances for unscheduled maintenance were 0.3% yearly of installed concentractor costs and 0.5% yearly of installed energy conversion, energy transport, and instrumentation costs. General plant overheads for O&M were estimated as 15% of total annual payments for scheduled and unscheduled maintenance.

B.7 SCALING PARAMETERS - SIMULATION CODE INPUTS

As described in Section 5.3.7, cost estimate scaling relationships were used in SOLSTEP to relate component costs to physical parameters describing the solar plant. In general, functional forms of cost estimate scaling relationships fare the same for all concepts, with different scaling parameters used to reflect individual cost behavior.

Scaling parameters used to estimate capital costs for all concepts are shown in Tables B.35 through B.50. Use of these parameters with the appropriate cost estimate scaling relationships allows direct calculation of capital cost estimates for various solar plant configurations. However, these estimates are subject to the constraints for which the systems were modeled. Cost estimate scaling parameters are not necessarily valid for other conditions.

TABLE B.35. Concentrator Cost Estimate Scaling Parameters[a]

Concept	Plant Rating, MWe	A	B	S
PFCR/R	1 5 10	0.0	80.0	1.0
PFCR/B	1 5 10	0.0	80.0	1.0
PFDR/R	1 5 10	0.0	116.0	1.0
PFDR/B	1 5 10	0.0	116.0	1.0
PFDR/S	1 5	0.0	116.0	1.0
FMDF	1 5 10	0.0	65.0	1.0
LFCR	1 5 10	0.0	72.0	1.0
LFDR-TC	1 5 10	0.0	67.0	1.0
LFDR-TR	1 5 10	0.0	70.0	1.0
LCNT	1 5 10	0.0	62.0	1.0

(a) Concentrator cost = $A + B(X)^S$
where X = collector field size, m^2.

TABLE B.36. Receiver Cost Estimate Scaling Parameters[a]

Concept	Plant Rating, MWe	A	B	C	S	T
PFCR/R	1 5 10	0.0	9.1597	494.284	0.9825	0.6889
PFCR/B	1 5 10	0.0	9.1597	555.878	0.9825	0.706
PFDR/R	1 5 10	0.0	25.0	0.0	1.0	0.0
PFDR/B	1 5 10	0.0	25.0	0.0	1.0	0.0
PFDR/S	1 5 10	0.0	40.0	0.0	1.0	0.0
FMDF	1 5 10	0.0	24.8	0.0	1.0	0.0
LFCR	1 5 10	-220559.0 -332769.0 -351382.0	77.568 59.6611 57.432	0.0	1.0	0.0
LFDR-TC	1 5 10	0.0	7.8	0.0	1.0	0.0
LFDR-TR	1 5 10	0.0	28.0	0.0	1.0	0.0
LCNT	1 5 10	0.0	29.0	0.0	1.0	0.0

(a) Receiver cost = $A + B(X)^S + C(X)^T$
where X = collector field size, m^2.

TABLE B.37. Thermal Energy Transport Cost Estimate Scaling Parameters(a,b,c)

Concept	Plant Rating, MWe	A	B	C	D	S	T	V
PFCR/R	1 5 10	0.0	0.0	0.0	0.0	0.0	0.0	0.0
PFCR/B	1 5 10	0.0	0.0	0.0	0.0	0.0	0.0	0.0
PFDR/R	1 5 10	0.0	3380.2	0.0	0.0	0.9553	0.0	0.0
PFDR/B	1 5 10	0.0	0.0	0.0	0.0	0.0	0.0	0.0
PFDR/S	1 5 10	0.0	0.0	0.0	0.0	0.0	0.0	0.0
FMDF	1 5 10	0.0	10239.8	0.0	0.0	1.0555	0.0	0.0
LFDR-TC	1 5 10	-1554.6	29.08	5780.7	54.269	1.0	1.0	0.5
LFDR-TR	1 5 10	0.0	21.179	0.0	0.0	1.1126	0.0	0.0
LCNT	1 5 10	0.0	163.74	0.0	0.0	1.0954	0.0	0.0
LFCR	1 5 10	51.02	5124.0 8564.0 9223.0	61.0 79.3 82.35		1.3059		

(a) For all concepts except the LFDR-TC, parameters are valid only for a specific value of ground cover ratio.

(b) For all concepts except the LFCR, thermal energy transport cost = $A + B(X)^S + \frac{C + D(X)^T}{Y^V}$

where X = number of collectors and Y = ground cover ratio.

(c) For the LFCR concept, thermal energy transport cost = $A + \left(\frac{X - B}{C}\right)^S$ where X = collector area, m^2.

TABLE B.38. Electric Energy Transport Cost Estimate Scaling Parameters[a]

Concept	Plant Rating, MWe	A	B	C	V
PFCR/R	1 5 10	0.0	0.0	0.0	0.0
PFCR/B	1 5 10	0.0	0.0	0.0	0.0
PFDR/R	1 5 10	0.0	0.0	0.0	0.0
PFDR/B	1 5 10	300.7	3464.25	346.3	0.5
PFDR/S	1 5 10	300.7	3464.25	346.3	0.5
FMDF	1 5 10	0.0	0.0	0.0	0.0
LFCR	1 5 10	0.0	0.0	0.0	0.0
LFDR-TC	1 5 10	0.0	0.0	0.0	0.0
LFDR-TR	1 5 10	0.0	0.0	0.0	0.0
LCNT	1 5 10	0.0	0.0	0.0	0.0

(a) Electric energy transport cost = $A(X) + \left[\frac{B + C(X)}{Y^V}\right]$

where X = number of collectors
Y = ground cover ratio.

TABLE B.39. Energy Conversion Cost Estimate Scaling Parameters[a,b]

Concept	Plant Rating, MWe	A	B	S	T
PFCR/R	1 5 10	0.0	856884.0	0.5753	0.0
PFDR/R	1 5 10	0.0	856884.0	0.5753	0.0
PFDR/B	1 5 10	4313.0	0.0	0.0	1.0
PFDR/S	1 5 10	3596.0	0.0	0.0	1.0
FMDF	1 5 10	0.0	856884.0	0.5753	0.0
LFCR	1 5 10	0.0	856884.0	0.5753	0.0
LFDR-TC	1 5 10	0.0	853976.0	0.7517	0.0
LFDR-TR	1 5 10	0.0	856884.0	0.5753	0.0
LCNT	1 5 10	0.0	853976.0	0.7517	0.0

		A	B	S
PFCR/B	1 5 10	162152.0	0.00025	0.9761

(a) For all concepts except the PFCR/B, energy conversion cost = $[A + B(X)^S](Y^T)$
where X = plant rating, MWe
Y = number of collectors.

(b) For the PFCR/B concept, energy conversion cost = $A(X)[B(X)]^S$
where X = collector field area, m^2.

TABLE B.40. Power Conditioning Cost Estimate Scaling Parameters[a]

Concept	Plant Rating, MWe	A	B	S
PFCR/R	1 5 10	7600.0	120000.0	0.52
PFCR/B	1 5 10	7600.0	120000.0	0.52
PFDR/R	1 5 10	7600.0	120000.0	0.52
PFDR/B	1 5 10	7600.0	120000.0	0.52
PFDR/S	1 5 10	7600.0	120000.0	0.52
FMDF	1 5 10	7600.0	120000.0	0.52
LFCR	1 5 10	7600.0	120000.0	0.52
LFDR-TC	1 5 10	7600.0	120000.0	0.52
LFDR-TR	1 5 10	7600.0	120000.0	0.52
LCNT	1 5 10	7600.0	120000.0	0.52

(a) Power conditioning cost = $A + B(X)^S$
where X = plant rating, MWe.

TABLE B.41. Thermal Electric Storage Cost Estimate Scaling Parameters[a]

Concept	Plant Rating, MWe	A	B	S
PFCR/R	1	232246.0	2.2842	1.0
	5	613783.6	1.5658	1.0
	10	1198747.0	1.3244	1.0
PFCR/B	1	160000.0	14.0	1.0
	5	800000.0	14.0	1.0
	10	1600000.0	14.0	1.0
PFDR/R	1	135929.0	1.8993	1.0
	5	348055.5	1.4431	1.0
	10	618238.0	1.3182	1.0
PFDR/B	1	160000.0	14.0	1.0
	5	800000.0	14.0	1.0
	10	1600000.0	14.	1.0
PFDR/S	1	160000.0	14.0	1.0
	5	800000.0	14.0	1.0
	10	1600000.0	14.0	1.0
FMDF	1	135929.0	1.8993	1.0
	5	348055.5	1.4431	1.0
	10	618238.0	1.3182	1.0
LFCR	1	135929.0	1.8993	1.0
	5	348055.5	1.4431	1.0
	10	618238.0	1.3182	1.0
LFDR-TC	1	128437.0	2.9580	1.0
	5	385334.3	2.0518	1.0
	10	686287.3	1.9292	1.0
LFDR-TR	1	135929.0	1.8993	1.0
	5	348055.5	1.4431	1.0
	10	618238.0	1.3182	1.0
LCNT	1	154591.0	3.6224	1.0
	5	491486.0	2.8002	1.0
	10	761137.0	1.9324	1.0

(a) Thermal electric storage cost $= A + B(X)^S$
where X = storage capacity, kWht.

TABLE B.42. Structures Cost Estimate Scaling Parameters(a)

Concept	Plant Rating, MWe	A	B	S
PFCR/R	1 5 10	0.0	171216.0	0.2226
PFCR/B	1 5 10	0.0	171216.0	0.2226
PFDR/R	1 5 10	0.0	171216.0	0.2226
PFDR/B	1 5 10	0.0	171216.0	0.2226
PFDR/S	1 5 10	0.0	171216.0	0.2226
FMDF	1 5 10	0.0	171216.0	0.2226
LFCR	1 5 10	0.0	171216.0	0.2226
LFDR-TC	1 5 10	0.0	171216.0	0.2226
LFDR-TR	1 5 10	0.0	171216.0	0.2226
LCNT	1 5 10	0.0	171216.0	0.2226

(a) Structures cost = $A + B(X)^S$
where X = plant rating, MWe.

TABLE B.43. Land Cost Estimate Scaling Parameters[a]

Concept	Plant Rating, MWe	A	B	C
PFCR/R	1 5 10	1.62	3340	902
PFCR/B	1 5 10	1.62	3340	902
PFDR/R	1 5 10	1.62	3340	902
PFDR/B	1 5 10	1.62	3340	902
PFDR/S	1 5 10	1.62	3340	902
FMDF	1 5 10	1.62	3340	902
LFCR	1 5 10	1.62	3340	902
LFDR-TC	1 5 10	1.62	3340	902
LFDR-TR	1 5 10	1.62	3340	902
LCNT	1 5 10	1.62	3340	902

(a) Land cost = $A\left[B + C(X) + \frac{Y}{Z}\right]$

where X = plant rating MWe
Y = collector field size, m^2
Z = ground cover ratio.

TABLE B.44. Instrumentation and Control Cost Estimate Scaling Parameters[a]

Concept	Plant Rating, MWe	A	B	C
PFCR/R	1	115000.0	0.01	0.03
	5	262000.0		
	10	370000.0		
PFCR/B	1	115000.0	0.01	0.03
	5	262000.0		
	10	370000.0		
PFDR/R	1	115000.0	0.01	0.03
	5	262000.0		
	10	370000.0		
PFDR/B	1	115000.0	0.01	0.03
	5	262000.0		
	10	370000.0		
PFDR/S	1	115000.0	0.01	0.03
	5	262000.0		
	10	370000.0		
FMDF	1	115000.0	0.001	0.03
	5	262000.0		
	10	370000.0		
LFCR	1	38000.0	0.01	0.03
	5	87000.0		
	10	123000.0		
LFDR-TC	1	38000.0	0.01	0.03
	5	8700.0		
	10	123000.0		
LFDR-TR	1	38000.0	0.01	0.03
	5	8700.0		
	10	123000.0		
LCNT	1	0.0	0.01	0.03
	5			
	10			

(a) Instrumentation and control cost = A + B(X) + C(Y)
where X = concentrator cost
Y = cost of receiver, structures, thermal transport, electric transport, power conditioning, energy conversion, land, thermal/electric storage.

TABLE B.45. Spare Parts Cost Estimate Scaling Parameters[a]

Concept	Plant Rating, MWe	A	S
PFCR/R	1	0.006	1.0
	5	0.002	
	10	0.001	
PFCR/B	1	0.006	1.0
	5	0.002	
	10	0.001	
PFDR/R	1	0.006	1.0
	5	0.002	
	10	0.001	
PFDR/B	1	0.006	1.0
	5	0.002	
	10	0.001	
PFDR/S	1	0.006	1.0
	5	0.002	
	10	0.001	
FMDF	1	0.006	1.0
	5	0.002	
	10	0.001	
LFCR	1	0.006	1.0
	5	0.002	
	10	0.001	
LFDR-TC	1	0.006	1.0
	5	0.002	
	10	0.001	
LFDR-TR	1	0.006	1.0
	5	0.002	
	10	0.001	
LCNT	1	0.006	1.0
	5	0.002	
	10	0.001	

(a) Spare parts cost = $A(X)^S$
where X = cost of concentrator, receiver, thermal transport, electric transport, energy conversion, power conditioning, thermal/electric storage, structures, and instrumentation and control.

TABLE B.46. Service Facilities Cost Estimate Scaling Parameters[a]

Concept	Plant Rating, MWe	A	S
PFCR/R	1	0.0089	1.0
	5	0.0085	
	10	0.0082	
PFCR/B	1	0.0072	1.0
	5	0.0070	
	10	0.0070	
PFDR/R	1	0.0099	1.0
	5	0.0095	
	10	0.0092	
PFDR/B	1	0.0072	1.0
	5	0.0070	
	10	0.0070	
PFDR/S	1	0.0072	1.0
	5	0.0070	
	10	0.0070	
FMDF	1	0.0039	1.0
	5	0.0035	
	10	0.0032	
LFCR	1	0.0059	1.0
	5	0.0055	
	10	0.0052	
LFDR-TC	1	0.0084	1.0
	5	0.0080	
	10	0.0077	
LFDR-TR	1	0.0084	1.0
	5	0.0080	
	10	0.0077	
LCNT	1	0.0064	1.0
	5	0.0060	
	10	0.0057	

(a) Spare parts cost = $A(X)^S$
where X = cost of concentrator, receiver, thermal transport, electric transport, energy conversion, power conditioning, thermal/electric storage, structures, and instrumentation and control.

TABLE B.47. Indirect Construction Cost Estimate Scaling Parameters(a)

Concept	Plant Rating, MWe	A
PFCR/R	1 5 10	0.18
PFCR/B	1 5 10	0.18
PFDR/R	1 5 10	0.18
PFDR/B	1 5 10	0.16
PFDR/S	1 5 10	0.16
FMDF	1 5 10	0.17
LFCR	1 5 10	0.17
LFDR-TC	1 5 10	0.17
LFDR-TR	1 5 10	0.17
LCNT	1 5 10	0.17

(a) Indirect construction costs = A(X)
where X = direct capital costs.

TABLE B.48. Contingency Cost Estimate Scaling Parameters[a]

Concept	Plant Rating, MWe	A
PFCR/R	1 5 10	0.07
PFCR/B	1 5 10	0.07
PFDR/R	1 5 10	0.07
PFDR/B	1 5 10	0.07
PFDR/S	1 5 10	0.07
FMDF	1 5 10	0.07
LFCR	1 5 10	0.07
LFDR-TC	1 5 10	0.07
LFDR-TR	1 5 10	0.07
LCNT	1 5 10	0.07

(a) Contingency costs = A (X)
where X = direct capital costs.

TABLE B.49. Ground Cover Ratios Used for Cost Estimation

Concept	Ground Cover Ratio
PFCR/R	0.23
PFCR/B	0.23
PFDR/R	0.44
PFDR/B	0.25
PFDR/S	0.25
FMDF	0.55
LFCR	0.75
LFDR-TC	0.50
LFDR-TR	0.25
LCNT	0.53

TABLE B.50. Base Year for Capital Cost Inputs

Subsystem	Base Year
Concentrator	1978
Energy Conversion	1978
Electric Energy Transport	1977[a]
Instrumentation and Control	1978
Land	1978
Power Conditioning	1977
Receiver	1978
Structures	1977
Electric Energy Storage	1978
Thermal Energy Storage	1977
Thermal Energy Transport	1977

(a) All 1977 costs were updated to 1978 costs by SOLSTEP during computer simulation.

APPENDIX B REFERENCES

AiResearch Manufacturing Company. 1975. Final Report, Core Engine Program, 40 HP Laboratory Closed Brayton Engine. Report 74-311002, Phoenix, Arizona.

Arthur D. Little, Inc. 1977. Conceptual Design and Analysis of a Compound Parabolic Concentrator Collector Array. Cambridge, Massachusetts.

Dodge. 1977. 1978 Dodge Guide to Public Works and Heavy Construction Costs. McGraw-Hill Information Systems Co., New York, New York.

Drumheller, K. 1978. Heliostat Manufacturing Analysis. PNL-2757, Pacific Northwest Laboratory, Richland, Washington.

Electric Power Research Institute. 1976. An Assessment of Energy Storage Systems Suitable for Use by Electric Utilities. EPRI EM-264, Palo Alto, California.

E-Systems, Inc. 1978a. Crosbyton Solar Power Project, Phase I Interim Technical Report. ETC/78 TR-01, Dallas, Texas.

E-Systems, Inc. 1978b. Crosbyton Solar Power Project, Phase I Interim Technical Report, Supplementary Reports to Technical Report ETC/78 TR-01. Dallas, Texas.

FMC Corporation. 1978. Proposal for Line Focus Solar Central Power System, Volume 1: Technical Report. FMC P-3750, Santa Clara, California.

Fujita, T. 1977. Projection of Distributed-Collector Solar-Thermal Electric Power Plant Economics to Years 1990-2000. DOE/JPL-1060-77/1, Jet Propulsion Laboratory, Pasadena, California.

Fujita, T., et al. 1978. Techno-Economic Projections for Advanced Dispersed Solar-Thermal Electric Power Plants to Years 1990-2000. DOE/JPL-1060-78/4, Jet Propulsion Laboratory, Pasadena, California.

Guthrie, K. M. 1974. Process Plant Estimating, Evaluation and Control. Craftsman Book Company of America, Solana Beach, California.

Holl, R. J. 1978. Definition of Two Small Central Receiver Systems. SAND78-7001, Sandia Laboratories, Albuquerque, New Mexico.

Honeywell, Inc. 1977. Solar Pilot Plant, Phase 1: Preliminary Design Report. Volume 7. CDRL Item 2, Pilot Plant Cost and Commercial Plant Cost and Performance. SAN/1109-8/9, Energy Resources Center, Minneapolis, Minnesota.

Jet Propulsion Laboratory. 1978. Thermal Power Systems Advanced Solar Thermal Technology Project, Advanced Subsystems Development, Second Semi-Annual Progress Report. DOE/JPL-1060-78/6, California Institute of Technology, Pasadena, California.

Martini, W. R. 1979. Survey of the Maintenance and Repair Requirement and the Lifetime of Stirling Engines. Martini Engineering, 2303 Harris, Richland, Washington.

Martin Marietta Corporation. 1975. Central Receiver Solar Thermal Power System, Volume 1, Preliminary Baseline Report and Conceptual Design Report. Denver, Colorado.

McDonnell Douglas Astronautics Company. 1976. Central Receiver Solar Thermal Power System, Phase 1 Final Report, CDRL Item 1, Pilot Plant Preliminary Design Baseline Report, Volume 1, Book 1, System Analyses and Design. MDC-G-6040, Huntington Beach, California.

McDonnell Douglas Astronautics Company. 1977. Central Receiver Solar Thermal Power System, Preliminary Design Report. SAN-1108-8/2, Huntington Beach, California.

Meador, J. T. 1977. ICES Technology Survey, Data Technology Evaluation of Steam Turbines. Oak Ridge National Laboratory, Oak Ridge, Tennessee.

Miska, K. H. 1978. "Costs Continue to Exert Pressure on Metal; Supply Generally Adequate." Materials Engineering. 87(1):71-74.

Mitre Corporation. 1977. Systems Descriptions and Engineering Costs for Solar-Related Technologies, Volume V. MTR-7485 V.5, McLean, Virginia.

Peters, M. S., and K. D. Timmerhaus. 1968. Plant Design and Economics for Chemical Engineers. 2nd ed. McGraw-Hill Book Co., New York, New York.

Robert Snow Means Company. 1976. Building Construction Cost Data, 1977. Duxbury, Massachusetts.

Robert Snow Means Company. 1977. Building Construction Cost Data, 1978. Duxbury, Massachusetts.

Schulte, S. C. 1977. Capital Cost Models for Geothermal Power Plants and Fluid Transmission Systems. PNL-2307, Pacific Northwest Laboratory, Richland, Washington.

Selcuk, M. K. 1976. Preliminary Evaluation of a Parabolic Dish-Small Heat Engine Central Solar Plant. 900-749, EM 342-341, Jet Propulsion Laboratory. Pasadena, California.

Selcuk, M. K. 1975. Survey of Several Central Receiver Solar Thermal Power Plant Design Concepts. 900-714, EM 342-311, Jet Propulsion Laboratory, Pasadena, California.

Sterlich, B. 1975. "The Equipment Side of Low Level Heat Recovery." Power. 119(6):71-77.

Texas Tech University. 1977. Crosbyton Solar Power Project Phase 1, Interim Technical Report Volume V. Lubbock, Texas.

Thaller, L. H. 1974. Electrically Rechargeable Redox Flow Cells. NASA TM X-71540, NASA-Lewis Research Center, Cleveland, Ohio.

Thaller, L. H. 1979. "Redox Flow Cell Energy Storage Systems." In Proceedings of AIAA Terrestrial Energy Systems Conference. CONF-79-0989, National Technical Information Service, Springfield, Virginia.

Warshay, M., and L. O. Wright. 1975. "Cost and Size Estimates for an Electrochemical Bulk Energy Storage Concept." In Proceedings of Energy Storage Symposium, Fall Meeting of the Electrochemical Society, pp. 130-140. CONF-751032, National Technical Information Service, Springfield, Virginia.

APPENDIX C

STEAM TURBINE GENERATOR PERFORMANCE AND COST - BECHTEL NATIONAL REPORT

December 29, 1978
Attachment A

SYSTEMS ANALYSIS STUDY OF SMALL SOLAR THERMAL POWER SYSTEMS

TOPICAL REPORT NO. 1

Prepared for

PACIFIC NORTHWEST LABORATORIES
BATTELLE MEMORIAL INSTITUTE
Richland, Washington

by

BECHTEL NATIONAL, INC.
Research and Engineering
San Francisco, California

Subcontract No. B-67820-A-L
Bechtel Job 13207

CONTENTS

ILLUSTRATIONS

Section 1

INTRODUCTION

The work reported herein was conducted by Bechtel under a subcontract to Pacific Northwest Laboratories of Battelle Memorial Institute (Subcontract No. B-67820-A-L) in support of their prime contract with the U.S. Department of Energy (Contract No. EY-76-C-06-1830). Under this contract, Pacific Northwest Laboratories (PNL) is ranking alternative solar thermal energy conversion systems that are potentially feasible for use in electric power generation facilities in the 1 to 10 MWe range, with initial commercialization by the mid-1980's. Bechtel is providing consulting services on the technical and cost aspects for the engineering and construction of the candidate system concepts.

The first task, assigned to Bechtel in the PNL letter of September 11, 1978 and subsequently modified in a meeting held on Setepmber 25, 1978 and telephone discussions, was to provide performance, costs and operational description of steam Rankine power cycles in the 1 to 10 MWe range. This report covers the results of the investigation by Bechtel.

Section 2

TURBINE SELECTION

2.1 REQUIREMENTS

The original requirements received from PNL for investigation of turbine cycle cost and performance were the following:

- Rated turbine-generator net electrical output to be from 1 to 10 MWe
- 100% of rated load to be generated from main steam at 1450 psia and 1000F
- 70% of rated load to be generated from storage steam at 960 psia and 540F (saturated)
- Site conditions of Barstow, California to be used including 74F design wet bulb temperature.

As a result of analysis by Bechtel and discussions with PNL, it was determined that PNL's desire to eliminate a storage superheater was not consistent with the limitation of steam turbine last-stage moisture to approximately 16% in order to prevent erosion. The steam conditions were therefore changed to coincide with those used by McDonnell Douglas Astronautics Company for their 10 MWe pilot plant study (Ref. 2-1):

- 100% of rated load to be generated from main steam at 1450 psig and 950F
- 70% of rated load to be generated from storage steam at 370 psig and 525F.

Subsequent investigations have shown that lower pressures should be evaluated for the low end of the 1 to 10 MWe range.

2.2 CONSIDERATIONS FOR TURBINE SELECTION

A turbine selected for a solar power plant in the 1 to 10 MWe range should have a high efficiency, be commercially available, and be adaptable to daily cyclic operation. In order to meet these requirements, the effects of turbine speed, control valve configuration and steam conditions were evaluated.

Two options are available in the 1 to 10 MWe range for turbine rotational speed. Operation at 3600 rpm with a direct coupling between turbine and generator is typical of large conventional power plant practice and was selected for the 10 MWe Barstow pilot plant studies. Operation at higher turbine speeds with the generator driven through a gear reduction unit is also possible in this capacity range. A high-speed turbine, with rated speed ranging from approximately 13,000 rpm for 1 MWe to 9,000 rpm at 10 MWe, has a higher efficiency than a 3600 rpm turbine for the same steam conditions and has a lower cost because it is less massive. Both turbine designs are commercially available for a 10 MWe rating but a 1 MWe turbine designed for 3600 rpm at the selected steam conditions is considered impractical by the manufacturers contacted.

Several arrangements for control of storage steam flow are available in the 1 to 10 MWe turbine designs. The mixed pressure design has one inlet section for both main and storage steam. The admission turbine has two steam inlets with a storage steam inlet control valve internal to the turbine casing, through which

both storage steam and main steam (after passing through the first few stages) are routed. The induction turbine also has two steam inlets but has a storage steam control valve external to the casing, that does not affect operation on main steam. The admission turbine recommended for the 10 MWe Barstow pilot plant has the best combination of performance efficiencies for all operating conditions typical of a solar plant. Induction and mixed pressure turbines are also available at ratings of 1 to 10 MWe. Siemens Corporation and Elliott Corporation were identified as potential suppliers of high-speed, 1 to 10 MWe turbine-generators.

The steam pressure of 1450 psig is higher than acceptable for many standard manufacturers' designs in the 1 to 10 MWe range. For pressures above 1000 psig, it is difficult to maintain flow passage dimensions with standard tolerances for the small volumetric flows involved. Therefore, for a 10 MWe turbine, a distinction in efficiency can be made between 1000 psig and 1450 psig inlet pressure but this difference becomes insignificant for a 1 MWe turbine. Other factors which influence cost should determine the inlet pressure for turbines in the low end of the 1 to 10 MWe range.

2.3 TURBINE SELECTION

Based on the considerations discussed in Section 2.2 above, the recommended turbine for the 1 to 10 MWe range is a high-speed (9,000 to 13,000 rpm) design which drives the synchronous

generator through a gear reducer. An admission turbine is the first choice. An induction turbine is the second choice if an admission turbine is not available for a particular rating between 1 and 10 MWe. The design main steam pressure of 1450 psig is practical for the analysis of the different concepts being evaluated by PNL; however, reducing the pressure to 1000 psig for the 1 MWe rating will not significantly affect turbine cycle efficiency.

Section 3

EQUIPMENT DESCRIPTION

The descriptive material in this section applies to a 10 MWe steam turbine system. Smaller systems are similar in most respects except as noted.

3.1 TURBINE-GENERATOR

The turbine selected is a single automatic extraction (admission) condensing steam turbine with three uncontrolled extraction connections. It consists of a two-stage high pressure section which is supplied by main steam and a 19-stage low pressure section which operates on steam from the high pressure section and/or admission steam. The rated power of the turbine is approximately 11 MWe since it must satisfy the auxiliary loads in addition to generating 10 MWe net power.

The design speed of the turbine is 9500 rpm and it drives the generator at 1800 rpm through a double helical spur gear reduction unit. The generator is a three phase, 60 hz, four pole synchronous unit rated at 13.8 kV with a power factor of 0.9. The generator is air cooled and is equipped with a brushless exciter.

Accessories for the turbine-generator include inlet steam stop and control valves, extraction stop valves, turning gear, lubrication system, steam seal system, electrohydraulic control

system and foundation plate with bolts. The approximate overall dimensions of the turbine generator are 34 feet long, 16 feet wide, and 20 feet high.

A similar turbine-generator rated at 1 MWe would operate at 13,000 rpm, have two uncontrolled extractions, and measure approximately 20 feet long and 15 feet wide.

3.2 TURBINE CYCLE EQUIPMENT

The turbine cycle equipment includes the condenser, feedwater heaters, the mechanical vacuum pump, condensate pumps, booster pumps, feedwater pumps, miscellaneous piping and valves, condensate demineralizers, condensate makeup and storage, instruments and controls, and auxiliary equipment such as air compressors and the auxiliary steam generator.

The two-pass, single-pressure surface condenser could be oriented to accept either a bottom or side discharging turbine. Tubes of 90-10 copper-nickel are often used for this application. A mechanical vacuum pump is used to remove non-condensibles. The condensate pump takes suction from the condenser hotwell.

The lowest pressure of the three feedwater heaters would be of the open deaerating type, with the two intermediate pressure shell and tube heaters operating at approximately 50 and 170 psia. The feedwater booster pumps draw from the deaerating heater drain tank and pump the condensate through the other two

feedwater heaters to the feed pump suction. For a 1 MWe cycle, there will be only one intermediate pressure heater and it would operate at approximately 80 psia.

3.3 HEAT REJECTION EQUIPMENT

The heat rejection equipment consists of cooling towers, circulating water pumps and piping, makeup water and blowdown piping, and water treatment equipment.

The mechanical draft cooling tower would consist of approximately 1 cell/MWe. Makeup requirements are estimated to be 2.5% of circulating water flow. Circulating water piping, probably fiberglass reinforced plastic (FRP), would be long enough to place the cooling towers beyond the collector field, so that water droplet drift does not impair heliostat performance.

Section 4

TURBINE CYCLE PERFORMANCE

Performance of a steam Rankine cycle has been calculated for the 1-10 MWe range, partial load conditions, and turbine back pressures.

4.1 EFFECT OF PLANT SIZE

The variation in net turbine cycle efficiency with plant size from 1 to 10 MWe is shown in Figure 4-1. The data shown are for admission turbines. Net cycle efficiency is based on the net electrical output, which is equal to the gross electrical output less the auxiliary loads.

The curve for high-speed turbines is based on turbine efficiency values received from Siemens Corporation for 1 MWe and 10 MWe turbine units. A slight adjustment of the original information was made to match the required steam conditions. The shape of the curve over the range is based on calculations done by Bechtel for a 3600 rpm turbine, shown as dotted lines in Figure 4-1.

Two sets of curves are shown for the two required inlet steam conditions. For a particular turbine, the rated efficiency with storage steam is based on a rating that is 70% of the rating on main steam. For example, a turbine rated at 5 MWe on main steam and 3.5 MWe on storage steam would have rated load efficiencies which correspond to those two values in Figure 4-1.

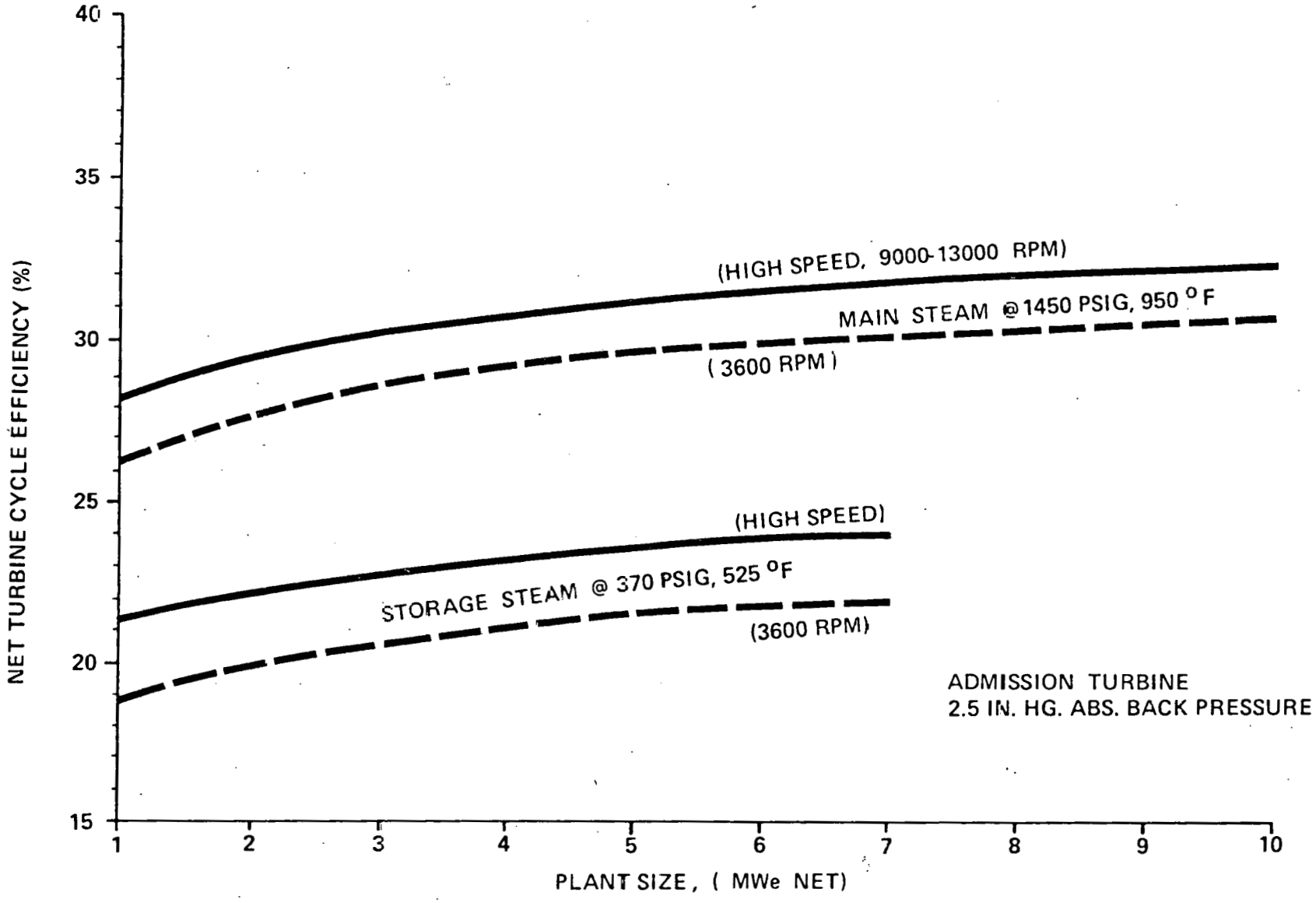

Figure 4-1 NET TURBINE CYCLE EFFICIENCY VS. PLANT SIZE

If an induction turbine is used, slightly higher main steam efficiencies would be expected although the efficiency on storage steam would be somewhat lower.

4.2 AUXILIARY LOADS

The auxiliary loads for the 1 to 10 MWe range as a function of gross electrical output are given in Figure 4-2. These percentages were determined from an examination of a much wider range of plant sizes.

Auxiliary loads with and without feed pump power are shown separately at PNL's request. It has been assumed that the pressure at the feed pump suction is approximately 500 psia.

4.3 EFFECT OF PART LOAD OPERATION

The variation of turbine cycle efficiency with operation at part load is shown in Figure 4-3. The effect of auxiliary loads is included. The basis for this information is the preliminary design reports for the 10 MWe Barstow pilot plant (Refs. 4-1 and 4-2).

When Figure 4-3 is applied to a particular turbine in the 1 to 10 MWe range, 100% of rated load on storage steam is equal to 70% of rated load on main steam.

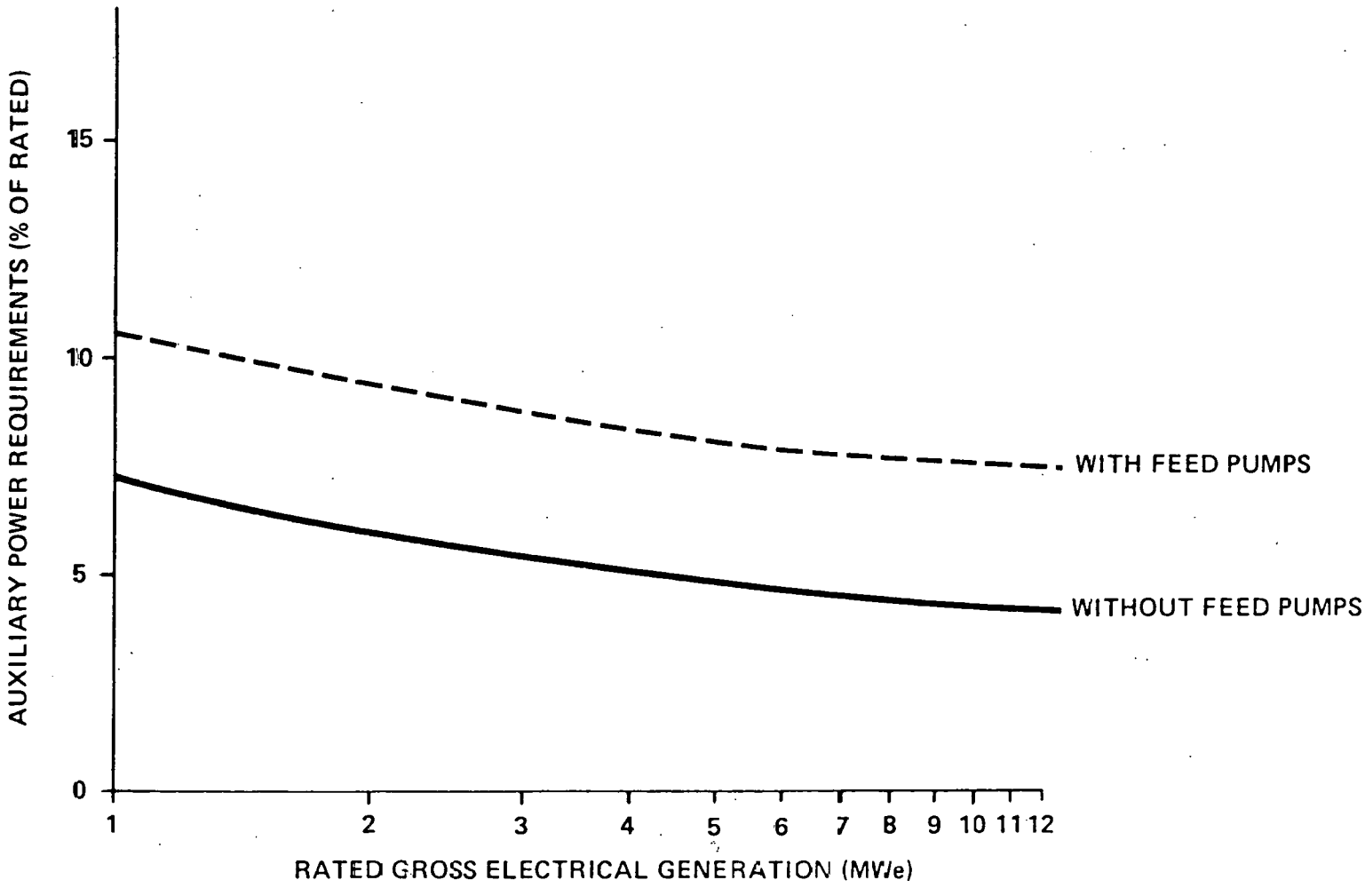

Figure 4-2 AUXILIARY POWER REQUIREMENTS

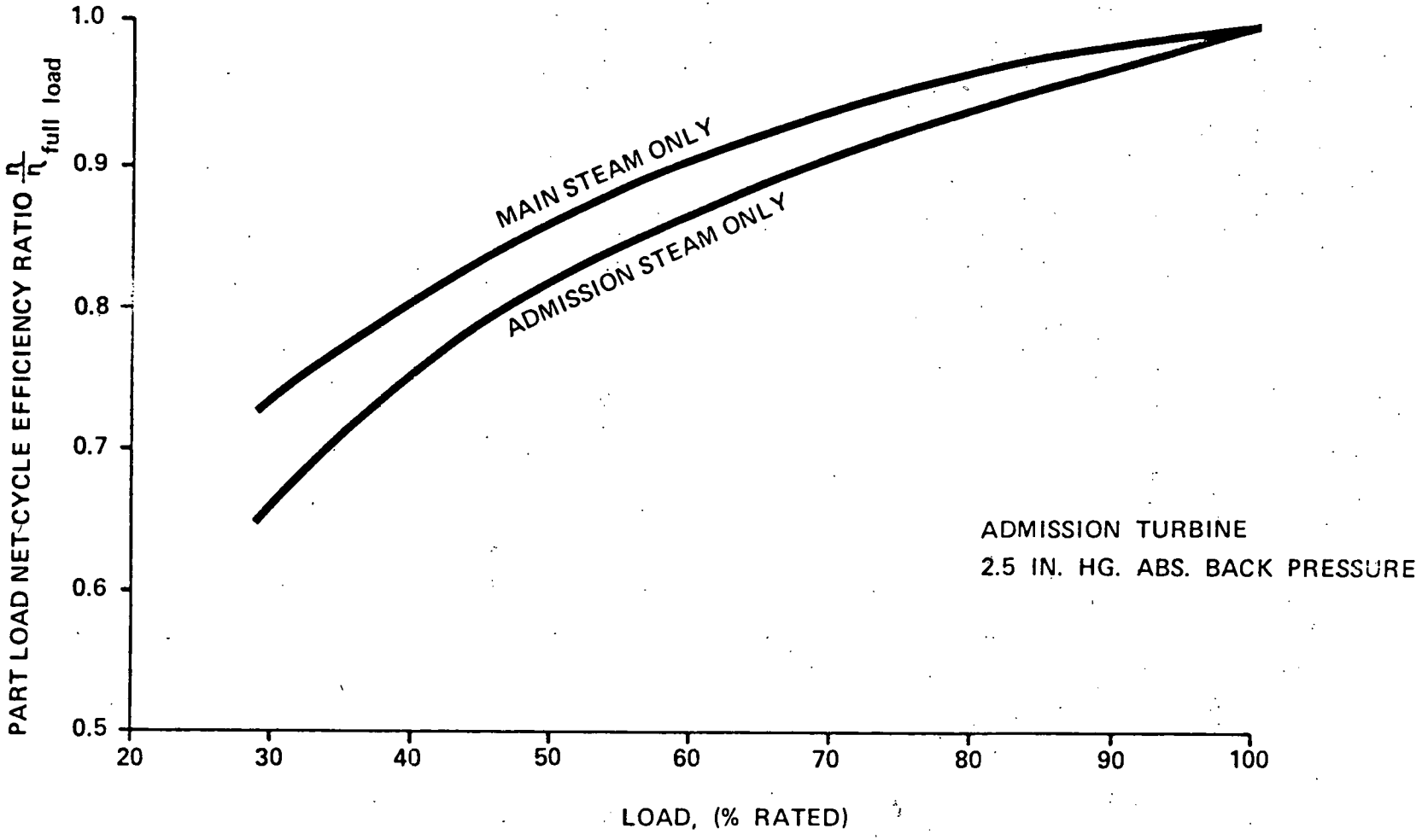

Figure 4-3 1 - 10MWe TURBINE CYCLE EFFICIENCY FOR PART LOAD OPERATION

4.4 EFFECT OF TURBINE BACK PRESSURE

The variation of turbine cycle efficiency with turbine back pressure is given in Figure 4-4. Main steam and storage steam operation are separate curves with interpolation between the curves necessary for combined operation. Performance is referenced to the design back pressure of 2.5 in Hg abs.

In order to correlate turbine cycle performance with ambient wet bulb temperature, the performance of the cooling tower is represented by Figure 4-5. An ambient wet bulb temperature of 74F is used as the design point.

The curves in Figures 4-4 and 4-5 are based on variation from rated load. For variations at other loads, both Figures 4-4 and 4-5 require modification to accurately model actual plant operation. Information on this relating to the 10 MWe pilot plant studies was given to Battelle in the meeting of September 25, 1978.

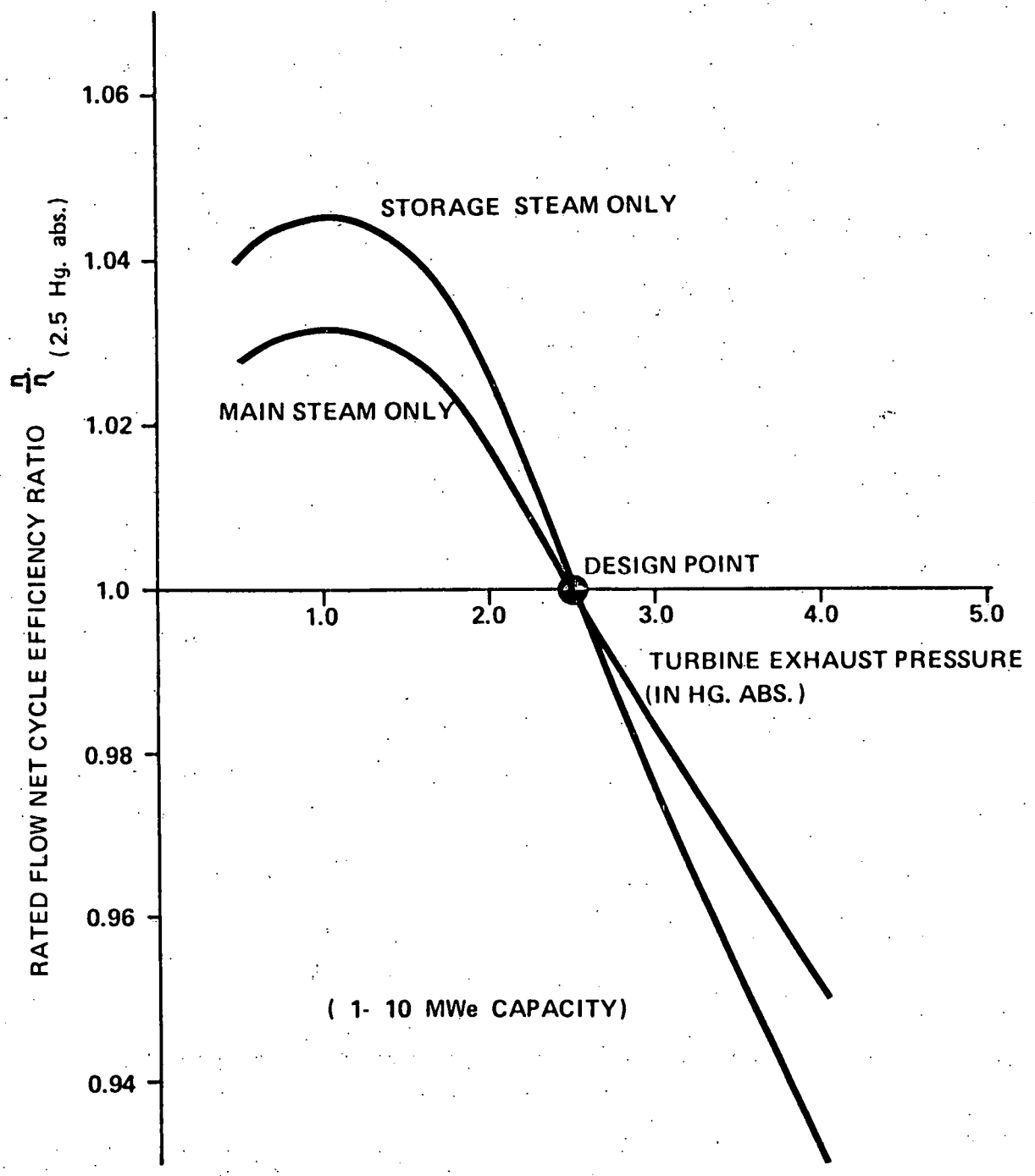

Figure 4-4 RATED FLOW TURBINE EXHAUST PRESSURE CORRECTION CURVES

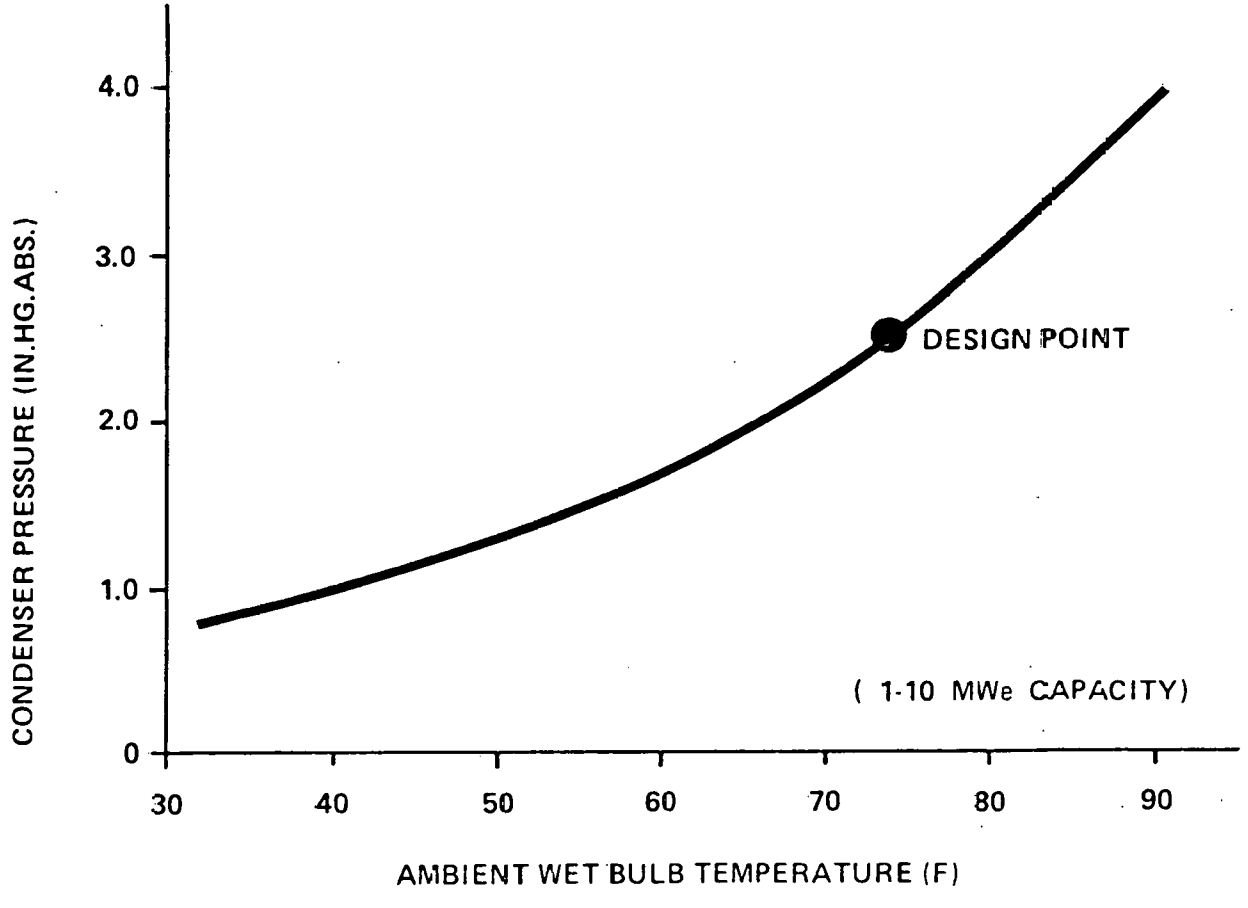

Figure 4-5 CONDENSER PRESSURE AS A FUNCTION OF WET BULB TEMPERATURE FOR RATED CONDENSER DUTY

Section 5

TURBINE OPERATION

5.1 NORMAL OPERATING MODES

Normal turbine steady state operating modes consist of main steam operation, storage steam operation, or operation on a combination of the two steam supplies. Load is controlled by throttling with the turbine main steam control or admission control valves. Several valves, each controlling a portion of the turbine arc, are individually positioned to minimize throttling losses.

When operating on storage steam only, a small portion (10%) of the inlet steam must be diverted through the high pressure section to prevent overheating due to aerodynamic friction.

It is reasonable to assume an overload rating of at least 105% although a particular manufacturers' standard designs may be able to handle greater overloads for some turbine sizes.

5.2 STARTUP AND SHUTDOWN

Startup for daily operation will require approximately the same time as the Barstow pilot plant designs (3600 rpm) because, although a high-speed turbine is less massive, it must be accelerated to a higher speed, and the closer tolerances of the smaller machine make differential expansion of components a relatively greater problem. The total time from roll of the

turbine to full load will be approximately 45 minutes for a system that is "bottled up" overnight and is kept hot. When shutdown duration is increased, the startup time will increase to approximately four hours for a cold start with no preheating.

Given these startup times, a lifetime of 10,000 startups should be reasonable. This same cyclic life should apply for quick excursions of up to 200F and large excursions at a rate not exceeding 500F per hour. This should require no special precautions for transition between steam supplies or shutdown.

5.3 SUPERVISION AND MAINTENANCE

With computerized plant control, this type of plant could be operated without constant on-site operator supervision. The usual complement of alarms and plant data could be monitored by a remote operator for several such plants.

A small maintenance crew would be required for one-shift per week day but they could service the whole plant, with only part time given to turbine cycle maintenance. Normal maintenance would include routine inspection to insure reliability. Scheduled periodic equipment maintenance would involve shutdown of the turbine-generator for a few cloudy days a year.

Section 6

TURBINE CYCLE EQUIPMENT COSTS

The development of realistic cost estimates for small, efficient, high pressure steam turbines is difficult for several reasons. The range from 1 to 10 MWe is seldom used for efficient power generation and therefore there has been little incentive for manufacturers to develop multistage turbines in this range. For applications with which the manufacturers are familiar, especially near 1 Mwe, it is impractical to use such high pressures and temperatures at the turbine inlet. The specific volume and steam flow rate cause a difficult design problem when standard manufacturing tolerances for internal fluid passages are considered.

One source of cost information is the contractors' cost estimates for the 10 MWe Barstow Pilot Plant (Refs. 6-1 and 6-2). However, the high-speed turbine-generator is less costly based on a quote obtained by Bechtel from Siemens Corporation for the Martin Marietta pilot plant study. Both the quote from Siemens and the cost from General Electric are shown on Figure 6-1.

Variations of cost with unit size are speculative in this range. Telephone quotes were obtained from Elliott Corporation for 1, 5 and 10 MWe turbine-generators and were used to obtain a scaling exponent relationship between installed $/kWe and unit size. This is the lowest curve shown in Figure 6-1.

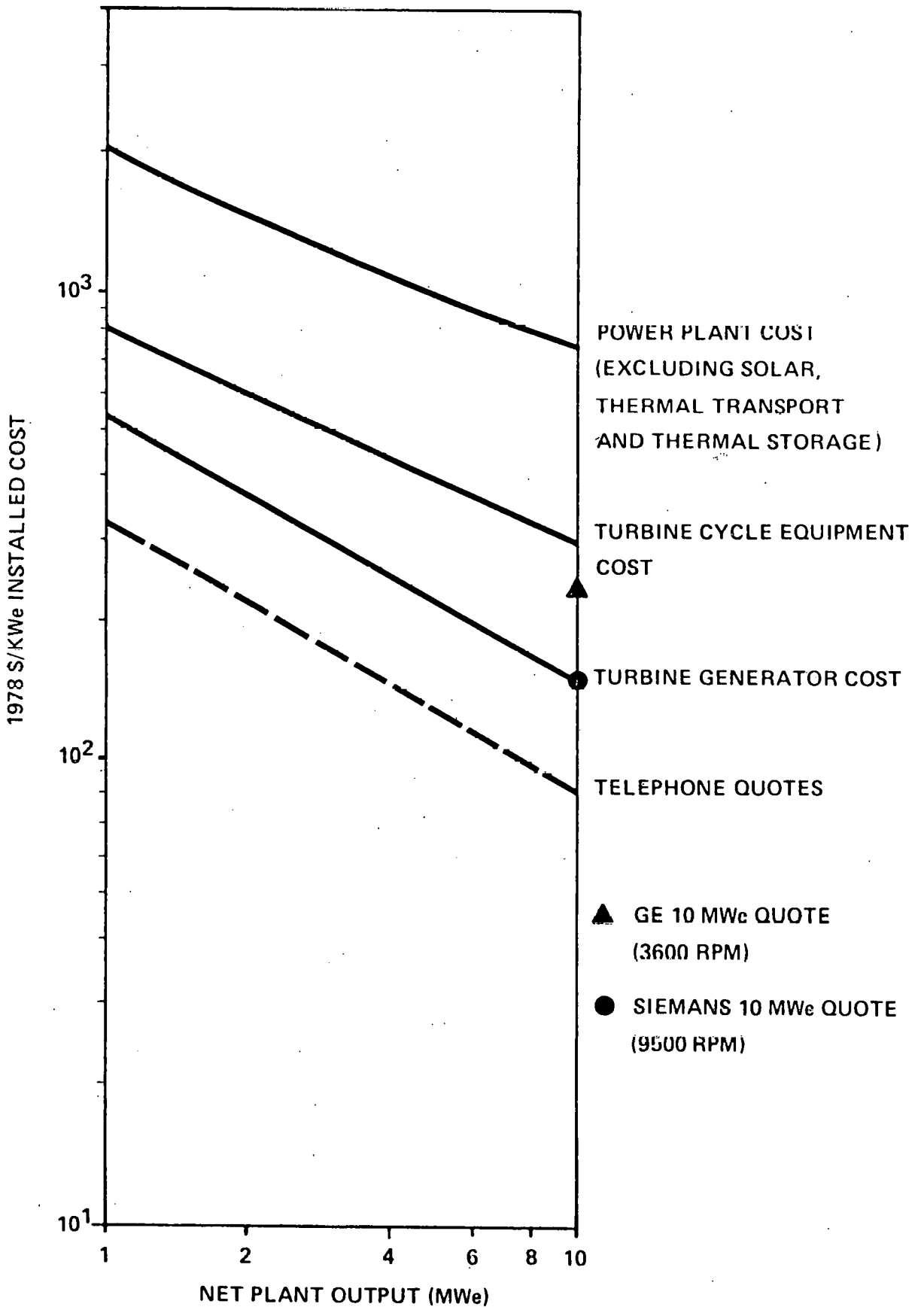

Figure 6-1 ESTIMATED STEAM TURBINE-GENERATOR EQUIPMENT AND PLANT COSTS

The combination of the estimated installed cost of the Siemens 10 MWe turbine-generator and the size exponent developed as described above has been used to determine the installed turbine-generator cost in Figure 6-1 for the 1 to 10 MWe range.

The installed cost of the turbine cycle equipment and heat rejection system equipment, based on the Bechtel estimate for Martin Marietta for the 10 MWe pilot plant, has also been shown in Figure 6-1. The dependency of the cost of the cycle equipment on unit size is estimated to be considerably lower than the turbine-generator because it represents standard equipment throughout the 1 to 10 MWe range.

The top curve in Figure 6-1 represents the total cost of the power plant excluding the solar, heat transport, and thermal storage subsystems. It is based on the Bechtel estimate for Martin Marietta, with a portion of yard work, master control, miscellaneous plant equipment, indirects, distributables, and contingency included; but based on a more modular approach using skid mounted modules, which is reasonable for the 1 to 10 MWe range. The dependency on unit size is based on examination of a much wider range of unit sizes.

These costs represent the best available preliminary estimates for the first few plants in the 1 to 10 MWe range. If a suitable market is demonstrated, these costs will probably decrease but no information is available at this time to evaluate such an effect.

REFERENCES

2-1 Hallet, R.W., Jr., and Gervais, R.L., (McDonnell Douglas Astronautics Company, Huntington Beach, CA), Central Receiver Solar Thermal Power System, Phase I, Electric Power Generation and Master Control Subsystems and Balance of Plant, Volume 6, CRDL Item 2, Pilot Plant Preliminary Design Report, SAN/1108-8/6, October 1977.

4-1 Hallet, R.W., Jr., and Gervais, R.L., (McDonnell Douglas Astronautics Company, Huntington Beach, CA), Central Receiver Solar Thermal Power System, Phase I, Electric Power Generation and Master Control Subsystems and Balance of Plant, Volume 6, CRDL Item 2, Pilot Plant Preliminary Design Report, SAN/1108-8/6, October 1977.

4-2 Central Receiver Solar Thermal Power System, Phase I, Electric Power Generation/Master Control Subsystems and Balance of Plant, Volume VI, Preliminary Design Report (Draft), Martin Marietta Corporation, Denver, Colorado, SAN-1110-77-2, MCR-77-156, April 1977.

6-1 Central Receiver Solar Thermal Power System, Phase I, Pilot Plant Cost and Commercial Plant Cost and Performance, Volume 7, Book 1 (Preliminary Draft), CRDL Item 2, Pilot Plant Preliminary Design Report, McDonnell Douglas Astronautics Company, Huntington, Beach, CA, SAN/1108/8, May 1977.

6-2 Cost and Schedule Estimates of Central Receiver Solar Thermal Power System, Phase I, 10 MWe Pilot Plant, prepared by Bechtel Corporation, San Francisco, CA, for Martin Marietta Corporation, April 1977.

DISTRIBUTION

No. of
Copies

OFFSITE

A. A. Churm
DOE Patent Division
9800 S. Cass Avenue
Argonne, IL 60439

6 J. E. Rannels
Division of Solar Thermal Energy Systems
U.S. Department of Energy
600 E Street, NW
Washington, DC 20585

27 DOE Technical Information Center

J. P. Thornton
Solar Energy Research Institute
1536 Cole Boulevard
Golden, CO 80401

ONSITE

2 DOE Richland Operations Office

H. E. Ransom
R. K. Stewart

90 Pacific Northwest Laboratory

D. T. Aase
W. J. Apley (71)
S. P. Bird
A. J. Currie
J. W. Currie
M. K. Drost
W. W. Laity (2)
B. A. Price
T. A. Williams
Technical Information (5)
Publishing Coordination (2)